HIGH TENSILE STEEL

AS NORMAL REINFORCEMENT IN CONCRETE

A thesis presented for the degree of

Doctor of Philosophy

by

Hamid Paulus Attisha

B.Sc., M.Sc.

Department of Civil Engineering,
The University of Salford.

May, 1972

ACKNOWLEDGEMENT

The author wishes to express his sincere gratitude to Professor T. Constantine, B.Sc., Ph.D., C.Eng., F.I.C.E., F.I.Mun.E., M.Inst.H.E., Chairman of the Department of Civil Engineering, and Professor E.R. Bryan, M.Sc., Ph.D., C.Eng., F.I.C.E., F.I.Struct.E., Professor of Structural Engineering, for providing the facilities to carry out the work reported in this thesis.

The author is also indebted to his Supervisor, Dr. N.J.Dave, M.Eng., Ph.D., D.C.T., A.M.I.E. (India), M.Am.Soc.C.E., for his constant experienced guidance and encouragement during the period of experimenting and writing the thesis.

Special thanks are due to Mr. D.C. O'Leary, M.Sc., C.Eng., M.I.C.E., for his advise and assistance in obtaining the materials and arranging the laboratory assistance.

The author wishes to thank Messrs. T.Clark, C. Lomax, W. Deacon and T. Ward and all the technical staff of the Civil Engineering Laboratories and Workshop for their assistance in making and testing the specimens and manufacturing the testing rigs.

Thanks are due to Mr. P. Burton for photographing the specimens and printing the plates.

Thanks to Miss S. Simister for typing the thesis.

The author would like to acknowledge the financial support provided by the Iraqi Ministry of Oil and Minerals to study for the degree of Ph.D. at the University of Salford. The author further acknowledges the Cement Marketing Corporation for the supply of cement, British Ropes Limited and Macaulls Limited (Sheffield) for the supply of reinforcement.

SYNOPSIS

The use of high tensile steel as normal reinforcement in concrete members necessitates the study of the behaviour of such members under the action of static, fatigue and sustained loading. The present state of knowledge of the effects of the type of steel and the type of loading on the serviceability and strength of concrete members has been reviewed. From a comparison of structures reinforced with ordinary and high tensile steels, it has been indicated that by increasing the permissible steel stresses great savings can be obtained, but the deflection and cracking become more pronounced, especially when the effects of long-term loading are considered. Limited information has been reported on the effect of the static cycles, subsequent to the first cycle, on these two limit states. In view of the above, the applicability of the limit state design, and the study of the recommendations of codes of practice of several countries, it was felt that an experimental investigation was required to study the behaviour, in cracking and deflection, of concrete members reinforced with high tensile steel and subjected to static, fatigue and sustained loading.

A programme of an experimental investigation was designed to study the behaviour of reinforced concrete beams. A total of twenty-one beams 152 mm x 305 mm with a span of 4570 mm, and two auxilliary beams with a span of 2740 mm, simply supported, singly reinforced beams were tested under static, fatigue and sustained loading. The main variables were the type and percentage of the steel reinforcement. The reinforcement consisted of (i) bars: plain round mild steel (276 N/mm^2 yield stress), deformed Unisteel 60 and Unisteel 80 (414 N/mm^2 yield stress and 550 N/mm^2 0.2% proof stress respectively), and deformed Kam 60 and Kam 90 steel (585 N/mm^2 yield stress and 897 N/mm^2 0.2% proof stress respectively) (ii) wires: crimped prestressing (1380 N/mm^2 0.2% proof stress), plain prestressing (1515 N/mm^2 0.2% proof stress) (iii) strands: prestressing (1690 N/mm^2 0.2% proof stress) and reinforcing Bristrand 100 (690 N/mm^2 0.2% proof stress). Only one design strength of concrete was used with a cube strength of 41.4 N/mm^2.

An empirical method was suggested for the evaluation of steel stresses under any applied short-term static load. This method was based on evaluating the neutral axis depth by assuming a bilinear relationship between the moment and the neutral axis depth, taking into account the movement of the neutral axis in the transition zone between the uncracked and cracked stages.

Formulae based on the present work are suggested for the prediction of crack width and deflection on the first and second cycles. The deflection and crack width on the first and second cycles were essentially proportional to the stress in the reinforcement. On the first cycle the deflection and crack width depended greatly on the cracking load stress. The remaining crack width was found to be directly proportional to the steel stress at design load, and the remaining deflection to be approximately $\frac{1}{4}$ of the design load deflection. The deflection was not affected by the surface characteristics of the steel, while there was a slightly better crack control with deformed bars than with plain bars or prestressing wires and strands.

The effects of long-term loading (sustained or fatigue) were found to cause an increase in the steel stress, the neutral axis depth, the compressive and tensile concrete strains, the deflection and cracking. The maximum increases in the maximum crack width at the level of reinforcement under sustained and fatigue loading were 67% and 50% respectively. The maximum increases in deflection were 116% and 32% after about 600 days and 3×10^6 cycles respectively. The increase in deflection under sustained loading was lower for higher permissible steel stress with corresponding smaller steel area.

In view of these findings and the limitations on the maximum allowable crack width suggested by the C.E.B., it has been concluded that the maximum steel strength is limited to 550 N/mm^2. The economic advantage of using such a high strength steel is a saving in the steel area of 51% of that of mild steel and 27.6% of that with a yield point of 414 N/mm^2. When the allowable maximum crack width of 0.3 mm, as suggested by the Draft Code, is considered, a steel with a yield strength of 690 N/mm^2 can be used. The saving in the steel area and cost can be further increased.

In Appendix (A) an illustrative example has been given using the various formulae developed in the present work for calculation of deflection, crack width and steel stresses.

Appendix (B) gives information on the effects of the geometric characteristics and the orientation relative to the bar axis of the ribs (transverse deformation) on the slip resistance and bond strength of deformed bars.

CONTENTS

The Use of High Tensile Steel as Normal Reinforcement in Concrete

NOMENCLATURE

A_e	effective concrete area in tension b(2C + D)
A_s	area of tensile steel reinforcement
A_s'	area of compressive steel reinforcement
a_{min}	minimum crack spacing
a_{max}	maximum crack spacing
b	breadth of beam
C	concrete cover (distance from point of measurement of crack to the surface of the bar)
C_c	creep coefficient (ratio of creep strain plus elastic strain to elastic strain)
D	bar diameter
d	over-all depth of beam
d_1	effective depth of beam (depth of the centroid of tensile reinforcement from the top surface of the beam)
dn	neutral axis depth
dn_{cr}	neutral axis depth for cracked condition
dn_{unc}	neutral axis depth for uncracked condition
E_c	initial tangent modulus of elasticity of concrete
E_c'	"effective" modulus of elasticity of concrete
E_s	initial tangent modulus of elasticity of steel reinforcement
e_t	concrete tensile strain
e_c	concrete compressive strain in the extreme fibre of the beam
e_o	plastic concrete compressive strain
e_{sh}	free shrinkage of prism
e_u	ultimate concrete compressive strain
F_c	crack width time dependent multiplier
F_d	deflection time dependent multiplier
f_c	compressive stress in concrete

f_s	tensile stress in steel reinforcement
f_{sc}	tensile stress in steel reinforcement at cracking load
f_{sp}	permissible tensile stress in steel reinforcement
f_t	modulus of rupture of concrete
f_t'	tensile strength of concrete
f_y	yield strength of steel reinforcement
I	second moment of area
I_c	second moment of area of cracked transformed section
I_o	second moment of area of uncracked transformed section
K	neutral axis depth coefficient
K'	constant defining the transition zone between the uncracked and cracked conditions
K_s	constant relating to the steel stress at cracking load
K_t	time dependent neutral axis depth coefficient
K_Δ	creep effect ratio
K_1, K_5	beam stiffness coefficients (ratio of the measured stiffness to the calculated stiffness based on the cracked transformed section for the first and second cycle respectively.)
K_4	ratio of the remaining deflection to the deflection at design load
K_2, K_3	coefficients relating to the mechanical properties of concrete
k_1, k_2	constants relating to the maximum remaining crack width
L	span length
l	anchorage length
l_a	moment arm
M	applied bending moment
M_c	cracking moment
M_D	design moment (using partial safety factors on material strengths and loads)
M_r	ultimate moment of resistance of section (using partial safety factors on material strengths)

M_t actual maximum test moment

M_u ultimate moment (using actual strengths of materials)

m modular ratio $\frac{E_s}{E_c}$

m_t time dependent modular ratio $\frac{E_s}{E_c^T}$

P_t actual maximum test load

P_u ultimate load (using actual strength of materials)

p percentage steel reinforcement

P_D design load (using partial safety factors on material strengths and loads)

P_e effective reinforcement ratio $\frac{A_s}{A_e}$

P_r ultimate load (using partial safety factors on material strengths)

Q shear force

q reinforcement index $p\frac{f_y}{U_w}$

R coefficient relating to the bond characteristics of the reinforcing steel

S stirrups spacing

s size reduction factor for shrinkage

u average bond strength

U_a anchorage bond

U_f flexural bond

U_w works cube strength

W applied load

W_{max_1} maximum crack width at the level of reinforcement on
W_{max_2} the first and second cycles respectively

$W_{(max)_T}$ time dependent maximum crack width

x,y parameters relating to the stress-strain design curve of concrete

α coefficient relating to the depth of the centroid of the resultant compressive force

β	deflection coefficient depending on the type of loading distribution and end conditions of the beam
Δ	allowable deflection
Δ_i	instantaneous deflection
Δ_{ct}	creep + instantaneous deflection
Δ_{rem}	remaining deflection
Δ_{sh}	warping due to shrinkage
Δ_T	time dependent deflection ($\Delta_{ct} + \Delta_{sh}$)
ΔW_{max}	maximum remaining crack width
$\Delta W_{s \text{ or } b}$	maximum remaining crack width at the side or bottom edge of the beam
$\Delta 1$	total deflection at design load, on the first cycle
$\Delta 2$	total deflection at design load, on the second cycle
ε	total time dependent compressive strain
ε_c	concrete compressive creep strain
ε_e	elastic concrete compressive strain
ϕ	beam curvature
γ	ratio of maximum concrete compressive stress in the beam to the cube strength of concrete
$\sum_o$	sum of bar perimeters

ABBREVIATIONS

A.C.I.	American Concrete Institute
C.P.	British Code of Practice
C.E.B.	Comite Europeen du Beton (European Concrete Committee)
F.I.P.	Federation Internationale de la Precontrainte (International Prestressing Federation)
B.S.	British Standard
I.A.B.S.E.	International Association for Bridge and Structural Engineering
P.C.A.	Portland Cement Association
P.C.I.	Prestressed Concrete Institute
I.C.E.	Institution of Civil Engineers
A.S.C.E.	American Society of Civil Engineers
A.A.C.E.	American Association of Cost Engineers
B.R.S.	Building Research Station
C. & C.A.	Cement and Concrete Association
A.S.T.M.	American Standards of Testing Materials
C.I.B.	Conseil International du Batiment pour la Recherche, L'etude et la Documentation
C.I.R.I.A.	Construction Industry Research and Information Association
A.I.S.I.	American Iron and Steel Institute

LIST OF TABLES

LIST OF FIGURES

59	Cube strength - modulus of elasticity curves for concrete
60-62	Load-deflection curves (static load - first and second cycles)
63-64	Load-deflection curves (static load)
65-66	Load-deflection curves (static load - virgin cycles)
67	Load-deflection curves first and second cycles (duplicate beams)
68	Steel stress-deflection curves (static load - virgin cycles)
69	Effect of high tensile steel on deflection
70	Effect of high tensile steel on strain of concrete
71-72	Variation in crack width under repeated loading
73	Effect of repeated loading on cracking
74	Increase in crack width under repeated loading
75	Additional crack width under sustained and repeated loading
76-77	Comparison of static and repeated loading beams (cracks at steel level)
78	Cracking pattern under repeated loading
79-80	Variation in crack width under sustained loading
81	Effect of sustained loading on cracking
82	Increase in crack width under sustained loading
83	Cracking pattern under sustained loading
84	Increase in deflection under repeated loading
85	Effect of repeated loading on load-deflection curve beam A33
86-89	Load-deflection curves (repeated loading)
90	Additional deflection (repeated loading)
91-92	Increase in deflection under sustained loading
93	Load-deflection relationship (sustained loading)
94	Comparison of deflection under sustained loading
95-99	Variation of strain distribution with time (sustained loading)
100	Variation of neutral axis depth with time (sustained loading)
101	Additional deflection (creep and shrinkage)
102-103	Strain distribution (repeated loading)
104	Variation of concrete strain with repetitions
105	Effect of repeated loading on the neutral axis position
106	Variation of concrete strain with repetitions
107	Variation of steel stresses with repetitions
108	Variation of concrete strain with time (sustained load)
109-110	Variation of steel stresses with time (sustained load)
111	Load-slip curves for Unisteel 80 and Kam 90.

LIST OF PLATES

CHAPTER 1

INTRODUCTION

1.1 General

The term "high tensile steel" as used in this investigation denotes reinforcing bars having yield points or 0.2% proof stresses of 414 N/mm^2 (60000 p.s.i.) or higher. Furthermore, high tensile steels must have a considerably higher bond resistance and higher anchorage than ordinary mild steel.

The present time usage of high tensile deformed reinforcing bars in combination with the ultimate load method of design has offered great economy in costs of construction as compared with structures reinforced with mild steel and designed by the conventional elastic method. During the last thirty years the development of high tensile steels with rolled-in deformation in Western Europe, e.g. Sweden and Austria, and in the United States, has saved sizeable amounts of steel and led to considerable economies due to the following factors:-

1) reduction in steel area which accompanies an increase in yield stress
2) reduction in width of section, resulting from reduction in steel area, which in turn also reduces dead weight
3) the amount of shuttering is reduced because of smaller section
4) anchorage hooks are often eliminated and less bending of bars is required
5) placement of concrete is facilitated by eliminating steel congestion
6) reduction in storey height and column sizes for tall buildings. Thus increases floor space and improves appearance, also permits reduction in beam and girder depths where head-room is a consideration.

The reduction in cost, using high tensile reinforcement, may vary widely between various types of structures. The limitations that are imposed on reinforced concrete structures by the performance requirements may prevent the utilization of high steel stress. These limitations are covered by the serviceability requirements:-

i) limited admissible width of crack
ii) adequate flexural rigidity, or limited deflection

Because less steel and smaller sections are made possible by high tensile

steel, the rigidity of the section is reduced and therefore the allowable stresses in steel may have to be determined on the basis of the limit state of either crack width or deflection rather than collapse.

In laboratories, due to the time factor, most of the structural elements are tested under one form of loading, namely, short term static loading. The effects of other types of loading, such as fatigue and sustained loading, are often included in terms of factors which are usually used in design, without any know-how of the actual behaviour of these elements. The unfavourable conditions created by these types of loading may lead to a great reduction in the allowable stresses determined on the basis of a static loading, and thus restrict the use of high tensile steel.

Limited fatigue and sustained loading tests have been carried out on reinforced concrete beams in laboratories and actual structures, and no definite conclusions have been drawn. In practice, the magnitude and incidence of loading, in some cases, are not similar to the loading employed in the laboratory. A structure can be under the effect of sustained or repeated loading or both. The ratio of live load to dead load could be very high, and thus the structure might be subjected to temporary cycles of high live loads and cycles of rest periods.

In practice, a member is under sustained loading when all or part of the imposed load is maintained for long periods of time, or when the self weight constitutes a substantial proportion of the total load. Fatigue loading occurs where there is machine vibration, or under the action of traffic.

Extensive work has been carried out on the performance of reinforced concrete structural members under static loading, and recently in some of these studies high tensile steel is considered as the major variable. Little research has been carried out on reinforced concrete, particularly using high tensile steel, under the action of sustained and/or repeated loading. It has indicated that many changes could occur in the behaviour of the structural members under such loadings. The ultimate strength, strain, cracking and deflection could well be affected, and associated with increased allowable stresses, any one of the limit states could well become a criterion for design. Further research, therefore, is required to determine the properties of concrete members reinforced with high tensile steel, in order to ensure adequate factors of safety against failure and unserviceability under sustained and/or repeated loading.

In view of the above reasons, the author has attempted to study in this thesis the behaviour of reinforced concrete beams with increased allowable steel stresses, i.e. using high tensile steel, under static, sustained and repeated loading. A great emphasis is placed on the serviceability of the beams as indicated by deflection, cracking and flexural strains. The author has tried to combine all the effects to produce a document on the use of high tensile steel as normal reinforcement in reinforced concrete beams. Design rules have been recommended to arrive at adequate load factors against failure and unserviceability.

Allowable stresses are determined in view of two basic requirements, namely ultimate strength and serviceability, as indicated by deflection and cracking. These two requirements must be considered under the action of static, sustained and repeated loading. The task of the engineer, therefore, is to study the behaviour under these forms of loading, which should be adequately assessed from the expected history, and to obtain information for design purposes which will result in a safe and serviceable structure over a long period of time.

1.2 High Tensile Steel

1.2.1 History and Development

The term high tensile steel[1,2,3,4,5,6,7] as distinguished from mild steel can be characterised by three conditions which must be fulfilled. It must have substantially higher strength and higher bond and/or anchorage resistance than mild steel, and the capability of being mass produced under mill condition.

The history and development of high tensile steel date back to the late nineteenth century when in 1898 Considere[8] suggested that "high steel" could with advantage be substituted for "iron or soft steel". The first American specification for "steel reinforcement bars" appeared in 1911 with three grades of bars: structural steel grade, hard grade, and cold twisted, with minimum yield points of 228 N/mm^2, 345 N/mm^2 and 380 N/mm^2 respectively. The first two grades could be either plain or deformed without any specification regarding the deformations.

Then in 1913 A.S.T.M. specifications for "Rail Steel Concrete Reinforcement Bars" were introduced with a minimum yield of 345 N/mm^2 for all types of bars, e.g. plain, deformed or hot twisted.

Although this type of steel has been in use in the United States for more than half a century, theworking stresses permitted were no greater than those for ordinary steel, e.g. 138 N/mm^2.

A great deal of experimental work has been done in the U.S.A., which proved the possibility of using deformed bars, and demonstrated their advantages, i.e. higher allowable stresses, better bond and better control of cracking.

European practice, in particular Austrian, German and Swedish, has benefited by American practice in the development of high tensile reinforcing bars leading to great advances in the structural concrete technology. It has advanced over the American practice, which was only concerned with increasing bond. It has led the rest of the world in using steels of higher strength and improved bond, resulting in more economical designs, provided adequate deflection and cracking control is exercised.

Investigation suggests that Germany[9] was probably the first country to permit the use of higher stresses in steel in 1925. In 1928 Austria introduced the twin twisted bars, known as Isteg steel, with a permissible stress of 167 N/mm^2, and in 1935 Torsteel was introduced with a permissible stress of up to 216 N/mm^2.

In the early 1930s, high tensile steel used as longitudinal reinforcement for columns [8,10] was under fundamental investigation. In the U.S.A. extensive tests on columns reinforced with steel of different grades and yield strengths, and under sustained loading, proved the direct relationship between the column strength and the yield strength of the reinforcement. The A.C.I. Building Code Requirements for Reinforced Concrete permitted the use of allowable compressive stress, in vertical column reinforcement, of 40% of its yield strength (e.g. 207 N/mm^2 for bars of 517 N/mm^2 yield value).

In 1941 the economic advantages of bars with 517 N/mm^2 yield point were well recognised in the U.S.A., and an allowable stress of 50% of the yield point was permitted in tension reinforcement for small diameter bars in short span slabs. However, practical implementation of high tensile steel in design did not begin until late 1950. Billet and Rail steels of high yield points ranging between 414 - 517 N/mm^2 spread in application initially from column reinforcement to beams, slabs and other structural elements. A.S.T.M. Standards were issued for this high quality steel,

which led to a wide spread usage of grades 414 N/mm^2 and 517 N/mm^2. A trend[11] of development towards higher steel qualities and higher permissible stresses is in progress.

For a long time St37 (with a yield of 37 Kg/cm^2) was the only type of steel used in Sweden[12]. The St44 (with a yield of 44 Kg/cm^2) appeared later by a progressive development. Considerable progress has been made in the use of St52 (52 Kg/cm^2) in reinforced concrete constructions. Initially, the Swedish specifications for constructions in reinforced concrete followed the German regulations. However, due to lack of experience in using reinforcing bars of high qualities, the Swedish engineers often used stresses lower than those recommended in the German code. For this reason, the work of the Swedish Committee for standardisation was retarded in its development to such an extent that there existed no official specifications for certain reinforcing steels.

The smooth round St52 reached the dominant position for use as reinforcement in concrete structures in 1940, whereas nowadays it seems to have completely disappeared from the Swedish market. Although St52 steel is treated in a detailed way in the Swedish specifications for reinforced concrete constructions, it is seldom used.

The first type of Swedish deformed bars, Kam Steel, appeared in 1941. This had such an economic success that other types of Kam deformed steels were produced by many Swedish firms.

During the last thirty years high tensile steel[8,9,10,11,12,13,14] with yield strengths ranging from 380 to 830 N/mm^2 has been developed and used. Reinforcing bars may differ significantly in different parts of the world in two aspects: the process of manufacture, the shape and characteristics of the surface deformation.

There are two major methods of producing high tensile reinforcement.[7,9,10] One is by hot rolling and increasing the amount of carbon content aided by small alloy components (by metallurgical means). An example of this type of steel is the Swedish Kam 60 steel. The other method is by cold-working of an ordinary grade of steel (cold twisting or cold stretching, or both) followed by ageing. An example of this is the Austrian Torsteel. The two types of steel, namely hot rolled and cold worked, differ in the following characteristics:

i) Hot rolled steels have sharp yield points with a rate of increase in yield stress the same as that for the ultimate strength. Cold worked steels are usually of gradual yielding type, with an increase in the ratio of yield stress to ultimate stress without affecting the ultimate strength significantly.

ii) Hot rolled (alloy steels) may be of a brittle nature with a lower ductility than the cold worked steel.

In Europe both types of bars are used. Cold worked bars are used in Germany, Austria and Switzerland, while hot rolled bars are produced in Sweden. In the United States hot rolled bars are in common use.

At the present time many types of high tensile steel are used in Britain. The majority are hot-rolled steels with a yield strength of 414 N/mm^2. Very few types of cold worked bars, e.g. square twisted and ribbed bars, are used in this country. The square twisted bars were introduced in Britain before 1914.

The cold worked ribbed bars are Tentor bar, Unisteel 80 and Tor bar. Tentor bars were produced in Britain in 1951, with an allowable stress of 186 N/mm^2. Unisteel 80 and the Tor bars are recent productions, with 0.2% proof stresses of 550 N/mm^2 and 475 N/mm^2 respectively. A new British reinforcement, formed by stranding three high tensile wires, with a yield strength of 690 N/mm^2, has also been recently introduced in the market.

1.2.2 Economics of High Tensile Steel

The economic nature of high tensile steel has been reported since early this century by Gilkey and Ernest[15]. They pointed out the invalid objections to the use of the high elastic limit steel (Rail steel). The economics of using high tensile steel and high quality concrete were discussed at length, and quantitative practical applications were undertaken. Several combinations of allowable concrete and steel stresses were used. It was concluded that the greatest economy, using elastic theory, was obtained by raising the working stresses for both concrete and steel to 11 N/mm^2 and 207 N/mm^2 respectively. Hognestad[11] also discussed the advantages and uses of high tensile steel, and he concluded that "the importance of high strength reinforcement to the economy and competitive position of reinforced concrete rested on basic engineering considerations.

Their importance is affected very little by international differences in trade practices. These differences are over-powered by the basic economy of high tensile steel."

Abeles,[16] based on Hognestad's[11] considerations, gave a comparison of the economics of using high tensile steel in the United Kingdom with other European countries and the United States. He concluded that a great many advantages can result from these high quality materials. Using high tensile steel of 690 N/mm^2 yield stress, a saving of 45%, with ordinary steel taken as a basis, was obtained.

In his paper Granholm[12] attempted to give a quantitative appreciation of the use of high tensile steel. A comparison, using a T-beam, of the prices of different types of reinforcing steel, shows that the high tensile steels are relatively less costly. In other words, one could say that the quotient of the price by the yield point or by the permissible stresses diminishes in proportion as the quality becomes better. The economical background of the development in Sweden of the special types of deformed bars, namely Kam 40 and 60, is discussed on the basis of the prices for concrete and steel in 1958.

Further economy can be achieved by using the ultimate strength design method as well as high tensile steel bars.[7,10,17,18,19,20,21] The replacement of smooth mild steel bars by high strength deformed bars, and designing by the ultimate strength method, will result in over 20% saving in the cost of steel in a structural framework, including the cost of erection and fabrication.[17] The savings in the over-all cost in using mild steel twisted bars were 12% and 15.5% for slabs and beams respectively.[18]

In the main, the above considerations lead to the conclusion that at higher allowable working stresses a safe, serviceable and economical structure is obtained if cracking and deflection can be limited under short and long term loading. It is in the next chapter that reference is made to previous investigators who carried out extensive research programmes, which form the basis of the present knowledge as far as the use of high tensile steel is concerned. Gaps in our knowledge are also pointed out. A schematic programme of investigation is undertaken in this thesis to study the behaviour of beams singly reinforced with high tensile steel, under static, sustained and repeated loading.

1.3 Object and Scope of Project

This thesis outlines the existing knowledge of the actual behaviour of reinforced concrete structures with high quality materials. It is shown that the present recommendations of C.P.114[22] limit the use of higher allowable steel stresses.

The methods of limiting crack widths and deflections in C.P.114 are unrealistic. The limit states method of design in the Draft Unified B.S. Code of Practice[23] gives a more realistic picture of the behaviour of reinforced concrete structures. The aims of the present investigation, are to study the performance of singly reinforced beams reinforced with high tensile steel in the light of the limit states of design, with particular reference to cracking and deflection. Design formulae are derived to predict the steel stress in beams in the uncracked and cracked conditions, the crack width and deflection at various stages of static loading.

The effects of creep and shrinkage of long term loading (sustained and fatigue) on crack widths, deflections, stresses and strains are determined for different grades of steel. Criteria are established for maximum allowable steel stresses for desing purposes and economic considerations.

1.4 Outline of Thesis

Chapter 2 deals with a review of previous investigations, aiming at an historical development of the uses and advantages of high tensile steel. A review of static, fatigue and sustained loading tests carried out by other investigators is presented.

The phenomena of creep and shrinkage and their effects on the behaviour of a reinforced concrete member are discussed.

In Chapter 3 it is pointed out that a structural member should comply with the limit states for determining its performance under load. There are four general performance requirements that should be satisfied for every structure: (i) safety against collapse (ii) limited cracking (iii) limited deflection (iv) durability.

The present code of practice, CP114[22], limits the possibility of using high quality materials by limiting the allow able steel and concrete stresses to much lower values than those which could occur

in serviceable structures. In CP114 the limit states of cracking and deflection are not directly considered. It is shown that the aspects of collapse and serviceability are better understood and controlled in a more rational way in the new Draft Code.[23] Recommendations of several other codes are also given, in particular those based on the concept of safety and serviceability.

Chapter 4 presents the factors that influence the three limit states of cracking, deflection and collapse under static bending. The theories and mechanisms of these limit states are also discussed. The major parameters that influence cracking, deflection and strength of reinforced concrete members are pointed out.

Chapters 5, 6 and 7 cover the programme of investigation, design and manufacture of test specimens, and instrumentation and test procedure.

In Chapter 8 procedures for the calculation of steel stresses from experimental results obtained for the static, fatigue and sustained loadings are explained. For the theoretical calculation of stresses under static loading a semi-empirical procedure has been developed. It has been shown that for both the cases the procedures depend on the determination of the position of the neutral axis in the cracked and uncracked conditions of the section. A transition zone between the cracked and uncracked conditions is established empirically.

In Chapter 9 the behaviour of the beams under static loading is discussed in terms of the strains and remaining strains, cracking and remaining cracking, and deflection and remaining deflection. A relationship between crack widths and stresses in steel is established and semi-empirical formulae for the prediction of crack width and deflection on the first and second cycles are proposed. A formula for the evaluation of span/depth ratio is given. The ultimate strength of beams is discussed and compared to those estimated according to the Draft Code. The effect of high tensile steel on the behaviour of reinforced concrete beams is studied.

The effects of sustained and repeated loading on the behaviour (cracking, deflection, ultimate strength, stresses and strains) of reinforced concrete beams are included in Chapter 10. A comparison between sustained and repeated loading is made in the same chapter, as regards the three limit states.

Chapter 11 contains the conclusions drawn from this investigation along with recommendations for the design of reinforced concrete members.

Points for future research are suggested in Chapter 12.

A list of references, tables, figures, plates and appendices are included at the back of the thesis.

CHAPTER 2

Summary of Previous Investigation

2.1 General

It has been indicated in the previous chapter that greater economy can be achieved by using high tensile steel as normal reinforcement with high allowable working stresses. By doing so not only will the section of steel be reduced but also the cross sectional area of the concrete. A greater reduction can also be achieved through the use of ultimate load design. A great amount of saving in materials and construction can be achieved if complete utilisation of the steel strength is attempted on the basis of safety against collapse alone. However, a structure must be designed on the basis of two requirements: safety against collapse and unserviceability. The allowable stresses could well be reduced to satisfy serviceability requirements, and thus restrict the use of high tensile steel in reinforced concrete structures. It is well known that serviceability is affected by long term loading. There is not at present a great deal of knowledge of this type of loading and its effect on serviceability, due to the limited number of tests and surveys carried out in this field.

Many research workers have tried to correlate the increase in the allowable stresses with the increase in crack widths as a criterion of design. However, very little has been published about the effect of using high tensile steel on deflection, and the effect of long term loadings (sustained and fatigue) on cracking and deflection.

In the following paragraphs a summary is presented of the work carried out by various investigators to ascertain the existing knowledge of the performance (strength, cracking and deflection) of reinforced concrete beams under static, sustained and fatigue loadings.

2.2 Review of Previous Research

2.2.1 Static Loading Tests

The idea of using high tensile steel as a means of economy in reinforced concrete structures has been suggested as early as the late nineteenth century. Gilkey and Ernest[15] reported, in 1935, that high elastic limit steel is suitable as reinforcement for concrete within the range of current working stresses if handled, fabricated and placed with

reasonable care. Though considerable economy results from the use of this type of steel with high working stresses, it was suggested that several precautions as regards anchorage, safety against diagonal tension failures and corrosion attacks, due to severe exposure and cracking, must be taken into consideration.

Hajnal Konyi conducted several series of tests on beams with different types of high tensile steel and under different types of loading. In 1943,[24] in his first series of tests, he tested beams reinforced with square twisted steel bars with a proof stress of up to about 480 N/mm^2 with 12.7 mm maximum bar size, and varying in number of twists per foot length and different steel percentages. Beams with mild steel of about 275 N/mm^2 yield point were also tested and compared with those with high tensile steel. He concluded that the full ultimate strength of square twisted steel could possibly be utilised, because at ultimate loads of the beams the yield points were greatly exceeded. Due to the superiority of bond of square twisted bars, the encased steel showed greater ultimate strength than the ultimate strength of the steel in the air. The ultimate strength of all beams agreed very well with thos predicted by Whitney's theory.

A crack width limit of 0.25 mm was reached at a steel stress not less than 275 N/mm^2 at first loading, irrespective of steel percentage. It was suggested that deflection should be controlled by limiting the span-deflection-depth ratios regardless of the type of reinforcement and allowable stresses.

In his second series of tests in 1951,[25] Hajnal Konyi carried out comparative tests on thirty-six beams, ranging from mild steel of 275 N/mm^2 yield point to 590 N/mm^2 proof stress Danish "Tentor" steel, both in ordinary and high grade concrete. Also two beams[26] reinforced with 2.65 mm plain wires of 1860 N/mm^2 tensile strength were tested. The tests have shown the superiority of deformed bars as against plain bars on the basis of bond and crack formation. Based on a permissible crack width of 0.25 mm, the stress in the steel in the majority of beams with cold worked steel was, as found before, between 275 N/mm^2 and 345 N/mm^2, and that in the beams with high strength wires it was 520 N/mm^2 to 576 N/mm^2. Considering warning before failure, cold worked bars were superior to bars having a definite yield point, due to the better bond characteristics and higher yield strength. As far as load bearing capacity was concerned it wasshown that Whitney's theory[27] was applicable to steel of any strength,

reasonable care. Though considerable economy results from the use of this type of steel with high working stresses, it was suggested that several precautions as regards anchorage, safety against diagonal tension failures and corrosion attacks, due to severe exposure and cracking, must be taken into consideration.

Hajnal Konyi conducted several series of tests on beams with different types of high tensile steel and under different types of loading. In 1943,[24] in his first series of tests, he tested beams reinforced with square twisted steel bars with a proof stress of up to about 480 N/mm^2 with 12.7 mm maximum bar size, and varying in number of twists per foot length and different steel percentages. Beams with mild steel of about 275 N/mm^2 yield point were also tested and compared with those with high tensile steel. He concluded that the full ultimate strength of square twisted steel could possibly be utilised, because at ultimate loads of the beams the yield points were greatly exceeded. Due to the superiority of bond of square twisted bars, the encased steel showed greater ultimate strength than the ultimate strength of the steel in the air. The ultimate strength of all beams agreed very well with thos predicted by Whitney's theory.

A crack width limit of 0.25 mm was reached at a steel stress not less than 275 N/mm^2 at first loading, irrespective of steel percentage. It was suggested that deflection should be controlled by limiting the span-deflection-depth ratios regardless of the type of reinforcement and allowable stresses.

In his second series of tests in 1951,[25] Hajnal Konyi carried out comparative tests on thirty-six beams, ranging from mild steel of 275 N/mm^2 yield point to 590 N/mm^2 proof stress Danish "Tentor" steel, both in ordinary and high grade concrete. Also two beams[26] reinforced with 2.65 mm plain wires of 1860 N/mm^2 tensile strength were tested. The tests have shown the superiority of deformed bars as against plain bars on the basis of bond and crack formation. Based on a permissible crack width of 0.25 mm, the stress in the steel in the majority of beams with cold worked steel was, as found before, between 275 N/mm^2 and 345 N/mm^2, and that in the beams with high strength wires it was 520 N/mm^2 to 576 N/mm^2. Considering warning before failure, cold worked bars were superior to bars having a definite yield point, due to the better bond characteristics and higher yield strength. As far as load bearing capacity was concerned it wasshown that Whitney's theory[27] was applicable to steel of any strength,

and that at least 85% of their ultimate strength was utilised, which would enhance the factor of safety.[28] However, the moment of resistance for balanced design was shown to decrease with increasing steel strength.

In this series of tests the effect of using high tensile steel on deflection as a limit state of serviceability was not considered. It was suggested[29] that the allowable stresses in the tensile reinforcement would be limited not only by the admissible width of cracks, but also by the deformation of the structure.

In a third series of tests Hajnal Konyi[30] tested twenty-eight singly and doubly reinforced rectangular beams as well as T-beams. The beams that failed due to the yielding of the reinforcement were designed on the basis of economic percentage for mild steel, using a permissible tensile stress of 124 N/mm^2. The reinforcement used in the tests were mild steel and Tentor bars with yield stresses of 275 N/mm^2 and 517 N/mm^2 respectively.

He concluded that "Tentor" steel may safely be substituted for mild steel in the inverse ratio of the permissible stresses up to the "economic" percentage for mild steel. The calculation of the ultimate bending moment of beams reinforced with Tentor steel may be based on the ultimate strength of the steel, if the percentage does not exceed the "economic" percentage for mild steel. There was a slight decrease in the moment of resistance in over-reinforced beams, as compared with beams reinforced with mild steel.

Evans[31] in 1937 tested two pairs of rectangular and two pairs of T-beams. One of each pair was reinforced with cold worked steel bars (two mild steel bars twisted together helically) with a yield point of 393 N/mm^2, and one with carbon steel bars with a yield point of 399 N/mm^2. These tests were conducted to study the effect of steel properties, e.g. modulus of elasticity, on the deflection and steel strains. It was concluded that for equal stresses in the tension reinforcement the deflection and steel strains in concrete beams reinforced with cold worked or overstrained twisted steel bars were greater than those in beams reinforced with high tensile or carbon steel bars of the same diameter, but having higher modulus of elasticity. The steel stresses are independent of the modulus of elasticity of the reinforcement.

Evans and Williams[32] tested 102 mm x 152 mm x 1680 mm long beams reinforced with 7.9 mm Square Grip steel with 488 N/mm^2 yield stress. It was found that the steel stress, at which a crack width of 0.25 mm was produced, was 517 N/mm^2. At a stress of 259 N/mm^2 the average and maximum crack widths were 0.053 mm and 0.064 mm respectively. It was concluded that a working stress of 241 N/mm^2 would provide an adequate factor of safety against dangerous cracking and bond failure even under sustained loading.

Lewis[33,34] carried out two series of tests, primarily to investigate the behaviour of typical beams and slabs with regard to cracking, deflection and factor of safety against flexural failure. A comparison was made between beams and slabs reinforced with Tentor bars of 490 N/mm^2 yield stress and those with mild steel of 275 N/mm^2 yield stress, with steel percentages inversely proportioned to the working stresses (124 and 228 N/mm^2). It was found that the distribution of cracks was slightly better in beams and slabs with deformed bars. In the beams the crack widths were considerably greater (2 - $2\frac{1}{2}$ times) for Tentor bars than for the mild steel bars at equal proportions of their working stresses. At the working stress the crack width was well below the critical value (0.2 mm) which was reached at a stress of 330 N/mm^2, and that the deflection was approximately 1.8 times greater in Tentor reinforced beams.

The warning of failure given by Tentor reinforced beams was excellent; they showed very large deflections near failure. It was suggested that high working stresses could be used for Tentor bars in slabs, and that more stringent limitations on the span-depth ratio at working load conditions would seem necessary. It was also suggested that Tentor bars can be used without hooks.

Hognestad has been engaged in the investigation on the use of high tensile steel as concrete reinforcement. He conducted a comprehensive study on full scale and model structural members.

In 1962[35] Gaston and Hognestad tested a full scale roof girder, which was of slender cross-section and had inclined stirrups, reinforced with high strength alloy steel bars of 577 N/mm^2 yield point. It was shown that a maximum crack width of 0.23 mm was reached at a steel stress of 275 N/mm^2, and the deflection at working load can be estimated from the static theory based on fully cracked section. It was concluded that deformed bars with 517 N/mm^2 yield points can be used successfully.

In 1962 Hognestad[36] reported on the control of cracking using old type deformed bars, plain bars and modern American deformed bars. He tested thirty-six beams with different bar diameters, beam widths, depths and thicknesses of concrete cover. It was shown that cracking occurred at a steel stress of 69 - 124 N/mm^2, all principal cracks had formed at a steel stress of 207 N/mm^2, and that crack widths were essentially proportional to the steel stress and the amount of concrete cover, and that, for deformed bars, the crack widths were less than half those for plain bars. Crack spacings and crack widths with variations of up to $\pm$ 50% from average values were entirely normal.

Wastlund in 1959[37] recognised three essential engineering requirements which a reinforced concrete structure had to fulfil. These are the adequate safety against failure, limited crack formation and limited deflection. He discussed these requirements and concluded that the limitations imposed on crack widths would limit the use of the maximum allowable stress, and when using high strength steel, the deflections were also regarded as a decisive factor, especially in view of the effect of sustained loading.

Mathey and Watstein in 1960[38] tested twelve rectangular beams to study the effect of the extent of stress and the stress-strain characteristics of the reinforcement on the resisting moment, crack widths, strain in the concrete and steel, deflection, load carrying capacity and manner of failure of beams.

The beams were reinforced with six different types of steel bars with yield strengths ranging from 294 - 720 N/mm^2. The ratio of reinforcement was inversely proportional to the yield strengths.

It was found that the load carrying capacity of the beams was not appreciably affected by the tensile properties of the longitudinal reinforcement, and that deflection, concrete strain and crack widths were greater, at a given load, in beams with lower ratios of reinforcement and corresponding higher allowable steel stresses. A comparison was made between the calculated and observed deflections, strains and stresses.

Guralnick[13,39] tested forty-two T-beams reinforced with high tensile deformed bars with yield strengths varying between 574 and 700 N/mm^2. It was found that the average enhancement in the calculated ultimate moment was 24%, as against 5 - 20% found by Wastlund.[37] The measured deflections at service load agreed with the calculated values based on

a fully cracked transformed section, the average crack width at a steel stress of 207 N/mm^2 ranged between 0.076 mm to 0.127 mm, and the average of two maximum crack widths ranged from 0.25 mm to 0.5 mm, the maximum value being at a steel stress of 345 N/mm^2.

Abeles[40] in 1952 analysed the results of his tests and those of several other investigators using high strength steel. He had shown that the high strength properties of steel and concrete can be fully utilised in reinforced concrete, provided that efficient bond is ensured. The resistance moments of beams reinforced with very low percentages of steel were higher than the theoretical moments, and sometimes the steel stresses at failure exceeded the ultimate strength of the bars.

As far as cracking was concerned high strength steel could be used provided bars of small size or of increased bond were used. Even plain high tensile wires might be used. However, it did not seem advisable to use plain high strength wires, in view of the great deflection of such members.

Abeles and Gill[16] in 1969 tested seven rectangular beams and two T-beams reinforced with three wire strand, having a guaranteed 0.2% proof stress of 690 N/mm^2 and a working stress of 345 N/mm^2.

They showed that this three-wire strand had excellent bond characteristics, which would ensure good crack distribution. A stress greatly in excess of the proof stress was reported for beams with low percentage reinforcement. Factors of safety in excess of 1.8 have been obtained, and an increase in permissible stress to 414 N/mm^2 seemed feasible. With a permissible stress of 345 N/mm^2 the maximum crack width in the rectangular beams for the second cycle of loading was within the limit of the C.E.B. recommendation:[41] between .10 and .20 mm.

The Building Research Station[42,43,44] and the C. and C.A.[45] have tested beams reinforced with high strength bars to assess the performance of these deformed bars in comparison with mild steel bars. The tests included fourteen different types of high strength bar, as well as mild steel, with yield stresses of 414 N/mm^2, 550 N/mm^2 and 690 N/mm^2. It was found that the variations in deflection and cracking did not appear to be significantly affected by the degree of surface deformation of the bar. The plain round bar, with a yield stress of 410 N/mm^2, was found to give a performance equal to the mean of all the deformed bars with this

yield stress. The cracking and deflection were controlled by the level of stress in the reinforcement. The magnitude of the allowable stress in high strength steel is determined by the limit state of deflection rather than cracking.[44]

Clark[46,47] tested beams reinforced with deformed high tensile steel with yield strengths ranging between 414 and 966 N/mm^2. It was concluded that cracking and deflection would probably limit the use of high tensile steel to 552 N/mm^2. Due to the stress-strain characteristics of the type of steel at high stress and a corresponding high elastic strain, the ultimate moments of resistance for balanced design seem likely to decrease with increasing steel strength, while a better agreement is reached for under-reinforced beams with steel having an indefinite yield point, and a modest ultimate strain, if the ultimate strength of the steel is substituted for the proof stress in the analysis.[47]

Some full scale structures have been under investigation to determine the effect of using high strength steel on their behaviour in service.

Holmberg in 1951[48] reported the design and construction of two full scale reinforced concrete highway bridges in Sweden, which were reinforced with high strength plain steel bars with end anchorage rings, having a yield point of 690 N/mm^2 with a maximum allowable stress of 294 N/mm^2, based on elastic theory, with a modular ratio of 15. This design resulted in reduced dimensions and economical design.

In 1959 Granholm[10,11,12,14] in Sweden used Kam 60 steel with a yield stress of 600 N/mm^2 in practice at allowable stresses of 324 N/mm^2. He reported great savings in the amount of steel. Another type of Kam steel has been used in laboratory tests. This has a yield stress of about 900 N/mm^2 and a working stress of 483 N/mm^2.[49] It was suggested that such a steel should be used for internal members.

In 1963,[50] it was reported that a saving in steel and concrete costs resulted from using high strength steel in a two lane, four span continuous girder bridge. This was the first concrete bridge reinforced with high strength steel bars (ASTM A432). A saving of 30% in steel costs alone was obtained.

Hognestad[51] reported on the use of high strength steel with a yield stress of 483 N/mm^2 in the construction of the girders of the Structural Laboratory and the Fire Research Laboratory. He reported

the satisfactory performance of the girders in service.

Antoni and Corbisiero[52] in 1968 reported on simple and continuous concrete bridges reinforced with deformed high strength steel of 435 N/mm^2 yield point, to describe their live load and long term dead load performance for the first eighteen months of service. It was concluded that both bridges were performing satisfactorily. Measurements during the test programme indicated that crack widths and depths might be approaching or had already reached maximum recommended values. The assumption of fully cracked section to check stresses and deflections proved to be too conservative. The long term dead load deflections were successfully estimated using the Yu and Winter method. After four and a half years another check was made on both bridges.[53] This showed that cracking of the continuous span deck was increasing, but the damage was not structurally significant.

2.2.2 Repeated Loading Tests

The earliest work on fatigue of reinforced concrete beams was reported by Van Ornum[54] in 1907. He discussed the elasticity, strength and bond of reinforced concrete under repeated loading and established a fatigue limit of 50% of the static ultimate load. From that time investigators became interested in the behaviour of reinforced concrete structures undergoing such a state of loading.

Berry[55] in his tests in 1908 on reinforced concrete beams with plain and deformed bars of varying percentages loaded to high working stresses pointed out that there was no significant effect on the ultimate strengths and deflections after one million repetitions of stress. The elastic deflection of any beam for a definite load remained nearly constant, but there was an increase in permanent set, the greatest part being on the first application and release of the load. The maximum deflection did not seem to be affected. Progressive cracking with repetitions was noticed, but the change in length of cracks was small. Hair line cracks became visible on the first few cycles of working load, and some cracks appeared after a great number of repetitions of loading.

The bond between the steel and concrete was not affected by repetitions of loading, and the position of the neutral axis was not changed either.[55]

Berry[55] also observed that the tensile strain in the plane of the reinforcement showed a rapid increase in the permanent set for the first

few applications of the load, and . became constant after the first few thousand cycles in some cases. While the strain in the compression sidewas similar to that in the case of deflection, the set increased rapidly for the earlier loading and increased directly with the stress and the number of repetitions.

Probst[56] reported that in reinforced concrete beams cracks do not appear under repeated loading so long as the maximum load of the repeated loading range does not exceed half of the static cracking load. When the loading range is within the limiting range, cracking and permanent deformation increase with increasing number of repetitions until stability is reached. At this stage thelength and size of cracks are also stabilized and the deformation is almost elastic. The permanent deformation and cracking are less significant in the aged concrete, and a condition of stability is reached after fewer repetitions than for younger concrete. No effect of the age or repetitions on the load carrying capacity of the beam was observed.

It would seem essential, therefore, to take account of the effects of repeated loading on the crack formation and stiffness of reinforced concrete beams. A fatigue limit is also of great importance and should be established to assess the required load factor against failure of this type.

Hajnal Konyi[57,58] found that although under static design loading the crack widths in a beam reinforced with mild steel and another with Tentor deformed bars may be similar the increase in the maximum crack width under repeated loading was much greater for the former than for the latter. Stabilisation of the maximum crack widths was reached after about two million cycles.

Saliger[59,60] reported fatigue tests on beams reinforced with four types of reinforcement, including mild steel, cold worked (Isteg) and high tensile steels, with ultimate strengths ranging between 428 N/mm^2 to 835 N/mm^2 and yield points ranging from 284 N/mm^2 to 432 N/mm^2.

The beams were subjected to one to three million cycles at a rate of 160 to 170 cycles per minute. The maximum stresses in the steel were about 55% of the ultimate strength. He concluded that at failure the cracking, deformation, position of the neutral axis, stress distribution, bond and ultimate load capacity appeared to be uraffected by previous repetitions.

Repeated stresses within the permissible limits have little effect on subsequent deformation at higher loads. Saliger also concluded that adequate safety against fatigue failure could be obtained by limiting the permissible stresses in steel and concrete to one half the yield point and one third the cube strength respectively.

Most failures of reinforced concrete beams were due to failure of the reinforcing steel. The effect of repeated loading on the ultimate carrying capacity of beams should be studied in two aspects: a) the load at which the beam fails reaching its fatigue strength while under repeated loading, and b) the effect of the history of previous repeated loading on the ultimate static strength. The former has been found to be much less than the static ultimate load, and depends on the range of stress and the number of cycles to which it is subjected. It is believed that beams critical in their reinforcement have an endurance limit of 60 - 70% of the static ultimate strength for one million cycles.[56,59,61,62] An endurance limit for ten million cycles of 43% and 70% have been reported by Chang and Kesler[63] and Lea[64] respectively. Repeated loads as low as 40% and 50% of the ultimate strength have been reported in tests in which beams have failed in shear[61] and bond.[64] It was found that beams subjected to repeated stresses below the critical stress were not materially affected in their ultimate static loads.[56,59,60,63]

An increase in static ultimate strength for under-reinforced beams subjected to previous fatigue loading of minimum of 100,000 repetitions was obtained by Verna and Stelson[65].

Verna and Stelson[66] concluded from repeated loading tests on reinforced concrete beams that the dynamic failure mode is dependent on the load level as well as the static failure mode. Beams failed statically by bond always failed by bond when subjected to repeated loading. This opinion was also shared by Chang and Kesler,[63] who concluded that for beams designed to fail in flexural tension under static load, a low magnitude of repeated load generally resulted in a flexural failure by fatigue of steel, while a high magnitude resulted in a shear failure.

Bate[67] reported on the effect of cold working on the fatigue strength of steel bars, and showed from results of Graf that the fatigue strength of plain bars is increased relatively by small amounts of cold working, but is reduced by larger amounts of cold working. From

test results given by Le Camus, Bate[67] showed that beams reinforced with mild steel, when subjected to fatigue loading, failed at higher proportions of their static ultimate loads than those with high tensile or cold worked steel.

It was suggested[67] that the load factor against fatigue failure is unlikely to be less than two for beams with normal amounts of mild steel, and may be greater for beams with larger or smaller amounts of mild steel, depending on the mode of failure. For beams with medium tensile or cold worked mild steel the load factor is likely to be between 1.3 and 2, depending on the ratio of dead load to live load. From tests carried out by Bate[68] the load factors against failure under one million repetitions of loading for beams reinforced with plain mild steel bars, and others with cold worked deformed mild steel bars were 2.2 and 1.6 respectively. The former beams failed by yield of steel, while the latter failed by fatigue fracture of the bars. The increase in deflection and crack width due to fatigue loading is shown by Bate[68] to increase only slightly, and the maximum crack width is not likely to be 0.25 mm with a little risk of corrosion.[67]

Bate[67] pointed out that the type and percentage of steel affected the strength and mode of failure of reinforced concrete beams under loading. Beams reinforced with mild steel of normal proportion, which generally fail statically as a result of yield of steel, leading to crushing of concrete, fail in the same manner when subjected to repeated loading, but the upper limit of the loading range is likely to be much less than the ultimate strength under static loading. Fatigue failure of the steel is unlikely, and the fatigue strength of the beam may not be influenced very much by the value of the minimum load in the range. If beams contain a small percentage of mild steel, fatigue fracture of the steel may occur, whereas sufficiently high percentage may result in fatigue of concrete.

Beams reinforced with a normal proportion of medium tensile steel or cold worked mild steel reinforcement fail statically in a fashion similar to those containing mild steel. Under repeated loading, however, these steels may fail in fatigue, with a maximum steel stress appreciably less than its yield value. The minimum value of the stress has an important influence on the maximum value in the critical range.[67]

In recent years, due to the development of high tensile steel,

some investigators followed the steps of Bate in investigating the effect of repeated loading on the ultimate strength and serviceability of beams reinforced with high tensile steel.

Hognestad[69] carried out an extensive programme of fatigue loading tests on 181 beams reinforced with three grades of steel. The number of repetitions of load were two million. Steel of different deformation patterns, all conforming to ASTM Designation A305, were used. It was concluded that for the same deformation pattern the stress range at a fatigue limit taken at two million cycles of load repetition is relatively insensitive to the magnitude of the minimum stress and to bar yield strength. The form of bar deformation has a great influence on the fatigue strength, depending primarily on the local geometry where transverse lugs meet the longitudinal ribs, and according to Kobrill and Sverchkor[70] the radii of curvature where the transverse rib joins the body of the bar, and also its inclination to the axis of the bar.[43] Similar observations have been reported by Kokubu et al.[71] It was shown by Hognestad, that for one pattern of deformation, the stress range and the fatigue limit may be 35% less than for another pattern of deformation. At a maximum stress below yield the stress range is the determining factor in design, and not the minimum or the maximum values, since the effect of minimum stress level is minor. These findings agreed well with those of Rehm[69] and disagreed with those of Blackwell[72] and Lash et al,[73] who stated that for a minimum stress of almost one quarter yield strength the stress range at two million cycles was higher for higher grade steel, provided the bars had the same deformation pattern.

Soretz[74] reported tests on fatigue strength of ribbed bars (Tor steel reinforcement) in rectangular and T-beams. The effect of repeated loading on the concrete, steel and bond, and the effect of unlimited repetition of stress on the cracking and deformation of the structural member were reported.

For the rectangular beams the maximum crack width after two million cycles between steel stresses of 30 and 330 N/mm^2 increased by 50% to a limited value of 0.25 mm. The residual crack width at the lower load limit around zero was about 0.13 mm. These results were obtained for concrete strengths of 16 and 60 N/mm^2. There was a large scatter in deflection due to crack formation. After two million cycles of stresses between 40 N/mm^2 and 330 N/mm^2, the residual deflection at the lower stress limit became one half of the total deflection under the

upper stress limit, and an average increase of 70% was reported.

Nakayama[71] reported an increase in crack width in beams with deformed bars of 0 - 20% after 10^5 cycles for a stress range of 560 - 2200 Kg/cm^2. For beams with a single reinforcing plain bar, the crack width was 1.5 times that in a beam with a single deformed bar, and increased to 1.8 as the number of repetitions increased. The elastic deflection increased by 5 - 20% after 100,000 cycles, and remained constant thereafter.

Russel and Webber[75] found that the deflection at working stress in beams reinforced with deformed bars increased by 60%, and the crack width by 15% after two million cycles of stress between about 86 - 173 N/mm^2.

2.2.3 Sustained Loading Tests

The effect of sustained loading or stress on the strength and serviceability of concrete structures must be studied with respect to creep in concrete. Creep is a phenomenon whereby concrete exhibits time-dependent stress-strain characteristics induced by an applied sustained stress. Concrete also exhibits a change in strain when subjected to drying without the application of external applied stress. This phenomenon is known as shrinkage. These two phenomena take place when the reinforced concrete members are subjected to long term loading.

It is well known that the creep behaviour of the extreme fibres of a beam under compressive or tensile stresses is much the same as in plain concrete. Many research workers have suggested methods of predicting creep in reinforced concrete beams, making use of the creep magnitude and characteristics of plain concrete. The inter-relation between the creep behaviour of both types of constructions is apparent and the existing quantitative knowledge of the creep of plain concrete can be used to analyse the creep behaviour of reinforced concrete structures. This procedure will be dealt with later in this chapter, after a brief historical review of the effects of creep and shrinkage on the strength and behaviour of reinforced concrete beams as reported from tests by other investigators.

Sustained stresses can be induced in a member either by sustained loads or from restrained deformation. The effect of sustained load on a statically determinate reinforced concrete structure is an increase of

deflection, at a decreasing rate, with time. The compressive strains in the concrete increase more rapidly with time than deflection. The reason for this behaviour is that, as the compressive strain increases, the neutral axis drops due to the tensile stresses not increasing in proportion. As a result there will be a relatively smaller rotation per unit length or deflection. A redistribution of stresses was noticed in the concrete compressive zone which led to a decrease in the lever arm of the internal stress and thus an increase in tensile steel stress.

Glanville and Thomas[76] reported this phenomenon, assuming the creep in compression and tension to be equal, by showing that the stress in the steel increased with time, and it was accompanied by a lowering of the neutral axis. As a result a lower rate of creep is obtained, because the concrete stress is reduced. They concluded that the steel stresses increased by 50%, the compressive strains increased by 3 - 4 times and the deflection by $2\frac{1}{2}$ times. The concrete stress was found to be 40% less than the initial value on loading.

Washa[77] in 1947 conducted tests on reinforced concrete slabs reinforced with intermediate grade steel, with an average yield point of 340 N/mm^2. It was concluded that after five years of sustained loading each slab exhibited a large number of tensile cracks, the ratio of final to initial deflection averaged about 3, the final deflection being 34% due to initial loading, 20% due to warping and 46% due to creep, the strain in the plane of the steel remained about the same, the top compressive strain increased at a faster rate than the deflection and attained a value about six times the strain at seven days, which again shows the effect of the lowering of the neutral axis due to creep. Of the total deflections 82% were obtained in the first half-year.

Inclusion of arbitrary amounts of compressive reinforcement resulted in a decrease in the plastic deflection and compressive strains.[78,79,80]

Washa and Fluck[80] reported the results of $2\frac{1}{2}$ years of sustained loading on thirty-four reinforced concrete beams reinforced with different sizes of deformed bars, with yield strengths ranging from 324 to 387 N/mm^2, with tensile reinforcement alone, and with different amounts of compressive reinforcement, and loaded at a 70 - 85°F temperature and 20 - 80% R.H. The plastic deflections were reduced to one half and one third, and the compressive strain by 60% and 40% by inclusion of compressive reinforcement equal in amount and half the

amount of the tensile steel respectively. The plastic deflection for beams with no compression reinforcement, and those with full compression reinforcement, were double and slightly greater than the immediate elastic deflection respectively, while for the compressive strains the ratios were $4\frac{1}{4}$ and $2\frac{1}{3}$ respectively. The plastic tensile strain was small, but the increase in the steel stress ranged from 18.6 N/mm^2, for beams without compressive reinforcement, to 49.7 N/mm^2 for beams with full compressive reinforcement.

The plastic deflections were found to increase with increasing span-depth ratio.[77,78,80]

After a sustained loading of up to $10\frac{1}{2}$ years, the ultimate strength was found to decrease by amounts of 5 to 10%, while the modulus of elasticity of concrete increased by up to 20%.[81,82,83] Washa and Fluck [84] reported that beams, which had been under sustained design load for three years and later loaded to 85% of the ultimate strength for nine months, and to 90% and 95% to the tenth and eleventh months, showed no significant changes in ultimate strengths. Similar observations have been reported by other investigators.[76,85]

Soretz[57] in 1957 reported test results on the effect of sustained loading on the cracking of concrete floor slabs reinforced with Tor 60 steel at a permissible stress of 330 Kg/mm^2. Initially, there was a rapid increase in crack widths and number, and then equilibrium of crack formation was reached, after a period of two months, in the case of beams loaded under their working load, and after five months in the case of beams loaded near failure. The crack width increased by 50% to a value of 0.225 mm, and the stiffness was found to increase.

Soretz[86,87] in 1961 reported observations, made on the crack formation and deformation, of two bridges of cellular cross section, under the same condition of service loading, reinforced with Tor 60 and Tor 40 respectively, and a foot bridge with Tor 60. In the twin bridges, at permissible stresses of 2400 kg/cm^2 and 3500 kg/cm^2 respectively, the cracks developed perpendicular to the axis of the bridge, and increased rapidly in number in the first months, and attained 90% of the final value after the first year, reaching stabilisation after three years. In the foot bridge, at a permissible stress of 3000 kg/cm^2, the beams behaved in a fashion similar to the twin bridges, but about 95% of the total number of cracks was attained after two years.

The lengths and widths of cracks and the deformation also increased rapidly during the first months, and then stabilised after three years. At the final state, the maximum crack width in the twin bridges was lower than 0.2 mm for the two types of steel used, whereas in the foot bridge the maximum crack width at the level of reinforcement was 0.28 mm with a mean of 0.14 mm, and at the middle height was 0.45 mm. In comparing the two twin bridges, despite the difference in permissible stresses of 50% between Tor 60 and Tor 40, the final values of the number of cracks were the same, and the crack widths were only 10% higher. The deformation due to creep and shrinkage and repeated overloading was only 20% higher for the bridge reinforced with Tor 60 than that with Tor 40.

Hajnal Konyi[1,88] tested beams with span-depth ratios of 20, 30 and 40, reinforced with mild steel and Tentor steel with permissible stresses of 138 N/mm^2 and 235 N/mm^2 respectively, and designed to carry the same ultimate moment. After $4\frac{3}{4}$ years of sustained loading, the deflection increased to 3.14 - 3.94 times the original deflection, and the average ratio of the maximum deflections of beams with Tentor steel to thos with mild steel was only 1.14, despite the fact that the ratio of area of mild steel to tentor steel was 1.7. The beams became unserviceable, implying that the recommended slenderness ratios in CP 114 (1957) are excessive if a substantial proportion of the design superimposed load is to be supported for a long period of time. The depth of the neutral axis was reported to have increased considerably.

A comparison of measured deflections with computed ones showed that the simplified C.E.B. method,[41] which takes account of concrete tensile stresses before cracking was in good agreement with the measured instantaneous deflections. Good agreement was also found using the Yu and Winter method[78] which included a "reduced modulus" for the prediction of long time deflection.

For design purposes it was suggested by Hajnal Konyi[1] that the tensile reinforcement index and the permissible stresses would have to be restricted as a function of the slenderness ratio of members subjected to bending. This is so because of three factors:

a) The ratio of the final to instantaneous deflection
b) The ratio of superimposed load to dead load
c) The initial position of the neutral axis as related to the tensile reinforcement index.

Corely and Sozen[89] in 1966 found from tests on beams under two years of sustained loading at 70°F and 50% R.H., and with permissible stresses of 138 and 207 N/mm^2, that the creep strain and deflection were 3 and 2½ times the instantaneous strain and deflection respectively, there was no escalation in deflection due to the use of higher permissible steel stresses, the length and number of cracks increased with the first 60 days and in later stages the upper portions of the cracks closed as the neutral axis moved to a position below the tops of some cracks.

Lutz et al[90] found that after five months of sustained loading at steel stresses of 207 N/mm^2, the ratios of the final deflection and compressive strains to the corresponding instantaneous values were 2.15 and 3.32 for a singly reinforced beam, and 1.62 and 2.09 for a doubly reinforced beam with equal amounts of compression and tensile steel. The average increase in the maximum crack width for a singly reinforced beam was about 40%, and was about 5% greater than that of doubly reinforced beams.

Evans and Paterson[91] reported sustained loading tests, over a period of 750 days, on lightweight aggregate Lytag and gravel concrete beams, reinforced with high bond bars. The instantaneous deflections at design load were greater for Lytag concrete beams than for gravel concrete beams, while the ratio of the final deflection to the instantaneous deflection was smaller, averaging 2.16 and 2.71 respectively. The crack widths at design load were greater, and in both cases did not exceed those regarded as permissible for conventional gravel concrete beams.[92]

2.2.4 Prediction of Creep

It is convenient to express the creep-time relation in a form of an equation, so that values of creep may be predicted without performing long-term tests.

Creep deformation, by definition, is a function of stress and time. Several expressions, e.g. hyperbolic, exponential, or logarithmic, have been suggested by many investigators.[93,94] The equations of Lorman and Ross[93] give satisfactory results. They are extremely easy to apply and have the advantage of quickly predicting the ultimate creep.

As suggested by Thomas,[95] the final creep does not exceed 4/3 of the creep after one year for specimens loaded at 28 days. This ratio

increases as the age of loading increases. Troxell et all[96] found that the average increase in creep, using a period of one year as a basis, is between 14% in two years to 36% in thirty years. Therefore it will be of interest to know the value of creep after one year. A quantitative method for the estimate of final creep strain is suggested by the C.E.B.[41] This method depends on the evaluation of several coefficients, from given charts, which are established on the basis of statistical analyses of concrete deforming under working loads, producing stresses of the order of 30 to 35% of the ultimate stress. These coefficients are derived for the effects of the member size, the water/cement ratio and cement paste content, the climatic conditions, the age at loading and the variation of creep with time.

2.2.5 Prediction of Shrinkage

In most cases it is assumed that the shrinkage-time relations can be treated in a similar fashion as for creep. Lyse[97,98] suggested that at a given relative humidity of the ambient atmosphere, if a given sustained stress is applied, the curve for creep will be nearly the same as that for shrinkage. He also found that creep and shrinkage are directly proportional to the amount of cement paste in the concrete. He suggested an exponential expression.

Hansen and Mattock[99] suggested that both expressions for creep and shrinkage can be given in a hyperbolic form, as given by Lorman.[93] They also investigated the effect of the size of the member (volume /surface ratio) on the variation of the final value of shrinkage.

Using this and the value suggested by the C.E.B.[41] a correction factor of 0.86 for the ratio of the free shrinkage strain in the top fibre of the beam to the free shrinkage of the companion prism was adopted, to allow for variation in size, in the author's calculations.

2.2.6 Prediction of the Time Dependent Behaviour of Reinforced Concrete Beams.

The influence of time on the behaviour of reinforced concrete structures subjected to sustained loading has been studied over a period of several years. Utilisation of higher quality materials and ultimate strength design has resulted in relatively slender flexural members. This has brought to light the greater significance of the various aspects of time effects. Concrete exhibits creep under sustained

stress, and even under a constant stress the time varying behaviour of reinforced concrete is characterised by a progressive redistribution of internal stresses in the concrete and steel, and by an increase in over-all deflection.

Early attempts to analyse creep in a cracked reinforced concrete beam were based on the "effective" or "reduced" modulus hypothesis introduced by Faber[79] and used by Glanville and Thomas,[76] Ross,[100] Yu and Winter[78] and Neville.[94] The author has included the methods presented by Pauw et al[101] and Gesund[102] in his calculations. The former has presented some refinements of the "effective" modulus technique, which permit estimation of neutral axis position, and steel and concrete stresses to be made. The latter recognised the fact that the plane of zero stress did not coincide with the plane of zero strain,[76,79] and in the rest of the analyses he used the "effective" modulus.

The "effective" modulus E_c' is defined as the ratio of the stress, f_c, to the total strain (elastic and creep), where the constant stress, f_c, is sustained:

$$E_c' = \frac{f_c}{\varepsilon_e + \varepsilon_c} = \frac{E_c}{C_c} \qquad \ldots\ldots\ldots\ldots\ldots (1)$$

Where ε_e = elastic strain

ε_c = creep strain

C_c = creep coefficient $\dfrac{\varepsilon_e + \varepsilon_c}{\varepsilon_e}$

For the calculation of creep deflection Pauw et al[101] has given the following steps:

$$mp = \frac{K^2}{2(1 - K)} \qquad \ldots\ldots\ldots\ldots (2)$$

$$m_t p = \frac{K_t^{\,2}}{2(1 - K_t)} \qquad \ldots\ldots\ldots\ldots (3)$$

$$K_\Delta = \frac{(1 - K)(3 - K)}{(1 - K_t)(3 - K_t)} \qquad \ldots\ldots\ldots\ldots (4)$$

$$\Delta_{ct} = K_\Delta \Delta_i \qquad \ldots\ldots\ldots\ldots (5)$$

Where m_t = time dependent modular ratio $C_c m$

K_t = time dependent neutral axis depth coefficient

K_Δ = creep effect ratio

Δ_i = initial deflection

$\Delta_{ct}-\Delta_i$ = creep deflection

The other terms, viz. m,p, and K have the usual meaning.

The other methods of analysis which are concerned with creep[76,100,103] of cracked reinforced beams are called the "rate of creep" method, the superposition method,[104] and the linear viscoelastic method.[105,106,107] All these methods of analysis are based on the assumption of the linear proportionality between creep and stress.

The choice of employing any one of the above methods depends on the importance of the problem, whether the state of stress is constant or variable, and the simplicity of the method. As has been pointed out by Ross,[100] for gradual loss of stress, the "effective" modulus method is extremely simple to use, and depends on creep data, which can be obtained experimentally from concrete specimens under sustained constant load.

The effects of shrinkage on warping of reinforced concrete structural members have been analysed quantitatively and qualitatively by several investigators.[101,108,109,110,111] The author has used the equation suggested by Pauw[101] in predicting warping due to shrinkage. The equation is in the following form:

$$\Delta_{sh} = \frac{3s\, e_{sh}}{8(3 - K_t)\, d} L^2 \qquad \ldots\ldots\ldots\ldots (6)$$

where Δ_{sh} = warping due to shrinkage

e_{sh} = free shrinkage of prism

s = size reduction factor (0.86)

Under certain circumstances, such as abnormal creep and/or shrinkage, the Draft Code[23] recommends separate consideration of creep and shrinkage, and the use of a method which is basically that due to Branson,[109] but with certain empirical coefficients adjusted in accordance with the creep and shrinkage coefficients given in the Code.

The time-dependent behaviour of reinforced concrete members is affected by the magnitude and characteristics of creep and shrinkage of concrete.

Creep and shrinkage of concrete depend to a great extent on the ambient conditions of humidity and temperature. The effect of environment is, therefore, a very important factor in influencing the long-time behaviour of reinforced concrete members.

CHAPTER 3

Building Codes

3.1 Concept of Safety and Serviceability

3.1.1 General

A historical review of the design procedures, given by Rowe et al,[112] Bate,[113] Abeles,[114] Beckett,[115] Torroja,[116] and Rose[117] shows that limit state design is the logical development. This has evolved, as Bate[113] puts it, "... from the intention expressed less rationally in the present codes."

The load factor method has been used, as early as the beginning of this century,[114] in the design of reinforced concrete structures. Large scale failure tests were taken as a basis for ensuring a definite load factor of safety against failure, and satisfactory behaviour under working load. No account was taken of the actual distribution of stresses.

The design of reinforced concrete entered a second stage when it was agreed that the tensile strength of concrete should be ignored, when considering resistance to bending, based on the elastic theory.[114] Since then until the more recent general acceptance of the ultimate load method, the elastic theory was included in the regulations of almost all countries. For over 75 years the analysis of concrete structures has largely been based on the assumption of the elastic theory, incorporating a stress factor of safety with limits imposed on span to depth ratios. Over the past 20 years, the inelastic behaviour of reinforced concrete has been gradually included in the codes.

In 1938 the Russians[112,115] abandoned the proportioning of reinforced concrete, based on the elastic theory, emerging with a well known fact that the elastic, or working load, theory of reinforced concrete gave a very good agreement with regard to safety against deflection, but varied to a great extent for the actual behaviour at failure. In the thirties they paid greater attention to a more rational design procedure, the limit state design, which was later generally accepted[112] in 1954 in the Russian code.

At present, many countries, e.g. Britain and the United States, are drafting their codes of practice in the light of the limit state design.

3.1.2 Current Codes and Limit State Design

The evolution of the current design procedures in the present codes can be clearly seen in the three kinds of design which have been developed during the last century. There are the working load design, the ultimate load design, and the limit state design. The working load design is based on the stress factor of safety and the cross section is dimensioned for the permissible stresses. The ultimate load design is based on a load factor of safety and the proportioning is based on yielding at failure. Limit design evolved from this method by assuming a failure mechanism in the structure, due to localised plastic hinges forming as a result of redistribution of stresses. The serviceability of the structure was also considered, because the ultimate load design allowed higher working stresses to be used.

As a result of the above development, a third method has emerged which considers three limit states for the design of reinforced concrete, namely, collapse, deflection and local damage (cracking), and which is now explicitly identified as limit state design. In the current codes a definite global load factor is used, whereas in the new approach flexible partial safety factors are introduced with regard to collapse, local damage and excessive deformation. These factors are related to loadings and strength of a probabilistic nature. The design must ensure the achievement of an acceptable probability that the structure being designed does not become unfit for the use for which it is required during its specified life. The acceptable probability should ideally be chosen to give a satisfactory balance between the initial cost, the maintenance cost and the insurance premiums related to the probability of structural failure. In any structure, unfitness for use may arise in various ways, the principal ones being collapse, excessive deflection and excessive local damage.

In the present codes the strength of individual members and sections can be calculated on plastic basis related to the actual behaviour of the materials. However, the analysis to obtain the force and moment system in a structure is still based on elastic assumptions.

The lack of freedom of choice in the design procedures and the misinterpretation of the concept of safety will render the structure generally conservative and uneconomical. The concept of failure must be treated in terms of probability of failure. Vague suggestions have

been made relating to the serviceability of a structure which render the methods employed in the current codes inadequate to apply.

All the above difficulties that are apparent in the current codes of practice are shown to be overcome once the concept of safety is based on the probability of failure relating to collapse, deflection and cracking associated with available statistical data on loads and materials. Based on this concept, the potential is available to produce satisfactory and cheaper structures.

3.1.3 The Statistical Concept of Safety

To calculate the probability of failure of a structure account must be taken of the expected and unexpected variation in the loads and materials, and of an acceptable probability of failure.

A choice of a "desirable" factor of safety has been investigated and discussed by Freudenthal,[118,119] Torroja,[120] Pugsly,[121] Thomas,[122] The Institution of Structural Engineers,[123] and Baker.[124] This suggests that a decision on an appropriate factor of safety must take into account economy as well as safety.

Granholm[49] proposed that the design should be based on reduced strengths (design strengths) and enhanced loads (design loads) which are obtained by applying certain factors to the probable strengths and loads (characteristic strengths and loads). This approach has been recommended by the C.E.B.[41]

3.2 C.E.B. Recommendations for an International Code of Practice for Reinforced Concrete

Since a complete probability analysis will be difficult and awkward to apply, the C.E.B. has adopted a semi-probabilistic method which, as compared with the present system, gives a clearer understanding of the behaviour of a structure and a better concept of the structural safety. Partial safety factors are introduced into the characteristic values of the strength (reduction factors) and loading (enhancement factors).

A coefficient of 1.64 was adopted to ensure that a probability of 5% of the results will be below the characteristic strength. For concrete the characteristic strength can be ascertained from the control

procedure intended, but for steel the characteristic strength is at present taken from the minimum strength.

For the present time the characteristic load cannot be defined on a statistical basis due to the lack of data concerning the occurrence of loading on structures.

The characteristic values of the loads and strengths take into account the expected variation, but do not allow for the following: loads significantly different from that assumed in design, the probability of different types of loads occurring at the same time, the degree of approximation in the calculation, the method and quality of construction, the cost of damage following a possible accident, the strength being significantly different from that determined by quality control, and the deterioration of the strength during the life time of the structure. Partial safety factors for strengths and loads are suggested for each limit state. The factors for the strength of the materials for the limit state of collapse are 1.5 and 1.15 for concrete and steel respectively, and that for loads is 1.4. These factors can be increased or decreased depending on the quality of construction, workmanship and risk of damage.

For the control of cracking the crack widths are limited to 0.3 mm for internal structural parts in normal atmosphere, 0.2 mm for internal structural parts in humid or aggressive atmosphere and external structural parts exposed to the weather, and 0.1 mm for internal or external structural parts exposed to a particularly aggressive medium or where watertightness is needed. The ratio of the maximum to the mean crack widths are assumed to be between 1.5 and 2.0. A method for the calculation of crack width is proposed.

For the calculation of the short term deflection, a method has been suggested, which takes into account the stiffening effect of concrete in the tensile zone.

3.3 Recommendations of the C.E.B. - F.I.P. Joint Committee 1970[125]

These recommendations are the result of combining the C.E.B[41] recommendations for international code of practice for reinforced concrete (1964) and the Draft F.I.P. - C.E.B. recommendations for the design and construction of prestressed concrete structures (issued in 1966 for the fifth F.I.P. Congress in Paris). This has been done with a view to

establishing a common basis for codes or standards, and achieving a uniform and appropriate structural safety for the design and construction of all civil engineering structures.

In this code the over-all correction factors with regard to strengths and loads have been sub-divided to include the separate effects of (1) the reduction in the strength of materials in the structure, as compared with the characteristic values, and the reduction due to local effects, (2) the possibility of a deviation of the loads from the characteristic values, (3) the low probability of simultaneous combination of loads all at their characteristic values, and (4) the possibility of adverse modification of the load effects. The design strength of the concrete is related to partial safety factors which depend on the quality and control of concrete.

For the control of cracking, four verification classes have been introduced to cover all structures with varying degrees of prestress, ranging from reinforced concrete to fully prestressed concrete. The different limit states of cracking are namely the limit state of crack width, the limit state of crack formation and the limit state of decompression. The limitations on crack width depend on the type of loading considered, short or long term loading, the conditions of environment and aesthetics reasons.

For the calculation of the limit state of crack width in reinforced concrete an equation is recommended, which includes the effects of cover, stress in the reinforcement, the bar diameter and the effective percentage of reinforcement.

For the control of deflection, span-depth ratios are given and methods for calculating the instantaneous deflection, taking account of the stiffening effect of concrete in tension and the amount of steel, are suggested.

For long term loads the instantaneous deflection should be increased by a factor of 2 in temperate or humid climates, and 3 in dry climates at an early application of the loads. The values of this factor should be reduced respectively to 1.5 and 2 when the age of loading is at least six months. In doubly reinforced beams the above increases should be reduced to 60% if $A_s' = \frac{1}{2}A_s$ and to 40% if $A_s' = A_s$.

3.4 Recommendations of the Draft Unified B.S. Code of Practice[23]

The C.E.B. Code was adopted by the B.S. Code Drafting Committee as a guide in the preparation of the new British Codes.

In considering the limit state of collapse the maximum values of the design loads are obtained by multiplying the dead load and the live load by separate partial safety factors of 1.4 and 1.6 respectively, and the minimum value of the design load can be obtained by considering the dead load alone with a factor of unity. Moment redistributions from the elastic distribution of up to 30% are allowed when certain conditions regarding the depth of the compression zone are fulfilled. The strength of individual sections is based on its inelastic properties, and may be assessed by using the following equations:

based on the yield strength of the reinforcement

$$M_r = (0.87)\, f_y\, A_s\, l_a \qquad \ldots\ldots\ldots\ldots (7)$$

$$l_a = \left(1 - \frac{1.1 f_y\, A_s}{U_w\, b d_1}\right) d_1$$

based on the strength of concrete in compression

$$M_r = 0.15\, U_w\, b d_1^2 \qquad \ldots\ldots\ldots\ldots (8)$$

The compressive concrete strain at the outermost fibre is taken as 0.0035, and the maximum stress is $0.45\, U_w$ or $0.4\, U_w$ for a rectangular-parbolic or a rectangular concrete stress distribution, extending to the full depth of the compression zone.

For the control of deflection the code has recommended the use of limiting values of span to depth ratios depending on the span length, the fixity condition, the percentage of tension reinforcement, the ratios of permanent to total load and of compression to tension reinforcement, the severity of the effect of creep, shrinkage and temperature changes and the criticality of deflection.

A formula for the calculation of deflection is given, which takes account of the stiffening effect of concrete in the tension zone.

The calculated deflections should not exceed the limiting values suggested in the code. They range between $L/250$ to $L/350$ (L being the span).

Two methods are suggested for the calculation of the additional long term deflection, due to creep and shrinkage. When the ultimate shrinkage strain is less or equal to 0.0006, and the ratio of creep/elastic strain is less or equal to 3.5, the following multiplying factors can be used:

	Age at Loading			
	14 days	28 days	90 days	1 year
$A_s' = 0$	2.0	1.8	1.5	1.3
$A_s' = \frac{1}{2}A_s$	1.2	1.1	0.9	0.7
$A_s' = A_s$	0.8	0.7	0.5	0.3

In controlling cracking the strain in the steel is limited to $\frac{0.75\ f_y}{E_s}$ or 0.0015, whichever is the lesser. The maximum surface cracks are limited to 0.3 mm and 0.1 mm for normal and aggressive environments respectively. A method for calculating the width of the most probable crack has been suggested, which includes the effect of concrete cover, the concrete strain and the stiffening effect of concrete in the tensile zone before cracking.

3.5 Codes of Practice

A. British Code CP114[22]

In the design of individual structural members two methods are permitted, namely the elastic method and the load factor method. The elastic method is based on a constant modular ratio of 15, and permissible stresses calculated by introducing factors of safety in steel and concrete of 2 and 3 respectively, which were later, in 1965, amended to include 1.8 and 2.73. The load factor method is based on permissible stresses to give the working load associated with a load factor of 1.8 to give the ultimate capacity of the section at failure. For the analysis of the structure to define the forces and moments acting on individual members the code allows 15% adjustment of moments obtained by elastic analysis.

The limitations on deflection and cracking are implicitly included in limiting the span-depth ratio and the permissible stresses respectively. No account is given of the possibility of calculating deflection or cracking.

The use of rolled steel bars, hard drawn steel wires, cold twisted steel bars and steel fabric is recommended. Other reinforcing steels may be regarded as suitable if due regard is given to yield stress, ductility, tensile strength and other essential properties. The permissible steel stresses were limited to a maximum value of 207 N/mm^2.

B. American Code A.C.I.[126]

The American Code (A.C.I. 318-63) is drawn up in the same manner as CP114, however, there are differences in details. A redistribution of moments of 10% is allowed only when using the ultimate strength design approach. Separate load factors are used for dead and live loadings, and a partial safety factor, taking account of the variation in strength of materials (cylinder strength), workmanship etc., is incorporated in the equations giving the strength of section. Minimum thickness, limiting values and methods of calculation are specified for the control of deflection. The additional long term deflection due to sustained loading is accounted for by multiplying the instantaneous deflection by a factor of 2 for $A_s' = 0$, 1.2 for $A_s' = \frac{1}{2}A_s$ and 0.8 for $A_s' = A_s$. The cracking is controlled by using deformed bars well distributed in the zone of maximum concrete tension, and by limiting the average crack widths to 0.38mm for interior members and 0.25 mm for exterior members.

C. Proposed Revision of A.C.I. 318-63[127]

Notable changes in the design of a structural member and in the control of deflection and cracking have been suggested. When using the ultimate strength design approach the load factors, for the dead and live loadings, were previously 1.5 and 1.8 respectively, but the proposed values are 1.4 and 1.7. For the control of deflection the minimum thickness, for a reinforcement having a yield strength greater than 414 N/mm^2, is a function of the yield strength, and the instantaneous deflection is calculated using elastic methods, and incorporating an effective moment of inertia obtained from a cubic equation, which includes the effect of cracking. The factor for additional deflection due to creep and shrinkage is obtained from a linear equation including the effects of the compression steel. Four different limiting deflection values are proposed, depending on thetype of member considered.

For the control of cracking only deformed bars are allowed and a

formula for the calculation of crack widths as a function of steel stress, concrete cover and distribution of steel reinforcement, is proposed, and limiting crack widths of 0.4 mm and 0.33 mm for interior and exterior exposures respectively are given. For deep beams with depths of 915 mm or more vertical face reinforcement, of a minimum value of 10% of the main tension steel area, with spacing not more than 300 mm or the width of the web, is recommended.

D. German Code DIN 1045[128]

The German Code allowed a saving in steel by increasing the permissible stresses. It distinguishes two types of steel: naturally hard steel and cold worked steel. These are in different forms: round and deformed twisted, knobbled and ribbed, and with various elastic limits ranging from 2200 kg/cm^2 to 5000 kg/cm^2.

The elastic analysis is based on a modular ratio of 15, and the allowable stresses for steel and concrete, which are given as a function of concrete and steel grades as well as the type and shape of the member considered. The maximum permissible steel stress in slabs is 2400 kg/cm^2 and in beams is 2000 kg/cm^2.

Cracking and deflection are indirectly controlled by specifying allowable steel and concrete stresses.

E. Danish Code [129]

The steel used for the reinforcement should generally be rolled steel. Cold worked steel can be used only if it is suitable for use in reinforced concrete. The permissible stresses for reinforcing steel depend on the types of steel and on the class of control measures. For loads of a purely temporary nature, the permissible stresses may be increased by 25%. With careful control the permissible stresses may be increased by 5%.

No limitations on cracking and deflection are given.

F. (Netherlands) Dutch Code GBV[130]

The code distinguishes three types of reinforcement according to the process of manufacture, e.g. hot rolled reinforcing steel (normal and high tensile) and cold worked steel. The bars may be plair, of prismatic, circular or oval shape, or deformed, of twisted oval, square or cruciform

with ribs perpendicular or inclined to the centre line.

For the calculation of stresses, either the elastic method, with a modular ratio of 15 or less, or the load factor method, with a load factor of 1.8, can be used. The values of the permissible stresses in the steel and concrete depend on the type of loading and the reinforcing steel used. The maximum permissible steel stress is 2600 kg/cm^2.

For the control of deflection, a minimum effective depth of a member can be calculated from an equation depending on the type of steel, the magnitude of loading and the length of the span.

A method of calculating crack width, depending on the type and form of bars, is recommended. Crack widths are limited to 0.25mm and 0.2 mm for exposed structures which come into contact with water and soil, and structures exposed to aggressive medium respectively.

CHAPTER 4

Calculations for the Limit States

4.1 General

The theories and mechanisms of the three limit states of excessive local damage (cracking), excessive deflection and collapse (ultimate strength) are discussed in this chapter. With the help of recommendations given in Chapter (3) for the limit state design, and the work of several investigators in this field, it is possible to arrive at simplified design rules for the prediction of crack width, deflection and ultimate strength of singly reinforced, simply supported concrete beams. With reference to early work by other research workers on cracking and deflection, only the main parameters are considered in the discussion for these limit states. These parameters will be shown to be in direct relationship with the limit state considered.

4.2 Calculation for the Limit State of Cracking

4.2.1 Mechanism and Theory of Cracking

A crack in concrete is a narrow, irregular opening of indefinite length and depth. Recent research has cast new light on the mechanism of cracking in reinforced concrete members under load, to achieve a better control over cracking, the widths and distribution of the cracks. Much of the work has been of a theoretical nature, often involving higher mathematical techniques. Extensive investigations have been carried out in the past, aiming at developing equations for spacing and width of flexural cracks in reinforced concrete members. Summaries of the causes, mechanism and control of cracking in reinforced concrete members can be found elsewhere.[57,131,132,133,134,135]

Three cracking mechanisms have been reviewed by Bianchini et al:[131]

(i) Observation of the surface cracking phenomenon and the assumption that concrete tensile stress is uniformly distributed over an effective area of concrete, and that a certain distribution of bond stresses exists.[36,133,134,135]

(ii) Redistribution of concrete stresses at crack formation that is compatable with observed internal and surface cracking as suggested by Broms.[136,137,138,139]

(iii) Fracture mechanics concept.[140,141]

The first mechanism is discussed here as follows:

In axially loaded reinforced concrete members the cracks initiate at critical locations where the limiting tensile properties of concrete have been exceeded, due to weak material or high stress and strain (see Fig. 1). These cracks, known as primary cracks, are randomly located through the concrete and propogate to the surface. At this stage the concrete surfaces at the cracked sections are free of stress and the force in the reinforcement equals the external load. Tensile stresses in concrete are present between the primary cracks due to the bonding action between steel and concrete which determines the distribution of concrete and steel stresses in this region. As a result, additional cracks form between the initial primary ones at higher loads where a uniform concrete stress exceeds the concrete tensile strength. Cracking will continue to take place until the bond is not sufficient to transfer enough stress to the concrete to cause another crack due to excessive slip and reduced distance between cracks.

Many investigators believe that the axially and concentrically loaded reinforced concrete tensile specimen is a satisfactory model for the tensile region of a flexural member between existing cracks. If the distance between two primary cracks is assumed to be twice the minimum crack spacing (a min.) (see Fig. 1) then a new crack will form when (a max) is slightly greater than (2a min.). However, if (a max) is slightly smaller than (2a min) then a new crack cannot form.

Since most theories on cracking are based on the same concepts and differ essentially in the assumption on bond and effective concrete area, a general theory has been established by the C.E.B.[36,73] regarding the mechanism of flexural crack formation:

$$a_{min} = \frac{f_t' \, A_e}{\sum_o u} \qquad \ldots\ldots\ldots\ldots (9)$$

$$a_{max} = 2a_{min} \qquad \ldots\ldots\ldots\ldots (10)$$

$$a_{max} = \frac{f_t'}{2u} \frac{D}{P_e} \qquad \ldots\ldots\ldots\ldots (11)$$

where $\sum_o = \frac{4A_s}{D}$, $\qquad P_e = \frac{A_s}{A_e}$

Assuming that the steel slips over concrete and neglecting the concrete extension:

$$W_{max} = a_{max} \frac{f_s}{E_s} \quad \ldots\ldots\ldots\ldots (12)$$

$$= \frac{f_t'}{2u} \frac{D}{P_e} \frac{f_s}{E_s} \quad \ldots\ldots\ldots\ldots (13)$$

However, because of bond, at some distance from the crack, the concrete is strained and therefore the steel stress and crack width are reduced:

$$W_{max} = K_1' \frac{D}{P_e} \frac{f_s}{E_s} \frac{f_t'}{2u} \quad \ldots\ldots\ldots\ldots (14)$$

$$= K_2' \frac{D}{P_e} \frac{f_s}{E_s} \frac{f_t'}{u} \quad \ldots\ldots\ldots\ldots (15)$$

This is similar to the relationship proposed by Rusch and Rehm.[57] It is assumed that f_t' and u are both dependent on the strength of concrete in compression. Therefore $\frac{f_t'}{u}$ will be constant:

$$W_{max} = K_3' \frac{D}{P_e} \frac{f_s}{E_s} \quad \ldots\ldots\ldots\ldots (16)$$

The previous investigation indicated that (i) crack widths were essentially proportional to steel stress[142] (ii) crack widths did not decrease significantly with decreasing bar size (D) and increasing effective reinforcement ratio (P_e).[36] Based on these facts, Efsen and Krenchel [57] suggested the formula:

$$W_{max} = K_4' + K_3' \frac{D}{P_e} f_s \quad \ldots\ldots\ldots\ldots (17)$$

and adopted by the C.E.B.[36,41] in the form

$$W_{max} = \left(4.5 + \frac{0.4}{P_e}\right) \frac{Df_s}{K_5'} \quad \ldots\ldots\ldots\ldots (18)$$

Based on their findings, it was pointed out by Broms,[138,139] Kaar and Mattock,[143] Hognestad[36] and the C. and C.A.[45] that crack width is strongly influenced by the steel stress, the distribution of the reinforcement over the effective concrete area, and the amount of concrete cover.

The C.E.B. simplified equation (Eq. 18) includes the effect of concrete cover, indirectly in the effective reinforcement ratio P_e (see Fig. 1)

$$P_e = \frac{A_s}{A_e} = \frac{A_s}{(2C + D)\ b} \qquad \ldots\ldots\ldots\ldots (19)$$

Hognestad[36] found that by varying the cover, and keeping the rest of the parameters constant, the C.E.B. equation gave values in good agreement with experimental crack widths.

It can be concluded, therefore, that the main parameters which directly influence the maximum crack width are the concrete cover and the stress in the reinforcement.

4.2.2 Cracking in Reinforced Concrete Members

It is generally accepted that cracks are only objectionable if they exceed a certain width. This limit has not been specified until recently. The codes, because of the low extensibility of concrete, have specified permissible steel stresses to limit the crack width, which becomes objectionable if it assists in the corrosion of the reinforcement, the disintegration of concrete, and mars the appearance of the structure.

In studying the crack formation in reinforced concrete members, it may be pointed out that the presence of the reinforcement in concrete has no appreciable effect on the strain capacity of the plain concrete. Microcracks occur at bending stresses which correspond to the direct tensile strength of concrete. The lengths and widths of the first micro-cracks were found, by Evans,[144] to be as small as 1.26 mm and 1.69 x 10^{-3} mm respectively. Kaplan[145] found that the strain at cracking varied depending on the volume of coarse aggregate in the mix. He observed an average of 110 microstrain in concrete before cracking in flexure. This cracking occured at loads considerably less than those required to cause visible cracking. Cracks became visible to the unaided eye when they were about 0.01 - 0.02 mm in width, and when the nominal tensile stress in concrete equalled the modulus of rupture.

Early work on the phenomenon of cracking has suggested that cracking can be controlled and limited by employing a higher percentage of steel, smaller bar diameter with high bond resistance, and limited permissible steel stresses.[57,146,147,148,149] Efsen and Krenchel,[57] from direct

tension tests, found that the crack widths were not affected by the surface characteristics of the bars. This finding opposes those of Watstein and Parson [142] and Watstein and Seese.[148] Watstein and Mathey[147] found that the crack width at the exterior surface of a deformed bar was about one half that at the exterior surface of the concrete at a steel stress of 138 MN/M^2.

Rusch and Rehm,[57] from test results on beams and slabs, concluded that the actual distribution of bond stresses along the bar is not essential in the calculation of crack spacing. Values of bond stress were estimated from pull-out tests on plain and deformed bars.

In the 1960s extemsive tests and analysis by various investigators [36,45,131,138,139,143,150,151] regarding the crack widths and spacings in flexural reinforced concrete members suggested that the magnitude of the crack width is greatly influenced by the magnitude of the steel stress, the amount of concrete cover, and the arrangement and distribution of reinforcement in the effective concrete tension zone. A variation of $\pm$ 50% of the average in the crack widths and spacings has been reported by Hognestad,[36] and Kaar and Mattock.[143] From these studies the following conclusions can be derived:

1. The term D/P_e is an insensitive variable.[36,131,138,139]
2. Crack widths and spacings depend on the amount of concrete cover.[36,45,131,138,139,143]
3. For the same concrete area (A), the crack widths vary with steel arrangement.[36,138,139,152.]
4. For a uniform distribution of reinforcement over the effective area of concrete, the parameter (A) appears to be significant.[131,152]
5. The steel stress is the major variable in the prediction of cracking,
6. The bottom and side cracks can be calculated from the same equation, except for the strain gradient,[45,139,153] provided the reinforcement is well distributed and the side crack width is little affected by the compression zone of the beam.
7. The maximum crack width, not the average crack width, is of practical significance in design.[36,131,154]
8. The surface characteristics of the reinforcing bar have little effect on the width of the cracks.
9. Appearance is controlled by cracks at the soffit of the beam, while durability (corrosion) is controlled by cracks at the reinforcement level on the side of the beam.[36]

4.3 Calculation for the Limit State of Excessive Deflection

4.3.1 Mechanism and Theory of Deflection

The problem of deflection in reinforced concrete structures has recently attracted the attention of several bodies and investigators to study the mechanism and theory of deflection more closely in order to arrive at a simplified formula for the design and control of deflection. The increase in the present day usage of high strength steel and concrete, and the ultimate load method of design has led to the adoption of slender members of less stiffness, resulting in increased deflection. Summaries of the mechanism and theory of deflection have been included in several papers, codes and bulletins.[41,134,155,156,157,158,159,160]

In reinforced concrete, three stages can be distinguished in the mechanism of deflection. Firstly, the concrete is uncracked and hence the section behaves elastically up to the cracking moment (Mc). Secondly, the tensile concrete has cracked, but concrete in compression and the steel continue to behave elastically up to the yield properties of the materials. The third stage is the zone of high concrete or steel stress, where the yielding characteristics of the steel or concrete affect the behaviour of the section, depending on whether the beam is over-reinforced or under-reinforced.

For the consideration of the limit states under working design load, the first two stages are of importance and many investigators have represented the behaviour of a beam in a bilinear relationship to allow for the stiffening effect of concrete before cracking.[23,41,156,158,159] On the other hand, several others allowed for the stiffening effect of concrete between the cracks.[78,159,160,161]

From elementary elastic theory a method of calculating the deflection of a reinforced concrete beam may be developed.[23,156,158] This theory is based on a commonly accepted expression:-

$$\phi = \frac{d^2y}{dx^2} = \frac{M}{E_c I} \qquad \ldots\ldots\ldots\ldots (20)$$

Where ϕ = curvature

M = applied moment

E_c = modulus of elasticity of concrete

I = second moment of area

The stiffness (E_cI) in the cracked condition, especially for reloading, undergoes the most change. It has been reported by Soretz[57] that the stiffnesses for initial loading and reloading of beams in the cracked state showed a considerably wide range of scatter of up to $\pm$ 20 and $\pm$ 50 respectively. These variations can be attributed to many factors, namely: percentage of reinforcement, cracking load, magnitude of stress at design load, extent of cracking, curing conditions, concrete strength, and shape of section.

The importance of the interdependence of the values of E_c and I has been emphasised by many investigators and codes.[155,158,162] Westlake[162] stressed the fact that the E_c and I values should be considered simultaneously.

Some of the previous codes have specified limiting values of the span-depth ratios for the control of deflection, but have not given the main factors that enter into the determination of this ratio. These factors are the span, steel quality, percentage of steel, amount of compression reinforcement and type of loading. For the short term loading the first three factors must be considered.

4.3.2 Deflection of Reinforced Concrete Members

The cracking moment in a beam with normal amount of reinforcement is only a fraction of the working design moment as compared to slabs,[163] and hence the deflections at design loads in beams are more critical than in slabs. More attention should therefore be placed on the control of deflection in beams and a reasonable assessment of their stiffness (EI) should be made.

Various recommendations as regards the stiffness of reinforced concrete members have been given by several codes. The variation of the stiffness with loads has been studied by many research workers.[57,159,160,164]

Eppes[164] found that the measured values of (EI) where the beams are uncracked are comparable with those calculated on the basis of a gross section with a transformed steel area, and the values where the beams are cracked with those calculated on the basis of cracked transformed section. It was reported, however, by Lash et al[73] that over a substantial part of the initial loading, the observed values of stiffness in some beams were less than the calculated values based on

a fully cracked section. In the working load range three stiffness values have been distinguished by Soretz.[57] The stiffness is greatest for the uncracked condition, and is least for the initial loading in the cracked condition; for subsequent reloading in the cracked condition the stiffness is greater than for the initial loading in the cracked condition.

The effects of the principal factors affecting deflection and comparisons of the measured and calculated deflections from various theories are included in the work of the A.C.I. Committee,[160] Bewtra,[165] and Beeby.[158] However, little information has been reported on the effect of long-term loading on the deflection of reinforced concrete.

4.4 Calculations for the Limit State of Collapse

For the calculation of the ultimate strength of reinforced concrete beams, it is essential to assume a distribution of the stress in the concrete compression zone, the maximum value of the compressive stress and the plastic strain in the concrete that can be attained at failure.

Many shapes of the stress distribution for concrete have been suggested by several authors and codes of practice.[23,27,41,125,166,167,168,169]

The C.E.B.[41] and the F.I.P. - C.E.B.[125] codes recognised the fact that the stress distribution at the ultimate limit state depends on many factors; for example, the position of the neutral axis, the rate and duration of the application of the loads, the quality of concrete and the geometric shape of the section. They also reported that basic theoretical approaches and the statistical interpretation of experimental evidence have shown that simplified stress distribution in the concrete compression zone can be used.

Ultimate strength theories, except that given by Baker,[57,170] assume that there is no slip between steel and concrete in tension. The assumption of no slip is recommended indirectly by the codes, via the assumption that plane sections remain plane after bending. Gray[171] has shown that there is a difference of 10% in the bonding characteristics at ultimate moment between plain and deformed bars. This has been shown by comparing the actual steel strain with the extrapolated strain, using Bernouli's theory. The effect of bond on the neutral axis position was noticed to be insignificant.[172]

Evans et al,[173] using X-ray technique in measuring slip, bond and steel stresses, showed that at ultimate loads and at 90% of ultimate loads, the ratios of interface to concrete surface strains were 116% and 108% respectively, and that the ratio (F) of the maximum strains in the steel to the measured average surface concrete strains at the level of reinforcement increased with increasing load and improved bond characteristics. This was contrary to Baker's finding[170,172] which, based on the values of concrete surface strains, at the level of steel, obtained from the measured values of the ultimate concrete compressive strains, and the neutral axis position, showed a decrease in (F) with increasing load.

Three different shapes of stress blocks have been recommended by the C.E.B.[41] These are the rectangular-parabolic, the parabola and the truncated rectangle for any shape of section and with certain limits on the maximum stress and strain and the position of the neutral axis. The Draft Unified Code, as has been discussed in Chapter (3), has recommended the use of two shapes of stress block, namely the rectangular-parabolic and the rectangular stress distribution. In the latest code by the C.E.B.-F.I.P. Joint Committee in 1970,[125] it was recommended that for sections subjected to uniaxial loadings in the ultimate limit state, the rectangular-parabolic design curve, formed by a second degree parabola extended by a straight line, is used. For sections subjected to bending, the rectangular-parabolic curve may be replaced by an equivalent simplified curve of rectangular form.

In considering under-reinforced beams, the shape of the compressive stress block has relatively little influence on the value of the moment of resistance of a member subjected to bending. This is because the compressive strength of the concrete has little influence in such cases. Also such beams with low percentages of reinforcement of good bond characteristics have been shown by many investigators to carry loads much higher than that expected on the basis of the yield strength of the steel. The stress in steel sometimes exceeds the tensile strength of the steel as tested in air. Results of this type have been reported by Hajnal Konyi,[24,25,26,28] Granholm[49] and many others.

As far as practical calculations are concerned, one must take into account not only the maximum ultimate moment, but also serviceability as given by deflection and cracking. Since hyper-strength is accompanied

by large steel strains, and even if the ultimate strength has not been reached, the concrete structure has already exceeded serviceability limits. At present agreement between theory and practice has been shown to be satisfactory and that the suggested calculating procedures result in values for the ultimate moment that are generally on the safe side. The European Concrete Committee recognised the effect of hyper-strength on the ultimate strength of weakly reinforced beams, and suggested its consideration in the calculation of the ultimate strength of such beams.

The recent codes of practice do not include consideration of hyper-strength in their recommendations.

The Draft Unified Code[23] recommends a simple equation based on the yield stress of the steel using a rectangular stress distribution and partial safety factors on the materials, as has been discussed in Chapter (3). This method, incorporating a load factor of 1.6, has been used in estimating the design moment. For the analysis of test results in controlled tests in the laboratory the partial safety factors should be eliminated and a rectangular-parabolic stress distribution, suggested by the Draft Code, can be used. This method has been used in estimating the ultimate strengths of beams.

The Need for the Proposed Programme

From the above review of the work of several investigators, it can be seen that there were differences in opinion as regards the suitability of high tensile steel as normal reinforcement in concrete. No definite conclusions were drawn as regards the design and prediction of the behaviour of reinforced concrete members using high tensile steel. The effects of raising the steel stresses and the effects of static, sustained and fatigue loading on the serviceability and safety of members with very high tensile steel have not been fully considered. The differences in the findings of several bodies and investigators suggested that no definite magnitude of the permissible steel stress could be arrived at. There is a need for a permissible steel stress which could be employed in design without jeopardizing the serviceability and safety even after a long period of sustained or repeated loading. They also suggested that the methods of controlling cracking and deflection are inadequate, and they should be derived on the basis of the second cycle as well as the first cycle of loading. The behaviour of the members which are already

cracked should be based on the cycles of loading subsequent to the first cycle, when they are first loaded in the uncracked state. Limited information has been given elsewhere regarding the effects of reloading cycles on the deflection and cracking behaviour of concrete members reinforced with high tensile steel.

The effects of the cracking and deflection and the effects of long term loadings on the choice of the strength of steel has not been considered before. The choice of steel strength and the economy resulting from using a certain type of steel should be based on the knowledge of the cracking and deflection behaviour under static, sustained and repeated loading.

The objective of the proposed programme of investigation, therefore, is to arrive at a set of design recommendations as regards the use of high tensile steel as reinforcement in concrete members. These recommendations should provide a safe, serviceable and economical structure. These three conditions can be achieved when the maximum permissible steel stress is found from the study of the behaviour of reinforced concrete members under short and long term effects.

CHAPTER 5

Programme of Investigation

5.1 General

The main objective of this investigation is the use of high tensile steel as normal reinforcement in concrete. The variables that are thought to be of primary importance and considered in the design of the test beams for the investigation are the surface characteristics, the diameter size, the percentage and the increase of permissible working stresses of the main longitudinal reinforcement. The type of loading (static, fatigue and sustained) is also considered as a major factor in this programme.

The aim of the investigation is to reach an acceptable limit of permissible working stress where a beam can be designed with a safe load factor against collapse, with adequate serviceability as regards deflection and cracking under instantaneous and long-term sustained and fatigue loading.

All the beams were designed to fail in flexure rather than shear or diagonal tension. This facilitated the study of beam behaviour at very high stresses. Mild steel stirrups were included only in the end spans of the beams. The main longitudinal reinforcement varied in yield points from 276 N/mm^2 to 897 N/mm^2, and in the surface characteristics, viz. plain round or deformed bars. Some beams were reinforced with prestressing steel with yield points up to about 1690 N/mm^2.

Two auxiliary beams were also tested. These beams were designed in a similar manner as the others, except that they contained exposed reinforcement for direct measurement of steel strains in the mid-span of the beam, and they had shorter spans than the main beams.

The working loads of the beams were calculated on the basis of the limit state of collapse with a global factor of 1.8, recommended by the Draft Unified B.S. Code of Practice.[23]

A summary of the programme of investigation is given in Table (1).

5.2 Beam Designation

The test programme included two main groups, and one auxiliary group,

of beams as shown by the following notation:

A - Group of beams with the same percentage of reinforcement and different types of steel, e.g. A11, A31

B - Group of beams with different percentages of steel and different types of steel, e.g. B11, B21

B_{st} - Auxiliary group of beams, e.g. B_{st1}

The first suffix number in A11, B21, A31 etc. refers to the type of loading. These are 1, 2 and 3 for static, sustained and fatigue loading respectively.

The second suffix number in A11, A12, A13 etc. refers to the number of beam within each group of beams. These are 1,2, 3 etc. for any type of loading.

For details of test beams refer to Tables 2, 3 and 4.

5.3 Beams with the Same Percentage of Steel and Different Types of Steel: Group A

Five types of reinforcement were used in this group, ranging from plain round mild steel (276 N/mm^2 yield point) to high tensile deformed Kam 90 (897 N/mm^2 proof stress). It was intended to design the beams of this group to include two bars of 19 mm diameter. Unfortunately, in beams reinforced with Kam 60 and Kam 90 the nearest available size was 16 mm.

5.4 Beams with Different Percentages and Types of Steel: Group B

This group consisted of nine types of steel reinforcement. The beams were reinforced with different percentages and strengths of steel and different bar sizes. Some of the beams had similar design loads.

5.5 Beams with Exposed Steel

Two beams (B_{st1} and B_{st2}) with exposed steel reinforcement over a length of 450 mm in the mid-span were tested as part of an undergraduate project supervised by the author.

5.6 Bond Tests

These tests were carried out as part of an undergraduate project supervised by the author to study the difference in bond resistance

between Kam 60 and Unisteel 80.

5.7 Types of Loading

5.7.1 Static Loading Tests

Beams designated A11,A12,A13,A14,A15,B11,B12,B15,B16,B17,B18, B19, B_{st1} and B_{st2} were tested under static loading.

Each beam was s ubjected to two cycles of loading before the final failure cycle. On the first and second cycles the beams were loaded up to approximately the design live load, and about 30% higher than the design live load respectively. In some beams the load was removed completely just before failure and was applied again. This was done to measure the amount of recovery in deflection.

5.7.2 Repeated Loading Tests

Beams A31, A32, A33 and A34 were first tested statically up to design load, which included the self weight of the beam. Repetitions of loading were applied with the upper limit corresponding to the design load and the lower limit to one half of the design load.

After every few hundred thousands of load repetitions the test was stopped and the beam was loaded statically up to design load. The beam was then unloaded again, and was subjected to repeated loading.

5.7.3 Sustained Loading Tests

Beams B21, B22, B23, B24 and B25 were tested statically up to design load, which included the self weight of the beam. This load was sustained on all five beams for the time durations indicated in Table (1).

5.8 Observations

In the three types of loading and for all the beams a standard of observation was followed. The following measurements were taken:

1) Strains in concrete (concrete surface)
2) Crack widths at bottom beam edge and at steel level
3) Length and distribution of cracks at various stages of loading

4) Deflections
5) Increase of deflection with time and repeated loading
6) Increase of strain with time and repeated loading
7) Increase in cracking with time and repeated loading
8) Residual deflection and cracking
9) Shrinkage of concrete

CHAPTER 6

Design, Description of Materials and Construction of Test Beams and Specimens

6.1 General

All beams were designed as singly reinforced with the same cross sectional dimensions of 152 x 305 mm, and the same span of 4570 mm, except the two beams with exposed steel, which had a span of 2740 mm.

The choice of the beam dimensions was to simulate the behaviour of actual members in building, and also to allow a comparison with other work elsewhere. This size of the beam provided ease of fabrication and handling in the laboratory.

In Tables (1-4) and Figs. (2-4), the beam marks, type of loading and properties of all beams are given.

6.2 Design of Test Beams

The details of the design of beams for safety against collapse, provision of shear reinforcement and check for bond and anchorage slip are given in Appendix A.

6.2.1 Ultimate Strength

Two main groups of beams were tested. The first group, designated as group (A), contained all beams reinforced with the same amount of steel but different surface characteristics and strengths of the reinforcing bars.

Beams A11 and A31 consisted of two 19 mm mild steel plain round bars. Beams A12 and A32 were reinforced with two 19 mm Unisteel 60 reinforcing bars. Beams A13 and A33 contained two 19 mm Unisteel 80 reinforcing bars. Beams A14 and A34 were reinforced with two 16 mm Kam 60 steel bars. Beam A15 was reinforced with two 16 mm Kam 90 steel bars.

The second main group (B) consisted of beams reinforced with different percentages, strengths, sizes and types of steel bars. The percentage of steel varied between 0.39 and 2.58.

Beams B11 and B21 consisted of two 25 mm diameter mild steel plain round reinforcing bars. Beams B12 and B22 were reinforced with two 22 mm Unisteel 60 reinforcing bars. Beam B23 was reinforced with two 19 mm Unisteel 80 reinforcing bars. Beam B24 contained two 16 mm Kam 60 steel bars. Beams B15 and B25 were reinforced with two 12 mm Kam 90 steel bars.

Prestressing wires and strands were also used in this group. Beam B16 contained six 7 mm diameter crimped prestressing wires. Beam B17 was reinforced with four 8 mm plain prestressing wires. Beam B18 was reinforced with four 7.94 mm seven ply prestressing strands.

In beam B19 four 14 mm three-wire Bristrand 100 were used.

The two beams B_{st1} and B_{st2} of the auxiliary group were reinforced with two 16 mm Kam 60 and Unisteel 80 reinforcing bars respectively. The reinforcement was left exposed in the mid-span. The size of the opening through which the bars were exposed was 100 x 450 mm. Two holes (0.79 mm diameter) were drilled on the outer exposed face of each bar, giving a gauge length of 200 mm.

All the beams had the same size of concrete cross-section of 152 x 305 mm, and equal side and bottom concrete covers to the surface of the reinforcing bar of 35 mm. Details of all the beams are shown in Figs. (3-4) and Tables (2-4)

The beams of all the groups were designed according to the Draft Unified B.S. Code of Practice.[23] The limit state of collapse was adopted as a criterion of design. The ultimate moment of resistance of the section was calculated, assuming a cube strength of 41.4 N/mm^2 with partial safety factors on steel and concrete of 1.15 and 1.5 respectively. The working load was calculated by dividing the calculated ultimate moment by a factor of 1.6.

6.2.2 Shear Reinforcement

The shear reinforcement of the beams was designed in accordance with the Draft Code. All beams were designed to contain the same number and uniform spacing of stirrups. The stirrups were 6 mm diameter mild steel, spaced at 152 mm centre to centre. These were only provided in the shear spans. The reason for not providing stirrups in the mid-span of constant moment was simply to avoid the initiation of cracks due to

the uniformly spaced stirrups, which had been shown to be crack initiators.

Four stirrup hangers were provided in each beam. These were 6 mm diameter mild steel bars. The stirrups were tied to the main reinforcement and the hangers, in a vertical position. Details are shown in Figs. (3 - 4).

6.2.3 Bond and Anchorage

The anchorage and flexural bond of all beams were considered carefully to ensure a tension mode of failure (yielding of reinforcing steel).

For the purpose of anchorage and prevention of slip, plain bars, wires and strands were supplied with hooks which were designed in accordance with the code recommendations. The hooks for mild steel were U - shaped, while those for the wires and strands were L - shaped.

Deformed bars were not supplied with hooks, except those in the auxiliary beams, which were L - shaped. In order to ensure that no slip takes place between steel and concrete at any level of stress, an extra length of bar was either welded, in the case of mild steel, or added, in the case of deformed bars, to the length of main reinforcement as shown in Fig. (3). The length protruding from each end of the beam was 50 mm only. This procedure was followed for nearly half the number of beams, and since there was no slip recorded it was abandoned for the rest of the beams.

In order to study the difference in slip resistance and bond strength of two reinforcing bars of almost the same 0.2% proof stress, but different surface characteristics, some pull-out tests were carried out. The pull-out test design was in accordance with the recommendations given in 1957 by the Rilem Symposium.[57] The concrete prism, in which the steel bar was embedded concentrically and horizontally while casting, was 145 mm square in cross-section and 190 mm long. The longitudinal steel bars were 500 mm long with diameters of 19 mm and 16 mm for Unisteel 80 and Kam 60 respectively. The prism was reinforced with a helix, of 6 mm diameter plain mild steel at 25 mm pitch, with an outside diameter equal to the size of the prism. Each end of the helix was welded to the next turn as recommended by CP114.[176] The specimen and test apparatus are given in Fig. (5).

A total of six specimens, three of each type, were made from the same concrete mix, as will be described later, and given the same conditions of curing as the cube specimens and the test beams.

6.3 Reinforcement

Nine different types of reinforcement were used in the investigation. These were:

a) Mild steel: plain round bars with a nominal yield stress of 276 N/mm^2:- 19mm and 25 mm diameter sizes.

b) Unisteel 60: deformed bars with deformation forming an oblique angle with the longitudinal axis of the bars, with a nominal yield stress of 414 N/mm^2:- 19 mm and 22 mm diameter sizes.

c) Unisteel 80: deformed bars produced by cold stretching Unisteel 60 by 3%, with a nominal yield stress of 550 N/mm^2:- 19 mm diameter size.

d) Kam 60: deformed bars, manufactured in Sweden, hard alloy steel with a nominal yield stress of 585 N/mm^2 and a size of 16 mm diameter. The transverse ribs are perpendicular to the longitudinal axis of the bar. On opposite sides of the bar two longitudinal grooves extend parallel to the axis of the bar.

e) Kam 90: deformed bars, produced by cold stretching Kam 60 steel by almost 5%, with a nominal yield stress of 897 N/mm^2, and sizes of 16 mm and 12 mm diameter.

f) Prestressing wires: crimped wires with a nominal yield stress of 1380 N/mm^2:- 7mm diameter size.
Plain wires with a nominal yield stress of 1515 N/mm^2:- 8 mm diameter size.

g) Strands: prestressing, 7-ply, with a nominal yield stress of 1690 N/mm^2 and 7.94 mm diameter size.
Bristrand 100 with a nominal yield stress of 690 N/mm^2 and 14 mm diameter size.

Before use, all the bars were degreased with Acetone.

Fig. (6), Plate (1) and Table (5) provide full details of the reinforcement modulus of elasticity, yield stress, ultimate strength and stress at fracture.

6.4 Concrete

The mix proportions were chosen after a few trial mixes were prepared and tested. These proportions were 1:2:4, using rapid hardening cement. In the trial mixes the water/cement ratio was varied from 0.40 to 0.60 in steps of 0.05. It was found that the most satisfactory ratio to attain the desired works cube strength of 41.4 N/mm^2 at 28 days was 0.55. The final mix adopted, therefore, was 1:2:4/0.55.

The concrete used in each test specimen contained rapid hardening Portland cement, and Croxdon gravel 19 mm maximum size, and Croxdon sand 4.7 mm maximum size.

Tests on the coarse and fine aggregates were made to determine the grading and water absorption factors of these dry aggregates. The absorption factor test was carried out after an immersion of the aggregates in water for a few hours. The absorption factors were 1.6% and 1.0% for fine and coarse aggregates respectively. The method followed was as described in the B.S. 812.[177]

The grading of the coarse and fine aggregates in Fig. (7) was determined by the seive analysis described in B.S.812.[177] It was found that the grading of the fine aggregates with maximum size of 4.7 mm down was within zone 3 of the B.S. 882,[178] while that of the coarse aggregates with maximum size of 19 mm down was almost within the B.S. 812 limits. The discrepancy was within the 5-15% allowance for over sized aggregate.

6.5 Control Specimens

At each casting nine 100 mm cubes, two 300 mm high x 150 mm diameter cylinders, three 100 x 100 x 500 mm prisms were made. A set of three cubes were tested at the age of 7 and 28 days and on the last day of the test, to determine the crushing strength of concrete. The cylinders were tested to determine the modulus of elasticity of concrete and the ultimate crushing strength. The flexure test specimens (prisms) served to measure shrinkage strains that occurred before and during the tests, and to determine the modulus of rupture of concrete.

6.6 Mixing, casting and curing

The mix weights were prepared a day in advance using mix proportions of 1:2:4/0.55 by weight. The concrete was mixed for three minutes in a

Liner Cum Flow horizontal pan mixer of 0.28 cubic metre capacity. The mix for each beam was made in two batches. From the first batch one half of the beam and the prism specimens were cast, and from the second batch the other half of the beam, the cubes and cylinders were cast.

Two types of moulds, wooden and steel, were used for the manufacture of the test beams. Steel moulds were used for all the control specimens.

Compaction of the beam was achieved by three Sinex Clamp vibrators attached to the bed of the mould and a Thor 110 V poker vibrator inserted in the mould for each layer of concrete cast. Triton vibrating table was used for the compaction of the control specimens.

For each batch the slump and compacting factor tests were performed as specified in B.S. 1881.[179] The values for the compacting factors and slump for all beams ranged between 0.85 to 0.95 and 25 mm to 112 mm respectively.

The beams were covered with wet hessian three hours after casting. The next day the moulds were stripped and the beams were marked to indicate the position of the supports, the loading points and the location of the Demec locating discs[180] for strain measurements, as can be seen in Fig. (8). Demec locating discs were also fixed on the four faces of each control prism specimen for measurements of shrinkage, and the cylinders to measure the modulus of elasticity of the concrete. Araldite was used to fix the Demec discs on the concrete faces. The first set of measurements was made 24 hours after fixing the Demec discs, The wet hessians were replaced immediately after fixing the Demec discs on the beams and the control specimens. Curing under these conditions continued for six days. The test beams and the control specimens were cured under the same conditions.

6.7 Final Condition of Beams

The beams had a fairly smooth finish on the three faces that were in contact with the mould, and in general a satisfactory finish on the fourth face.

CHAPTER 7

Instrumentation, Test Arrangement and Test Procedures

7.1 General

The loading arrangement was chosen to simulate a uniformly distributed loading. The loads were applied tp the beam through a steel spreader beam at two points, equidistant from the centre of the beam, which produce a third point loading system. The deflections under this sytem of loading are greater than would occur under a uniform load of the same magnitude. If the deflections are compared under the same moment both corresponding deflections will be approximately of the same magnitude.

In the following sections the description of the test arrangement and procedures, the test rigs and instrumentations is given.

7.2 Design of Test Rigs

Static Loading Tests

The static loading tests were run in two different restraining frames: one was a simple frame transferring all the applied loads to the floor and the other a self-restraining frame. The two frames are shown in Plate (2).

The simple frame, a pin base portal frame with a capacity of 150 KN, was made of two round 150 mm diameter bright mild steel columns fixed to the floor, through two heavy footings with MacAlloy bars in strong floor sockets. At the top ends of the columns a large welded plate girder was fixed over a span of 3600 mm. The jack was attached to the middle of the bottom flange of the girder. Two different capacity hydraulic jacks were employed in the investigation, namely 100 KN and 200 KN.

The test beam was placed in a position perpendicular to the longitudinal direction of the girder, with its centre exactly under the centre of the jack. It was supported on rigid non-yielding supports, which were spaced 4570 mm apart as shown in Fig. (2) and Plate (2).

The hydraulic jacks were operated by a Denison model T60 J Console

machine with a capacity of 1000 KN. A ball bearing and socket of the jack transmitted the load, through a spreader beam which was 150 mm wide x 250 mm deep, 1800 mm long and stiffened at the locations of the point loads, to two 75 mm diameter 150 mm long rollers, resting on distribution plates 150 mm x 100 mm x 25 mm thick, which were plastered to the top of the beam. The weight of the spreader was 91 KN. All the applied loads were transmitted from the beam to the reaction supports through 38 mm diameter x 150 mm long rollers, sandwiched between two 150 mm x 100 mm x 25 mm thick plates, one of which was stuck to the soffit of the beam and the other to the steel supports by means of Evostick.

The loading arrangements, supports, conditions and the restraining simple frame which were used in the static tests were also used in the fatigue tests.

Fatigue Loading Tests

The fatigue tests were carried out using Losenhausenwerk Fatigue Testing Machines. These were of two types, SBE 120 and SBE-WE 80, the former having a maximum pump capacity of 120 c.c., and the latter having a capacity of 80 c.c. and an alternating device to operate two jacks at one time pushing in opposite directions.

The loading jacks (EPZ) were of several capacities, ranging from 40 KN to 600 KN, and could be operated by either machine. Only EPZ4 and EPZ10 were used in the fatigue tests.

The maximum dynamic load that could be applied was 80% of the static capacity of the jack. The minimum dynamic load was theoretically zero.

The rate of cycling depended on the deflection of the beam at its range maximum limit, the volume of oil needed for the strokes, the size of the jack, the type of machine, SBE 120 or SBE-WE 80, and the type of frequency required, 1:1 or 2:1. A top speed of 100 cycles per minute, and a low speed down to 5 cycles per minute were possible.

Both machines were used for the fatigue tests in the investigation, with a range of speed of 60 cycles per minute to 100 cycles per minute, and with an average of 90 cycles per minute. The machines could also be used for static loading, using a load maintainer. Safety devices were

available to enable the machine to switch off automatically in case of beam failure or excessive loading.

Sustained Loading Tests

Two types of sustained loading arrangements were designed. In one two beams were loaded simultaneously in a self-straining system, and in the other only one beam could be loaded, with the reaction from the loads being transferred to the floor. They both followed the leverage principle for loading. The leaverage ratio for beams B22, B24 and B25 was 10, and for beams B21 and B13 was 9 (see Fig. 9).

The loads applied were by means of dead weights, some of which were round cast iron, and the others were hexagonal concrete flat blocks made in the concrete laboratory, each of which weighed about 0.45 KN.

Due to the lack of loading area to include all sustained loading tests, it was decided to load beam B22 in the Heavy Structures Laboratory employing the arrangement commonly used. The other four beams were loaded in pairs in the Concrete Laboratory in the self-straining sustained loading system. This sytem is principally the same as the first one, except that the reaction forces are transferred to a heavy Steel Universal beam, as can be seen in Fig. (9).

The problems involved in the system of sustained loading were very few. Firstly, as the reinforced concrete beam deflected by a certain amount the end of the lever, where the weights were hanging, deflected 9 or 10 times as much, depending on the leverage ratio. This problem was overcome by tightening up the nut, bringing the free end of the lever on a level with the other end in a horizontal position, and this was checked with a spirit level. The effects of having a big deflection at the free end were the creation of a horizontal component of loading on the reinforced concrete beam, as well as the bending of the MacAlloy tie. Secondly, in the self-straining system, the cracks could only be checked on the outer side of the beam, and this was not in accordance with the static and fatigue tests in which both sides were checked. However, the results of the one-sided measurement were not significantly different from those obtained by measurement on both sides.

Fig. (9) and Plate (3) show the sustained loading arrangements.

Pull-out Tests

The apparatus consisted of two mild steel plates, as shown in Fig. (5). The bottom plate, with 57 mm diameter hole at its centre, provided the base plate for the concrete specimen, and the top plate, with a 27 mm diameter hole at its centre, formed the reacting member. The two plates were connected by four MacAlloy ties.

The top of the apparatus was anchored to the upper set of jaws of the machine through a MacAlloy bar tied to the centre of the top plate. The lower end of the reinforcing bar, passing through the hole in the bottom plate, was gripped by the lower set of jaws. A packing of 3.18 mm plywood was placed between the concrete and the base.

The pulling load was applied to the lower end of the reinforcing bar by a 500 KN capacity Denison machine.

The slip of the free end of the reinforcing bar at the top of the concrete specimen was measured with a simple apparatus. A dial gauge, with 25 mm travel and a least division of .01 mm was attached to a 75mm diameter round base stand with a hole in the centre passing over the end of the bar and resting on the top of the concrete specimen. The spindle of the dial gauge was in contact with the top end of the bar, and exactly at its centre.

Fig. (5) and Plate (4) show the pull-out test arrangement.

7.3 Instrumentation

For the measurement of deflection, three 50 mm travel dial gauges with magnetic bases were used. These gauges were fixed on a 1830 mm long universal beam, the centre line of which was exactly below the centre line of the reinforced concrete beam. Three square 50 mm x 50 mm x 1.58 mm thick mild steel plates were fixed with Evostick to the soffit of the beam at the middle and at points of applied loads at 761.5 mm on either side of the centre of the beam, for the spindles of the deflection dial gauges to bear against. Near ultimate loads the dial gauges were removed and replaced with a scale and a magnetic stand at the centre of the beam only to measure deflection at higher loads.

On either end of the beam a 25 mm travel dial gauge was used to measure any movement of the steel relative to concrete, as explained

in Section 6.2.3. The spindles were bearing against 50 mm x 50 mm x 1.58 mm thick mild steel plates fixed to the concrete faces near the centres at the ends of the beam.

The strains were measured on the concrete surface with a 200 mm Demountable Mechanical Strain Gauge[180] known as a "Demec" gauge, and stainless steel locating discs, which were 6.3 mm in diameter with a central hole of 0.79 mm diameter. The least division in this gauge was $.99 \times 10^{-5}$. Also a 50 mm Demountable Strain Gauge with a least division of 1.248×10^{-5} was used for the determination of the modulus of elasticity of concrete. The gauge was always checked against a calibrating bar for temperature changes.

For beams A11 and B11 strains on the reinforcing bars were also measured by electrical strain gauges. Two pairs of "6k" felt back paper gauges were used in each beam. The gauges were placed on the top and bottom surfaces of the reinforcing bar at the central section in each case. The gauges were fixed by Araldite, and were then water-proofed with a layer of fibreglass followed by epoxy resin.

The detection and measurement of crack widths were made with a hand microscope of 40 magnifications illuminated from a 6 volt battery cell. The least division of the inner scale of the microscope was 0.01 mm, and it could read a crack width as fine as .001 mm.

Very bright lamps were used to facilitate the detection of the initial visible cracks on the sides of the beam.

The distribution plates on the top of the beams were fixed with plaster of Paris. In the case of sustained loading tests the reaction supports were levelled by applying a layer of plaster of Paris between the supports and the floor.

7.4 Test Procedures

7.4.1 Static Loading Tests

Fourteen beams were tested under static loading. All the beams were subjected to two cycles of loading before the final failure cycle, except beam B18 which was accidentally cracked, and was therefore tested for the final failure cycle only. The first and second cycles were up to design live load, and one and a third times the design live load. In

some cases the beams were loaded below or above these limits.

On the first and second cycles deflection readings were taken at every increment of loading. On the third cycle the deflection readings were taken until the theoretical failure load of the beam was approached when the dial gauges were replaced with a 300 mm scale at the centre of the beam. The deflections were read more frequently before the cracking load was reached, and at bigger increments thereafter.

In some beams, deflections were also read after unloading from a high overload near ultimate load.

Strains were measured with a Demec gauge over a 200 mm gauge length on either face on the central section of the beam at various levels as shown in Fig. (8). In order to locate the neutral axis position accurately, more locating discs were used in the compression zone than in the tension zone. In only two beams, B16 and B17, strains were measured at the level of reinforcement and at the soffit over the entire mid-span. The strains in the reinforcement, over a 200 mm gauge length in the mid-span of the auxiliary beams, were directly measured with a Demec gauge.

Strain measurements were taken during the cycles of loading and unloading at uniform and fewer intervals than was the case with deflection measurements.

On the third cycle the strain measurements were stopped just before the calculated ultimate load was reached.

The use of bright lights, the change in the shape of the load-deflection curve, and the change in strain reading gave a good indication of the initiation of cracking.

With the aid of a hand microscope, frequent measurements were made of the width, number, depth and direction of penetration of the cracks. Different coloured marks were used for the three different loading cycles. At the end of the unloading cycle the widths of the cracks that remained open were recorded.

After the failure of each beam, the ultimate load and the mode of failure were recorded. The crack pattern was taken down on graph paper, including the spacings and lengths of all cracks. The cracks were marked

with a black marker, and the beam was photographed.

7.4.2 Repeated Loading Tests

It was intended to test five beams in this series, but beam A35 was not tested, therefore only four beams were tested under repeated loading. Beams A31, A32 and A33 were designed to contain the same amount of steel, e.g. two 19 mm diameter bars, with different types and strengths of steel. Beam A34 was reinforced with two 16mm diameter bars.

The load ranges of all four beams were chosen to reach a maximum load equal to the design load (applied load + self weight of beam) and a minimum load of half the design load.

Firstly, the beams were subjected to a single static loading cycle up to the design load, during which measurements of cracks, deflection and strains were recorded in the same manner as in the static tests. After unloading on the first cycle the remaining deflections, strains and crack widths were recorded, and the fatigue test was started. In some cases the test was interrupted by mechanical failure of the machine, which lengthened the testing period.

After every few hundred thousands of repetitions, the machine was stopped and the beam was subjected to another static load cycle up to design load. The strain, deflection, number, width and travel of cracks were recorded in the same way as in the static loading tests.

At the end of fatigue loading after 2 to 4 million cycles, as given in Table (1), the beams were loaded statically up to failure, recording all the observations as in the static loading tests.

After failure the beams were marked with a black marker and were photographed.

7.4.3 Sustained Loading Tests

Five beams were tested under sustained design load (live + dead loads) by applying the lever principle as described earlier.

The ages at which the beams were loaded varied between 44 days and 100 days, as indicated in Table (1), depending on the availability of the apparatus and space. As mentioned earlier, it was possible to

load only one beam in the Structures Laboratory, in which the temperature and relative humidity were maintained. The other four beams were loaded in couples in the Concrete Laboratory, where there was a considerable variation of temperature and humidity. Seasonal and daily variations in temperature and relative humidity were noticed, and a daily record of these atmospheric conditions of both laboratories was maintained, as shown in Fig. (10)

The sustained loading was maintained on beams B21 and B23 for a period of 623 days, on beams B24 and B25 for a period of 553 days and on beam B22 520 days, as shown in Table (1).

After the beams were fixed into position, the spreader and the loading arrangement were carefully placed, causing a load on the beam which was sufficiently heavy to initiate cracking in some of the beams. One weight at a time was applied, causing a load on the beam of approximately 4.5 KN. The beams that were tested in pairs were loaded simultaneously. This procedure was continued up to the design load.

Deflections, strains and cracking were recorded before and after the placing of the spreader beam and the loading arrangement, and at every increment of loading up to the design load. The deflection readings were taken every day for the first 4 to 7 months, and every week for the next nine months, and then every month for the rest of the test period. The strain readings were taken daily for the first week, weekly for the first two months and then monthly for the rest of the test period. The crack widths, the extent of travel of the cracks and the number of cracks were measured for the first year at the same intervals as for the strain measurements.

The concrete shrinkage strain on the Demec locating disc, fixed on four faces of a 100 x 100 x 500 mm control prism, were also recorded each time strain measurements were taken.

7.4.4 Control Tests

With each beam tests were carried out to ascertain the compressive strength (cube and cylinder), modulus of elasticity, modulus of rupture and shrinkage.

7.4.4.1 Compressive Strength Tests

Nine 100 mm cubes were cast, and tested in groups of three cubes after 7 and 28 days and at the time of failure of the beam. They were tested

in a dry condition in axial compression in an 1800 KN Avery Compression Testing Machine at a rate of 13.8 N/mm^2 per minute, in accordance with B.S. 1881, 1952.[179]

Two cylinders, 300 mm high x 150 mm diameter, were tested in compression in a 3000 KN Denison Compression and Transverse Testing Machine to determine the modulus of elasticity of concrete. The tests were carried out just after the failure of the test beam, at increments of loading of 50 KN. At each increment of loading the strains were measured over four sets of 50 mm Demec gauge points, which were fixed in such a way that they were parallel to the axis of the cylinder, symmetrical about the mid-height and spaced 90^o apart, The cylinders were capped, three hours after casting, with a thin layer, 3.18 mm thick, of a mortar of high alumina cement and Leighton Buzzard sand. A plane surface was obtained by working down on oiled flat glass on top of the mortar.[181] Measurement of strain was stopped when there was a rapid change in the rate of strains. The cylinders were then taken to failure to determine the maximum compressive strength.

The results are shown in Table (6).

7.4.4.2 Modulus of Rupture of Concrete and Shrinkage Control Specimens

Two 100 x 100 x 500 mm prisms were tested in flexure just after the first cracks appeared in the test beam. The third prism, on which Demec locating discs were fixed for shrinkage readings, were tested after the failure of the beam. The prisms were tested with a 150 KN Denison Transverse Testing Machine, at a rate of 1.78 N/mm^2 per minute, in accordance with B.S. 1881, 1952.[179]

The results are given in Table (6).

7.4.4.3 Bond Tests (Pull-out Tests)

Six 145 x 145 x 190 mm prisms were cast using a similar concrete mix as that used for the main investigation. Three were reinforced with 19 mm diameter Unisteel 80 bars, and the other three with 16 mm Kam 60 bars. They were all reinforced with spiral reinforcement.

The loads were applied in increments of 5 KN in a 500 KN Denison Testing Machine. The slip at the free end was measured with a 25 mm travel dial gauge at every load increment up to failure. Plate (4) shows the test arrangement.

At the end of the test the mode of failure was noted, and the failed specimens were photographed as shown in Plate (4).

Details of the test specimens are given in Table (7).

7.4.4.4 Modulus of Elasticity and Ultimate Strength of Steel

Three 450 mm long specimens for each type and size of bar from the batches of deformed and mild steels used in the investigation were tested and the stress-strain curves were obtained.

The tests were carried out in a 500 KN capacity Denison hydraulic testing machine, using a Huggenberger strain measuring gauge with a gauge length of 25 mm. The results are shown in Fig. (6) and Table (5).

7.4.4.5 Temperature and Relative Humidity Measurement

A daily record of the temperature and relative humidity of the Structures Laboratory and Concrete Laboratory was maintained during the first year of the sustained loading tests. The temperatures were recorded by a Zecol maximum-minimum temperature thermometer. The relative humidity was measured by a Gallenkamp humidity meter. The recorded values are shown in Fig. (10).

CHAPTER 8

Analysis of Stresses in the Reinforcement

8.1 General

In reinforced concrete structures, the stresses in the reinforcement due to applied loads or forces are usually calculated on the basis of either uncracked homogeneous section, or a fully cracked section. The transition zone between uncracked and fully cracked states is usually ignored in design. In this zone the neutral axis position changes gradually, with the applied load between the uncracked value and the fully cracked value.

The centroid of the composite section in the unloaded state, and the position of the neutral axis in a fully cracked state can be predicted by the elastic theory using a specified modular ratio. The neutral axis position at failure can be predicted fairly accurately by the many suggested plastic theories. The method of determining the neutral axis depth at any loading stage in the transition zone will be given in this chapter.

Once the neutral axis depth and the centroid of compression in the concrete are found, the stresses in the reinforcement can be found from the moment compatibility at any load level.

8.2 Formulation for the Calculation of Stresses in the Reinforcement of a Simply Supported, Singly Reinforced Concrete Beam.

The proposed method is based on experimental analysis of the position of the neutral axis. It is, therefore, a semi-empirical analysis whereby the neutral axis position is a function of the varying applied moment. The assumptions used in this formulation are as follows:

1) Plane section remains plane after bending, i.e. a linear strain distribution is assumed in the concrete in compression at all stages of loading.

2) The depths of the neutral axis of strain and stress may be derived from the assumption that the neutral axis depth is a linearly decreasing function of the moment from uncracked stage up to a value of K' x the ultimate moment, which represents fully cracked state. After this point, it is assumed to be constant until near failure, as

shown in Fig. (11). The calculations of the neutral axis depths for the uncracked as well as the fully cracked sections are based on the elastic theory.

The uncracked neutral axis depth measured from the extreme top fibre is calculated from: (See Appendix A)

$$d_{n\ unc} = d - \frac{d/2 + (m - 1)\ p(d - d_1)}{1 + (m - 1)\ p} \qquad \ldots\ldots\ldots\ldots(21)$$

and the cracked neutral axis depth from: (See Appendix A)

$$d_{n\ cr} = d_1 \sqrt{m^2p^2 + 2mp} - mpd_1 \qquad \ldots\ldots\ldots\ldots(22)$$

where m is the modular ratio; p is the steel ratio; d_1 is the effective depth.

For $o < \frac{M}{M_u} \leq K'$

the neutral axis depth is: (See Fig. 11)

$$d_n = d_{n\ unc} - \frac{(d_{n\ unc} - d_{n\ cr})}{K'} \frac{M}{M_u} \qquad \ldots\ldots\ldots\ldots(23)$$

For $K' < \frac{M}{M_u} < 1.0$

$$d_n = d_{n\ cr} \qquad \ldots\ldots\ldots\ldots(24)$$

3) The distribution of compressive stresses in the concrete is assumed to be of the simplified shape considered in Fig. (12). The strain at the maximum stress ($\mathcal{K}U_w$) is equal to $e_o = \frac{\sqrt{U_w}}{5000}$ and the strain at failure in the uppermost top fibre in concrete is 0.35%. The position of the centroid of the resultant compressive force α can be found, by trial and error, from the strain and force compatibility: (See Fig. 12)

for $e_c \leq e_o$

$$\alpha = 0.33 \text{ and } 0 < f_c \leq U_w$$

for $e_c \geq e_o$

$$\alpha = \frac{3e_c^2 - 3e_c e_o + e_o^2}{6e_c^2 - 3e_o e_c} \qquad \ldots\ldots\ldots\ldots(25)$$

$$f_s = \frac{M}{A_s (d_1 - \propto d_n)} \qquad \ldots\ldots\ldots\ldots(26)$$

$$x = \frac{e_o}{e_c} d_n \qquad \ldots\ldots\ldots\ldots(27)$$

$$x + y = d_n \qquad \ldots\ldots\ldots\ldots(28)$$

$$f_c = \frac{f_s A_s}{(x/2 + y)b} \qquad \ldots\ldots\ldots\ldots(29)$$

and $f_c = \gamma U_w$

4) The stresses in the steel reinforcement are calculated from the equilibrium with applied moment

$$f_s = \frac{M}{A_s (d_1 - \propto d_n)} \qquad \ldots\ldots\ldots\ldots(26)$$

The factor K,' in assumption (2) § 8.2, is determined from the plot of the experimental results of the neutral axis depth with the moment.

8.3 Calculation of Stresses in the Reinforcement using Experimental Results

8.3.1 Static Loading Tests

In the calculation of stresses in the steel reinforcement the position of the neutral axis, and the centroid of the compressive force in the concrete, were the main parameters, varying with the magnitude of the applied load. A computer programme was developed incorporating the following procedure for the calculation of stresses in the steel reinforcement. (Reference should be made to Fig. 13):

1) The average neutral axis position of strains for each increment of loading is located by passing the best fit line through the experimental strain readings in the compression zone.

2) The neutral axis of stress is assumed to be coincident with the neutral axis of strain, neglecting the effect of shrinkage.

3) The centre of compression is assumed to be a function of the load and thus a function of the compressive strains.

4) Assuming a parabolic distribution of stresses up to a strain

$e_o = \frac{\sqrt{U_w}}{5000}$ in the uppermost top fibre of the concrete, and a parabolic and rectangular distribution at loads producing strains higher than e_o, the centroid of compression at any level of loading can be found from geometric consideration.

5) The maximum strain in the concrete at failure is equal to 0.35%.

6) The total force in the reinforcement is calculated from the moment compatibility relationship at any applied moment. Thus the stress in the steel is found by considering the amount of the reinforcement.

8.3.2. Sustained and Repeated Loading Tests

In the analysis of stresses, in these long term tests, the effects of creep and shrinkage on the distribution of strains in the central section are taken into account. With reference to Fig. (14) the following assumptions are made:

1) Upon instantaneous loading the neutral axes of stress and strain coincide.

2) Both neutral axis depths of stress and strain increase with time (under sustained and fatigue loading) and then remain constant.

3) After a period of time the stress neutral axis and strain neutral axis do not coincide, due to shrinkage and effects of stresses in the concrete tensile zone.

4) For the calculation of stresses, the stress neutral axis due to creep is equal to the strain neutral axis, obtained by deducting a uniform shrinkage strain from the measured over-all strain due to creep and shrinkage.

5) The stress distribution in concrete in compression is assumed triangular (under sustained and fatigue design load) and from this and the position of the neutral axis, calculated in (4) above, the value of the steel stress is obtained.

8.4 Experimental and Theoretical Steel Stresses under Short Term Static Loading

It has been mentioned above that the determination of the neutral axis position at any moment level is required a priori for the calculation of steel stresses. The variation of the depth of the neutral axis with

increasing applied moment can be seen in Figs. 15-18. In these figures the ratio of the actual neutral axis depth to the effective depth is plotted against the ratio of the applied moment to the actual ultimate resistance moment of the beam. It can be seen from the results that a bilinear relationship can be fitted through the points in the manner described in § 8.2, which will give a value of K'= 0.3. This value of K'can be used in the formulae given in § 8.2 to predict the stress in the steel reinforcement.

Figs. (19) and (20) show the variation of the theoretically calculated steel stresses, with the total applied load (dead load + live load) superimposed on the experimental stresses, which are calculated using actual experimental neutral axis depths.

Fig. (21) shows the variation of the actual steel strains in the central section of the constant moment region, with the applied loading for the three cycles of loading. These strains were measured with electrical strain gauges. On the same graph, the load-strain curve, calculated using the measured neutral axis depths obtained from the strain distribution as shown in a typical graph in Fig. (22), is also included.

In Fig. (23) another comparison is made, in the case of auxiliary beams, between calculated stresses based on the actual strain measurement on the surface of the reinforcement, and the calculated stresses based on the actual measured neutral axis depths. Only the results of beam B_{st1} are considered here, since the measured strains of beam B_{st2} gave non-uniform results.

From all the relationships and graphs listed above, the following general conclusions about the stress in reinforced concrete beams can be derived.

1) The variation of the average neutral axis depth with load was independent of the type (plain or deformed) of steel used, and thus the stiffening effect of concrete between cracks for all beams was almost of the same order, regardless of the various surface characteristics of the different steel reinforcing bars. Figs. (15) - (18) show that there is a transition zone between the uncracked and the cracked states, which can be estimated fairly accurately by a straight line which gives a K'value of 0.3. The line representing the fully cracked state of the

beam can be taken as a lower bound in most of the beams.

2) There was some scatter in the position of the neutral axis. This was because of the scatter in the estimation of the line of best fit, which passed through the strain values at different locations through the compressive depth of the beam. Also in these figures it can be seen that in most cases the depth of the neutral axis increases slightly during the second and third cycles of loading. This might be attributed to the cumulative effect of creep.

3) The neutral axis depth in the cracked state was found to depend mainly on the percentage of the steel, the modular ratio and the strength of concrete. The design strength of concrete was the same for all the beams, however there was a variation from the design value in some cases. The effect of the variation of strength is obvious in the cases of beams A11,A12 and A13. Beam A11 showed a greater depth of the neutral axis than the other two beams, due to the lower concrete strength.

4) The extent of cracking is another factor which can affect the average depth of the neutral axis. A study of the crack patterns of beams A11,A12,A13,A14 and A15 indicated that the extent of cracking, the height of travel and the number of cracks within the 200 mm gauge length influenced the position of the neutral axis.

Also the direction of movement of the cracks had a great bearing on the strain distribution. On increasing the loading a crack may change direction and may become outside or inside the 200 mm gauge length.

5) With reference to Figs. (19) and (20), the theoretical and experimental plots show a uniform and linear relationship between load and stress in the steel, which can be extended back to the origin.

6) The theoretical and experimental curves agreed at all load stages up to and beyond the design load. There was a slight divergence at relatively high loads. At these loads the theoretical values of stresses were slightly lower than the experimental values.

7) The actual stresses measured, using electrical and mechanical strain gauges, as shown in Figs. (21) and (23), were always lower than

the stresses calculated in accordance with § 8.3.1. In Fig. (21) the stiffening effect of concrete before cracking can be seen to affect the tensile steel strains.

It was intended to calculate values of α (centroid of compressive force) in beams with exposed steel and one with electrical strain gauges. However, when using the measured steel strains the values of α obtained were inconsistent.

8) The magnitude of the maximum stress (δU) in the stress block depends on the position of the neutral axis, the rate and duration of loading and the quality of concrete. The values of δ varied from 0.75 to 0.90.

9) Fig. (21) shows that when the load was removed the steel stress did not go back to zero, but some residual tensile stresses developed in the steel. On the second application of loading to a magnitude equal to or higher than that of the first application, the relationship was again that of the virgin cycle.

10) At the ultimate load condition the stress in steel in most of the beams exceeded the yield point or proof stress of the material.

Column (14) in Table (8) gives the ratios of the calculated steel stresses at failure to the actual steel stresses as measured from tnesion specimens tested in air. The calculated steel stresses at failure were computed in accordance with the Draft Code of Practice[23] with the assumptions used in § 8.3 and Fig. (13), and a value of δ of $\frac{2}{3}$. It can be seen from the values of these ratios that there is an enhancement in the steel stress over the yield stress of up to 27%, as in the case of beam B19. In beams reinforced with the prestressing wires and strand the ratios were based on the nominal strength of these steels. The range of increase in stress over the yield stress was from 0 to 16% for beams reinforced with mild steel bars, from 12 to 20% for beams reinforced with Kam steels, and from 0.99 to 17% for beams with Unisteel bars, the low value being for the beam with exposed steel. In beam B16, which was reinforced with crimped prestressing wires, the increase was 20%, which indicated that the bond between steel and concrete was maintained. However, in beam B17, with prestressing wires, the ratio of the failure stress to the yield strength was very low, which indicated that failure was not a tension

failure of steel, but probably a bond failure resulting in crushing of concrete.

In general, the amount of steel for these under-reinforced beams did not show any particular trend as regards the hyperstrength of the beams.

Therefore, neglecting the partial safety factors on the materials, The Draft Code method can be utilised in predicting the stresses in steel reinforcement at failure. It is suggested that this method can be used in conjunction with the proposed method in predicting the stresses in the reinforcement at any load level even at ultimate.

The effects of long term loading (sustained and fatigue loading) on the stresses in the steel reinforcement will be discussed in Chapter (10). The initial steel stresses which are recorded in Tables (9) and (10) were calculated by assuming a triangular concrete stress distribution and using the experimental neutral axis depths.

CHAPTER 9

Behaviour of Beams under Static Loading

9.1 General

Design procedures for predicting the behaviour of beams, in terms of cracking and deflection, under static loading are presented. The reliability of the procedures is indicated by comparisons between computed results and experimental data of this study for 12 beams reinforced with different types and percentages of steel.

A detailed study is presented on the effects of static loading on cracking, deflection, ultimate strength, steel stresses and concrete strains. The effects of using high tensile steel (with different strengths and surface characteristics) on the three limit states are also discussed.

9.2 Limit State of Cracking

9.2.1 General

In § 3.2 and § 3.4 limits on crack widths have been established following the recommendations given by the C.E.B.[41] and the Draft Unified Code[23] for the different conditions of exposure. In this section formulae for the prediction of the maximum crack width on the first and second cycles of loading are suggested. A formula for the determination of the maximum remaining crack width is also given. These formulae are useful for the design of concrete members reinforced with different types, percentages and sizes of high tensile steel.

In the light of these formulae the experimental results are analysed and a detailed study of the crack formation and crack width under static load is presented. A comparison is made between the computed and experimental crack widths. The agreement between the computed results and experimental data indicates the reliability of the proposed methods in predicting the crack widths of concrete members reinforced with high tensile steel.

In the analysis of cracking, engineering judgment rather than a statistical approach was adopted. However, regression lines were plotted to establish the linear relationships between the major variables which were included in the formulation.

9.2.2 Proposed Crack Width Formulae

In § 4.2 the various parameters involved in the spacing and width of cracks were reduced into three major parameters:

1) stress in the steel reinforcement
2) concrete cover
3) distribution of reinforcement within the effective concrete area

In the present investigation the parameters which would directly affect the crack width are:

1) the stress in the steel reinforcement (f_s)
2) the stiffening effect of concrete before cracking ($\frac{K_s}{p}$)
3) the percentage of steel reinforcement (p)
4) the type of steel reinforcement (surface characteristics) (R)
5) the effects of the loading cycles subsequent to the first cycle
6) the concrete cover (C)

The concrete cover was kept constant for all the beams. The value of the effective reinforcement ratio (P_e), the bar size and hence the ratio (D/P_e) were varied.

9.2.2.1 Crack Width: First Cycle

On the first cycle of loading the concrete cracks when the stress in the steel is equal to a certain magnitude (f_{sc}). The magnitude of this stress depends on the amount of tension steel in the beam. This stiffening effect of the concrete before cracking has a great influence on the crack width and it can be suggested that the following expression can be used for predicting the maximum crack width on the first cycle:

$$W_{max_1} = RC\left(f_s - \frac{K_s}{p}\right) \times 10^{-6} \qquad \text{.....(30)}$$

where W_{max_1} - maximum crack width (mm) at the level of reinforcement on the first cycle

R - coefficient depending on the surface characteristics of the reinforcing steel ($^1/_{N/mm^2}$)

C - concrete cover (mm) at the reinforcement level

f_s - stress in steel (N/mm^2) calculated in accordance with § 8.2.

K_s - constant depending on the strength of concrete and related to the steel stress at cracking load (N).

p - percentage of steel (percent)

9.2.2.2 Remaining Crack Width

In a reinforced concrete member, when the applied load exceeds the cracking load on unloading a certain number of cracks will not close. However, if the beam is severely cracked then most of the cracks will not close. The magnitude of the maximum remaining crack width depends on:

1) the steel stress at the maximum load applied on the previous cycle
2) the concrete cover

It can be suggested that the maximum remaining crack width can be expressed as follows:

$$\Delta W_{max} = k_1 C (f_{sp} - k_2) \times 10^{-6} \quad \text{.....(31)}$$

where ΔW_{max} - maximum remaining crack width (mm)

k_1 - proportionality constant ($1/N/mm2$)

C - concrete cover

f_{sp} - permissible steel stress ($\frac{f_y}{1.8}$) (N/mm^2)

k_2 - design steel stress (N/mm^2) under the effect of which all the remaining cracks will be closed.

9.2.2.3 Crack Width: Second Cycle

The stiffening effect ($\frac{K_s}{p}$) of concrete in the tension zone, which influences the crack width on the first cycle is no longer available for the second cycle, and hence can be neglected. The cracks start increasing in width as soon as the load is applied. The crack width increases above that value which remains after unloading at the end of the first cycle. It is suggested, therefore, that the maximum crack width on the second cycle of loading can be expressed as the combination of equations (30) and (31), but neglecting the term ($\frac{K_s}{p}$) as in the following:

$$W_{max_2} = C \left| f_s (R + k_1) - k_1 k_2 \right| \times 10^{-6} \quad \text{.....(32)}$$

where W_{max_2} - maximum crack width (mm) at the level of reinforcement on the second cycle

k_1 - constant related to the maximum remaining crack width ($^1/N/mm^2$)

k_2 - design steel stress under the effect of which all the cracks will be closed (N/mm^2)

The other terms have the usual meanings.

9.2.3. Determination of the Coefficient (R) from Test Results

In equation (30) the influence of the bond characteristics of the reinforcement is included in the coefficient (R), which had different values for different surface characteristics. The surface characteristics tend to modify the influence of steel stress and concrete cover on cracking.

The values of the coefficient (R) can be determined from the slopes of the best fit lines through the results correlating crack width at the level of reinforcement with steel stress for the three categories of beams as shown in Figs. (24) and (25) for the first cycle and in Figs. (26) and (27) for the second cycle.

The values of R obtained were:

Beam Category (Type of steel)	Values of (R)	
	First Cycle	Second Cycle
Deformed bar	16.0	12.9
Plain bar	18.6	13.5
Wire and Strand	25.0	24.2

In the comparison of the results of the different types of bars, it was found that the maximum crack width for plain round bars was only 7 percent greater than that for deformed bars. The increase in width for the wires and strands over that of deformed bars was 67 percent. Snowdon[43] reported 12 percent wider cracks for the plain bars, while the C. and C.A.[45] found the difference to be 13 percent.

9.2.4 Determination of the Constants K_s, k_1 and k_2 from Test Results

The stiffening effect of the uncracked concrete in the tension zone on the first cycle of loading can be obtained from the relation

between the stress in steel at first cracking, and the percentage of steel. This relation for the present investigation is shown in Fig. (28). In this figure the stresses (f_{sc}) at cracking moment, as obtained from the deflection curves, are plotted against the percentage of steel reinforcement (p) for an average concrete strength of 41.4 N/mm^2. It can be seen that the stress at first cracking is inversely proportional to the steel percentage and the relationship is of the form:

$$f_{sc} = \frac{K_s}{p}$$

where $K_s = 69.5\ N/mm^2$ for $U_w = 41.4\ N/mm^2$

The value of K_s depends on the tensile strength of the concrete which is related to the cube strength.

Considering this effect, the steel stress at first cracking for each beam was deducted from the total steel stresses for loads higher than the cracking load. The results were plotted against the maximum crack widths and lines of best fit were passed through the points. Figs. (24) and (25) show the plots for the three categories of beams as designated by the type of steel viz. deformed bars, plain bars, and wires and strands. In these figures it can be seen that the relationship between the maximum crack width and the steel stress beyond the cracking load stress is linear, and it starts from the origin.

The constants k_1 and k_2 can be obtained from the relationship between the maximum remaining crack width and the stress in the steel at design load as shown in Fig.(29). Even though a big scatter can be observed to occur, the trend was a direct proportionality between steel stress at design load and the remaining crack width. Best fit lines were passed through the experimental points and the following values for k_1 and k_2 were obtained:

	Steel Level	Bottom Edge
k_1 ($^1/_{N/mm^2}$)	5.28	5.00
k_2 (N/mm^2)	138.00	41.40

9.2.5 Relation between Crack Width and Concrete Cover

The effect of concrete cover C (the distance from the point of measurement of cracks to the surface of the nearest reinforcing bar)

on the crack width was studied as follows:

The average concrete surface tensile strains (e_t) were extrapolated from the linear strain distribution diagram in the compression zone. The crack slopes (W/e_t) were obtained from the slopes of the regression lines of the plots of the maximum and average crack widths against the average concrete tensile strains at the level of measurement of the cracks. Typical graphs of W v.s. e_t are shown in Figs.(30) and (31) for plain and deformed bars.

The slopes of W/e_t were plotted against the cover (C) for all the beams. The effect of the distance (C) for both deformed and plain bars can be seen in Figs. (32) and (33). For the same value of (C) the results showed a big scatter in the values of W/e_t. However, the scatter fell within the scatter reported by the C. and C.A.[45] based on the results of 133 test beams, and the relationship between the crack width and concrete cover can be assumed to be linear. A similar conculsion has been reported by Hognestad[36] and Broms,[138,139] by plotting the average and maximum crack widths against the concrete cover.

9.2.6 Relation between Crack Width and Steel Stress

9.2.6.1 Comparison between Theoretical and Experimental Results

In Figs. (34-37) a comparison was made between the calculated and measured crack widths. The theoretical lines were superimposed on the experimental results for the first and second cycles of loading. The theoretical values agreed satisfactorily with the experimental ones for both cycles. In only three cases did the theory underestimate the maximum crack width on the first cycle. This resulted from experimental scatter in the magnitudes of the maximum crack widths. However, beam B17 was heavily cracked and failed due to bond slip. The same reasoning may be applied to the deviation observed between experimental and theoretical results on the second cycle.

In Table (11) a comparison was made between the maximum crack widths calculated using the Draft Code formula and those based on the proposed formula (Eqn. 30). It can be seen that the Draft Code formula under-estimated the measured maximum crack width in most cases, while the proposed formula showed a good agreement. Another comparison with the equation recommended in the Code reveals that the Code has recommended the use of plain and deformed bars and reinforcing wires, but it does not give any indication of the difference in the crack

control characteristics of each type of reinforcement. The proposed formulae in § 9.2.2. indicate that the crack control of the three types of reinforcement depends on the characteristics of the reinforcement. The different values of (R) in the equations in § 9.2.2 account for the different surface characteristics of the reinforcement.

In Table (11) the measured average and maximum remaining crack widths of the beams tested under static load are given. The maximum remaining crack widths calculated according to Equ (31) are also given. It can be seen that the steel stress at design load has a great influence on the remaining crack width. It can also be seen that the values of the maximum crack width calculated according to Equ.(31) agreed fairly well with the measured ones.

9.2.6.2 Behaviour of Test Beams

Before any discussion of the results is undertaken it is necessary to define the maximum and the average crack width used in the analysis of the results. In this investigation the maximum crack width is that of the largest crack that occurs at any loading stage i.e. it need not necessarily be the same crack. The average crack width is the total widths of cracks divided by the total number of cracks at any loading stage. There are four values which should be considered in this investigation. These are the maximum and average crack widths at both the bottom edge and the steel level.

The crack widths were measured for all the cycles of loading, but not while unloading.

The graphs shown in Figs. (38-49) give the relationship between the measured crack width and the calculated steel stress for the virgin cycles (first cycleand loading stages of the second and third cycles above the maximum load of the first cycle) from near cracking load up to near failure. The sudden increase in the crack width as seen on the graphs was due to the unloading and reloading effect.

The steel stresses were calculated using the measured depths of the neutral axis (§ 8.3). This was adopted to avoid the use of assumed values of the modular ratio, and allow the use of the proposed method (§§ 8.2) in the calculation of the average steel stresses. These figures show the effects of the major variables used in this investigation on the crack widths. These variables are the type of steel, percentage

and diameter of the reinforcing bars and the stress in the steel.

Figs. (38) and (39) respectively give the relationship for the maximum crack width at the bottom edge and the level of steel in beams reinforced with equal amounts of steel. Beams A11, A12 and A13 have 1.44 percent of steel, and beams A14 and A15 have 1.01 percent of steel. The comparison is made on the basis of the type of steel used in these five beams. The behaviour showed a direct relationship between the maximum crack width and the steel stress beyond the cracking load stress, as has been predicted theoretically in § 9.2.4.1. The importance of steel stress on crack width has been observed by other investigators.[36,41,45,146,149]

In comparing beam A11, reinforced with plain round bars, with beams A12 and A13, containing deformed bars, it can be seen in Figs. (38) and (39) that the cracks were of comparatively equal magnitude from stresses as low as those corresponding to initiation of cracking up to about 200 N/mm^2. After this the maximum crack width in beam A11 increased more rapidly than in the case of the other two, reaching a maximum (at the bottom edge) of 0.3 mm at about 220 N/mm^2. Beams A12 and A13 reached the same value of crack width at steel stresses of 320 N/mm^2 and 300 N/mm^2 respectively.

Stresses in Steel (N/mm^2) (For Crack Widths at Bottom Edge)

Beam Mark	A11	A12	A13	A14	A15
% Steel	1.44	1.44	1.44	1.01	1.01
Type of Steel	Plain	Deformed	Deformed	Deformed	Deformed
Crack Width					
0.2 mm	180	245	194	345	400
0.3 mm	220	320	300	510	483

The steel stresses reached in beams A11, A12 and A13 at a crack width of 0.2 mm at the bottom edge were about 180, 245 and 194 N/mm^2 respectively (see the table above). Even though the strength of concrete in beam A11 was much below that of beams A12 and A13, the three beams showed similar behaviour, and the divergence at higher load levels was due to the typical behaviour of beams reinforced with plain round bars. At high loads, in beam A11, the increase in width was concentrated in the maximum crack at the section at which the concrete eventually failed in compression as can be seen in Plate (5).

In beams A14 and A15 the reduction in the area of steel and bar size resulted in the $^{D}/P_{e}$ ratio and thus it was expected from the theoretical consideration in § 4.2 to obtain higher crack widths than those for beams A11, A12 and A13 at the same steel stress. However, the experimental results from the present investigation showed lower values of maximum crack widths in beams with higher values of $^{D}/P_{e}$.

For a crack width of 0.2 mm, at the bottom edge level, the steel stresses for A14 and A15 were about 345 and 400 N/mm^2 respectively. All the five beams (A11 - A15) developed similar cracking patterns with sensibly equal number of cracks, but the crack widths were smaller for lower percentages of steel.

Thomas[146] pointed out that the steel stress for zero crack width increased as the percentage of steel decreased, and hence this effect tended to keep the cracks small at working stresses for low percentages of steel. The same conclusion can be drawn from the results given by Clark[149]. These observations confirm the validity of the assumptions used in formulating equation (30).

In the present investigation at the same stress levels smaller crack widths were observed in beams A14 and A15 (with Kam steel of 1.01%) as compared with beams A11 (with mild steel of 1.44%), A12 and A13, (with Unisteel of 1.44%). The superiority of Kam steel bars in controlling crack widths may be further attributed to two probable reasons: the smaller bar diameter and good bond characteristics. Kam steel bars have surface deformation pattern with the transverse lugs perpendicular to the axis of the bar, whereas in Unisteel bars the lugs are oblique. Pull-out tests (Appendix B) on specimens containing two types of steel indicated the superiority of the steel with perpendicular lugs as far as initial slip and working stress range are concerned.

According to the Draft Code[23] two conditions must be fulfilled a) the maximum crack width for normal conditions of exposure is limited to 0.3 mm, b) the strain in the tension reinforcement, neglecting the stiffening effect of concrete in the tension zone, is limited to $\frac{0.75f_y}{E_s}$ or 0.0015, whichever is the lesser. To comply with the first condition in this investigation it can be seen in Figs. (38-39), (42-43) and (46-47) that the range of stresses in the

reinforcement (including all types) is between 250 - 511 N/mm^2 at the bottom edge, and between 500 - 700 N/mm^2 at the level of steel. With these ranges of stresses the strain in the reinforcement, assuming E_s = 200 KN/mm^2, ranged between 0.00125 to 0.00350 and in most of the beams exceeded the value (0.00150) given in (b) above. The value of 0.0015 in the Code suggests that the maximum yield strength (f_y) should be limited to about 400 N/mm^2. However, the findings in this investigation suggest that steels with very high yield strengths can be used without violating the first condition of the Code.

In practice most engineers are unwilling to accept cracks that are 0.3 mm wide permitted by the Draft Code[23] for unprotected structures under normal conditions of exposure. However, the C.E.B.[41] recommends a limiting value of 0.2 mm for these types of structures which may be regarded as reasonable.

In Figs. (40) and (41) the average of the crack widths are plotted against the stress in steel. It is obvious that the average crack widths at all stress levels for beams A14 and A15 were smaller than those for the other beams, and they also appeared to be increasing more uniformly.

Figs. (42) and (43) show the maximum crack width at the bottom edge and steel levels, for beams reinforced with different types and percentages of steel. Beams B11, B12, A13 and B19 have approximately the same design load, while beam B15 has a lower design load than the rest. In considering the results of beam B11, B12 and A13, it can be seen that the type of bar (plain or deformed) and the percentage of steel did not have significant effects on the rate of increase of crack width.

An objection might be raised that the conclusion regarding the percentage of steel is based on various sizes of bar diameters. However, the findings of C. & C.A.[45] and Hognestad[36] confirmed that even when the bar size is kept constant the amount of steel reinforcement does not affect the rate of increase of crack width. On the other hand, Thomas[146] and Clark[149] reported a higher rate of increase of crack width with lower percentages of steel.

Beam B15, with Kam 90 steel deformed bars, showed lower crack widths, at the bottom edge level, than the other beams. Beam B19 with Bristrand 100, had a better cracking control, when considering

the crack width at the bottom edge, than B11, B12 and A13, and even better control than B15 when considering the crack widths at the steel level up to about 385 N/mm^2. When the average crack widths were compared, Figs. (44) and (45), beam B15 was superior to all the other beams. Beam B19 also showed a good crack control. The superiority of these two beams (B15 and B19) to the rest of the beams (B11, B12 and A13) was due to the low percentage of steel which affected the steel stress at first cracking. The steel percentages for beams B15 and B19 were 0.564% and 1.09% respectively, and those for beams B11, B12 and A13 were 2.58%, 1.96% and 1.44% respectively.

Figs. (46) and (47) show a comparison of the maximum crack width of beams, reinforced with wire, strands and bars, and which have similar design ultimate loads. Fig. (46) reveals the superiority of the bar over other types of steel. Beam B16, with crimped prestressing wire, showed a better crack control than beam B19, which was reinforced with Bristrand 100. This may possibly be explained by the larger number of small wires used in this beam, and consequently the smaller area of concrete, in the tension zone, surrounding each bar. It may also be explained by the lower steel stress at first cracking, due to a smaller area of steel. Beam B17, with four 8 mm diameter plain prestressing wires, and beam B18, with four 7.94 mm diameter prestressing strand, showed much wider cracks than beam B15, B16 and B19. This may be because of the fewer and widely spaced cracks that are likely to form with this type of steel due to less efficient bond (see Fig. 50).

In the present investigation B17 and B18 showed similar crack widths up to a steel stress of 750 N/mm^2. The great difference after this level was due to unloading and reloading in beam B17. Hajnal Konyi[26] reported a crack width of 0.25 mm at an average steel stress of 550 N/mm^2 in beams reinforced with 28-12 gaugewires, and a steel area of 154 mm^2. At the same crack width the stress in this investigation was about 360 N/mm^2 in beam B17, with a steel area of 201 mm^2.

Abeles[182] found that the maximum crack widths were greater in a beam reinforced with rough surface wires than in the beam with strands. This was attributed to the smaller number of cracks due to the less satisfactory bond efficiency of prestressing wires. The cracks were much wider in a beam reinforced with very smooth surfaced wires.

Figs. (48) and (49) show the average for beams with wires, strands and bars. Again the crimped prestressing wires (B16) showed a comparatively good control over cracking, while beam B15, with deformed bars, showed the best crack control.

The relationship between the maximum and average crack widths with increasing steel stress over the whole range of loading can be seen in Figs. (51) and (52) to vary essentially in a random manner. The average values of the ratio, maximum crack width/average crack width, were 1.96 and 1.86 for deformed and plain bars respectively. These ratios, obtained at the level of steel, were greater than that at the bottom edge with a value of 1.7 for both types of steel, For the purpose of clarity only five beams were included in the figures. For beams reinforced with wires and strands, the average ratios over the whole range of loading for the steel level and the bottom edge were 1.7 and 1.6 respectively.

The ratios reported by other investigators[36,43,44,45,138,139,149,183] ranged between 1.5 and 2.0.

9.2.7 Relation between Crack Width and Bar Diameter (D) and Effective Reinforcement Ratio (P_e)

In the present tests the value of the bar diameter (D), the effective reinforcement ratio (P_e), and the ratio (D/P_e) were varied. In Fig. (53) a plot is shown of the ratio (D/P_e) with the measured maximum crack width. No significant trend can be observed of the effect of the ratio D/P_e on the crack width. Similar observations have been reported by other investigators.[36]

The figure shows the suggested relationship of the C.E.B. theory[36] to be linear, and in comparison with test results it is far from true. The direct relation of crack widths with D/P_e ratio given by the C.E.B. seems to over-estimate the effect of the diameter (D) and the effective reinforcement ratio (P_e). It can be concluded, therefore, that the ratio D/P_e is an insensitive variable as has been indicated in (§ 4.2.2).

9.2.8 Relation between Crack Width and Crack Spacing

The classical theory predicts the average crack widths from the assumption of all the slips that would occur between the steel and concrete over the average spacing. If this relationship is being

sought from the results of the present investigation, a relationship pf the form given in Fig. (54) is obtained. It is apparent that there is no definite trend from the relationship. However, a linear direct relationship was assumed in the classical slip theory. The graph was plotted for a steel stress of 207 N/mm^2, which was assumed to be the limit after which no more cracks formed. One important fact that could be deduced from this figure was that there was a significant bond between the cracks at this level of stress Rush and Rehm[57] pointed out that this relationship depended on the magnitude of the steel stress, the existence of secondary cracks and the concrete strength.

Broms[138] has shown that the theoretical minimum spacing of cracks is equal to the concrete cover (the distance from the point of measurement to the centre of the bar). The theoretical average spacing is 1.5 times the theoretical minimum spacing. However, tests carried out by Broms showed that the average spacing was 2.0 times the minimum spacing. Assuming the latter to be true, the results of the present investigation gave different values from the calculated values when the plain and deformed bars only were considered (the level of measurement was at the bottom edge). The calculated average spacing was equal to 120 mm as compared to the experimental average value of 102 mm. (see Table 11), which was comparable to the value of 1.5 x the minimum spacing, i.e. an average of 90 mm. In considering the results of these beams and beams B16, B17 and B18, reinforced with prestressing wires and strands, a factor, K, should be used, as has been suggested by Morita[152], to take into account the different bond characteristics of the different types of steel.

Crack widths and spacings are inherently subject to great experimental scatter[36,51,73,143,183] and the variability might be as high as $\pm$ 50% from the average.[36] Beams A11, A31, B11 and B21 with plain round bars showed the greatest scatter at all the loading stages. This was so because of the variability of the formation of the secondary cracks, which were included in the evaluation of the average crack spacing. Due to the wider spacing of aracks in beam A11 (see Table 11), the crack widths were observed to be relatively greater than in the other beams with the same type of steel.

9.2.9 Cracking Pattern

In the present tests cracks were usually detected when they had a width of about 0.015 to 0.02 mm, which was wide enough to be

visible to the unaided eye of an experienced observer. However, the cracking load was established by adopting a bilinear relationship of the load-deflection curves. On this basis cracks occurred at calculated steel stresses (based on experimental neutral axis depth) ranging from 20-100 N/mm^2 depending on the amount of reinforcement employed in the beam. The flexural tensile strength of concrete, based on the above, was found to vary from 2.0 to 4.0 N/mm^2.

For all the test beams, the development of the cracking pattern was recorded at several load stages. At the cracking load, as defined above, in a typical beam, a number of cracks occurred simultaneously at a spacing which averaged about 300 mm, though subject to a great variation. This spacing was reduced as the load was increased, and more cracks developed. There was a tendency for the mean spacing to reach a minimum value, and virtually no more cracks formed after a stress of 200-250 N/mm^2 was reached. On increasing the load above this limit the cracks increased in width and in length. In most of the beams with deformed and plain bars, the mean spacing reached a minimum value of about 100mm, while in those beams with plain prestressing wires and prestressing strands the cracking patterns showed widely spaced cracks with an average spacing between 150-200 mm. The behaviour of the beam reinforced with Bristrand 100, B19, was similar to that of the beams reinforced with deformed or plain bars.

The cracking patterns at failure, for beams reinforced with different types of steel, are shown in Figs. (55) and (56). It can be seen that in some of the beams with deformed bars, small cracks, usually called secondary cracks, were observed between the well established main cracks. These cracks extenied just above the level of steel and were smaller in width than the primary ones. Some of these cracks formed at the steel level, and propagated upward towards the neutral axis. With increasing load all the cracks became wider and longer, reaching the level of the theoretical elastic neutral axis, based on cracked transformed section. In beams with deformed bars or prestressing wires or strands, most of the cracks extended beyond the elastic neutral axis level towards the theoretical plastic neutral axis. In beams with prestressing wires or strands the cracks were seen to bifurcate as they approached the elastic neutral axis.

Generally, the cracking patterns shown in Figs. (55) and (56) did not show any significant difference between the plain round and

deformed bars. However, the use of prestressing wires and strands resulted in a significant difference in the formation, number and width of cracks (see Table 11). Due to the presence of the indentation on the surface of the prestressing wires, beam B16 showed relatively more cracks, clearly spaced, than beams B17 and B18, even though B18 contained stranded wires. This behaviour is confirmed in Fig. (50) where the crack spacing was plotted against the steel stress. It can also be noticed that the use of a lower percentage of steel resulted in higher steel stresses at the formation of the first cracks. The spacings varied with the amount of steel and up to a stress level of about 200-250 N/mm^2, after which the spacings in the case of deformed or plain steel bars became more or less the same.

All the cracks that formed, whether primary or secondary, were included in the analysis of the results and in the construction of the graph discussed above. The variability of crack spacing was not taken into account, even though a scatter was found as regards crack widths and spacings for beams of similar design. This is because the sample of beams with similar design was very small.

9.2.10 Effect of High Tensile Steel on Cracking

In the present investigation it has been shown that the effect of reducing the area of steel was to increase the steel stress at first cracking. It has also been shown here and elsewhere[36,45] that the percentage of steel did not significantly influence the rate of increase of cracking. Therefore, a reduction in the steel area seems beneficial, since it tends to keep the cracks small at working stresses for low percentages of steel. Using high tensile steel, higher steel stresses are allowed, leading to decreased steel percentages. The crack widths will be increased as a result of increased stresses, but will be decreased as a result of decreased percentages of steel.

Comparison of the results for beams with plain round mild steel bars, and those with high tensile deformed steel bars showed an average difference in the average and maximum crack widths of only 11% and 7% in favour of the deformed bars. There was a considerable overlap between the results of the two types of steel. These results may not be considered as conclusive since the sample of beams with plain round mild steel bars was very small. Better results can be obtained by testing larger numbers of beams of similar design and using a statistical

approach to deal with the variability that exists in the crack widths and spacings. However, the difference in behaviour between plain and deformed bars found in this investigation is in agreement with those found by Snowdon[43] and the C. & C.A.[45] of 12% and 13% respectively as mentioned earlier.

If the allowable stress of mild steel, 150 N/mm^2, is taken as the basic stress to which the allowable stresses of different types of high tensile steel is related, a very useful relationship, for design purposes, can be obtained. For steel stresses, which are multiples of the basic stress, the behaviour of beams, as indicated in cracking and deflection, can be evaluated.

Fig. (57) gives the effect on the width of cracks of using high tensile steel with higher permissible stresses. It gives a plot of the ratio between the allowable stress of high tensile steel (H.T.S.) and that of mild steel (M.S.) as against the ratio between the crack width, maximum or average, at the allowable stress of high tensile steel, and that at the allowable stress of mild steel. A linear relationship was obtained, which could be used in the design of a reinforced concrete beams, or in the case of replacement of mild steel by high tensile steel once the requisite steel stress is known.

It can be seen from this graph that when the permissible steel stress is doubled or tripled, the maximum crack width becomes respectively about 1.8 and 2.5 times that for mild steel. The beams included in the construction of the graph in Fig. (57) were intended to be of the same design load. However, beams B12 and A13 had the same design load, but B11 was smaller and A15 was greater by about 10%. This is mainly because of the replacement of the mild steel bars by high tensile bars of areas relatively bigger than should be used for the same design load.

It has been shown previously that the type of steel, deformed or plain round, has no significant effect on the crack spacing even at very high stresses, as can be seen in Fig. (50).

9.3 Limit State of Deflection

9.3.1 General

In § 3.4 the limitations on the allowable deflections and span/depth ratios have been discussed. It has been shown by many

investigators that deflection may exceed the allowable limits and may constitute a criterion for design, when high steel stresses or shallow members are used. In this study formulae are suggested for the prediction of deflection on the first and second cycles of loading. Comparison between computed results and experimental data of this study indicates that these formulae can be successfully used for concrete members reinforced with different types, percentages and sizes of high tensile steel. The experimental results are used to determine the constants which are included in the proposed formulae.

The relationship between the span/depth ratio and the stress in the steel is also established. This relationship is useful in controlling the deflection of members with high steel stresses.

In the light of the proposed formulae for deflection the relationships between deflection, stress and load are discussed and the effects of high tensile steel on deflection are studied.

9.3.2 Proposed Deflection Formulae

In § 4.3 it has been emphasised that the stiffness as given by the term (EI) is an important and a major parameter in the formulation of deflection.

In this study the parameters which would influence deflection are:

1) The stiffness of the uncracked section (E_cI_o) and the stiffness of the cracked section (E_cI_c).
2) The stiffening effect of concrete in the tension zone before cracking (the cracking moment M_c).
3) The effect of cracking (K_1)
4) The applied moment (M)
5) The effects of the loading cycles subsequent to the first cycle
6) The span (L).

The beam span and depth were kept constant for all the beams.

9.3.2.1 Deflection: First Cycle

There are three distinct stages in the behaviour of the load-deflection curve history of reinforced concrete beams:

1) Uncracked elastic stage: this represents the behaviour

of the beam prior to cracking and deflections are predicted using the value of the second moment of area of the uncracked transformed section (I_o)

2) Cracked elastic stage: this represents the behaviour of the beam after cracking and deflections are predicted using the value of the second moment of area of the cracked transformed section (I_c) adjusted for the gradual deterioration of the tension stiffening capacity of the concrete.

3) Yielding stage: this represents the behaviour of the beam after the yielding of the steel. This is the case in an under-reinforced beam.

Only the first two stages are of interest when considering the limit state of deflection, as has been pointed out in §§ 4.3. A bilinear relationship can, therefore, be suggested:

$$\text{Stage (1)} \quad \Delta_{11} = \beta \frac{M}{E_c I_o} L^2 \quad \text{for} \quad M \leq M_c \qquad \ldots\ldots\ldots(33)$$

$$\text{Stage (2)} \quad \Delta_{12} = \beta \frac{M - M_c}{K_1 E_c I_c} L^2 \quad \text{for } M \geq M_c \qquad \ldots\ldots\ldots(34)$$

$$\Delta_1 = \Delta_{11} + \Delta_{12} \leq \beta \frac{M}{E_c I_c} L^2 \qquad \ldots\ldots\ldots(35)$$

$$\text{where } M_c = \frac{f_t I_o}{d - dn} \qquad \ldots\ldots\ldots(36)$$

β - deflection coefficient depending on the type of loading distribution and end conditions of the beam.

M - applied moment (KN - mm)

E_c - modulus of elasticity of concrete (KN/mm^2)

I_o - second moment of area of the uncracked transformed section (mm^4)

L - span length (mm)

K_1 - ratio of the stiffness of the beam to the stiffness of the cracked section

I_c - second moment of area of the cracked transformed section (mm^4)

M_c - cracking moment (KN - mm)

Δ_1 - total deflection (mm) on the first cycle

f_t - modulus of rupture of concrete (N/mm^2)

The terms E_c and f_t can be expressed in terms of the cube strength (U_w in N/mm^2) of concrete as in the following:

$$f_t = K_2\sqrt{U_w} \qquad \text{.....(37)}$$

$$E_c = K_3\sqrt{U_w} \qquad \text{.....(38)}$$

where K_2 and K_3 are constants of proportionality as determined in § 9.3.3.

9.3.2.2 Remaining Deflection

The remaining deflection, when unloading from a load above the first cracking load, depends on:

1) the deflection at the maximum load of the previous cycle
2) the extent of cracking at the maximum load and the number of the remaining cracks on unloading
3) the ratio of the maximum load to the cracking load

A meaningful and practical interpretation of the remaining deflection can be achieved when the latter is expressed in terms of the deflection at the maximum load of the previous cycle:

$$\Delta_{rem.} = K_4\Delta_1 \qquad \text{.....(39)}$$

where K_4 - the ratio of the remaining deflection to design load deflection

9.3.2.3 Deflection: Second Cycle

The stiffening effect of concrete in the tension zone which influences the deflection on the first cycle is no longer effective on the second cycle and hence the stiffness of the beam becomes less than that on the initial loading prior to first cracking. The increase of deflection with loading will be above that value of the remaining deflection and, therefore, the total deflection is expressed as

$$\Delta_2 = \beta \frac{M}{K_5 E_c I_c} + K_4\Delta_1 \qquad \text{.....(40)}$$

where Δ_2 - total deflection (mm) on the second cycle
K_5 - ratio of the stiffness of the beam on the second cycle to the stiffness of the cracked section
$K_4\Delta_1$ - remaining deflection (mm)

The other terms have the usual meanings.

9.3.3 Determination of the Coefficients K_2 and K_3 from Test Results

Since the equation for the calculation of deflection (Eq.35) was assumed to be bilinear, the point where the two straight lines meet should be determined. This point is the cracking moment (M_c) at which visible cracks are assumed to occur. Visible cracks appeared when the tensile force in the extreme fibre of the concrete in the tension zone reached the modulus of rupture of the concrete (f_t). Fig. (58) gives the relationship between the cube strength and the modulus of rupture based on the measured cracking moments of the test beams. From this relationship the coefficient (K_2) in (Eq. 37) was found to be equal to 0.458.

The values of the modulus of elasticity (E_c) obtained from the consideration of the cracking moments of the test beams were plotted, in Fig. (59), against the cube strength (U_w) for all the beams. From this plot the coefficient (K_3) in (Eq .. 38) was found to be equal to 4.0.

The results of the modulus of elasticity and modulus of rupture obtained from the control specimens were also included in Figs.(58) and (59). They were always higher than those obtained from the results of the test beams (based on the measured cracking moments of the test beams).

9.3.4 Determination of the Coefficients K_1 and K_5 from Test Results

The slopes taken from load-deflection curves have been used as a measure of the stiffness of the beam on the first and second cycles. The values of the coefficients K_1 and K_5 were obtained by dividing the measured stiffness (EI) (based on the slopes of the load-deflection curves) by the calculated stiffness ($E_c I_c$) of the cracked transformed section. The average values of the coefficients K_1 and K_5 in Eqs . (34 and 40) were found to be equal to 0.9 and 1.3 respectively. The values of (E_c) used in the determination of the values of (I_c) were obtained from Eq . (38) with $K_3 = 4.0$.

9.3.5 Determination of the Coefficient K_4

Table (12) shows the deflections at the design loads and the remaining deflections at the end of the first cycle. The ratios of the remaining deflection to the design load deflection for all

the beams tested under the first and second cycles are also given. The average of these ratios on the first cycle was found to be 24% which was approximately $\frac{1}{4}$. The results of beam B17 were ignored, because of a bond slip failure.

9.3.6 Relationship between Deflection and Load

9.3.6.1 Comparison between Theoretical and Experimental Results

Figs. (60-64) give the load-deflection curves for the three categories of beams. (beams with deformed or plain bars and beams with wires and strands. Only the curves for the first and second cycles of loading are given. The theoretical lines of deflection have been drawn for comparison with the experimental results. In all cases the deflections obtained using the proposed methods were on the safe side, except in beams A12, A13, A31 and B25, where the calculated deflections for both cycles were smaller than the actual values. This could be due to many reasons, such as the calculated values of the cracking moments in these four cases being higher than the actual ones. In beams A12 and A13 the underestimation may also be due to the overestimation of the stiffness (EI). The calculated deflections at the design load agreed reasonably well with the observed deflections and the average ratios of the observed to the calculated deflections for both cycles were 0.970 and 0.967 respectively, as can be seen in Table (12).

The proposed methods for the calculation of deflection can be safely employed even if very high strength steels are used. The good agreement between the theoretical and experimental values indicates the reliability of the proposed methods in predicting deflection for the four types of steel: deformed steel, plain mild steel, wires and strands.

9.3.6.2 Behaviour of Test Beams

It has been indicated previously (9.3.2.1) that the load-deflection behaviour of a reinforced concrete beam can be studied in three stages. In Figs. (65) and (66) the deflection characteristics are seen to consist of these three stages: the first stage is before and up to first cracking, the second stage after first cracking to yielding, and the third stage at and after yielding.

Fig. (65) gives the relation between load and deflection for beams reinforced with equal amounts but different types of steel. Beams A11, A12 and A13 showed exactly the same deflection characteristics over a substantial part of the curve. Beams A14 and A15 could have given the same deflection characteristics if the amount of steel and the cracking moments were of the same magnitude as that in the other beams. Beams with the same amount of steel and cracking moments had all the points lying almost exactly on the same straight line. Beams A14 and A15 had the same amount of steel but different cracking moments and thus, at any load level, beam A14, with greater cracking moment, showed smaller deflections than beam A15. The points did not fall on the same line but they fell on two lines which were almost parallel. If the cracking moments were made equal then the two lines would coincide.

In Fig. (66) the deflections of beams reinforced with different types and amounts of steel are shown. Some of the beams had almost equal design loads. Beams B12 and A13 had the same design load (46.6 KN). However, the deflection was greater in the latter than in the former. The deflection of beam B12 at design load was greater than $^{L}/360$ (12.7 mm), but less than $^{L}/250$ (18.2 mm). Beam A13 showed a deflection greater than $^{L}/250$. This was because of the smaller percentage of steel in A13 due to the use of steel of higher strength.

Beams B_{11}, B_{16}, B_{17} and B_{19} have almost the same design loads but different steel types, viz. plain round bars, crimped and plain prestressing wires and Bristrand. Again, it can be seen that the increase in permissible stresses resulted in decreased steel area, giving increased deflection for the same design load. The least deflection of $^{L}/360$ was observed with beam B11, which had the lowest permissible steel stress. When beams A14 and B19 were considered, the two beams had almost the same percentage of steel, however, the deflection of beam B19 was much more than that of A14 at the same load level, The only reason for this difference lies in the magnitude of the moduli of elasticity of both types of steel. Beam B19 had a lower modulus of elasticity than A14 and thus the deflections of the two beams were different, since they deformed in a manner similar to the shape of the stress-strain curve of the steel. If all the beams with the same design load had the same (E_s) value for steel, then the

deflections would be greater for beams with higher permissible steel stresses.

Fig. (66) shows that there is no significant difference in the behaviour of beams reinforced with deformed bars and those with prestressing wires. The deflections of beam B16 with crimped prestressing wires were comparatively similar to those of beam B15 with deformed bars, even at very high percentages of the ultimate load. Beam B17 with plain prestressing wires behaved differently as it contained less area of steel compared to beams B15 and B16 and its failure mode was also different (it failed in bond slip).

The graphs in Fig. (66) indicated that up to the cracking load there was very little difference in the values of deflection for the different beams. After first cracking, the rate of deflection increased with decreasing percentage of steel.

Figs. (60-64) show the load-deflection curves on the first and second cycles of loading. The remaining deflections are also included. The deflections for the second cycle were drawn only up to the design load, which was of practical importance. The deflections at design load on the second cycle seemed to increase slightly in all beams, thus indicating the time-dependent effects due to creep during the test.

It has been indicated in § 9.3.4 that the slopes of the load-deflection curves can be taken as a measure of the stiffness of the beam. In Figs. (60 - 64) it could be seen that the stiffnesses of the beams on the second cycles of loading were less than those on the initial loading in the uncracked stage, while they were greater than those in the cracked stage. Similar observations have been reported elsewhere.[57,184,185]

It has been found by Soretz[57] in his tests on 115 beams that the deflections on the initial loading (first cycle) in the cracked stage showed deviations of $\pm$ 20% from the average, while those on the subsequent cycles showed deviations of $\pm$ 50% from the average. In the repeated loading range too many factors were assumed to have affected the stiffnesses, and the remaining deflections, and it was observed that a deviation of $\pm$ 20% is unavoidable.

In Fig. (67) the idealized load-deflection curves for comparable beams of similar design are shown. It could be seen that the loads to produce first cracking in each pair of similar beams were different. This fact affected the deflection at design load; beams with lower cracking loads showed greater deflections at the same design load. The stiffnesses of the beams in each pair, on the first cycle, differed slightly, depending upon their relative concrete strengths. The cube strengths for beams A11 and A31 were 32.4 and 52.7 N/mm^2, for beams A13 and A33 were 41.4 and 48.9 N/mm^2, and for beams A14 and A34 were 41.4 and 35.7 N/mm^2 respectively.

In comparing these beams the extent of cracking did not seem to influence the stiffness (which is proportional to the slope of the load deflection) of the beams, even though beams of similar design, e.g. A11 and A31, A13 and A33, had different crack distribution. However, the steel stress at first cracking and the extent of cracking appeared to affect the stiffness of the beams on the second cycle. Beams A11, A12, A13 and A14, which had lower steel stress at first cracking than their companion beams, showed lower stiffness characteristics on the second cycle of loading. This could be explained by the fact that the ratio of the applied steel stress at design load to the steel stress at first cracking was comparatively high, and thus the beam stiffness was gradually reduced as cracking progressed. This phenomenon, that the ratio of applied stress to stress at first cracking has a significant influence on the stiffness of the beam on the reloading cycles, has been observed by Soretz[57] and Burns et al.[155] However, Kripanarayanan and Branson,[184] in a recent theoretical approach to the effective second moment of area on the reloading cycle suggested that an increase in the above ratio to a levelwhere the beam was severely cracked increased the stiffness to a value of that of the gross section.before cracking. The findings of the present investigation do not agree with Branson's findings, and support the opposite point of view; on the reloading cycles the stiffness of the beam decreases and gradually approaches the value of that of a cracked section as the load increases.

Soretz[57] pointed out that while the ratio of the applied steel stress to steel stress at first cracking had very little influence on the remaining deflection for the same beam, it had significant influence on the relative magnitudes of the remaining deflections of

the comparable beams with different values of steel stress at first cracking. In Fig.(67) beams A11 and A13 had a high ratio of design stress to stress at first cracking, and at the same time developed lower remaining deflection than their companion beams. It seemed that the remaining deflection depended on various other factors in addition to the ratio of applied stress to stress at first cracking considered by Soretz. These factors have been indicated in § 9.3.2.2, and they include the number of cracks that do not close (remaining cracks) on removal of the load, the wedging action of the particles trapped between the crack faces and the crack formation and distribution.

Another factor that affected the remaining deflection was the stiffness of the beam in the uncracked zone, and the modulus of elasticity of concrete in compression. This stiffness depended on the modulus of elasticity (E_c) of concrete, which in turn depended on the strength of concrete, and on the second moment of area of the uncracked section. The graph in Fig. (67) shows some slight differences in the stiffnesses of the companion beams on the first loading in the uncracked stage.

Table (12) gives the behaviour of the beams under the effects of loading and unloading on the first, second, and third cycles. It could be seen in columns (2) and (9) that reloading on the second cycle to a given design load level (P_D) did not increase the magnitude of the deflection significantly, except for a small increase due to creep.

A comparison of the figures in columns (5) and (6) show ed that the remaining deflection increased as the load increased to a level of about 30% above the design load. This increase in the remaining deflection was due to the increased degree of cracking and the creep effects. However, comparison of columns (7) and (9) showed that when the load was increased there was a reduction in the ratio of remaining deflection to deflection at the maximum load of the previous loading cycle. These findings suggested that there was an increase in the recovery ratio as opposed to the findings of Kripanarayanan and Branson[184], who reported a reduction in the recovery ratio with increasing load.

From the results of beams unloaded from loads between 76 and 89% of their maximum failure loads, the recovery of deflection

amounted to about 77% to 88%. It was observed that the recovery decreased with decreasing steel area, and it was not affected by the type of steel (deformed or plain). For a beam reinforced with three 10 mm diameter strands (Bristrand 100), Abeles[16] found a recovery of about 60%, and reported the decrease of this recovery with decreasing steel area.

The effect of the hysterisis loops can be observed in the difference of the values in columns (10) and (11) of Table (12). The difference between these values is very small, and it is suggested that the effect of the hysterisis loop can be ignored, and that the deflection curves on unloading and reloading are assumed to coincide. Similar conclusions have been reported by Kripanarayanan and Branson.[184]

9.3.7 Relation between Deflection and Steel Stress

Fig. (68) shows the direct proportionality between the stress in the steel and the deflection. The deflection increased linearly with increasing steel stresses. It is clearly seen that the stress at cracking was much higher in beams reinforced with low percentages of steel and that the limits of $^{L}/360$ and $^{L}/250$ were reached at much higher stresses than those with normal or high percentages of steel. On the same graph the permissible stresses at 0.55 f_y in the different types of steel are indicated. From this it is observed that for the same permissible steel stress the relative values of deflection decreased as the reinforcement percentage was decreased. Table (13) shows how this increase in the steel stress affected the span-deflection ratios, for a particular span and depth of beam, for all the beams concerned.

Another factor of importance when dealing with the effect of stress on deflection is the modulus of elasticity of the steel. This is reflected in beam B19 (with Bristrand 100) in which the E_s value is lower than those for the rest of the beams which have almost the same percentage of steel. The curve of B19 in Fig. (68) appeared to change at a higher rate than those of beams A14 and A15, with approximately equal steel percentage, thus emphasising the effect of the modulus of elasticity (E_s) on deflection.

In design, therefore, it is essential, when using high strength steel, to take account of the effect of high permissible

stresses on deflection, either by limiting the span-depth ratio or by using sufficient camber.

When a reinforced concrete member is designed with a limiting span /depth ratio the following factors should be considered:

1) stress in steel (f_s)
2) allowable deflection (Δ)
3) extent of cracking (K)
4) time effects (F)

The Draft Code has proposed a design procedure whereby the span/depth ratios can be obtained by multiplying four different factors, including the effect of creep and shrinkage. In this study, in order to take account of the above factors, the proposed equation of the span/depth ratio is:

$$\frac{L}{d} = \frac{\Delta}{L}\,\frac{1}{F}\,\frac{E_s}{f_s}\,\frac{1}{\beta}\,\frac{d_1}{d}\,(1 - K) \qquad \text{.....(41)}$$

where Δ - allowable deflection (mm)

f_s - calculated steel stress § 8.2

K - neutral axis depth coefficient, which takes into account the extent of cracking § 8.2.

F - creep and shrinkage factor which can be obtained from Fig. (101)

The other terms have the usual meanings.

When Eq . (41) is used the calculation of deflection will no longer be required. The results of this equation agreed fairly well with the results of the cubic equation suggested by the A.C.I. Committee.[161]

9.3.8 Effect of High Tensile Steel on Deflection

In considering the effect of high tensile steel on the deflection of the reinforced concrete beams tested in this investigation, three factors must be discussed: i) the scatter that occurred in duplicate beams ii) the surface characteristics of the reinforcing bars, and iii) the increase in the permissible stresses with or without a decrease in the steel percentages.

The first of these factors, the scatter in duplicate beams, can easily be seen in Fig. (67). These beams, of the same design and type of steel, showed a significant difference in the deflection at all levels of loading. It is essential, therefore, to compare beams that have exactly the same cracking load and similar in all respects except in the type of steel. In Fig. (67) it can be seen that beams A11, A12 and A13 can be chosen to serve this purpose since they have almost the same cracking load, moduli of elasticity (E_s) for the steel, and similar design except for the type of steel employed. Beam A11 contains plain round mild steel bars, and beams A12 and A13 contain deformed Unisteel 60 and 80 respectively. They all contain the same amount of steel, 1.44%. A comparison of these beams in Fig. (65) shows that the three beams give the same deflection characteristics regardless of the type of steel used. It is, therefore, concluded that the surface characteristics of the reinforcing bars, as long as bond is not lost, have no significant effect on the deflection of a reinforced concrete beam. In this case the only variable to be considered should be the strength of the steel, and the permissible stresses that can be used without jeopordizing the stiffness of the beam at working load. A beam designed to include two plain round mild steel bars can be used to carry higher design loads by replacing the bars with the same size of steel of higher strength, provided the limiting declection is not exceeded. The effect of replacing mild steel with a smaller size of high tensile steel to give the same design load is two-fold: i) the increased steel stress at working load ii) the decrease in the stiffness owing to a smaller steel percentage.

Two beams can be designed with different types and percentages of steel to carry the same amount of loading. Looking back at Fig. (66) beams B12 and A13 have almost the same ultimate load, but they contained different amounts of steel, and hence they gave different deflections for the same applied load. Beam A13, with a steel percentage of 1.44% gave greater deflection than beam B12, with a steel percentage of 1.96%, at all load levels. The same logic can be applied to beams B11, B16, B17 and B19, except that in beam B19, due to the low modulus of elasticity of the Bristrand, bigger deflection was attained, even though it contained a higher percentage of steel.

A relationship can be established between the ratio of the allowable steel stress of high tensile steel (H.T.S.) to that of

mild steel (M.S.) and the ratio of their respective deflections. Fig. (69) shows such a relationship for beams of almost the same design loads. From this figure the value of deflection at any allowable stress can be attained by multiplying the ratio of deflections by the basic deflection of mild steel.

Beams B19 and A15, with Bristrand 100 and Kam 90 respectively, appeared to deviate from the straight line in Fig. (69). These were marked points (1) and (2) on the graph. The reason that point (1) lies outside the straight line is due to the fact discussed above, concerning the low value of the modulus of elasticity of this type of steel. The deviation of point (2) is believed to be due to a relatively high percentage of steel. Similar observations have been reported by Mathey and Watstein.[38]

One of the advantages of using high tensile steel can be clearly seen in Figs. 65 and 66. As discussed later, beams A11,A12,B11 and B12, reinforced with steel having a definite yield point, showed a difference in behaviour, from the rest of the beams at near collapse. In these beams collapse occurred suddenly after the yield point was reached. There was not enough warning before failure. The beams with high tensile steel with an indefinite yield point (with gradual yield), e.g. A13 and A15, continued to undergo large deflections before collapse and thus gave enough warning before failure.

9.4 Limit State of Collapse (Ultimate Strength)

9.4.1 Ultimate Strength

All the beams tested in this investigation were designed in accordance with the Draft Unified B.S. Code of Practice.[23] The formulae given in this code were used in defining the ultimate moment from which the design moment, based on nominal strengths of materials, was obtained by applying the factors for dead and live loads for the limit state of collapse as explained in § 3.4. However, it was decided to use a factor of 1.6 by assuming the total load acting as superimposed load. The ultimate strengths of the beams, employing the actual values of steel and concrete strengths without incorporating the material partial safety factors were also determined.

The compressive stress distribution in concrete was assumed to be rectangular-parabolic as recommended in the Draft Code.

Table (8) gives the details of the experimental maximum moments and the moments calculated by the methods given above. In each case, except in beam B17, the experimental value was greater than the calculated value. This can be seen in column (11) of the table, where the ratio of the experimental to calculated ultimate loads is greater than unity. In the case of beam B17, the ratio was 0.76. The reason for this low ratio was the formation of a vertical hinge in the vicinity of the point load outside the constant moment zone. This crack initiated on the first cycle at a load lower than the design load and remained widely open after removal of the load. This was believed to be a bond failure, caused by slip between steel and concrete which was followed by the crushing of the concrete at the top of the hinge. However, the maximum flexural bond stress that occurred at that section was only 1.4 N/mm^2, as against the permissible bond stress, in the Draft Code, of 3.1 N/mm^2. The anchorage bond stress was found to be about 1.45 N/mm^2 as against the permissible value of 1.7. Therefore, the failure was not due to critical shear stress or insufficient embedment length. It could be a slip failure due to accidental contact of the wires with grease. Failure at the support nearer to the failure crack was also observed. The concrete was seen to have disintegrated.

It can also be noticed from column 11 of Table (8) that the ratios are highest for the beam reinforced with Bristrand 100. The enhancement for this beam was 22%.

The steel stresses at failure were calculated from the actual bending moments at which the beam collapsed, using a rectangular-parabolic concrete stress distribution, and assuming a maximum concrete stress at the top fibre of $^2/_3$ times the nominal strength of concrete. These stresses are shown in column (13) of Table (8). A comparison of these stresses with the actual yield stresses obtained from bars tested in the air are given in column (14) in the form of ratios. It can be noticed that in all but two beams, A31 and B_{st2}, the steel stresses exceeded the yield stresses. Beam B19 showed the highest ratio of 1.27.

Most of the beams subjected to repeated loading prior to static loading up to failure showed higher strengths at failure than their companion beams. The reasons for this increase will be given in the next chapter.

In column (12) of Table (8), the ratios of the experimental maximum moments to design moments are given. It can be observed that the ratios are greater than 2. The calculated design moment was based on the nominal concrete strength of 41.4 N/mm^2, and the nominal steel stress, with the inclusion of the material partial safety factors. The ratios ranged from a maximum of 2.52 to a minimum of 2.05. The reason for this fluctuation may partly be due to the use of the nominal values of the strengths of the materials.

In Table (6) the average cube strengths at failure are given for all beams tested to failure. It can be seen that using an average strength of 41.4 N/mm^2 in calculating the design moments seems justifiable, since the variation from the mean in the strength of concrete in these under-reinforced beams did not affect the ultimate strength significantly, and also because nominal strengths are usually employed in design.

9.4.2 Effect of High Tensile Steel on Ultimate Strength of Beams

For a balanced or over-reinforced design, the ultimate strength of a reinforced concrete beam is limited by the magnitude of the plastic strain in the extreme fibre of the concrete in the compression zone. This strain is usually given a value of 0.0035. For an under-reinforced design the crushing of concrete is a secondary failure after steel yielding. Theoretically, in order to produce a high stress in the tensile steel, there must be a high elastic strain of the material which will, for the same value of concrete strain at failure, reduce the depth of the neutral axis. This will result in smaller area of concrete subjected to the compressive stress loading to premature failure of concrete in compression.

In this investigation the beams were under-reinforced and the crushing of concrete was only a secondary failure. In none of the beams was the primary failure due to strain in the concrete reaching

the plastic failure strain. Table (14) gives the measured concrete strain at the extreme compressive fibre, the neutral axis depth and the strain in the steel at yield or 0.2% proof stress. It can be observed that the strain in the concrete fibre increased with higher grade of steel. In beam B16, reinforced with crimped prestressing wires, the strain was 278×10^{-5} at 90% of the ultimate load. The corresponding figure for beam B11 with mild steel was 189.5×10^{-5}, the yield strain for prestressing wire being 0.887% against 0.16% for the mild steel.

Two groups of beams must be considered; beams with the same percentage of steel but different types of steel (Group A in the table) and beams of the same ultimate strength but with different types and percentages of steel (Group B in the table).

In group (A) in Table (14) beams A11, A12 A13, A14 and A15 had steel strains at their respective yield strengths of 0.16%, 0.22%, 0.53%, 0.29% and 0.63% respectively. The increase in the steel strains did not affect their neutral axis depth, even at loads of very high percentages of the ultimate load. The difference in the neutral axis depths was due to the difference in the cube strengths. The strain in the concrete extreme fibre increased with increasing working load, and at loads of very high percentage of the ultimate loads, the strains increased with increasing steel strain at the yield strength of the steel.

In comparing beams of group (B), it can be observed from Table (14) that the neutral axis depth decreased with an increase in the grade of steel. This rise in the neutral axis was due to the smaller area of steel employed. For the same working load the concrete strain increased with an increase in the steel strain at its yield, and corresponding decrease in steel area. At loads near failure the steel strain reached values many times that of mild steel, and yet the concrete strain has not reached the plastic failure strain.

It can be concluded, therefore, that in under-reinforced beams high tensile steel provides better utilisation of the concrete strength in compression, and produces no rise in the neutral axis owing to the increased strains in the steel in beams using the same or different areas of steel. It has no effect, therefore, on the ultimate strength

of under-reinforced concrete beams. This conclusion has also been reached by Clark and Eastwood[46,47] and Hajnal Konyi.[186]

9.5 Flexural Strain

9.5.1 Flexural Strain Distribution

The flexural strains on the surface of the beam were measured over a gauge length of 200 mm across the depth on both sides of the beam. The average values of the strains on both sides of the beam were plotted.

The strain distribution obtained for the compression zone of the beam was almost linear, but not so for the tension zone. The over-all strain may not be continuously linear.

The reason for the non-linearity in the tension zone of the beam was the presence of tensile cracks within the length of measurement. An attempt was made at measuring the strains at two levels, near the bottom edge and at the level of the bottom layer of the steel, for the entire constant moment zone of beams B16 and B17. This procedure involved a lot of time abd labour. The results obtainedwere averaged and compared with the average strain measured over the middle gauge length, which was usually adopted for the other beams. The difference between the two in beam B17 was only 14.2% and 15.2%, while in beam B16 it was 52% and 37% for the steel level, and the bottom edge respectively. This was so because in the former only a few cracks formed, one within each gauge length, while in the latter in two of the gauge lengths two cracks formed and in each of the other gauge lengths only one crack formed.

The average tensile strain obtained for the entire constant moment zone was also compared with the average tensile strain obtained from the extension of the strain profile in the compression zone. They appeared to compare reasonably well. Therefore, it was decided to use this procedure in determining the average tensile strain at the steel level and at the bottom edge of the beam for the analysis of the cracks.

The neutral axis position was located by fitting a straight line through the points of strain measurements in the compression zone.

This depth can be assumed to be the average neutral axis depth and was used, as described earlier, in the calculation of the stresses in the steel. The neutral axis depth seemed to change with the magnitude of the load up to about 30% of the ultimate value, after which it remained almost constant, as can be seen in Fig. (11) and as discussed in Chapter (8).

The strain distribution in the compression zone remained linear as the load increased, while the concrete stresses redistributed themselves in such a way as to maintain equilibrium with the forces in the steel.

9.5.2 Remaining Compression Strain

Remaining compression strain is defined as the compressive strain remaining immediately after the removal of the load. It is not the permanent strain which remains even after a rest period when the beam is unloaded.

The beams tested in this investigation showed remaining compressive strains on unloading after they had been loaded to design load. The remaining strains did not increase significantly after the second cycle of loading.

The remaining strain is characteristic of the plastic nature of the concrete under compression, and the extent of cracking in a cracked reinforced concrete. The stress-strain diagram for concrete in compression is never a straight line, and owing to the rate of loading of these beams, plastic strain in the concrete must be present. Some of the remaining compressive strains were seen to diminish when the beams were left in the unloaded condition after the first cycle.

9.5.3 Effect of High Tensile Steel on Strains

The effect of high tensile steel on strains must be studied under two aspects. Firstly, the effect of increasing the steel stresses keeping the percentage of steel constant, and secondly the effect of increasing the steel stresses while decreasing the steel percentage to attain the same ultimate moment capcity. Fig. (70) considers the latter aspect. For beams with the same ultimate capacity the effect of increasing the stress in steel, relative

to that of mild steel, on the compressive strains in concrete is shown. The points on the graph that are seen to deviate from the curve are those for beam B19 with Bristrand 100, having a low modulus of elasticity, which affected the stiffness of the beam, and thus gave a bigger deformation.

This diagram is very useful in estimating the amount of strain increase that will occur when the allowable steel stress exceeds or is a multiple of that of mild steel. As far as the ultimate capacity of an under-reinforced beam is concerned, it has been shown in § 9.4.1. that there is no significant effect. Only deflection and cracking are very much affected by the increase in the steel strains.

Table (14) gives the effect of increasing the steel strains on the compressive strains in the concrete by increasing the steel grade or strength. In beams of Group (A) when the steel area was kept the same, the concrete strain increased with increasing working load due to the higher grade of steel. In beams of Group (B) when the working load was kept constant the concrete strain increased with higher grade of steel.

The increase in tensile strain in the steel, when using high tensile steel will bring about an increase in the crack widths in the concrete tension zone. The increase was more pronounced when the crack pattern was well developed. Most of the tensile strain will be taken by the steel reinforcement at the cracks, and thus the cracks will increase in width.

It can be seen that the effect of using high tensile steel on concrete strains is another way of describing its effect on the serviceability, viz. deflection and cracking. This effect must be closely considered in the design of beams which are stressed to very high strains.

9.6 General Behaviour of Beams

On the first application of the load the beams behaved elastically up to the cracking load, which ranged between about 10 KN and 15 KN. These values were obtained from the observations of the change of slopes of the load-deflection curves and from the first visible cracks, as can be seen in Figs. (60-64). At the cracking load the

width of the visible cracks were, generally, of the order of 0.015 mm and the deflections ranged between 1.3 mm to 2.6 mm (see Figs. 60-64), depending on the cracking load and the stiffness (EI) of the section in the uncracked state.

As the load was increased above the cracking load the deflection increased more rapidly due to the change of the stiffness of the section. The deflection at the design moment in some instances exceeded even the one calculated on the basis of fully cracked section. In all beams except B17, the increase in deflection, in the cracked state, was uniform and was almost linear. At loads approaching the yield of the steel reinforcement the load-deflection curve followed the slope of the stress-strain curve of the reinforcement.

On each side of the beam, at the initiation of cracking, a number of cracks (primary cracks) appeared simultaneously at a steel stress depending on the percentage of steel in the beam. As the load increased the spacings between the primary cracks were reduced by the formation of secondary cracks. The crack widths increased to values depending on the magnitude of the stress in the tension steel. The length of the cracks was also noticed to increase with loading. At the design load a fully developed pattern formed and a stabilised condition was reached as far as the number and, in some cases, the length of the cracks was concerned.

On unloading the shape of the deflection curve was concave towards the load axis. At zero load the remaining deflection (recoverable and irrecoverable) formed an appreciable part of the total design load deflection. The remaining deflection consisted mostly of residual deflection, which was irrecoverable. It was observed that the rest period in the state of unloading had some influence on the recovery of deflection.

The widths of all the cracks were measured on the removal of the applied loads. In most beams it was found that most of the cracks remained open and the rest closed completely. The width of the maximum remaining crack varied depending on the magnitude of the stress in the steel at the design load.

On reloading the stiffness of the beam was greater than the stiffness in the cracked condition when loaded initially. The

transition zone that was clearly noticed in the initial loading between the uncracked and the cracked elastic states could be faintly recognised on the second cycle. The deflections observed on the reloading cycles were slightly smaller than those on the previous unloading cycles.

At the design load the deflection on the second cycle of loading was greater than that on the first cycle; the increase ranged between 0.07 mm and 2.00 mm, as can be seen in Figs. (60-64). At higher loads the deflection curve followed the extrapolated first cycle (virgin cycle).

The crack widths were also noticed to increase slightly at the same level of load previously applied. This increase ranged between 0 and 0.05 mm, as can be seen in Figs. (38-49).

When unloading from a load about 30% above the design load there was an increase in the remaining deflection. The remaining crack widths were not affected very much.

When reloading, on the third cycle, the stiffness of the beam was noticed to have reduced significantly. The increase in deflection at the design load was also significant. The crack widths appeared wider in some cases, and remained unchanged in other cases, when the design load was applied.

At loads higher than previously applied on the second cycle the deflection curve took the shape of the steel stress-strain curve. The slope of the deflection curve, in the case of steel with an indefinite yield point, changed gradually and the deflection increased more rapidly and the cracks became excessive. In the case of beams with steel having a definite yield point, the deflection increased suddenly as the yield point was reached, resulting in the crushing of concrete. Before collapse, beams with gradually yielding steels gave good warning, as indicated in both the excessive crack width and deflection. In this respect cold worked bars, (with an indefinite yield point) were superior to hot-rolled bars (with a definite yield point). However, when the latter has good bond and high strength, as in the case of Unisteel 60 and Kam 60 steel, sufficient warning can be obtained.

Failure, in all beams except B17, occurred in the constant moment zone. Concrete crushing occurred at the weakest section in beams with steel having indefinite yield point, and at the section where there were two or three prominent maximum cracks in beams with plain mild steel bars. Plate (5) shows the final condition of beam A11, reinforced with two 19 mm plain mild steel bars. It is apparent that after the bars have yielded the crushing of the concrete occurred at the top of three widest cracks, which happened to be near the point of loading. This type of failure was also reported by Hajnal Konyi[28] and Lewis[33], and it can be taken as typical of plain mild steel bars.

The mode of failure was typical of that of under-reinforced beams; the steel yielded first, as a primary failure, as expected, and then it was followed by crushing of the concrete with a loud noise, as a secondary failure. Plate (6) shows the final condition of beams. Two types of failure could be distinguished: a) yielding with a sudden increase of the deformation and b) gradual yielding and deformation with increasing load.

The first type of failure is characteristic of concrete beams reinforced with steel having a definite yield point: mild steel, Unisteel 60, Kam 60, and the second type (gradual failure) is characteristic of concrete beams reinforced with cold worked bars: Unisteel 80, Kam 90, prestressing wires and strands and Bristrand 100.

The short yield plateau and the excellent bond of Kam 60 caused the tensile zone of the central portion, in Beam A34, to completely disintegrate. The mode of failure was similar to that of beam A11, in that the beam failed at a maximum crack by concrete crushing, as can be seen in Plate (5). However, there were some important differences: there were a few wide cracks on either side of the failure crack, and a horizontal crack extending along the entire length of the constant moment zone at the steel level where the concrete was found to be broken into very small pieces. The adhesion between the steel and the concrete was seen to be broken. The loss of adhesion and the formation of the horizontal crack with small pieces of chipped concrete indicated thepressure exerted by the interlocking of the transverse lugs of the reinforcing bars

and the surrounding concrete due to high bond stresses and wedging action developing at failure.

Beams reinforced with Unisteel 60 bars showed a pattern of failure similar to that of beams with Kam 60 steel, even though the two steels had different deformation patterns. This can be seen in beam B12 in Plate (5).

In beams reinforced with steel having an indefinite yield point, the distribution of cracks near failure was uniform and crushing of concrete occurred at the weakest section. Two horizontal cracks formed in beam A15, with Kam 90 steel, one at the top and one at the bottom parallel to the reinforcing bars. The top crack ran along the ends of the cracks causing a big block of concrete in the top zone to be displaced from the rest of the beam. The bottom crack caused complete disintegration of the tensile zone of the central portion, and covered almost the entire constant moment zone. The concrete at the steel-concrete interface was ground like powder. In both beams A15 and A34 the horizontal crack joined the crushed zone by a diagonal crack. Similar failure patterns were observed in beams with Unisteel 80 and Bristrand 100. Beams A13 (Unisteel 80) and B19 (Bristrand 100) are shown in Plate (5).

In general, failure in beams with deformed bars of both types of yield was of a similar pattern. This mode of failure has been studied theoretically by Broms.[136,137]

Beams with wires and strands gave very good warning and were safer than the beams reinforced with steel having a definite yield point, e.g. mild steel. The mode of failure was different from those of beams with mild steel or deformed bars, crushing of concrete and disintegration of concrete on the tension side occuring only in a limited zone of failure. Beam B17 with plain wires failed as a result of bond slip just outside the constant moment zone. A hinge appeared and increased in width and length, pushing the neutral axis towards the compression face until crushing occurred over a very small area.

By way of conclusion, the serviceability of the test beams depended mainly on the magnitude of the steel stress. The higher the allowable stress, the bigger are the deflections and crack widths. The safety of a structural member depended on the amount of warning

that it could give to the occupants before failure, and the mode in which it failed. Beams reinforced with steel with a definite yield point, e.g. mild steel, might not give sufficient warning before failure, due to the sudden collapse that would occur after the steel yield is reached, while in beams reinforced with steel with an indefinite yield point, e.g.Unisteel 80, Kam 90 steel, strands and wires, the deflection and crack widthswere sufficient to cause alarm before the collapse occured.

9.7 Conclusions

The foregoing paragraphs summarise the actual behaviour under static loading of the reinforced concrete beams. From the present investigation conclusions regarding the three limit states of cracking, deflection and collapse can be drawn as follows.

9.7.1 Limit State of Cracking

1. At the initiation of cracking a number of cracks formed simultaneously at greatly varying specings with an average spacing of 300 mm.

2. Under increasing load the number of cracks increased and hence the crack spacing decreased until a stabilised condition was reached at a steel stress of 200-250 N/mm^2

3. The cracking pattern was not significantly affected by the surface characteristics of steel, viz. deformed or plain round bars. An average crack spacing of 100 mm was obtained.

4. The cracking pattern in beams with prestressing wires and strands showed relatively wider crack spacings than in beams with deformed or plain bars. An average spacing of 150-200 mm was attained. Crimped prestressing wires were superior to the plain wires and the strands.

5. The beams with the three wire strand (Bristrand 100) showed a cracking pattern similar to those in beams with deformed and plain bars.

6. The average crack spacing, in beams with deformed and plain bars, was equal to about 1.5 x the concrete cover.

7. The proportionality between crack width and crack spacings as suggested by the C.E.B. did not appear to exist.

8. In all beams initially the cracks increased in length with increasing load, reaching the level of the theoretical elastic neutral axis. In beams with deformed bars and prestressing wires and strands the cracks extended beyond the elastic neutral axis.

9. The steel stress for zero crack width increased as the percentage of steel decreased. This effect tended to keep the average and maximum cracks smaller at working stresses for lower percentages of steel. The stress in steel at first cracking can be predicted from: $f_{sc} = \frac{K_s}{p}$

10. The maximum crack width on the first cycle of loading was proportional to the stress increase in the steel reinforcement above its value at initial cracking, and to the concrete cover.

11. For the second cycle of loading the maximum crack width beyond the remaining crack width was proportional to the steel stress and the concrete cover.

12. The maximum remaining crack width was proportional to the stress in the steel reinforcement at design load and the concrete cover.

13. The parameter D/P_e had no significant effect on the width of cracks, while the C.E.B. formula over-emphasises the effects of the bar diameter (D) and the effective reinforcement ratio (P_e).

14. Over the whole range of loading the ratio of maximum to average crack widths varied essentially in a random manner with increasing steel stress. The average values of the ratio were 1.96 for deformed bars, 1.86 for plain bars and 1.7 for wires and strands.

15. In beams with equal or different percentages of reinforcement the surface characteristics of the reinforcing bars had no significant effect on cracking for a substantial portion of the loading ranges. The difference in the maximum crack width between plain round and deformed bars was only 7% in favour of the latter.

16. In beams with similar designed ultimate loads the bar was superior to the wires and strands in controlling cracking. Prestressing

crimped wires and Bristrand 100 showed good crack control over the plain prestressing wires and the prestressing strands. The increase in the maximum crack width for the wires and strands over that of deformed bars was 67%.

17. At a crack width of 0.2 mm at the reinforcement level the stresses in the reinforcement were 400-510 N/mm^2 for Kam steel deformed bars, 300-360 N/mm^2 for Unisteel deformed bars, and 275-385 N/mm^2 for prestressing wires and reinforcing and prestressing strands.

18. At a crack width of 0.2 mm at the bottom edge level the stresses in the reinforcement were 325 to 400 N/mm^2 for Kam steel deformed bars, 180 to 230 N/mm^2 for plain round mild steel, 194 to 245 N/mm^2 for Unisteel deformed bars, and 255 to 275 N/mm^2 for the prestressing wires and the reinforcing and prestressing strands.

19. The crack width at the bottom edge of the beam was not directly related to the crack width at the level of reinforcement.

20. In beams having the same design load, but reinforced with different grades, types and percentages of steel as the permissible stresses doubled or tripled the crack widths became 1.8 or 2.5 times that for the beam reinforced with mild steel.

9.7.2 Limit State of Deflection

1. For the first cycle of loading the deflection varied with the magnitude of the applied and cracking moments, the stiffness of the section in the uncracked and cracked states.

2. For the second cycle of loading the deflection beyond the remaining deflection varied with the applied moment and the stiffness of the section neglecting the stiffening effect of concrete in tension before cracking.

3. The stiffness of the beam on the reloading cycle was smaller than the stiffness on the first loading in the uncracked state, but greater than the stiffness on the first cycle in the cracked state.

4. The deflection after cracking was greatly affected by the magnitude of the cracking load. The smaller the cracking load the bigger the deflection, and vice versa.

5. At low values of applied moment (in the uncracked state) the stiffness (EI) exceeded that calculated on the basis of the uncracked transformed section.

6. After cracking the stiffness of the beam decreased with increasing bending moment to a value very near to that calculated on the basis of a cracked transformed section.

7. The stiffness on the reloading cycle was greatly affected by the ratio of applied steel stress to stress at first cracking on the previous

loading and the extent of cracking. An increase in the ratio caused a reduction in the stiffness.

8. The remaining deflection was influenced by the applied load and the extent of cracking.

9. The average ratio of the remaining deflection at the end of the first cycle to the deflection at the design load may be taken as $\frac{1}{4}$.

10. The ratio of the remaining deflection to the deflection at the maximum load of the previous loading cycle decreased as the load was increased, i.e. the recovery ratio increased with increasing load.

11. The reloading curves were approximately linear (due to the little effect of the hysterisis loops) up to the previous maximum load, after which the curve bent sharply along the initial load-deflection curve (virgin cycles).

12. On unloading from a value of 76 to 89% of the maximum load the recovery in deflection amounted to 77 to 88% for the deformed and plain bars. The recovery decreased with decreasing steel area.

13. The span to depth ratio varied directly with the allowable deflection and inversely with the stress in the reinforcement.

14. In beams with the same percentage but different types of steel the surface characteristics of the reinforcing bars had no significant effect on deflection, even at loads as high as the first yield of the material. The deflection was greatly influenced by the magnitude of the stress in the reinforcement.

15. In beams with different amounts and types of steel reinforcement, the deflection was greatly influenced by the magnitude of the steel stress and the amount of the reinforcement.

16. In beams with the same design loads, but with different grades, types and percentages of steel the deflection increased with decreasing area and the decreasing modulus of elasticity of the reinforcement.

9.7.3 Limit State of Collapse (Ultimate Strength)

1. The ratio of the actual maximum moment to the calculated ultimate moment was always greater than unity. The beam with Bristrand 100 showed the greatest ratio of 1.22.

2. The theoretical ultimate moments (calculated in accordance with the Draft Code, neglecting the partial safety factors on the materials) were in good agreement with the experimental values.

3. The ratios of the experimental maximum moments to design moments (calculated according to the Draft Code with a global load factor of 1.8) were greater than 2. The maximum ratio was 2.52.

4. The actual steel stresses at failure exceeded the yield strength of the reinforcement. The beam with Bristrand 100 showed the greatest increase of 27%.

5. In under-reinforced concrete beams, high tensile steel provides better utilisation of the concrete strength in compression.

6. In under-reinforced concrete beams the stress-strain characteristics of the reinforcement have no effect on their ultimate strength.

7. Cold worked steels were superior to hot rolled steels as regards the warning before collapse. However, hot rolled steel with high yield strength and good bond characteristics were superior to mild steel.

9.7.4 Flexural Strains

1. The strain distribution in the concrete compression zone was almost linear, while that for the tension parts of the beam might not be linear.

2. Some recovery in the compressive strain occurs when the beams are left in the unloaded condition after previous loading cycle.

3. The effect of increasing the permissible stress in the reinforcement for beams with equal or different percentages of steel was to increase the compressive and nominal tensile s trains oocurring in concrete.

4. The type (plain or deformed) of the reinforcing bars had no effect on the concrete strains.

CHAPTER 10

The Effect of Long-Term Loading on the Behaviour of Beams

10.1 General

The behaviour of nine beams reinforced with different types and percentages of steel was studied under the action of sustained and fatigue loading. Five beams were kept under sustained design load for the durations noted in Table (1). Four beams were subjected to repeated loading between full and half the design load. The number of cycles each beam was subjected to is given in Table (1).

The behaviour of the beams with time was examined in relation to cracking, deflection, stresses and strains. The change in the serviceability and safety characteristics were examined very closely at frequent stages.

A detailed study of the long-term behaviour of beams is reported. Practical considerations of the prediction of the behaviour (cracking and deflection) under sustained and fatigue loading are presented. The effects of the long-term behaviour on the economic use of high tensile steel are discussed.

10.2 Limit State of Cracking

10.2.1 Repeated Loading Tests

In the beams tested statically in this investigation the stresses in steel at the first cracking of concrete varied between one third to one eighth of the design load steel stresses, with an average of one fifth. At the static design load before the fatigue loading, the crack widths were of certain magnitude, as shown in Figs. (71) and (72).

In these figures the crack widths can be seen to increase with the number of repetitions of loading. In all beams most of the increase seemed to have occurred during the first million repetitions. After two million repetitions the maximum crack widths stopped increasing, while the average crack widths continued to increase. Considering the maximum crack width at the bottom edge

of the beam, the increase was not uniform, and as the repetitions increased there were some changes in the slope of the curves. The maximum crack width at the steel level and the average crack widths at both levels increased more uniformly. At some stages there appeared to be a decrease rather than an increase in the total and average widths of cracks in the constant moment zone. This may be due to the formation of new cracks, which tended to extend at the expense of the neighbouring cracks. The new cracks formed either in the constant moment zone or in the shear spans. Only the cracks in the constant moment zone were recorded. Most of the increase in the number of cracks took place within the first few thousand repetitions, as can be seen in Fig. (73). In beam A32 the increase continued until approximately two million repetitions occurred, while in beam A33 a new crack formed at the last static load cycle after about 3.3 million repetitions.

In Figs. (71) and (72) and in column (7) of Table (15) it is observed that after 3.5 million repetitions the maximum crack width at the level of steel, under design load, did not exceed the permissible crack width (0.2 mm) for normal conditions, as suggested by the C.E.B.[41] The crack width at the bottom edge level, further away from the surface of the reinforcing bar may exceed the permissible crack width as in the case of beam A34, in which the maximum crack width was about 0.235 mm. The initial stress in steel in this beam was 326 N/mm^2.

Column (9) in Table (15) gives the ratio at design load of the crack width extrapolated for 3.5 million repetitions (see Fig. 74) to the crack width at the first cycle. It can be observed that the ratios did not exceed 1.5. This suggests that a value of 1.5 for the ratio of final to instantaneous width of cracks for fatigue loading seems to be reasonable. An initial crack width at the reinforcement level of 0.12 mm under a design steel stress for static loading of 320 N/mm^2 can be adopted without any danger of corrosion to be expected in normal conditions of exposure.

In Fig. (75A) increases in crack width due to repeated loading are given for all types of steel. It can be noticed that the increase for mild steel was bigger than the average of those for deformed bars. This conclusion was based on only one beam, and is therefore

of limited validity. In beam A34, where the stress in steel was as high as 326 N/mm^2, the increase approached that of mild steel.

After 0.33×10^6 repetitions an increase in crack width of 25% at design load steel stress ranging between 138-380 N/mm^2, has been reported[43] for beams with different types of steel, including plain round, deformed, square twisted and strands. An increase as low as 8% has also been reported[44] for the same number of repetitions for a steel stress of 345 N/mm^2. In the present investigation (ref. Fig. 75A) the increases were 37.5, 15, 7.8 and 40% for beams with plain round bars (A31), deformed Unisteel 60 bars (A32), deformed Unisteel 80 bars (A33) and deformed Kam 60 bars (A34). Nakayama[71] found that the increase in crack widths for beams with plain bars was the same as that for beams with deformed bars when a greater number of small sized bars were used. When the beam contained only one plain bar the crack width was 1.5 times as large as that using a deformed bar of the same diameter, and this ratio became 1.8 as the load was repeated. For deformed bars an increase of 0 to 20% was observed at a steel stress of 220 N/mm^2 after 10^5 repetitions.

Hajnal Konyi[57] observed that the crack width in the beam with mild steel increased by 167%, while that with deformed bars remained constant after two million repetitions, even though in the latter the stress in the steel was 210 N/mm^2. The number of the maximum cracks seemed to have increased in beams with deformed bars. For the same number of repetitions, increases in crack width of 15%, 17.5% and 50% have been reported by other investigators[44,71,75] for maximum steel stresses of 173 N/mm^2, 345 N/mm^2 and 330 N/mm^2 respectively. In the present investigation the increases in the maximum crack width after two million repetitions were 50%, 38%, 25% and 50% for beams A31, A32, A33 and A34 respectively.

The increase in crack width for beams with mild steel was more likely to be due to loss of bond between steel and concrete in the vicinity of the cracks, owing to its surface characteristics. The increase in beams with deformed bars might be caused by a) the increase in steel stresses between the cracks due to creep of concrete in tension and b) the increase and formation of internal cracks at the steel level at high values of stresses in steel. This was

shown to be true by Lutz.[90]

On the removal of the live load, most of the cracks remained open with certain widths. After repetitions of load some of the remaining crack widths increased. Remaining crack widths are shown in Fig. (74). The biggest remaining crack width was in beam A34 with a value of .08 mm at the steel level after 3.5 million cycles. In beam A31 the remaining crack width after 3.5 million repetitions was .05 mm. For beams A32 and A33 the respective maximum remaining crack widths after 3.5 million cycles were 0.03 and 0.035. These were well within the accepted figure of 0.2 mm.

Throughout the stages of fatigue loading the crack formation and the increases in crack widths were recorded for several increments of loading up to design load. At the last static test the measurements were recorded up to failure. Figs. (76) and (77) show the effect of previous repeated loading on the manner in which the crack widths changed with the load. It can be seen that in beam A31 there was a big increase in crack width at design load after about 2 million cycles, while in the other beams it was less severe. Also the remaining crack widths and the changes in the slopes can be noticed. However, when a comparison is made between beams tested statically (e.g. A11) and those with previous repeated loading (e.g. A31) as in Figs. (76) and (77) no definite conclusions can be drawn as regards the effect of repeated loading on crack width. This is because of the random nature of the crack widths on the first application of the load. In most of the static beams the crack widths were greater than those of the fatigue beams in the first cycle. This behaviour was observed until failure. In beam A34 the crack width on first application of the load was greater than that in beam A14 and it seemed to have increased relatively under the effect of repeated loading at the design and at near failure loads.

The cracking patterns at failure on one side of each of two typical fatigue test beams are shown in Fig. (78). This figure shows the initial spacings of cracks at first application of load, the height of travel of cracks at various increments of loading, at design load and at near failure load. The changes in the cracking patterns and crack formations due to repeated loading can be seen

from the development of new cracks and the increase in the height of travel of the initial cracks. In only one beam, A34, after over three million repetitions of loading was it noticeable that the cracks decreased in length, i.e. the tops of most of the cracks were seen to have closed. At the last static test to failure, one crack in beam A31 and two cracks in beam A33 formed at very high loads. They travelled from the bottom edge to the mid-depth of the beam.

10.2.2. Sustained Loading Tests

The increase in crack width and crack propagation were studied under the effect of sustained design load, which was the design live load plus the self-weight of the beam.

Figs. (79) and (80) show the initial values of the maximum and average crack widths at both the steel level and the bottom edge of the beam. The major increase in these crack widths took place within the first 3 to 4 months after which the maximum crack width attained a sensibly stable condition. The average crack widths continued to increase at an ever decreasing rate until a stable condition was reached after about a year. A decrease in the average crack widths can be seen in beams B21, B22 and B23 after a period of six months. This decrease may be due to the formation of new cracks during this period of time, as can be seen in Fig. (81). Most of the new cracks initiated at the level of steel, on the surface of the concrete, and travelled downwards and upwards and in some cases did not reach the bottom edge. In beams B21 and B25 most of the new cracks formed in this manner. There were more new cracks in these two beams compared to other beams.

Lutz et al[90] found that the major portion of the crack width increase occurred in the first 3 to 4 weeks after loading, after which the cracks increased at a much slower and continuously decreasing rate. Soretz[57] reported that a state of equilibrium in the widths and number of cracks of floor slabs was reached after 2 months. In other tests on bridges[86,87] he reported that 90% of the final number of cracks was reached after one year, and that complete stability was reached after three years. Corely and Sozen[89] noticed that the number and length of the cracks increased during the first 60 days.

All the beams showed a well developed pattern of cracking and beam B21, reinforced with mild steel, showed a larger number of cracks at the level of the centroid of steel than the rest of the beams.

Table (15) shows the values of crack widths at the steel level extrapolated for 1000 days of sustained loading. This extrapolation was deduced from Fig. (82) in which the crack widths were plotted on a semi-logarithmic scale. It can be observed from column (5) in Table (15) that the maximum value occurred in beam B25. A value of 0.29 mm was recorded. This was because of the very high steel stress (460.5 N/mm^2) at the design load, which caused the initial value of the crack width to be of a high value (0.22 mm). However, the ratio of the final to the initial crack widths, from column (8) in Table (15), was highest in beam B21, and lowest in beam B22. These ratios were 1.67 and 1.22 respectively. The ratio reported by Lutz et al[90] was 1.4, while others[42,146] reported a ratio of 1.5

In Fig. (75B) the average increase in the maximum crack widths of all the beams with deformed bars were smaller than that for the beam reinforced with mild steel, even though the design steel stresses in the case of deformed bars were much higher than that in the case of mild steel bars. The initial applied steel stresses, as shown in Table (10) ranged from 175 N/mm^2, for mild steel, to 460.5 N/mm^2, for Kam 90 steel. A difference of only 10% in the final values of the crack width has been observed by Soretz[86,87] when the steel stress under sustained loading was increased from 2400 kg/cm^2 to 3500 kg/cm^2.

At the maximum value of the stress (460.5 N/mm^2) the crack width exceeded that which is permissible by the C.E.B.[41] This limit has been superimposed on the graphs of the variation of maximum crack width with time. As regards the maximum crack widths at the bottom edge of the beam, the limit of 0.2 mm was exceeded in three beams, B21, B23 and B25, as shown in Fig. 79. These beams developed final values of 0.22mm, 0.22 mm and 0.38 mm respectively. In the other two beams, B22 and B24, the final values were 0.20 mm and 0.19 mm respectively. These values, along with the ratios of the final to initial crack widths depended greatly on the initial values, which in turn depended on the random probability of the formation of the cracks.

There are three main reasons for the increase of crack width under sustained loading: a) the increase in steel stresses due to progressive breakdown of the concrete in tension at sections between cracks, resulting in an increase in width and number of internal cracks, b) the increase in steel stresses due to the creep of concrete in compression and the subsequent lowering of the neutral axis c) creep in bond between steel and concrete, causing increased slip of concrete over the steel. Similar observationshave been noted by Lutz[90] and Thomas.[146]

One single side of each of two typical beams under sustained loading is shown in Fig. (83). The cracking patterns are shown for the first application of loading. The height of travel of the cracks were marked at various increments of loading and up to design load. In these same figures the effect of sustained design load for a duration of one year is shown. It can be seen that some of the cracks increased in length within the first few days, after which, due to the effect of creep in the concrete, they tended to close at their tops. Due to the same effect, the heights of the cracks became more uniform, throughout the constant moment zone. A similar observation of closing of the tops of cracks after a period of 60 days has also been reported by Corely and Sozen.[89]

10.3 Limit State of Deflection

10.3.1 Repeated Loading Tests

When a reinforced concrete beam is cracked it exhibits a change of stiffness with increasing load. The stiffness decreases, causing an increase in rotation and thus an increase in deflection. The same beam will behave in a similar manner under the influence of repeated design load, with the stiffness deteriorating with an increase in the number of repetitions of loading. However, when the applied repeated loads stay the same in magnitude a state of stability in the change of stiffness may be reached, after a certain amount of fatigue loading.

Fig. (84) shows the increase in deflections during the repeated loading test. These deflections at design and zero live loads were measured during the static load cycles carried out after every few

hundred thousands of repetitions during the fatigue loading tests. It can be noticed that the maximum increase in deflection took place during the first few thousand repetitions. There was a rapid increase during the first 400,000 - 500,000 cycles, after which the rate of increase in deflection was decreasing. With a maximum permissible stress in steel of 168 N/mm^2 in beam A31, and a span-depth ratio ($^L/d_1$) of 17.6, the maximum deflection at the end of the repeated loading test did not reach the value of $\frac{L}{360}$. In beam A32, in which the steel stress was 229 N/mm^2, the maximum deflection exceeded the value of $\frac{L}{360}$, but never reached the value $\frac{L}{250}$. Beam A33 had a deflection greater than $\frac{L}{360}$ at a steel stress of 259 N/mm^2 on first application of the load. The maximum deflection approached the value of $\frac{L}{250}$. In beam A34 at a steel stress of 326 N/mm^2, the value of $\frac{L}{250}$ was reached in the first 200,000 cycles, after which it was exceeded as the number of repetitions increased.

Again in Fig. (84) it can be observed that the increase in the total deflection at design load, after one million cycles or more, was mainly due to the increase in the remaining deflection at zero live load. This effect can also be seen in Fig. (85) which includes typical load-deflection curves for static load cycles applied at frequent intervals during the repeated loading test. The load-deflection relationships for all the beams were recorded and the typical behaviour is shown in Fig. (85). On the first application of the load the curve was not a straight line. It was slightly concave towards the deflection axis. When it was unloaded the curve became concave towards the load axis, with a remaining deflection at zero live load. The beam was then subjected to repeated loading, and after about 679,000 cycles the relationship became straight lines for both loading and unloading conditions, as can be seen in the figure. The deflections at both zero and design live loads increased due to increasing elastic and remaining deflections. Further repetitions of loading affected the remaining deflection only while the elastic deflection became stabilized. The remaining deflection tended to stabilize just after two million cycles. The loading curve did not coincide with the unloading curve, even at a very high number of repetitions. In Fig. (85) the two curves started from almost the same point and then they diverged up to a load which represented about 60% of initial cracking load, after which they changed slope and moved towards almost the same

point, forming a hysterisis loop. The loop did not appear to diminish even after more than three million cycles.

The remaining deflection at zero live load, after the first application of loading, was higher in the case of beam A31 than that of A32, in spite of the fact that the working steel stress in the former was lower. However, the remaining deflections became the same for both beams after the first 800,000 repetitions, and they remained approximately equal until over two million repetitions at which the test of beam A31 was stopped. It seemed that the extent of cracking was responsible for such behaviour. On the first application of loading the cracking pattern of beam A32 was not fully developed, so within the first few thousand repetitions more cracks formed, and thus more remaining deflection occurred. This can be clearly seen in Fig. (87) where the load-deflection curve on the first application of the load was not linear, but the stiffness was gradually decreasing, thus indicating the incomplete development of the cracking during the first cycle of loading.

In Figs. (86-89) a comparison is made between beams of similar design which were tested statically to failure. The companion beam in each pair has been subjected to previous repeated loading. In the figures beams with lower cracking loads showed bigger deflection at the static design load than their companion beams. However, it can be clearly seen that repetitions at design load tended to increase the stiffness of all the beams regardless of the type of steel. When a static load higher than the maximum repeated loading was applied the elastic deflection of the beam under this load was less than that for the companion beam subjected to the same load without previous repetitions of loading. It may also be seen in the figures that a clear discontinuity in the load-deflection curves marks the limit of the earlier repeated loading. It can be concluded, therefore, that the damage occurring under repeated loading is that which under static loading would occur at higher load, and that less further damage occurs in beams with prior repetitions of loading when loaded statically beyond the upper limit of the loading range. Consequently, the maximum deflection at failure was not significantly affected by previous repetitions. Similar behaviour has also been reported by Saliger,[59,60] Bate,[68]

and Russell et al.[75]

Table (16) summarises the value of the deflections under the design load at the first application of loading, and at the static loading cycle at the end of 3.5 million repetitions. In beams A33 and A34 the value of $\frac{L}{360}$ was exceeded even before the repeated loading was applied (Fig. 84). After 3.5 million repetitions of loading the value of $\frac{L}{360}$ was exceeded in beam A32, while the value of $\frac{L}{250}$ was exceeded in A34 only.

The ratios of final to initial deflections are given for all the beams, the maximum value being 1.33 for A31, reinforced with plain round mild steel bars, and the lowest being 1.22 for A33 with deformed bars. Fig. (90) shows the effect of repeated loading on the increase of deflection, the average being taken for the beams reinforced with deformed bars. It can be seen that the increases in the remaining deflections at zero live load were greater than those for the deflection at design loads.

Bate[68] found an increase in the total deflection of not more than 20% for any number of repetitions within the working range between half and full design load. Similar increases of 10 - 20% after 2 to 3 x 10^6 repetitions was found by Hajnal Konyi.[58] Russell et al[75] found an increase of 50 to 60% after 2 x 10^6 repetitions. It was recently reported[44] that the deflection continued to increase with repetitions, and an increase of 43% after 10 x 10^6 was obtained.

Soretz[74] reported that the total and residual deflections increased by an average of 70% during 2 x 10^6 repetitions, and that the residual deflection was finally about half of the total deflection. Other investigators[43,71] reported increases in the total deflection of 5 to 25% regardless of the type of steel used.

10.3.2. Sustained Loading Tests

It is well known that when concrete is subjected to a constant sustained stress it will creep. Initially, these creep deformations increase rapidly, and then they increase at an ever-decreasing rate as time elapses. The same phenomenon of creep occurs in reinforced

concrete beams subjected to any level of sustained load. The beams in the present investigation were subjected to their design loads producing a range of stresses in the steel from 175 N/mm^2 for beam B21, with plain round mild steel bars, to 460.5 N/mm^2 for B25, with deformed Kam 90 steel bars. The properties of the beams and the stress ranges are shown in Table (10).

The time dependent deflections, including creep and shrinkage, are plotted, in Fig. (91), on ordinary scale, and in Fig. (92) on semi-logarithmic scale, in which they were extrapolated to one thousand days. Fig. (91) shows typical creep deflection curves, with an increase in deflection at a decreasing rate for a very long time. The instantaneous deflections, for all beams, were above the value of $\frac{L}{360}$, and in the case of beam B25 it was even above the value of $\frac{L}{250}$ due to very high steel stress. In beams B21, B22, B23 and B24 the value of $\frac{L}{250}$ was exceeded within the first four weeks of the application of load. Therefore all the beams became unserviceable from the point of view of limit state of deflection. Fig. (93) shows the deflections of the five beams after one year of sustained loading. The limits of $\frac{L}{360}$ and $\frac{L}{250}$ are indicated on this curve. It is clearly seen how these limits are exceeded under sustained loading.

In order to study the difference in the behaviour under sustained loading of beams reinforced with different types of steel bars, namely plain round and deformed steel bars, Fig. (91) has been reproduced as Fig. (94) for only the first 67 days. It can be seen that the instantaneous deflections of the beams increased with an increase in the permissible steel stress, and a decrease in the steel percentage. The increase in the inelastic deflection with time seems to be less in beams reinforced with deformed high tensile steel (H.T.S.) bars than that reinforced with plain round mild steel (M.S.) bars. The ratios of the deflection of the beams with deformed bars to those with plain bars are indicated in Table (17) for durations of six months and one year. It is apparent from these ratios that after one year of sustained loading the ratios of total deflection of deformed bars to total deflection of mild steel are 0.969, 1.060, 0.917 and 1.247 for beams B22, B23, B24 and B25, as against

the ratios (1.09, 1.27, 1.12 and 1.72 respectively) for the instantaneous deflections of deformed bars to mild steel. Hajnal Konyi[88] found that the average ratio of maximum deflection between high strength steel and mild steel decreased from 1.24 to 1.14 after a period of $4\frac{3}{4}$ years.

In Fig. (94) the time deflection curves of beam B24 crossed that of beam B21 at about 33 days, and its deflection continued to increase at a lower rate. The curve of beam B22 crossed that of beam B21 at about 43 days and continued at the same rate of increase as that of B21. Therefore, the curves of the beams with high tensile steel showed smaller increases in the deflection than that with mild steel during the whole period of sustained loading. This indicates the advantage of high tensile steel in controlling time dependent deflection.

This phenomenon can be explained with the following reasoning: the increase in the neutral axis depth with time (due to creep) was greater for beams with high tensile steel (H.T.S.) (with less area of steel) than that with mild steel (M.S.), as can be seen in Figs. (95-100). The percentage increases after three weeks of sustained loading for beam B21 with M.S. bars and beams B22, B23, B24 and B25 with H.T.S., were 12%, 20%, 14%, 25% and 25% respectively. After a period of one year the increases were 30%, 41%, 37%, 53% and 58% respectively. As a result of this movement of the neutral axis a redistribution of stresses in the concrete occurred and this reduced the rate of creep, causing a lower rate of creep deformation and deflection. The biggest increase in the neutral axis depth was in beam B25, in spite of the formation of a new crack within the gauge length of strain measurement. The increases in the average crack widths for beams with deformed bars, after seven weeks of sustained loading were 36%, 26%, 50% and 26% for beams B22, B23, B24, and B25 respectively. These percentages are bigger than the increase in beam B21 with plain round bars, which was only 7%. Therefore, the differences in the increase of deflection cannot be due to cracking. It cannot be due to the age differences of the beams. The age of beam B21 when first loaded was 97 days, the other beams were loaded at ages varying between 44 to 100 days.

From the above reasoning, therefore, the differences in the rate of creep of concrete, for the different types of steels, was due to the effect of different stress redistributions resulting from the lowering of the neutral axis. This will, therefore, account for the difference in the increase of the time dependent deflections for beams with different types of steel; the increase was lower for beams with higher steel stresses and corresponding smaller steel area.

Hollington[187] found that beams containing high tensile reinforcement (414 N/mm^2 yield point) have a greater rate of deflection during the first few months after loading than those with mild steel, but subsequently the deflection curves become very similar. He attributed the cause of the different ratios of deflections at early ages to the breakdown of the tension stiffening effect in the concrete, which is bigger in beams with high tensile steel due to less steel area. However, Corely and Sozen[89] did not find any escalation in deflection due to the use of higher permissible steel stresses.

Table (16) shows the final deflection extrapolated from Fig. (92) for one thousand days duration. The last measurements were taken after 623, 520, 623, 553, 553 days for beams B21 to B25 respectively. Column (8) in the Table (16) shows the ratio of the deflection at the end of 1000 days to the instantaneous deflection. These ratios decreased with an increase in the applied steel stress, being highest (2.22) for beam B21 with a permissible stress in the steel of 175 N/mm^2 and lowest (1.57) for beam B25 with a permissible stress of 460.5 N/mm^2. Additional deflections for different permissible stresses sustained for long periods of time, are given in Fig. (101). The maximum additional deflection was 122%. This was much lower than the value given by Yu and Winter.[78] Therefore, the factors suggested by Yu and Winter cannot be applied when using very high tensile steel, as can be seen in Fig. (101). Also the beams tested by Yu and Winter were loaded at ages different from the ages reported in this investigation.

Because of the different span-depth ratios, different applied steel stresses, and different ages at loading , values of the ratio

between the final deflection and the instantaneous deflection of 3 to 4 for a period of about five years have been reported by different investigators.[77,78,80,88] Lutz et al observed[90] a total deflection of 2.15 times the instantaneous deflection after five months of sustained loading. For a duration of 182 days it has been reported[44] that an increase of 38% in deflection was found in a beam with Bristrand 100 for a steel stress of 290 N/mm^2 and a steel percentage of 1.51. In this investigation the increase was found to be 56% for the same steel stress but different type (deformed) and percentage of steel (1.01%).

To take into account the influence of long term loading, including creep and shrinkage, it is therefore important to know about the level of stress to which the reinforcing steel is being subjected. Given that part of the load which is considered to be of a long duration the stress in the steel can be found and consequently, using Fig. (101), a multiplier (F) for additional deflection due to creep and shrinkage can be obtained.

This factor (F) may be incorporated in the denominator of the expression, developed in § 9.3.6. for the L/d ratio, which can be used in the design of a reinforced concrete member, to give a total deflection (instantaneous + creep + shrinkage) not exceeding a permissible limiting value.

The factor of age at loading should also be included, as has been suggested by the Draft Code.[23] At an age of loading of 14 days a factor of 2.0 for additional deflection is recommended. At an age of 90 days a factor of 1.5 is recommended. In the present investigation beam B21 was loaded at an age of 97 days, and the factor for additional deflection due to creep and shrinkage obtained was 1.22. Beams B24 and B25 were loaded at 85 and 100 days respectively, and the factors for additional deflection were 0.78 and 0.57 respectively. These values for B24 and B25 are much lower than the Code's value, and this, as above, is due to the higher permissible steel stresses and corresponding smaller steel areas.

In the present investigation, as mentioned earlier, the beams under sustained design loads were intended to be designed to contain steel percentages and permissible stresses which will give the

same design load. So the above conclusions apply to beams with equal design loads but different percentages and working stresses of steel. However, more information can be gained if in addition beams with equal amounts of steel and different degrees of permissible stresses were tested under sustained design load.

Table (18) shows the calculated and measured deflections after one year of sustained design loading. The calculated deflection has been obtained using an "effective" modulus of elasticity for concrete and the equations provided by Pauw and Meyers,[101] as has been shown in Chapter (2). The calculated deflections were found to be less than the measured ones. In Fig.(91) a deflection curve has been superimposed on the experimental curve for beam B21. Again it could be observed that the calculated deflections were always less than the measured ones; the difference between the two curves increased with time until about 140 days after which it became nearly constant. This increase can be attributed to the formation of additional cracks, mainly internal cracks, between the surface cracks, which made the steel strains greater and more uniform in that region than existed initially, and hence larger deflections occurred. The increased internal cracking is produced by (1) the increase in steel strains due to the lowering of the neutral axis caused by creep, and (2) theprobable decrease in the tensile strength of concrete under sustained loading. Similar observations have been reported by Lutz et al.[90]

In Table (18) the time-dependent deflections calculated on the basis of the proposed method in § 9.3.2.1., and the percentage increase given in Fig.(101) are compared with the measured deflections. It can be seen that the two deflections agreed satisfactorily and in all beams the proposed method over-estimated the measured ones. The proposed method accounted for the increase in deflection due to the increase in cracking.

Only three beams were unloaded and their deflection recoveries were recorded. The load was removed from beam B22 after 520 days and from B24 and B25 after 553 days of sustained loading. Table (19) gives the recoveries of deflection that were measured over a period determined by the limited availability of test area. It can also be seen from the table that additional recoveries after one day and 28 days were respectively 0.27 mm and 0.84 mm for beam B24, and

0.29 mm and 1.08 mm for beam B25. The additional recovery observed by Hollington[187] was the same after 1 day and 40 days. The residual deflection in this investigation was about half of the final deflection, while Hollington found an average residual deflection of 75% of the final deflection. From the figures in the table it can be observed that the grade of steel did not have any effects on the recovery of deflection.

10.4 Limit State of Collapse (ultimate strength)

10.4.1 Repeated Loading Tests

All beams, except A31, were subjected to more than three million repetitions between full and half the design load. Under this range of loading the stresses in the steel reinforcement as a percentage of the yield stress were 53%, 50%, 40% and 53.8% for the upper limit and 38%, 24.8%, 22% and 27.4% for the lower limit for beams A31 to A34 respectively. The percentages based on the ultimate strength were 35%, 37%, 37.5% and 35% for the upper limit and 18.5%, 18.5%, 20.8% and 18% for the lower limit respectively. The stresses in the concrete compression zone as a percentage of the cube strength were respectively 25%, 40%, 46% and 54% at the upper limit of loading and 11.7%, 17%, 25% and 22% at the lower limit. It was expected that fatigue failure would not occur and that the ultimate static strength would not be significantly affected after this number of loading repetitions, since these limiting ranges of stresses were well within the limiting failure stress ranges of the modified Goodman diagrams for the component materials, i.e. steel and concrete.

At the end of the fatigue test, the static strengths were found to be very nearly the same or slightly higher than the static strengths of the corresponding beams, which were not previously subjected to repeated loading. The ratios of the experimental to calculated ultimate strengths are given in column (11) of Table (8). It can be seen that there is a good agreement between experimental and theoretical values of the ultimate strength of beams.

Beam A33 could sustain higher loads than that indicated in Table (8). The test was stopped because the capacity of the loading jack used was not big enough to destroy the beam, The reason for the

increase in the strength of the beam under fatigue loading, over that of the companion static beam, may be due to the ageing of concrete with time, and may also be due to the compacting effect on the concrete under compression. Similar observations have been given by Saliger,[59,60] Bate,[67,68] Verna and Stelson[66] and Probst.[56] From results of tests carried out on prestressed concrete beams similar observations have been reported by Abeles,[188,189] Dave,[190] and Rimmer.[191]

In general, fatigue failure of a reinforced concrete beam can occur either as a fatigue failure of the reinforcing bars or a failure in the concrete in compression. The latter mode of failure depends on the magnitude of loading, and can be either flexural failure or bond and shear failure, which may induce a crushing failure of concrete in compression. According to Chang and Kesler,[63] and Verna and Stelson,[66] when a reinforced concrete beam fails in flexural tension, as is the case with the static beams in this investigation, it can either fail in tension or shear under fatigue loading, depending on the magnitude of the applied repeated loading. If the upper limit of the repeated loadings was low, the failure will be flexural, and if it was high the failure will be in shear. When the failure is a fatigue fracture of the reinforcing bar, then the minimum stress becomes an important factor which influences the fatigue resistance of the beam.

Since the static ultimate strength of the concrete beam with low and normal percentages of steel reinforcement is conditioned by the behaviour of the steel, the properties of the reinforcing steel may, therefore, be expected to have a considerable influence on the behaviour of reinforced concrete members under repeated loading. The mode of failure under static loading with normal percentage of steel is first yielding of the reinforcement, and then crushing of the concrete. The mode of failure under repeated loading is likely to be the same in beams reinforced with mild steel, with a reduction in ultimate strength. The beams with high tensile steel may fail at the value of the stress in the steel appreciably less than that of a beam subjected to static loading only. This value of stress in steel also depends upon the range of loading.

In this investigation none of the beams failed under repeated loading. Since the range of loading and the number of repetitions

were comparatively low to cause such failure.

10.4.2 Sustained Loading Tests

There is an abundant evidence on the effect of sustained loading on the ultimate strength of the structure. Many investigators reported[57,76,81,82,83,84,85] no significant change in the static ultimate strength of the beams subjected to previous sustained design loading, and in some cases even sustained over-loads. A reference can also be made to prestressed concrete beams subjected to sustained design loading and over-load. Dave,[190] and Cottingham, Fluck and Washa[192] confirmed that there is no reduction in strength, while Kimmer[191] and Gadre[193] reported losses in ultimate strengths of 5.57% for over-loaded beams, and 8.5 to 17% for composite beams under design load for a period of six months.

Experimental evidence, therefore, suggests that the ultimate static strength of reinforced concrete beams is not affected even after very long periods of sustained design load.

10.5 Flexural Strains and Stresses

10.5.1 Repeated Loading Tests

Figs. (102) and (103) give typical history of the flexural strain distribution of the beams subjected to repeated loading, ranging between full and half the design load. Beam A31, reinforced with plain round mild steel bars was subjected to just over two million repetitions. The stress range in the concrete in the compression zone was between 6.17 and 13.1 N/mm^2, with an average of 9.63 N/mm^2. The compression strain in the concrete top fibre increased from 38×10^{-5} to 65×10^{-5} for the upper limit of the loading range, and from 15×10^{-5} to 45.5×10^{-5} for the lower limit. The variation of the compressive strain can also be seen in Fig. (104) as related to the number of repetitions. The strains increased rapidly during the first few thousand repetitions and then they increased at a decreasing rate. Both the elastic and the remaining strains increased with the number of repetitions, the remaining strain at a faster rate, and they both would attain a stable state eventually.

In the beams with high tensile deformed bars, the initial compressive strains at the first application of the loads were higher than those for beam A31. They increased with the

increase in the concrete stress caused by the increased permissible steel stresses. The ranges of concrete stresses to which the beams were subjected were (7.3 - 17.0 N/mm^2), (12.5 - 22.6 N/mm^2) and (7.93 - 19.2 N/mm^2) for beams A32, A33 and A34 respectively. The initial strains at the corresponding levels of stress were (15×10^{-5} - 47.5×10^{-5}), (32×10^{-5} - 63.5×10^{-5}) and (24.5×10^{-5} - 68.5×10^{-5}), for beams A32, A33 and A34 respectively. At the end of the fatigue testing the compressive strains measured were (41.5×10^{-5} - 68.5×10^{-5}), (48.5×10^{-5} - 76.0×10^{-5}) and (73×10^{-5} - 112.5×10^{-5}) at their corresponding stress levels.

From these figures it can be noticed that after the final cycle the increases in concrete compressive strains due to creep were not dependent on the magnitude of the stresses in the steel. Shrinkage strain being a fraction of the total strain, the increase in strain (creep + shrinkage) in A33 was only 19.7%, which was the lowest, while for beam A31 the percentage increase was 71%, which was the highest. For beams A32 and A34 the percentage increases were 44.4% and 64.5 % respectively. It can be concluded that the increase in compressive strains is likely to be affected by the level of stress in the concrete, the strength of concrete and the age of concrete at loading. In this study the cube strengths of the concrete at failure were 52.7, 42.7,48.9 and 35.7 N/mm^2, and the ages at loading were 60, 140, 200 and 139 for beams A31, A32, A33 and A34 respectively.

The increase in compressive strains in the concrete can be due to either a) fatigue creep or b) movement of the neutral axis. The former is more likely to be the reason, because the neutral axis dropped as the number of repetitions increased. The behaviour of the four beams under repeated loading indicated a drop in the neutral axis and thus a redistribution of stresses occurred, which tended to reduce the rate of creep.

A careful study of Figs. (102) and (103) reveals the behaviour of the lower portion of the beam in tension at both the bottom edge and the steel level. This behaviour is greatly influenced by the extent of cracking and to a lesser degree by fatigue creep of concrete in tension. The concrete in the tension side between the cracks is restrained by the steel reinforcing bars, and thus the rate of creep of concrete at the level of steel is usually less than that at the

top fibre in compression. This causes the neutral axis to drop slightly. At the same time the cracks already existing tend to travel towards the compression face at a different rate, which causes the neutral axis at the crack to rise, so the net movement, as seen in Figs. (102) and (103) is the lowering of the neutral axis and an increase in the nominal tensile strains at the steel level. Under repeated loading, in some cases, the increase in the nominal tensile strains due to crack widening and creep of the concrete exceeded the compressive strains for the same number of cycles. In beam A32, for example, at design load, the increase in the nominal tensile strains at the steel level after 761,092 cycles was 22.5 x 10^{-5} as compared to 10.0 x 10^{-5} increase in compressive strains. This is because the neutral axis remained constant over the first 761,092 cycles, as seen in Fig. (105). The increase was due to the widening of cracks, creep of concrete and breakdown of tension stiffening effect.

In beam A33 after 679,250 cycles, a new crack formed within the 200 gauge length of the strain measurement. The neutral axis did not change its position and there was an increase in the nominal tensile strains greater in magnitude than the increase in the compressive strains at the top fibre. The increase in tensile strains was 6.0 x 10^{-5} as compared to 4.0 x 10^{-5} in compression.

In beam A34 again the increase in tensile strains was 16.5 x 10^{-5} after 1,914,143 cycles, which was higher than the increase in the compressive strains of 9 x 10^{-5}. This was because of the formation of a new crack.

The general behaviour was a rapid increase in the nominal concrete tensile strains in the initial stages of load repetitions. This increase depended on the extent of cracking and fatigue creep in both the compression and tension zones of the beam. Generally the rate of increase of strains decreased with increasing number of load repetitions, unless new cracks formed.

Fig. (106) shows that after two million repetitions of loading, there was either a rise in the curve of the tensile strain as in beam A31 or a decline as in beams A32 and A33. The reason for this is that the depth of the neutral axis in the former case decreased, while in the latter it increased at a higher rate than usual.

In order to find whether a component of the increase in the tensile strains is due to slip between steel and concrete, a study of the crack pattern of beam A33 was made. Initially, there was one crack, on side B, within the Demec gauge length. After 679,250 repetitions the increase in the measured nominal tensile strains at the steel level was 9.0×10^{-5}, while the increase in the crack width was 5.0×10^{-5}.

On side B of beam A31 the increase in the nominal tensile strains was 8.0×10^{-5} after 350,000 repetitions, while the increase in crack width was 15.0×10^{-5}. This discrepancy might be due to a) the pr esence of compressive strains between the tension cracks and their increase with load repetitions, and b) the possible forking of the crack at the steel level, and the width indicated above being where the two cracks meet.

Due to the limitations of the measurements and the variation in the readings of cracks, it cannot be inferred that the slip between steel and concrete has occurred. A value of 0.01 mm crack width is equivalent to 5×10^{-5} strain, and there is always a $\pm$0.01mm difference in the reading of the cracks, which the observer cannot avoid. Even so, it is believed that slip due to repeated loading has occurred in beam A31, in which plain round mild steel bars were used.

Fig. (107) shows the variation of the maximum stress in steel under repeated design load for all the four beams. The stress ranges to which beams A31,A32,A33 and A34 were subjected are given in Table (9).

It can be seen from this figure that the initial stresses at the design load increased with the grade of steel. The increase in steel stresses with repetitions depended on the movement of the neutral axis. If the neutral axis moves upward with repeated loading a decrease in stress is expected. This is so because the lever arm increases and thus the stress in the steel decreases. If the neutral axis moves downward the situation reverses and there will be an increase in steel stress.

In all the beams except A31, the neutral axis depth remained constant during the first few thousand cycles, and then it started

moving downwards with increasing number of repetitions until it became practically constant, as can be seen in Fig. (105). The neutral axis position depended onthe rate of creep and the rate of travel of the cracks. It may be noted that the strains were measured across a 200 mm gauge length within which the number of cracks varied randomly.

At the end of fatigue loading the increases in the steel stresses due to the lowering of the neutral axis were 2.56%, 1.75%, 1.16% and 3.4% for beams A31, A32, A33 and A34 respectively. These increases are very small and hence it can be concluded that there is no substantial change in the stress in steel due to fatigue loading.

Comparing the beams reinforced with different grades of steel, it can be emphasised that the differences in the increases in the steel stress did not bear any relation to the type of steel used or to the level of stress at which the repetitions were taking place.

In repeated loading the effects of the type of steel and the increased permissible steel stresses,(with constant steel area) on the deformation of reinforced concrete beams can only be related to the extent of cracking, the bond characteristics between steel and concrete and creep of concrete. No distinct trend in the tensile strain development can be traced to the differences in the types of steel used.

10.5.2 Sustained Loading Tests

Figs. (95-99) show the history of the flexural strain distribution of beams B21, B22, B23, B24 and B25 under sustained design load, These graphs have been drawn for a duration of one year.

The initial stresses in concrete and steel under the sustained design load are shown in Table (10). The concrete compressive stresses varied between 19.0 N/mm^2 and 22.4 N/mm^2, the average being 20.7 N/mm^2.

Fig. (108) shows the increase in the compressive strains in all the beams. Theincrease is attributed to two factors a) shrinkage of the concrete (without any applied stress) and b) creep of the concrete (under applied stress). From the figure it is apparent that the more severe effect is that of the creep. The factors affecting creep and shrinkage have been outlined in Chapter (2), so suffice it to point out here that the beams were loaded at an age of 44 days,

while beams B21, B24 and B25 were loaded at 97 days, 85 days and 100 days respectively. The younger the concrete, as measured by the degree of hydration, the higher the creep.

The initial compressive strains, under the sustained design load, for beams B21, B22, B23,B24 and B25 were 82.5 x 10^{-5}, 68.5 x 10^{-5}, 77.5 x 10^{-5}, 60.5 x 10^{-5} and 68 x 10^{-5} respectively. The variation in the initial strains in the beams was as high as 22 x 10^{-5}, even though the applied compressive stresses, as given above, were nearly equal for all the beams. The variation in the concrete strains cannot be due to the difference in the concrete cube strengths, because the results did not bear any direct relationship to the differences that occurred in the strengths of concrete inthe different beams. The variation in strengths between the beams was quite small. The variation in the compressive strains, therefore, should be attributed to the random nature of the concrete. This has been observed previously in the case of the static tests on beams of similar design.

Fig. (108) shows the increase in the compressive strains with time. During the first few days of sustained loading, there was a rapid increase in the strains. With time the curves changed and tended to take a flatter shape with a diminishing rate of increase in strains. The strains were ever increasing up to the last day of measurement. Similar behaviour has been reported from tests on sustained uniaxial compressive stress on plain concrete specimens.[93]

The increase in the compressive strains for all the beams during a period of one year was 149 x 10^{-5}, 110 x 10^{-5}, 113 x 10^{-5}, 93 x 10^{-5} and 88.5 x 10^{-5} for B21, B22, B23, B24 and B25 respectively. It is apparent that the increase in strains decreases with increasing permissible steel stress, i.e. creep depends on the steel stress and percentage as well as on the concrete stress.

In Fig. (108) it can be seen that the change of stress with time is not uniform, i.e. the curves are not smooth. There are some curious changes in the shapes of the curves. This is so because there was a variation in temperature and relative humidity in the test area, as can be seen in Fig. (10). Beams B24 and B25 particularly were situated near the exit, which was kept open during

the day, so the controlled conditions (20°C and 50% R.H.) could not be maintained.

The increase in the nominal tensile strains depended greatly on the downward shift in the neutral axis, the rate of increase of crack width and length, the rate of creep of concrete in tension, and the creep in bond and slip between steel and concrete. From Figs. (95-99) it is apparent that there was a rapid increase in the nominal tensile strains during the first few days, after which they increased at a diminishing rate untile a practically stable condition was reached. The increase in nominal tensile strains at the reinforcement level after one year of sustained design loading for beams B21 to B25 were 18×10^{-5}, 11.5×10^{-5}, 21.5×10^{-5}, 22.5×10^{-5} and 29×10^{-5} respectively. These increases were found to be less than the corresponding increases in the compressive strains for the same period of time, The biggest increase, which was in beam B25 with Kam 90 steel, was due to the formation of a new crack. The smallest increase, in beam B22, was due to the existence of only one primary crack within the 200 mm gauge length.

Comparing beams B21, B23 and B25, it can be seen thatthe increases in the nominal tensile strain were not much different, but the increases in the compressive strains varied greatly with different grades of steel, being lowest for the highest grade and corresponding lowest steel area. This suggests that good bond characteristics exist between steel and concrete, and a bigger stress redistribution occurs in the beams with high tensile deformed bars with less steel areas than with plain mild steel bars which reduces the rate of creep. As can be seen in Fig. (100), the neutral axis depths have increased by 12%, 20%, 14%, 25% and 25% for beams B21 to B25 respectively after three weeks of sustained design load. After one year the increases were 30%, 41%, 37%, 53% and 58% respectively. A bigger area of concrete will, therefore, be under compression, and thus for the same applied moment the average and maximum stresses in the concrete become smaller, which result in a smaller rate of creep.

The measured strains at the level of steel reinforcement were much larger than those due to the increased steel stress caused by the lowering of the neutral axis. Similar observations have been reported by Hollington.[187]

A comparison, therefore, between beams reinforced with mild steel bars with those reinforced with high tensile steel bars with lower percentages of steel, suggests that the former has a higher rate of increase in compressive strains than the latter. This is so in the initial stage when the neutral axis was increasing in depth and in the final stage when the neutral axis remained practically constant..

For all the types of steel and throughout the sustained loading tests, the flexural strain distribution in the compression zone remained sensibly linear. The strain distribution in the tension zone was less uniform. This general pattern of time dependent strain distribution in the compression zone has been reported by Hajnal Konyi,[88] Corely and Sozen[89] and Hollington,[187] and has been predicted theoretically by Sackman and Nickell.[106]

Figs. (109) and (110) show the variation of the stress in the steel reinforcement under sustained design load. The change in stress seems to be higher than that in stress during the first few days. As the time elapsed, there was a decrease in the rate of incfease until a practically stable state was reached. The increases in the steel stress were brought about by the lowering of the neutral axis as seen in Figs. (95 - 100). This effect reduces the lever arm resulting in an increase in steel stress, which will increase the crack width and the height of travel of the cracks. The steel stress between cracks will also increase due to the creep of concrete in tension and the formation of internal cracks at the surface of the steel bars. It is important, therefore, to note that there was a general trend in the increase of stress in the steel reinforcement: the higher the applied steel stress, the bigger was the increase in stress. The increase in beam B21, with a permissible stress of 175 N/mm^2, was 11 N/mm^2, and in beam B25, with a permissible stress of 460.5 N/mm^2 was 22.5 N/mm^2. However the percentage increase in the steel stress was lower for higher applied steel stress. The percentage increases for B21 and B25 were 6.3% and 4.88% respectively.

10.6 Comparison between Sustained and Repeated Loadings

10.6.1 Limit State of Cracking

Table (15) should be considered in comparing the effect of sustained and repeated loading on the maximum crack widths.

Columns (8) and (9) give the ratios of the final to the instantaneous maximum crack widths at the level of steel for the sustained and repeated loading respectively. Both types of loading seem to have similar effects on the crack width, giving average ratios, after 3.5 million cycles and 1000 days, of 1.43 and 1.46 respectively. Therefore, in the consideration of the limit state of cracking, both types of loading are equally critical.

When considering the maximum crack width at the bottom edge of the beam, it was found that the ratios for sustained loading were 1.29, 1.54, 1.10, 1.72, and 1.36, with an average of 1.44, as against 1.64, 1.03, 1.06 and 1.19, with an average of 1.23 for repeated loading tests. The effects of sustained loading on cracking seem to be more critical.

The ratios of the average crack widths were higher at the steel level than at the bottom edge for the two types of loading. The ratios obtained at the steel level were 1.5 and 1.73 and at the bottom edge were 1.40 and 1.24 for repeated and sustained loading respectively.

The number of cracks was affected by repeated loading more than by sustained loading. In most of the fatigue beams the number of cracks increased, particularly at the level of steel. Whereas in the sustained loading beams the increase was insignificant except in beams B21 and B25.

The height of travel of the cracks in most of the fatigue beams increased, and only in beam A34 the cracks, after extending towards the compression face, closed within very short lengths at their tops. In the sustained loading beams some of the cracks extended towards the compression face during the first few days. After a period of one year the cracks were noticed to have shortened in length.

10.6.2. Limit State of Deflection

In comparing the effects of the two types of loading, repeated and sustained, Table (16) should be referred to. It can be observed from the ratios given in Columns (8) and (9) for the sustained and repeated loadings respectively, that the ratios in Column (8) are higher than those in column (9), indicating that the effects of sustained loading are more severe than those of repeated loading. The sustained loading effects, therefore, are more critical than

the repeated loading in the consideration of the limit state of excessive deflection. The magnitude of the allowable steel stress has a great influence on the long-term deflection in the case of sustained loading. Thus the grade of steel must be considered in the design, when considering the effects of sustained loading on deflection a value of the factor for additional deflection can be obtained from Fig. (101).

10.6.3 Limit State of Collapse

Only the repeated loading test beams were loaded to failure at the end of the tests. Three of the sustained loading beams were unloaded, but not loaded to failure.

From the present and past findings these types of loading do not affect the static ultimate strength of a beam significantly. However, the present tests have shown an increase in the ultimate strength for some of the beams subjected to previous repeated loading, over their companion static beams.

10.7 Economic Considerations

In the previous sections the behaviour of the beams reinforced with high tensile steel under static, sustained and repeated loading has been discussed. The increase in crack width and deflection with steel stress and with time has been emphasised. In this section an attempt is made, using these results, to find out what strength of steel can justifiably be used as reinforcement for concrete, and how much saving in cost can be achieved by utilising such a type of steel.

The choice of higher strength steel in preference to mild steel is controlled by cracking and deflection considerations.

The deflection of a member depends on the span/depth ratio, steel stress and area, and the strength of concrete, so the magnitude of deflection is not controlled only by the magnitude of the stress in the steel. As a smaller area of higher strength steel is used the corresponding moment of inertia is reduced and deflections will be correspondingly greater. In Fig. (69) at working load a reduction of 27.6% in the steel area corresponding to an increase in steel

strength from 414 to 550 N/mm^2, i.e. 33%, would produce an increase in deflection of 13%. The deflection at the working load for 550 N/mm^2 steel was $\frac{L}{214}$ which is above the permissible value of $\frac{L}{250}$ as recommended in the Draft Code. The deflections for steel with strengths higher than above are considerably greater (e.g. Kam 90).

In order to use steels of higher strength in design, a balance should be found between the span/depth ratio and the magnitude of stress and area of steel, as recommended in the Draft Code. A smaller deflection under short term static design load could have been obtained in this investigation for 550 N/mm^2 steel if, for the same steel area, a smaller span-depth ratio had been used. Another factor which is extremely important is the type of loading. When the member is subjected to sustained design loading, the deflection increases in amounts depending on the level of steel stress at working load. (Ref. Fig. 101)

The relationship between the permissible maximum crack width and the possibilities of using high strength steels depends on the conditions of exposure and the type of loading. If well protected internal members are used very high strengths of steels can be used. However, for unprotected members exposed to severe atmosphere and loaded for a long time under sustained or repeated design loading the possibilities of using steels of high strengths are very limited.

In the present investigation the maximum crack width for each beam on the second cycle of loading is plotted against the steel stress at several loading stages, as can be seen in Figs. (26) and (27). The maximum crack width, as has been discussed earlier, increased linearly with increasing steel stress. From § 9.2.2., Eq . (32), derived from Figs. (26) and (27), can be used to calculate the steel stresses corresponding to the permissible maximum crack widths for the three conditions of exposure suggested by the C.E.B. § (3.2) Eq. (32) predicts the maximum crack width under a short term static loading. To include the effects of sustained or repeated loading a reduction factor of 1.5 is applied to the permissible maximum crack width. Combining all these effects and using Eq. (32) the maximum allowable steel stresses that can be used are as follows:

Maximum crack width (mm)	Maximum steel stress (N/mm^2)
0.20	250 (36200 p.s.i.)
0.25	303 (44000 p.s.i.)
0.30	355 (51500 p.s.i.)

When the working load steel stress is $\frac{1}{1.8}$ of the yield or proof stress, it can be seen from above that for beams reinforced with 550 N/mm^2 (80000 p.s.i) steel the maximum crack width is 0.25 mm. The cracks could possibly be reduced by using a smaller amount of concrete cover.

It can be concluded that the maximum crack width at the working load will probably limit the possibilities of using steel of strengths higher than 550 N/mm^2 when the concrete cover is 35 mm.

For the same section, when mild steel is replaced by 550 N/mm^2 steel, there is a saving of 51% in the steel area and 45.1% in the steel cost. When the steel strength is increased from 414 N/mm^2 to 550 N/mm^2 there is a saving of 27.6% in the steel area and 25.42% in the steel cost. In determining the cost of steel it is estimated that 414 N/mm^2 steel will cost £5 per ton more than mild steel and 550 N/mm^2 steel will cost £2 per ton[47] more than 414 N/mm^2 steel. In Appendix (A) an illustrative example is given showing the percentage saving when mild steel bars are replaced by steel bars with yield stress of 550 N/mm^2.

10.8 Conclusions

In the foregoing the effects of sustained and fatigue loading on serviceability and strength have been studied. The following conclusions as regards the behaviour of reinforced concrete beams of the type considered in this investigation and under such types of loading can be drawn:

10.8.1 Limit State of Cracking

A. Repeated Loading

1. The crack widths increased with the number of repetitions and after about two million repetitions a stabilised condition in the width of the maximum crack was reached, while the average crack width continued to increase.

2. The number and length of cracks increased with the number of repetitions and most of the increase occurred within the first few thousand repetitions, after which they stabilised.

3. The increase in the maximum crack width at the level of reinforcement was about 50%, and in no case did it reach the limiting value (0.2 mm).

4. The increase in the maximum crack width in the beam with mild steel was greater than the average increase for beams with deformed bars.

5. The remaining maximum crack width increased with repetitions, and a maximum value of 0.08 mm at the level of reinforcement was reached which was within the accepted limit (0.2 mm)

B. Sustained Loading

1. The major increase in the maximum crack width occurred in the first three to four months, after which it attained a reasonably stable condition, while the average crack width continued to increase until a stable condition after about one year was reached.

2. The number and length of cracks increased with time, and most of the increase occurred during the first few days, after which they stabilised. The cracks closed at their tops at a later date, due to the compressive creep of concrete.

3. The increase in the maximum crack width at the level of reinforcement was about 50%, regardless of the type of steel.

4. The average increase with time in the maximum crack width in beams with deformed bars was smaller than that for the beam with mild steel.

5. With an initial steel stress of up to 300 N/mm^2 the maximum crack widths at both the reinforcement level and bottom edge level, even after a long period of sustained design load, were within the accepted limit (0.2 mm). With an initial steel stress of 460,5 N/mm^2 the maximum crack width at the level of reinforcement exceeded the accepted limits within the first few days.

10.8.2. Limit State of Deflection

A. Repeated Loading

1. The deflections increased rapidly during the first 400,000 to 500,000 repetitions, after which they increased at a much lower rate. The maximum increase in deflection took place during the first few thousands of repetitions.

2. The maximum increase in the total deflection at design load after 3.5 million repetitions was 33%.

3. After one million repetitions the increase in the total deflection at design load was mainly due to the increase in the

remaining deflection at zero live load.

4. At a static load higher than the maximum limit of the repeated loading range, the elastic deflection was less than that for the companion beam subjected to the same load, but without previous repetitions of loading.

B. Sustained Loading

1. Creep deflection increased rapidly during the first few days, after which it increased with time at an ever-decreasing rate.

2. Throughout the sustained loading period the increase in deflection was more rapid in beams with mild steel than those with high tensile steel (with less steel area). i.e. the rate of increase diminished with higher grade of steel and corresponding lower steel area.

3. The difference in the increase of deflection of the beams with two types of steel was not due to the difference in the cracking or age of concrete at loading, but was due to the different concrete stress redistributions, owing to the different movements of the neutral axes of the beams with time.

4. The maximum increase in the total deflection after 1,000 days of sustained design load was 122% in the beam with mild steel with an initial steel stress of 175 N/mm^2, and steel area of 2.58%. The lowest increase was 57% in the case of the beam with Kam 90 steel, with an initial steel stress of 460.5 N/mm^2, and steel area of 0.564%. The age at first loading was about 100 days in both cases.

5. The average increase in deflection after six months was 66% and after one year was 83% of the 1000 day value.

6. The calculated time dependent deflections based on an "effective" modulus were less than the measured ones.

7. The recoveries of deflection after unloading from sustained design loading were independent of the grade of steel and the major portion of the recovery occurred immediately after unloading, and it was about (on average) 83% of the elastic deflection. The residual deflection was half the final deflection.

10.8.3. Limit State of Collapse (Ultimate Strength)

1. The ultimate static strength was retained even after many millions of repetitions of design load.

2. The ultimate static strength was retained even after a very long period of sustained design load.

10.8.4. Flexural Strains and Stresses

A. Repeated Loading

1. The compressive strains increased rapidly during the first few thousands of repetitions, then they increased at a decreasing rate until they nearly stabilised.

2. The increase in thecompressive strains depends on the age at loading, the level of stress in the concrete, and the strength of the concrete, all of which affect the creep of concrete.

3. The increase in the concrete compressive strains varied greatly between 19.7% to 71%. This was independent of the grade of steel.

4. The remaining compressive strains increased with repetitions at a faster rate than the elastic ones.

5. The increase in the nominal concrete tensile strains was due to many factors, e.g. the lowering of the neutral axis, creep of concrete in tension, cracking and break-down of the tension stiffening effect of concrete.

6. The nominal concrete tensile strains increased rapidly in the initial stages of load repetitions, and then they increased with time at a much lower rate. In some cases the increase in the nominal tensile strains was greater than the increase in compressive strains.

7. The stress in the steel remained practically constant even after many repetitions of loading.

B. Sustained Loading

1. During the first few days the compressive concrete strains increased rapidly then they continued to increase with time at a much lower rate.

2. The increase in the concrete compressive strains decreased with higher grade and corresponding lower percentages of steel reinforcement.

3. The increase in compressive strains after one year was 180% in the beam with mild steel with an initial steel stress of 175 N/mm^2 and steel area of 2.58%. In the beam with Kam 90 with an initial stress of 460.5 N/mm^2 and steel area of 0.564 % the increase was 130%.

4. The strain distribution in the compressive zone remained reasonably linear throughout the sustained loading period.

5. During the first few days the nominal concrete tensile strains increased rapidly and they then increased at a lower rate until they nearly stabilised.

6. After one year the greatest increase in the neutral axis depth of stress was 58%. This increase was greater for higher grade and

corresponding lower percentage of steel reinforcement.

7. The stresses in the steel increased rapidly during the first few days and then they increased at a lower rate until stability was reached.

8. The percentage increase in steel stress with time was lower for higher grades and corresponding lower percentages of steel.

10.8.5. Economic Considerations

1. The maximum crack width at working load, including the effects of sustained or repeated design loading will probably limit the yield strength of steel to 550 N/mm^2.

2. The possibilities of using higher strengths of steel are also limited by the deflection which in turn is limited by the span-depth ratio and the steel stress and percentage.

3. For the same section, when the steel strength is increased from 276 N/mm^2 (mild steel) to 550 N/mm^2, there is a saving in steel area of 51% and steel cost of 45.1%. When the steel strength is increased from 414 N/mm^2 to 550 N/mm^2, the savings are 27.6% and 25.42% .

CHAPTER 11

Summary and Conclusions

11.1 Conclusions from the Present Investigation

These conclusions have been derived from the results of the present investigation on singly reinforced, simply supported rectangular concrete beams.

11.1.1 Neutral Axis

1. Under short-term static loading the neutral axis depth can be predicted from:

$$dn = dn_{unc} - \frac{dn_{unc} - dn_{cr}}{0.3} \frac{M}{M_u} \qquad \text{.....§ 8.2}$$

where:

$$dn_{unc} = d - \frac{d/2 + (m-1)\ p(d-d_1)}{1 + (m-1)p} \qquad \text{.....§ 8.2}$$

for $M/M_u > 0.3$

$$dn = dn_{cr} = d_1 \sqrt{m^2p^2 + 2mp} - mpd_1$$

2. The neutral axis depths of both stress and strain increased with time (under sustained or repeated loading) and then stabilised. After a period of time they did not coincide due to shrinkage and stress effects in the concrete tensile zone.

11.1.2. Stresses in the Reinforcement

1. Under short-term static loading the stresses in the steel reinforcement depend primarily on the applied moment, the amount of steel and the position of the neutral axis, at any loading stage.

2. The stresses in the steel reinforcement can be predicted from:

$$f_s = \frac{M}{A_s(d_1 - \alpha dn)} \qquad \text{.....§ 8.2}$$

The value of α can be obtained from:

$$\alpha = \frac{3e_c^2 - 3e_c e_o + e_o^2}{6e_o^2 - 3e_o e_c} \qquad \text{.....§ 8.2}$$

3. The experimental and theoretical steel stresses increased linearly under short term, static loading: from small loads around zero to very high percentages of the ultimate load.

4. Due to the stiffening effect of concrete in the tension zone, before cracking, the actual measured steel stresses were lower than those calculated on the basis of the measured compressive strains and the position of the neutral axis.

5. Under the effects of repeated design loading, the maximum variation in the steel stress took place during the first few thousand repetitions. The maximum increase was 3.4%.

6. Under the effects of sustained design loading the maximum variation in the steel stress took place during the first few days. The maximum increase was 6.7%.

7. In most beams the steel stresses under the short-term static failure loads exceeded the yield strength of the reinforcement.

11.1.3 Strains

1. The strain distribution in the concrete compressive zone is almost linear, while that for the tension parts of the beam may not be linear.

2. Under the effects of sustained and repeated design loading the concrete compressive strains at design load increased rapidly during the first few days and the first few thousands of repetitions. After two million repetitions the maximum increase was 27×10^{-5} (71%). The maximum increase after one year of sustained loading was 149×10^{-5} (181%).

3. Under the effects of repeated design loading the remaining concrete compressive strains at zero live load increased rapidly during the first few thousand repetitions. The maximum increases after about two million repetitions and one year of sustained loading were 25×10^{-5} (23%) and 29×10^{-5} (16.5%) respectively.

11.1.4 Ultimate Strength

1. The safety factor against collapse under short-term static loading exceeded a factor of 2 against a global load factor of 1.8 as recommended in the Draft Code.

2. Sustained and repeated design loads had no appreciable effect on the ultimate strength of reinforced concrete beams. In some cases repeated design load caused an increase in the ultimate strength.

11.1.5 Deflection

1. The deflection is influenced by the magnitude of the cracking and applied moments, the span and the flexural rigidity. The deflection can be predicted for the first cycle from:

$$\Delta_1 = \beta \frac{Mc}{E_c I_o} L^2 + \beta \frac{M - Mc}{K_1 E_c I_c} L^2 \qquad \ldots\ldots\ldots \S\ 9.3.2.$$

and for the subsequent cycles

$$\Delta_2 = \beta \frac{M}{K_5 E_c I_c} L^2 + K_4 \Delta_1 \qquad \ldots\ldots\ldots \S\ 9.3.2.$$

where $K_1 = 0.9$
$K_4 = 0.25$
$K_5 = 1.30$

2. The span-depth ratio can be evaluated from:

$$L/d = \frac{\Delta}{L} \frac{1}{F} \frac{E_s}{f_s} \frac{1}{\beta} \frac{d_1}{d} (1 - K) \qquad \ldots\ldots\ldots \S\ 9.3.7.$$

3. The remaining deflection was influenced by the extent of cracking and the ratio of the applied steel stress to steel stress at first cracking.

4. The average ratio of the remaining deflection at the end of the first cycle to the deflection at the design load may be taken as $\frac{1}{4}$.

5. The recovery of deflection on unloading of a beam loaded to a very high percentage of the ultimate load, decreased with decreasing area of steel reinforcement.

6. Under the effects of repeated design loading most of the increase in deflection occurred during the first four to five hundred thousand repetitions. After 3.5 million repetitions the ratios of the final to initial deflections ranged between 1.22 and 1.33.

7. Under the effects of sustained design load the deflection increased rapidly during the first few days. After 1000 days the ratios of the final to initial deflections varied between 1.57 to 2.22, the age at first loading varying between 44 and 100 days.

8. The average increases in deflection after six months and one year of sustained design loading were 66% and 83% respectively of the increase after 1000 days.

9. The stiffnesses of the beams at loads higher than the upper range of repeated loading increased after previous repeated design loading.

10. The major portion of the recovery of deflection after unloading from sustained design loading occurred immediately after unloading and it was about (on average) 83% of the elastic deflection. The residual deflection was about half the final deflection.

11.1.6 Cracking

1. The crack width is controlled by the level of the stress in the reinforcement, the distance from the point of measurement to the surface of the bar, the percentage of reinforcement as affecting the steel stress at first cracking, and the surface characteristics of the bars.

2. The maximum crack width at the level of reinforcement in static load tests can be predicted from the following equations:

$$W_{max_1} = RC \left(f_s - \frac{K_s}{p}\right) \times 10^{-6} \qquad \ldots\ldots \S\ 9.2.2.$$

where R = 18.6 plain round bar
= 16.0 deformed bar
= 25.0 wire and strand

K_s = 69.5 N/mm^2

for the subsequent cycle of loading:

$$W_{max_2} = C \left[f_s (R + k_1) - k_1 k_2\right] \times 10^{-6} \qquad \ldots\ldots \S\ 9.2.2.$$

where R = 12.9 plain round bar
= 13.5 deformed bar
= 24.2 wire and strand

k_1 = 5.28 $1/N/mm^2$ k_2 = 138 N/mm^2

3. Under short-term static loading a fully developed cracking pattern was reached at stresses between 200 - 250 N/mm^2.

4. The average crack spacing in beams with deformed and plain bars was approximately equal to 1.5 x the concrete cover.

5. At a crack width of 0.2 mm at the reinforcement level, the stresses in the reinforcement were: 400 - 510 N/mm^2 for Kam steel deformed bars, 300 - 360 N/mm^2 for Unisteel deformed bars, and 275 - 385 N/mm^2 for prestressing wires, and reinforcing and prestressing strands.

6. At a crack width of 0.2 mm at the bottom edge of the beam, the stresses in the reinforcement were: 325 - 400 N/mm^2 for Kam steel deformed bars, 180 - 230 N/mm^2 for plain round mild steel bars, 194 - 245 N/mm^2 for Unisteel deformed bars, and 255 - 275 N/mm^2 for

prestressing wires and reinforcing and prestressing strands.

7. The ratio of the maximum to average crack width varied greatly with the level of reinforcement stress.

8. Under the effects of repeated design loading, most of the increase in the maximum and average crack widths and the height of travel of cracks occurred during the first million repetitions After 3.5 million repetitions the maximum crack width at the bottom edge slightly exceeded the permissible value (0.2mm) when the initial design steel stress was 326 N/mm^2. The ratio of the final to instantaneous crack widths can be taken as 1.5.

9. The maximum remaining crack width increased with load repetitions.

10. Under the effects of sustained design loading, most of the increase in the maximum and average crack widths occurred during the first 3 to 4 months. After a period of 1000 days and an initial steel stress of up to 300 N/mm^2 the maximum crack widths at the reinforcement level were much lower than the permissible value (0.2 mm). While those at the bottom edge were about equal to the permissible value. However, when the initial steel stress was 460.5 N/mm^2, the maximum crack widths at the steel and bottom edge levels were 0.29 mm and 0.38 mm respectively. The ratio of the final to the initial maximum crack width can be taken as 1.5.

11. Most of the increase in number and length of cracks was during the first few days of sustained design loading. However, due to the effect of creep, these cracks closed within short distances from the top.

11.1.7. Type and Grade of Steel Reinforcement

1. The average neutral axis depth under short-term static loading was not affected by the surface characteristics (deformed or plain) of the reinforcement.

2. Under the effects of sustained design loading the percentage increase in the neutral axis depth and the increase in the steel stress were greater for higher design steel stress and corresponding lower steel percentage.

3. Under the effects of repeated design loading, when the steel percentage was constant, the increase in the steel stress did not depend on the type or grade of the steel reinforcement.

4. Under short-term static loading the concrete compressive strains were not affected by the surface characteristics (deformed or plain) of the reinforcement, but they increased with higher design steel

stress and corresponding lower steel percentage.

5. Under the effects of repeated design loading, when the steel percentage was constant, the increase in the concrete compressive strains did not depend on the surface characteristics and the magnitude of the design steel stress.

6. Under the effects of sustained design loading the increase in the concrete compressive strains was lower for higher design steel stress and corresponding lower steel percentage. When the initial steel stresses were 175 N/mm^2 and 460.5 N/mm^2 the increases in concrete compressive strains after one year were 149 x 10^{-5} and 88.5 x 10^{-5} respectively.

7. The ultimate strength was not affected by the surface characteristics or quality of steel reinforcement, however, the strength of concrete was much better utilised when high tensile steel was used.

8. The mode of failure and the amount of warning before failure were affected by the surface characteristics and the type of the steel reinforcement. Cold worked steels (with indefinite yield point) were superior to hot rolled steels (with definite yield point, and hot rolled steels with high yield strength and good bond characteristics were superior to mild steel, in that they gave better warning before collapse.

9. Under short-term static loading, when the section properties were constant, the deflection was not affected by the surface characteristics of steel. However, the deflection was greatly influenced by the magnitude of the design steel stress. When the design stresses were double or triple the deflections were 1.74 and 2.48 times that of mild steel respectively.

10. Under the effects of sustained design loading the creep deflection and the ratio of final to initial deflection decreased with higher design steel stress and corresponding lower steel percentage.

11. The percentage recovery in deflection after unloading from sustained design load was very little affected by the magnitude of the design steel stress.

12. Under short-term static loading the crack spacings were not significantly different for beams with deformed or plain round bars, but they were bigger for beams with prestressing wires and strands.

13. The average difference in the maximum crack width between beams reinforced with plain round and deformed bars was only 7% in favour of the latter, while the difference in crack width for beams with prestressing wires and strands and the deformed bars

was 67% in favour of the latter.

14. The maximum crack width at working load ($^1/1.8$ of the yield or proof stress) including the effects of sustained or repeated design loading, will probably limit the possibilities of using steels of strengths higher than 550 N/mm^2 proof stress. The reduction of concrete cover could raise the limit of permissible stresses higher than in the above case.

15. The possibilities of using higher strengths of steel are limited by deflection which in turn is limited by the span-depth ratio and the steel stress and percentage.

16. Providing the section and the ultimate design load are constant, there is a 51% saving in steel area and 45.1% saving in the cost of steel when mild steel (276 N/mm^2 yield point) is replaced by steel with yield of 550 N/mm^2. There is a 27.6 % saving in steel area and 25.42% saving in cost of steel when 414 N/mm^2 steel is replaced by 550 N/mm^2 steel.

11.2 Design Recommendations for Reinforced Concrete Members

11.2.1. General

The aim of this thesis is to arrive at simple design rules for concrete beams reinforced with high tensile steel. These rules can be applied when the type and distribution of loading and forces on the structure are determined. The major step in applying these design rules is to satisfy the ultimate limit state of collapse by designing a safe structure. The grade of steel and the magnitudes of the permissible stresses to be used, however, will be controlled by the limit states of deflection and cracking, the type (sustained or repeated) and the conditions (normal or severe exposure) of loading.

The methods recommended in the thesis are confirmed by the results of the investigation carried out on a small number of beams of particular size and shape. Therefore, the design methods are applicable to the type of member studied in the present investigation. In Appendix (A), the methods recommended are used and a comparison is made between the behaviour of beams calculated on these principles, and the actual behaviour of the test beams.

In the following, the major steps in the design of a reinforced concrete member, complying with the limit states of collapse, deflection and local damage (cracking) are described. Methods of determining steel stresses, ultimate strength, deflection and crack width are recommended.

11.2.2. Recommendations for the Calculation of the Limit State of Collapse

The section properties of the beam may be obtained in accordance with the Draft Unified B.S. Code of Practice recommendations. From the knowledge of the magnitude and distribution of the characteristic loads, the design loads can be obtained by incorporating certain partial load factors. From the design load acting on the member, the width and depth of the section and the percentage reinforcement can be determined by using the formulae and tables given in the Code. It is essential to take account of the characteristic and design values of the strength of the materials by using certain appropriate partial safety factors. After the section has been fixed, the stresses at any stage of loading can be determined and the limit states of cracking and deflection can be examined as given in the following sections.

11.2.3. Recommendations for the Calculation of the Stresses in the Steel Reinforcement

1. From the section properties, the neutral axis depth of the uncracked section can be determined according to equation (21).
2. The neutral axis depth of the cracked section can be obtained from equation (22).
3. From equation (23) the transition neutral axis depth can be determined Ref. Fig. (11).
4. For $\frac{M}{M_u} \leq K$ use the neutral axis depth determined in (3).
5. For $\frac{M}{M_u} > K$ use the neutral axis depth determined in (2).
6. A rectangular-triangular concrete compressive stress distribution can be assumed. Ref. Fig. (12).
7. The position (α) of the resultant compressive force in the concrete zone is determined as follows: if the strain (e_c) in the extreme fibre is less than $e_o = \frac{\sqrt{U_w}}{5000}$ then the stress distribution is triangular and $\alpha = 1/3$. If e_c is greater than e_o then the stress distribution is rectangular-triangular, and α can be determined from equation (25) from the stress and strain compatability.
8. The stress block coefficient (γ) can be assumed to be 0.8.
9. The stresses in the reinforcement are obtained from the compatability with the applied moment from equation (26).

11.2.4. Recommendations for the Calculation of the Limit State of Deflection

The limit state of deflection will not be required to be considered

if the beam is designed with a span-depth ratio $^{L}/d$ in accordance with the following:

$$^{L}/d = \frac{\Delta}{L} \frac{1}{\beta F} \frac{E_s}{f_s} (1 - K) \qquad \ldots\ldots (41)$$

The increase in deflection due to sustained loading may be obtained from Fig. (101). The reduction factor (F) in the above equation can then be found by adding a unity to the value obtained from Fig. (101). The values of the allowable deflection $\frac{\Delta}{L}$ are given in the Draft Code.

When the calculation of deflection is required for a given applied moment, equation (35) or (40) can be used. However, when it is required to determine the maximum steel stress as limited by the allowable deflection, the following procedure can be applied:-

1. The allowable deflection can be established.
2. A reduction factor (F) due to sustained loading is assumed and applied to the allowable deflection.
3. Using equations (36) and (37) the cracking moment and the modulus of rupture can be determined.
4. From equation (35) the working moment can be determined.
5. The stress in the steel reinforcement may be determined from the procedure recommended in § 11.2.3.
6. With the steel stress found in (5), Fig. (101) can be used to determine a new value of F. If this F is different from the one assumed in (2) repeat steps 2,4, and 5 until the correct permissible steel stress and the value of F are found.

11.2.5. Recommendations for the Calculation of the Limit State of Cracking

When the calculation of the maximum crack width is required in design for a given applied stress, equation (30) or (32) can be used. However, if the maximum steel stresses corresponding to an allowable crack width is being sought, the following procedure can be applied:

1. The maximum permissible crack width appropriate for the conditions in which the member is considered can be established Ref. § 3.2.
2. A reduction factor of 1.5 for the long term effects (sustained or fatigue loading) is applied to the permissible crack width.
3. The steel stresses corresponding to the permissible crack width can be determined from equation (30). The value of R to be adopted depends on the type of steel.

CHAPTER 12

Suggestions for Future Research

1. Sustained and Repeated Loading Tests

In this investigation only one beam with round plain mild steel bars was tested under sustained loading, and another under repeated loading. Therefore, the findings from these beams are of limited validity. A few beams should be made with each type of reinforcing bar.

The beams tested under repeated loading had the same amount of steel reinforcement. While the beams tested under sustained loading had different amounts of steel, some had similar design loads. The effects of these two aspects should be studied under both types of loading. It can, therefore, be suggested that an investigation be carried out under sustained and repeated loading on beams (a) with equal amounts of steel, and (b) with similar design load (with different amounts of steel).

2. Lightweight Concrete

In the present investigation normal concrete was used in the design and manufacture of the test specimens. The dead weight was only a fraction of the design load. In practice the weight of the structure may constitute a major problem as far as serviceability and handling are concerned. Lightweight concrete can, therefore, be used with advantage in reducing the dead weights, which will help in increasing the span. On the other hand, lightweight concrete will induce bigger deflection and crack width, due to the lower value of the modulus of elasticity of concrete, the cracking load and the bond characteristics. It would, therefore, be interesting to study the over-all effects that are produced if lightweight concrete is used in place of the normal concrete.

The type of loading, i.e. static, sustained or repeated, must also be considered, since the effect of creep with such concrete is of great importance.

In using this type of concrete along with high tensile steel, the economic advantages must be fully considered.

3. Fibre Reinforced Concrete

The effect of the tensile strength of concrete on cracking and deflection is greatly dependent on the value of the load at which the concrete cracks. By increasing the tensile strength and extensibility of concrete, the amounts of cracking and deflection can be reduced.

Using fibre reinforced concrete in place of normal concrete in the tension zone of the beam may lead to an increase in the tensile strength of concrete and hence an increase in the cracking load, which will reduce cracking and deflection of the beam. It would therefore be possible to increase the permissible stresses in the steel reinforcement to very high values.

The use may be suggested of the fibre reinforcement either in the form of chopped fibres, or in the form of a layer of mesh placed at a certain level of the tensile zone to act as a crack arrester and prevent cracks from reaching the reinforcement.

4. Other Shapes of Section

The beams used in this investigation had a rectangular cross-section, and the results are valid only for such a type of section. Similar investigations should, therefore, be carried out on beams with different shapes of section, in particular those which are commonly used in practice, i.e. T-section.

LIST OF REFERENCES

1. Special Reinforcements for Reinforced Concrete. Rilem Symposium on Special Reinforcements for Reinforced Concrete and on Prestressing Reinforcements, Liege 1958. Final Report, pp. 117-180.

2. Roberts, N.P., Steel in Reinforced Concrete. Consulting Engineer (London) Vol. 33 No. 7, July 1969, pp. 52-53.

3. Bannister, J.L., Steel Reinforcement and Tendons for Structural Concrete. Part 1. Steel for Reinforced Concrete. Concrete Vol. 2 No. 7, July 1968, pp. 295 - 306.

4. Western Construction, Re-Bars take a New Step Forward, Vol. 35, No. 3-A, March 1960, pp. 38,43.

5. The Structural Engineer (London). The Use of Deformed Steel Bars in Reinforced Concrete. Results of an investigation by an ad hoc committee of science and research committee of the Institution of Structural Engineers, Vol. 31, Aug. 1953, pp. 222-225.

6. Reese, R.C., New-Style Deformed Reinforcing Bars, A.C.I. Journal Vol. 21, No. 9, Proc. Vol. 46, May 1950, pp. 681-688.

7. Ramaswamy, G.S., Zacharia, G. and Prasala, R.A., High Strength Deformed Bars for Concrete Reinforcement, Journal of the National Buildings Organisation, Vol. 11, No. 1, 1966, pp. 3-14.

8. Lash, S.D., and Blackwell, W., High Strength Reinforcement in Reinforced Concrete Beams, Part 1: A Selective Bibliography. O.J.H.R.P. Report No. 37, Ontario Dept. of Highways 1965.

9. Hajnal Konyi, The Use of High Tensile Steel Reinforcement, Concrete and Constructional Engineering (London) , Vol. 52 No. 6, June 1957.

10. Hognestad, E., High Strength Bars as Concrete Reinforcement, Part 1, Introduction to a series of experimental reports. P.C.A. Research and Development Laboratories (Chicago), Vol. 3 No. 3, Sept. 1961,pp.23-29.

11. Hognestad, E., Trends in Consumer Demands for New Grades of Reinforcing Steel, P.C.A. Development Dept., Bulletin D.130, 1967.

12. Granholm, H., Kam 40, Kam 60 and Kam 90, Transaction of Chalmer University of Technology (Goteborg, Sweden) No. 213, 40 pages, 1959 (In Swedish).

13. Guralnick, S.A., High Strength Deformed Steel for Concrete Reinforcement, A.C.I. Journal, Vol. 32, Proc. Vol. 57, No. 3, Sept. 1960, pp. 241-282.

14. Hognestad, E. and Winter, G., High Strength Reinforcing Steels for Concrete Bridges, Proceeding Highway Research Board (Washington), Vol. 39, 1960, pp. 103-119.

15. Gilkey, H.J., and Ernest, G.C., Report of Project Committee on the Use of High Elastic Limit Steel as Reinforcement for Concrete, Proceeding Highway Research Board (Washington), Vol. 14, 1935, pp. 255-314.

16. Abeles, P.W. and Gill, V.D., High Strength Strand Reinforcement for Concrete. Concrete Vol. 3, Apr. 1969, pp. 127-133.

17. Ramaswamy, G.S., Chandra, R. and Narayanan, R., Savings in Reinforced Concrete Structures by Using Ultimate Strength Design Procedure and High Strength Deformed Bars. Indian Concrete Jounral Vol. 41 No. 10, Oct. 1967. pp. 370-373.

18. Chetty, S.M.K. and Singh, S., Mild Steel Twisted Bars for Concrete Reinforcement, Indian Concrete Journal, Vol. 41, No. 5, May 1967, pp. 183-185.

19. Cherry, J.R., Estimating the Cost of Concrete Structures, A.A.C.E. Bulleting, Vol. 8 No. 4, Dec. 1966.

20. High Strength Reinforcing Bars, A.I.S.I. Committee of Concrete Reinforcing Bar Producers, Vol. 1 and 2, 1964.

21. Mukherjee, P.K., Economy in Steel - How to Achieve it. Bulletin of the Institution of Engineers (India), Vol. 15 No. 12, Aug. 1966, pp. 12-24.

22. British Standard Code of Practice C.P.114,(1957). The Structural Use of Reinforced Concrete in Buildings, British Standards Institution (Reset and re-printed in 1965).

23. British Standards Institution, Draft Unified Code of Practice for the Structural Use of Concrete, circulated for comment, Sept. 1969.

24. Hajnal Konyi, K., Tests on Square Twisted Bars and their Application as Reinforcement of Concrete, The Structural Engineer (London), Vol. 21 No. 9, 1943.

25. Hajnal Konyi, K., Comparative Tests on Various Types of Bars as Reinforcement of Concrete Beams, The Structural Engineer (London), Vol. 29 No. 5, May 1951, pp. 133-148.

26. Hajnal Konyi, K., Tests on Concrete Beams Reinforced with 12 Gauge Wires of an Ultimate Strength of 120 tons per sq. in. Magazine of Concrete Research, Vol. 3 No. 9, Mar. 1952, pp. 113 - 129.

Discussion Vol. 4 No. 12, Apr. 1953, pp. 127-142.

27. Whitney, C., Plastic Theory of Reinforced Concrete Design. Transaction A.S.C.E., Vol. 107, 1942, Paper 2133, pp. 251-326.

28. Hajnal Konyi, K., Reinforcing Steel in Concrete and the Comcept of Safety, A.C.I. Journal Vol. 23, No. 7, Proceeding Vol. 48, Mar. 1952, pp. 561-580.

29. Hajnal Konyi, K., The Use of High Strength Steelas Concrete Reinforcement, I.A.B.S.E. Fifth Congress 1956, (Lisbon, Porto).

30. Hajnal Konyi, K., Recent Research on Deformed Reinforcing Bars. The Reinforced Concrete Review, Vol. 3, No. 7, 1955, p. 393.

31. Evans, R.H., Experiments with Cold-Worked Steel as reinforcement. Concrete and Constructional Engineering (London), Oct. 1937. pp.567-573.

32. Evans, R.H. and Williams, A., Bond Stress and Crack Width in Beams Reinforced with Square Grip Reinforcement, Rilem Symposium on Bond and Crack Formation in Reinforced Concrete, Vol. 1, Stockholm 1957, p. 105.

33. Lewis, H.E., Tests to Determine the Behaviour of Tentor Steel as Tensile Reinforcement for Concrete, Technical Report, T.R.A./1974 C. & C.A. London, Nov. 1954.

34. Lewis, H.E., Comparative Tests on Concrete Beams and Slabs Reinforced with Mild Steel and Tentor Bars, Preliminary Publication Fifth Congress I.A.B.S.E. Lisbon 1956, pp. 763-781.

35. Gaston, J.R., and Hognestad, E., High Strength Bars as Concrete Reinforcement Part 3: Tests on full-scale roof girder. P.C.A. Research and Development Laboratories, Chicago, Vol. 4, No. 2, May, 1962. Bulletin D54 pp. 10-23.

36. Hognestad, E., High Strength Bars as Concrete Reinforcement, Part 2: Control of Cracking, P.C.A. Research and Development Laboratories, (Chicago) Vol. 4 No. 1 Jan. 1962.

37. Wastlund, G., Use of High Strength Steel in Reinforced Concrete, A.C.I. Journal Vol. 30, No. 12. Proceeding Vol. 55, June 1959, pp. 1237-1250.

38. Mathey, R.G. and Watstein, D., Effect of Tensile Properties of Reinforcement on the Flexural Characteristics of Beams. A.C.I. Journal, Vol. 31, No. 12, Proceeding Vol. 56, June 1960, pp. 1253 - 1273.

39. Guralnick, S.A. and Winter, G., An Investigation of High Strength Deformed Steel Bars for Concrete Reinforcement. Report No. TSR 4730-7146. Part 2. Department of Structural Engineering Cornell University Nov. 1958.

40. Abeles, P.W., The Use of High Strength Steel in Ordinary Reinforced and Prestressed Concrete Beams. International Congress for Bridge and Structural Engineering Fourth Congress, Cambridge and London 1952, pp. 871 - 891.

41. C.E.B. Recommendations for an International Code of Practice for Reinforced Concrete, A.C.I. and C. & C.A. 1964.

42. Thomas, F.G., Concrete Research at B.R.S., Concrete Vol. 2, No. 3 Mar. 1968, pp. 123-128.

43. Snowdon, L.C., The Static and Fatigue Performance of Concrete Beams with High Strength Deformed Bars, B.R.S. C.P.7/71, Mar. 1971.

44. Report of Special Investigation on the Behaviour of Full Scale Concrete Beams with Bristrand 100 Reinforcement when Tested under Static Sustained, and Fatigue Conditions of Loading, B.R.S. Oct. 1970.

45. Base, G.D., Read, J.B., Beeby, A.W. and Taylor, H.P.J., An Investigation of the Crack Control Characteristics of various types of Bars in Reinforced Concrete Beams. Research Report 18, Parts 1 and 2, C. & C.A. Dec. 1966.

46. Clark, L.A., The Flexural Strength of Concrete Beams Reinforced with Very High Strength Steels. Ph.D. Thesis, University of Sheffield, Aug. 1968.

47. Clark, L.A. and Eastwood, W., The Flexural Strength of Concrete Beams Reinforced with very high strength steel. The Structural Engineer, London, Vol. 48, No. 7, July 1970.

48. Holmberg, A., Two Highway Bridges with High Grade Steel Reinforcement. I.A.B.S.E. Publications, Vol. 11, 1951, pp. 247-252.

49. Granholm, H., A General Flexural Theory of Reinforced Concrete. John Wiley & Sons, New York, London, Sydney, 1965.

50. Civil Engineering. Texas Concrete Bridge Reinforced with High Strength Steel Bars. Vol. 33 No. 9, Sept. 1963.

51. Hognestad, E., Development of High Strength Reinforcement. Journal Of Metals, Vol. 18 No. 6, June 1966, pp. 692-697.

52. Antoni, C.M., Corbisiero, J.A., Instrumentation and Testing of Concrete Bridges Reinforced with High Strength Steel. New York (State Dept. - Transportation - Research Report 68 -3) Sept. 1968.

53. Beal, D.B., Performance of Concrete Bridges Reinforced With High Strength Steel. First Interim Report on Research Project 211. Research Report 69-16. Mar. 1970. Eng. Research and Development. Bureau New York State Dept. of Transportation.

54. Van Ornum, The Fatigue of Concrete. Transaction of the A.S.C.E. Vol. 58, 1917, pp. 294-320.

55. Berry, H.C., Some Tests on ReinforcedConcrete Beams Under Oft Repeated Loading. A.S.T.M. Proc. Vol. 8, 1908, p. 454.

56. Probst, E., The Influence of Rapidly Alternating Loading on Concrete and Reinforced Concrete. The Structural Engineer (London) Vol. 9, No. 10, Oct. 1931. pp. 326-340, No. 12 Dec. 1931, pp. 410-429.

57. Rilem Symposium on Bond and Crack Formation in Reinforced Concrete, Stockholm 1957, Vols. I, II and III.

58. Hajnal Konyi, K., Comparative Tests on Beams Reinforced with Plain and Tentcr Bars under Repeated Loading. Structural Concrete Vol. 1 No. 3, May 1962.

59. Saliger, R., Fatigue Tests on Reinforced Concrete Beams. Engineering News Record. Vol. 115, 1935, p. 611.

60. Saliger, R., American Fatigue Tests on Reinforced Concrete Beams, Engineering News Record, Vol. 114, No. 20, May 1935, p. 697.

61. Noredby, G.M., Fatigue of Concrete. A Review of Research. A.C.I. Journal, Vol. 30, No. 2, Proc. Vol. 55, Aug. 1958, pp. 191-219.

62. Stelson, T.E. and Cernica, J.N., Fatigue Properties of Concrete Beams. A.C.I. Journal Vol. 30 No. 2, Proc. Vol. 55, Aug. 1958, pp. 255-259.

63. Chang, T.S., Kesler, C.E., Static and Fatigue Strength in Shear of Beams with Tensile Reinforcement. A.C.I. Journal Proc. Vol. 54, No. 10, June 1958.

64. Lea, F.C., Repeated Stresses on Structures, Part II, The Structural Engineer (London), Vol. 18, No. 2, Feb. 1940.

65. Verna, J.R. and Stelson T.E., Repeated Loading Effect on Ultimate Static Strength of Concrete Beams. A.C.I. Journal Proc. Vol. 60 No. 6, June 1963, pp. 743-749.

66. Verna, J.R., and Stelson, T.E., Fatigue of Small Reinforced Concrete Beams under Repeated Loads. A.C.I. Journal Proc. Vol. 59, No. 10, Oct. 1962, pp. 1489-1504.

67. Bate, S.C.C., The Strength of Concrete Members under Dynamic Loading. Symposium on the strength of concrete structures. Session D., Paper 2, London 1956. Proc. of Symposium on the strength of concrete structures May 1958, Cement and Concrete Association, London.

68. Bate, S.C.C., A Comparison between Prestressed Concrete and Reinforced Concrete Beams under Repeated Loading. I.C.E. Proc. Vol. 24, Mar. 1963, pp. 331-358.

69. Pfister, J.F. and Hognestad, E., High Strength Bars as Concrete Reinforcement, Part 6. Fatigue Tests. P.C.A. Research and Development Laboratories (Chicago) Vol. 6, No. 1, Jan 1964, pp. 65-84.

70. Kobrin, N.M., and Sverchkov, A.G., Effect of Component Elements of Deformation Patterns on the Fatigue Strength of Bar Reinforcement. A.I.S.I. Library, Experimental and Theoretical Investigation of Reinforced Concrete Structures.

71. Japan Society of Civil Engineers, Transactions, Vol. 122, Oct. 1965.

72. Blackwell, W., Behaviour of Reinforced Concrete Beams Subjected to Repeated Loads, with Particular Reference to High Strength Steel. M.Sc. Thesis, Queen's University, Kingston, Ontario, April 1964. 77 pages.

73. Lash, S.D., Macleod, N., and Blackwell, W., High Strength Reinforcement in Reinforced Concrete Beams. Part 2. O.J.H.R.P. Report No. 38 Ontario Department of Highways. 1965.

74. Soretz, S., Fatigue Behaviour of High Yield Steel Reinforcement. Concrete and Constructional Engineer (London), Vol. 60, No. 7, July, 1965, pp. 272-280.

75. Russell, T.H. and Webber, J.R. , High Strength Reinforcement in Reinforced Concrete Beams Subject to Repeated Loading at Room and Sub-Zero Temperatures. The Institution of Engineers, Australia, Civil Engineering Transaction Vol. CE9 No. 2, Oct. 1967.

76. Thomas, F.G., and Glanville, W.H., Further Investigations on the Creep Flow of Concrete under Load. Building Research. Technical Paper 21, (London), Dept. of Scientific and Industrial Research,1939.

77. Washa, G.W., Plastic Flow of Thin Reinforced Concrete Slabs. A.C.I. Journal Proc. Vol. 44 No.3, Nov. 1947, pp. 237-260.

78. Yu, W.W. and Winter, G., Instantaneous and Long-Term Deflections of Reinforced Concrete Beams under Working Loads. A.C.I. Proc. Vol. 57, No. 1, July, 1960, pp. 29-50.

79. Faber, O., Plastic Yield, Shrinkage, and other Problems of Concrete and Their Effect on Design. Proc. I.C.E., Vol. 225, Part I, (London) (1927-28) p. 27.

80. Washa, G.W. and Fluck, P.G., Effect of Compression Reinforcement on the Plastic Flow of Reinforced Concrete. A.C.I. Journal, Proc. Vol. 49, No. 2, 1953, pp. 89-108.

81. Washa, G.W. and Fluck, P.G., Effect of Sustained Loading on Compressive Strength and Modulus of Elasticity of Concrete. A.C.I. Journal Vol. 21, No. 9, Proc. Vol. 46, 1950, pp. 693-700.

82. Sell, R., Investigation into the Strenth of Concrete under Sustained Load. Rilem Bulletin, No. 5, Dec. 1959.

83. Shank, J.R., Plastic Flow of Concrete at High Overload. A.C.I. Journal, Vol. 20, No. 6, Proc. Vol. 45, Feb. 1949, pp. 493-498.

84, Wash, G.W. and Fluck, P.G., Effect of Sustained Overload on the Strength and Pladtic Flow of Reinforced Concrete Beams. A.C.I. Journal, Proc. Vol. 50, 1954.

85. Grinter, C.E. and Kepford, B., Long Time Overload Tests on a T-beam Floor Panel. A.C.I. Journal. Proc. Vol. 37, Feb. 1941, pp. 433-438.

86. Soretz, S., Research on Concrete Members Reinforced with Deformed Bars. Concrete and Constructional Engineering (London), Vol. 59, No. 3, Mar. 1964.

87. Soretz, S., Contribution to Research on Reinforcing Steel and Reinforced Concrete. (in French) Annale de l'Institut Technique du Batiment et des Travaux Publiques (Paris) Vol. 14, Nov. 1961, pp. 1200-1218.

88. Hajnal-Konyi, K., Tests on Beams with Sustained Loading. Magazin of Concrete Research, Vol. 15, No. 43, Mar. 1963. pp. 3-14.

89. Corely, W.G., and Sozen, M.A., Time Dependent Deflections of Reinforced Concrete Beams. A.C.I. Journal Proc. Vol. 63, No. 3, Mar. 1966. pp. 373-386.

90. Lutz, L.A., Sharma, N.K., Gergely, P., Increase in Crack Widths in Reinforced Concrete Beams under Sustained Loading. A.C.I. Journal Proc. Vol. 64, Sept. 1967, pp. 538-546.

91. Evans, R.H. and Paterson, W.S., Long-Term Deformation Characteristics of Lytag Lightweight Aggregate Concrete. The Structural Engineer, (London), Vol. 45 No. 1, Jan. 1967.

92. Evans, R.H., Orapgun, C.O., Behaviour in Flexure of Reinforced Lightweight Aggregate (Lytag) Concrete Beams. Civil Engineering and Public Works Review, Part I, May 1964, Part 2, June 1964.

93. Neville, A.M. and Meyers, B.L., Creep of Concrete, Influencing Factors and Prediction. Symposium on Creep of Concrete. A.C.I. Sp.-9, 1964.

94. Neville, A.M., Creep of Concrete: Plain, Reinforced and Prestressed. North Holland Publishing Co. - Amsterdam 1970.

95. Thomas, F.G., A Conception of the Creep of Unreinforced Concrete, and an Estimation of the Limiting Values. Structural Engineer. Vol. 11, No. 2, Feb. 1933.

96. Troxell, G.D., Raphael, J.M. and Davis, R.E., Long Time Creep and Shrinkage Tests of Plain and Reinforced Concrete. A.S.T.M. Proc. Vol. 58. June, 1958 pp. 1101-1120.

97. Lyse, I., The Shrinkage and Creep of Concrete. Magazine of Concrete Research, Vol. 11, No. 33, Nov. 1959.

98. Lyse, I., The Shrinkage and Creep of Concrete, A.C.I. Journal, Vol. 31 No. 8, Proc. Vol. 56, Feb. 1960, pp. 775-782.

99. Hansen, T.C., and Mattock, A.H., Influence of Size and Shape of Member on Shrinkage and Creep of Concrete. A.C.I. Journal, Proc. Vol. 63, No. 2, Feb. 1966, pp. 267-290.

100. Ross, A.D., Creep of Concrete under Variable Stress. A.C.I. Journal, Vol. 29, Proc. Vol. 54, No. 9, Mar. 1958. pp. 739-758.

101. Pauw, A. and Meyers, B.L., Effect of Creep and Shrinkage on the Behaviour of Reinforced Concrete Members. Symposium on the Creep of Concrete. A.C.I. Sp-9, 1964, pp.129-150.

102. Gesund, H., Shrinkage and Creep Influence on Deflection and Moments of Reinforced Concrete Beams. A.C.I. Journal Proc. Vol.59, No. 5, May 1962, pp. 687-703.

103. Illston, J.M. and England, L., Creep and Shrinkage of Concrete and Their Influence on Structural Behaviour. A review of methods of analysis. The Structural Engineer (London) Vol. 48, No. 7, 1970.

104. McHenry, D., A New Aspect of Creep in Concrete and Its Application to Design. A.S.T.M. Proc. Vol. 43, pp. 1069-1084. 1943.

105. Miller, C.A. and Guralnick, S.A., Reinforced Concrete Beams Subjected to Repeated Loads. Journal of Structural Div. A.S.C.E., Proc. Vol. 93, No. ST5, Oct. 1967, pp. 67-84.

106. Sackman, J.L. and Nickell, R.E., Creep of a Cracked Reinforced Concrete Beam. Journal of the Structural Div. A.S.C.E. Proc. Vol. 94, No. ST1, Jan. 1968, pp. 283-308.

107. Leong, T.W. and Warner, R.F., Creep and Shrinkage in Reinforced Concrete. Journal of Structural Div. A.S.C.E. Proc. Vol. 96 No. ST3, Mar. 1970.

108. Miller, A.L., Warping of Reinforced Concrete due to Shrinkage. A.C.I. Journal Vol. 54, No. 11, May 1958, pp. 939-950.

109. Branson, D.E., Design Procedures for Computing Deflection. A.C.I. Journal, Vol. 65, No. 9, Sept. 1968, pp. 730-742.

110. Ferguson, P.M., Discussion of Warping of Reinforced Concrete due to Shrinkage by Miller. A.C.I. Journal. Proc. Vol. 54, No. 6, Dec. 1958.

111. Elvery, R.H. and Shafi, M., Analysis of Shrinkage Effects on Reinforced Concrete Structural Members. A.C.I. Journal, Vol. 67, No. 1, Jan. 1970. pp. 45-52.

112. Rowe, R.E., Cranston,W.B. and Best, B.C., New Concepts inthe Design of Structural Concrete. The Structural Engineer. (London) Vol. 43, No. 12, Dec. 1965.

113. Bate, S.C.C., Why Limit State Design ? Concrete. Vol. 2 No. 3, Mar. 1968.

114. Abeles, P.W., The Limit States of Design in Reinforced and Prestressed Concrete. The Consulting Engineer. (London). June 1968.

115. Beckett, D., Introduction to Limit State analysis of Reinforced Concrete Beams. Building Science, Vol. 4, No.1, June 1969, pp. 1-21.

116. Torroja, E., Load Factors, Report by the International Council for Building Research. A.C.I. Journal Vol.30, No. 5, Proc. Vol. 55, Nov. 1958. pp. 567-572.

117. Rose, W.H., The Structural Use of Precast Concrete and the British Standard Code of Practice C.P.116 (1965). The Structural Engineer (London) Vol. 44, No. 10 Oct. 1966.

118. Freudenthal, A.M., The Safety of Structures, Transactions of the A.S.C.E. Vol. 112, 1947, pp. 125-159.

119. Freudenthal, A.M. Safety and Probability of Structural Failure, Transactions of A.S.C.E. Vol. 121, 1956, pp. 1337-1375.

120. Torroja, E., Philosophy of Structures. University of California Press, Berkeley and Los Angeles, 1958.

121. Pugsly, A.G., Design for Safety and Efficiency. The Structural Engineer, (London) Jan. 1957.

122. Thomas, F.G., Basic Parameters and Terminology in the Consideration of Structural Safety. C.I.B. (Bulletin No. 3) 1964.

123. Report on Structural Safety, The Structural Engineer, Vol. 33, No. 5, May 1955.

124. Baker, A.L.L., Limit State Design of Reinforced Concrete. Published by C. &. C.A. Butler and Tanner Ltd. France and London 1970.

125. C.E.B.-F.I.P. Joint Committee International Recommendations for the Design and Construction of Concrete Structures. June 1970, F.I.P. Sixth Congress, Prague.

126. A.C.I. Committee 318. Building Code Requirements for Reinforced Concrete (A.C.I. 318-63) Detroit, 1963.

127. Proposed Revision of A.C.I. 318-63. Building Code Requirements for Reinforced Concrete. A.C.I. Journal, Feb. 1970.

128. DIN 1045 (German Code of Practice) Regulations of the German Sub-Committee for Reinforced Concrete. "Regulations for the Construction of Reinforced Concrete Buildings." Nov. 1959, C. & C.A. (London). Library Translation.

129. "Betong-og Jernbetonkonstructioner" (Danish Code of Practice) Copenhagen, Teknisk Forlog 1949. C. & C.A.(London) Library Translation.

130. G.B.V. (Netherlands) (Dutch Code of Practice) 1962. C. & C.A. (London) Library Translation.

131. A.C.I. Causes, Mechanism and Control of Cracking in Concrete. A.C.I. Committee 224. A.C.I. Annual Convention March 1966, Philadelphia. Pa; Anon; Publication Sp-20., Detroit,Mich. 1968,244pp.

132. Reis, E.I., Moze, J.D., Bianchini, A.C. and Kesler, C.E., Causes and Control of Cracking in Concrete Reinforced with High Strength Steel Bars. A Review of Research, Engineering Experiment Station, University of Illinois, Bulletin No. 479.

133. C.E.B. Bulletin d'Information No. 12, Paris, Feb. 1959. (Permanent Secretariat)(English Translation from French) Issued by C. &. C.A. London 1959.

134. C.E.B. Bulleting d'Information No. 24, Paris, June 1960, (Permanent Secretariat). Proceeding of the Fifth Working Session, Vienna. (English Translation from French) Issued by C. & C.A. April 1959. London.

135. Concrete Construction. Some Questions and Answers on Mechanism of Cracking. Vol. 13 No. 9, Sept. 1968, pp. 321-2.

136. Broms, B.B., Stress Distribution, Crack Patterns and Failure Mechanisms of Reinforced Concrete Members. A.C.I. Journal, Proc. Vol. 61. Dec. 1964.

137. Broms, B.B., Stress Distribution in Reinforced Concrete Members with Tension Cracks. A.C.I. Journal. Proc. Vol. 62, No. 9, Sept. 1965, pp. 1095-1103.

138. Broms, B.B., Crack Width and Spacing in Reinforced Concrete Members, A.C.I. Journal, Proc. Vol. 62 No. 10, Oct. 1965, pp. 1237-1256.

139. Broms, B.B. and Lutz, L.A., Effect of Arrangement of Reinforcement on Crack Width and Spacing of Reinforced Concrete Members. A.C.I. Journal, Proc. Vol. 62, No. 11, Nov. , 1965, pp. 1395-1410.

140. Griffith, A.A., The Phenomenon of Rupture and Flow in Solids. Philosophical Transactions, Royal Society London, A-221, 1921.

141. Batson, G.B., Journal of Engineering, Mechanics Div., A.S.C.E., Proc. Vol. 89, no. EM3, June 1963, pp. 147-168.

142. Watstein, D. and Parson, D.E., Width and Spacing of Tensile Cracks in axially Reinforced Concrete Cylinders. Journal of Research, National Bureau of Standards, 31, R.P. 1545 (1943).

143. Kaar, P.H. and Mattock, A.H., High Strength Bars as Concrete Reinforcement. Part 4, Control of Cracking. P.C.A. Research and Development Laboratories. Vol. 5, No.1, Jan. 1963, pp.15-38.

144. Evans, R.H., Extensibility and modulus of rupture of concrete. The Structural Engineer (London), Vol. 24 No. 12, Dec. 1946,

145. Kaplan, M.F., Strains and Stresses of Concrete at Initiation of Cracking and Near Failure. A.C.I. Journal Proc. Vol. 60, No. 7, July, 1963.

146. Thomas, F.G., Cracking in Reinforced Concrete, The Structural Engineer (London), Vol. 14, No. 7, July 1936, pp. 298-320.

147. Watstein, D. and Mathey, R.G. Width of Cracks in Concrete at the Surface of Reinforcing Steel, Evaluated by Means of Tensile Bond Specimens. A.C.I. Journal, Vol. 31, No. 1, Proc. Vol. 56, July 1959, pp. 47-58.

148. Watstein, D., and Seese, N.A., Effect of Type of Bar on Width of Cracks in Reinforced Concrete Subjected to Tension. A.C.I. Journal, Vol. 16, No. 4, Proc. Vol. 41,, Feb. 1945. pp293-304.

149. Clark, A.P., Cracking in Reinforced Concrete Flexural Members. A.C.I. Journal, Proc. Vol. 52, April 1956. pp. 851-862.

150. Blakey, F.A., and Anson, M., Design for Cracking. Constructional Review. Vol. 40, No. 7, July 1967, pp. 19-22.

151. Nawy, E.G.,Crack Control in Reinforced Concrete Structures. A.C.I. Journal, Proc. Vol. 65, No. 10, Oct. 1968, pp. 825-836.

152. Morita, S., Effects of Arrangement of Reinforcement on Crack Width and Spacing of Reinforced Concrete Members. Discussion of the paper by B.B. Broms and L.A. Lutz. A.C.I. Jounnal Part 2, June 1966, Proc. Vol. 62, 1965, pp. 1807-1812.

153. Kaar, P.H. and Hognestad, E., High Strength Bars as Concrete Reinforcement. Part 7, Control of Cracking in T.-Beam Flanges. P.C.A. Research and Development Laboratories. Jan. 1965.

154. Abeles, P.W., Brice, L.P. and Hajnal-Konyi, K., Cracking in Reinforced Concrete Flexural Members. Discussion of Paper by P. Clark. A.C.I. Proc. Vol. 52 1955-56, pp. 1433-1439.

155. C.E.B. Bulletin d'Information No. 19, Paris.

156. Blakey, F.A., A Theory of Deflection of Reinforced Concrete Beams under Short-Term Loads. Magazine of Concrete Research. Vol. 3 No. 7, Aug. 1951.pp. 3-8.

157. Guralnick, S.A., A study of deflection of reinforced concrete beams, M.Sc. Thesis Cornell University, 1955.

158. Beeby, A.W., Short-term Deformations of Reinforced Concrete Members. Technical Paper TRA408. C. & C.A. March, 1968.

159. Branson, D.E., Design Procedures for Computing Deflection. A.C.I. Journal, Proc. Vol. 65, No. 9, Sept. 1968 pp. 730-742.

160. A.C.I. Committee 435. Deflection of Reinforced Concrete Flexural Members. A.C.I. Journal, Proc. Vol. 63, No. 6, June 1966.pp.637-674.

161. A.C.I. Committee 435, Subcommittee 1, Allowable Deflections, Proc. Vol. 65. No. 6, June 1968, pp. 433-444. Discussion Dec. 1968 pp.1037-8.

162. Westlake, B.J. and Hawkins, N.M. The Inclusion of Deflection Consideration in the Design of Reinforced Concrete Beams. Constructional Review, Technical Supplement, Vol. 42, No. 4, Nov. 1969, pp. 58-64.

163. Attisha, H.P., A Study of the Behaviour and Design of Reinforced Concrete Slabs with an Experimental Investigation on Some Aspects of Membrane Action. M.Sc. Dissertation, University of Manchester, Jan. 1969.

164. Eppes, B.G., Comparison of Measured and Calculated Stiffness for Beams Reinforced in Tension only. A.C.I. Journal, Vol. 31, No. 4, Proc. Vol. 56, October 1959. pp. 313-325.

165. Bewtra, S.K., A Study of Different Methods for Predicting Short-Time and Long-Time Deflection of Reinforced Concrete Beams. M.Sc. Thesis, University of Iowa, Aug. 1964.

166. Hognestad, E., Hanson, N.W. and McHenry, D., Concrete Stress Distribution in Ultimate Strength Design. A.C.I. Journal, Proc. Vol. 52, Dec. 1955, pp. 455-480.

167. Mattock, A.H., Kriz, LB., and Hognestad, E., Rectangular Concrete Stress Distribution in Ultimate Strength Design. A.C.I. Journal. Vol. 32, No. 8, pp. 875-928, Proc. 57, Feb. 1961.

168. Prentis, J.M., Analysis of Inelastic Bending Stress in Concrete Beams. A.C.I. Journal Vol. 28, No. 3, Proc. Vol. 53, Sept. 1956.

169. Prentis, J.M., The Distribution of Concrete Stress in Reinforced and Prestressed Concrete Beams when Tested to Destruction by a Pure Bending Moment. Magazine of Concrete Research. Jan. 1951. No. 5. pp. 73-77.

170. Baker, A.L.L., Recent Research at Imperial College on the Design of Reinforced Concrete Frameworks, by Ultimate Load Theory. Reinforced Concrete Review. Vol. 3 No. 6, 1954, pp. 313-353.

171. Gray, J. de C., The Influence of Bond on Neutral Axis Position and Crack spacing in Reinforced Concrete Beams. Imperial College of Science and Technology (London), M.Sc. Thesis, 1953.

172. Baker, A.L.L., Discussion on a Paper by R.H. Evans and A. Williams "The Relation between the Strains in the Concrete and the Steel in Reinforced and Prestressed Concrete Beams." Magazine of Concrete Research, Vol. 12, No. 34, Mar. 1960.

173. Evans, R.H. and Williams, A., The Relation between the Strains in the Concrete and the Steel in Reinforced and Prestressed Concrete Beams. Magazine of Concrete Research, Vol. II, No. 32, July 1959, pp. 55-64.

174. Evans, R.H. and Robinson, G.W., Bond Stresses in Prestressed Concrete from X-Ray Photographs.. Proc. I.C.E., Part I, Vol. 4, No. 2, Mar. 1955, pp. 212-235.

175. Evans, R.H. and Williams, A., The Use of X-Rays in Measuring Bond Stresses in Prestressed Concrete. World Conference on Prestressed Concrete. San Francisco, July 1957, pp. A32-1 - A32-8.

176. Glanville, W.L.S. and Thomas, F.G., Explanatory Handbook on the B.S. Code of Practice for Reinforced Concrete (C.P.114 1957).

177. B.S. 812 (1967) "Methods for Sampling and Testing of Mineral Aggregates, Sands and Filters" British Standards Institution.

178. B.S. 882 (1965) Specification for Aggregates from Natural Sources for Concrete. British Standards Institution.

179. B.S. 1881,(1952) Methods of Testing Concrete. British Standards Institution.

180. Morice, P.B. and Base, G.D., The Design and Use of a Demountable Mechanical Strain Gauge for Concrete Structures. Magazine of Concrete Research, Aug. 1953. pp. 37-42.

181. Neville, A. M., Properties of Concrete. Sir Isaac Pitman and Sons Ltd. 1963.

182. Abeles, P.W., Cracking and Bond Resistance in High Strength Reinforced Concrete Beams, Illustrated by Photoelastic Coating. A.C.I. Journal, Proc. Vol. 63. No. 11, Nov. 1966. pp. 1265-1278,

183. Macleod, N., Cracking and Deflection Characteristics of Concrete Beams Reinforced with High Strength Steel. M.Sc. Thesis. Queen's University, Kingston, Ontario. 221 pages, April, 1963.

184. Kripanarayanan, K.M., and Branson, D.E., Short-time Deflections of Beams under Single and Repeated Load Cycles. A.C.I. Journal No. 2 Proc. Vol. 69. Feb. 1972.

185. Burns, N.H. and Siess, C.P., Repeated and Reversed Loading in Reinforced Concrete. Journal of the Structural Div. Proc. of the A.S.C.E. ST-5 Oct. 1966.

186. Hajnal Konyi, K., The Use of High Tensile Steel Reinforcement. Concrete and Constructional Engineering, Vol. 52, No. 12, pp. 397-409. Dec. 1957.

187. Hollington, M.R., A Series of Long-Term Tests to Investigate the Deflection of a Representative Precast Concrete Floor Component. C. & C.A. Technical Report. TRA442, April 1970.

188. Abeles, P.W., Prestressed Reinforced Concrete Sleepers Tested as Simply Supported Beams. Concrete and Constructional Engineering, I Vol. 42, No. 4, p. 123-132, Apr. 1947, II No. 5 May,1947, pp.155-161.

189. Abeles, P.W., Static and Fatigue Tests on Partially Prestressed Concrete Constructions. A.C.I. Journal. Vol. 26 No. 4, Proc. Vol. 51, Dec. 1954. pp. 361-376.

190. Dave, N.J., Limited Prestressing as a Means of Economy in Structural Concrete, Ph.D. Thesis, University of Leeds, July 1967.

191. Rimmer, B., A study of some prestressed concrete beams under sustained and repeated loadings. Ph.D. Thesis, University of Leeds, Aug. 1964.

192. Fluck, P.G., and Washa, G.W., Cottingham, W.S., Creep of Prestressed Concrete Beams, A.C.I. Journal, Proc. Vol. 57, Feb. 1961, p. 929.

193. Gadre, A.H., Sustained Load on Prestressed Composite Beams, Ph.D. Thesis, University of Leeds, 1961.

194. Lutz, L.A., The Mechanics of Bond and Slip of Deformed Reinforcing Bars in Concrete. Ph.D. Thesis, Cornell University 1966.

195. Lutz, L.A. and Gergely, P., Mechanics of Bond and Slip of Deformed Bars in Concrete. A.C.I. Journal, Proc. Vol. 64, No. 11, Nov. 1967. pp. 711-721.

TABLE (1)

Test Programme

Beam Mark	Type of Loading	No. of Cycles or Duration of Sustained Loading	Age at Loading (days)	
			Test	Failure
A11	Static	3 cycles	28	30
A12	"	"	30	32
A13	"	"	30	32
A14	"	"	30	32
A15	"	"	30	32
B11	"	"	60	62
B12	"	"	35	37
B15	"	"	30	32
B16	"	"	75	77
B17	"	"	110	112
B18	"	1 cycle	120	120
B19	"	3 cycles	45	47
B_{st1}	"	"	28	30
B_{st2}	"	"	21	28
A31	Fatigue	2,108,000 cycles	60	151
A32	"	3,597,000 "	140	176
A33	"	3,326,000 "	200	243
A34	"	3,250,000 "	139	243
B21	Sustained	623 days	97	-
B22	"	520 "	44	-
B23	"	623 "	44	-
B24	"	553 "	85	-
B25	"	553 "	100	-
P1	Pull-out		35	35
P2	"		"	"
P3	"		"	"
P4	"		"	"
P5	"		"	"
P6	"		"	"

TABLE (2)

Properties of Test Beams (Static Loading Tests)

Beam Mark	Beam Size (mm)			Steel Reinforcement				Calculated Loads#	
	b	d	d_1	No. & Size of Bars (mm)	Steel Area (sq.mm)	Type of steel	Yield Point or 0.2% Proof Stress N/mm^2	x Design P_D	Ultimate P_r
A11	152	305	260	2-19	570	Mild Steel	276	25.0	40.0
A12	152	305	260	2-19	570	Unisteel 60	414	37.2	59.5
A13	152	305	260	2-19	570	Unisteel 80	550	46.6	74.5
A14	152	305	262	2-16	401	Kam 60	585	37.2	59.5
A15	152	305	262	2-16	401	Kam 90	897	51.0	81.5
B11	152	305	257	2-25	1020	Mild Steel	276	42.0	67.0
B12	152	305	259	2-22	774	Unisteel 60	414	46.6	74.5
B15	152	305	264	2-12	226	Kam 90	897	33.2	53.0
B16	152	305	253	6-7	231	C.P.S.W.+	1380	42.5	68.2
B17	152	305	252	4-8	201	P.P.S.W.&	1515	41.4	66.3
B18	152	305	254	4-7.94	150	P.S.S.‡	1690	38.0	60.5
B19	152	305	247	4-14	412	Bristrand 100	690	40.0	64.0
B_{st1}	152	305	262	2-16	401	Kam 60	585	62.5	100.0
B_{st2}	152	305	262	2-16	401	Unisteel 80	550	60.0	95.0

+ Crimped Prestressing Wire & Plain Prestressing Wire ‡ Prestressing Strand

Calculated in accordance with the Draft Unified Code using nominal $U_w = 41.4\ N/mm^2$ and nominal steel yield point (Incorporating Partial Safecty Factors on Materials) x Calculated using a load factor of 1.6 i.e. $P_D = \frac{Pr}{1.6}$

TABLE (3)

Properties of Test Beams[x] (Repeated Loading Tests)

Beam Mark	Beam Size (mm) b	d	d_1	Steel Reinforcement: No. & Size of Bars (mm)	Steel Area (sq.mm)	Type of Steel	Yield Point or 0.2% Proof Stress N/mm^2	Calculated Loads (KN): Design P_D	Ultimate P_r
A31	152	305	260	2-19	570	Mild Steel	276	25.0	40.0
A32	152	305	260	2-19	570	Unisteel 60	414	37.2	59.5
A33	152	305	260	2-19	570	Unisteel 80	550	46.6	74.5
A34	152	305	262	2-16	401	Kam 60	585	37.2	59.5

TABLE (4)

Properties of Test Beams[x] (Sustained Loading Tests)

Beam Mark	Beam Size (mm) b	d	d_1	Steel Reinforcement: No. & Size of Bars(mm)	Steel Area (sq.mm)	Type of Steel	Yield Point or 0.2% Proof Stress N/mm^2	Calculated Loads (KN): Design P_D	Ultimate P_r
B21	152	305	257	2-25	1020	Mild Steel	276	42.0	67.0
B22	152	305	259	2-22	774	Unisteel 60	414	46.6	74.5
B23	152	305	260	2-19	570	Unisteel 80	550	46.6	74.5
B24	152	305	262	2-16	401	Kam 60	585	37.2	59.5
B25	152	305	264	2-12	226	Kam 90	897	33.2	53.0

x Same notations as Table (2)

TABLE(5)

Properties of Steel Reinforcement

Mark	Size (mm)	Type of Reinforcement	Yield Point or .2% Proof Stress N/mm^2	Ultimate Tensile Stress N/mm^2	Fracture Stress N/mm^2	Modulus of Elasticity E_s KN/mm^2
A	19	Mild Steel	317	482	372	210
A	25	"	317	484	378	215
B	19	Unisteel 60	420	620	500	205
B	22	"	438	620	490	198
B	19	Unisteel 80	650	690	506	200
C	16	Kam 60	605	924	1131	205
C	12	Kam 90	845	945	788	202
C	16	"	870	924	1225	207
D	14	Bristrand 100	744	927	-	190
E	7.94	P.S.S.[x]	1690	1940	-	196.5
F	8	P.P.S.W.[x]	1515	1600	-	218
G	7	C.P.S.W.[x]	1380	1690	-	201

x See Table (2) for notations

TABLE (6)

Properties of Concrete

Beam Mark	Cube Strength N/mm² 28 days	Strength of Concrete at Time of Test N/mm²			
		Cube Strength U	Cylinder Strength f_c	Modulus of Rupture f_t	Modulus of Elasticity E_c
A11	32.4	32.4	21.2	2.44	21.8
A12	40.4	46.0	28.8	3.76	28.8
A13	41.9	41.4	28.8	3.24	30.2
A14	40.0	41.4	28.2	3.28	32.1
A15	34.4	42.7	27.0	2.84	33.4
A31	41.0	52.7	31.9	4.14	29.2
A32	35.0	42.7	28.3	3.42	36.6
A33	41.0	48.9	31.8	3.76	31.8
A34	36.8	35.7	-	5.30	-
B11	38.0	47.5	32.3	4.14	30.7
B12	31.0	35.5	25.9	3.94	27.3
B15	35.5	36.5	28.4	2.70	28.5
B16	33.6	37.6	29.7	5.10	31.0
B17	39.3	37.6	33.7	4.20	32.2
B18	41.4	41.4	37.4	3.80	32.4
B19	35.8	37.2	38.3	3.63	29.0
B21	41.9	-	-	2.96	-
B22	47.3	-	-	3.79	-
B23	35.5	-	-	3.79	-
B24	38.7	-	-	3.00	-
B25	42.6	-	-	3.72	-
B_{st1}	-	39.1	-	3.13	-
B_{st2}	-	41.6	-	3.85	-

TABLE(7)

Pull-out Test Results[X]

Specimen Size = 145 x 145 x 190 mm

Specimen No.	Type of Steel	Size of Bar (mm)	Average Cube Strength N/mm^2	Average Bond Stress (N/mm^2) at		Max. Load (KN)	Max. Bond Stress (N/mm^2)	Mode of Failure[+]
				Slip of 0.025(mm)	Slip of 0.25 (mm)			
1	Unisteel 80	19	41.6	3.31	11.05	176.5	15.4	Bond
2	"	19	41.6	3.09	9.72	176.5	15.4	"
3	"	19	41.6	4.86	11.50	185.0	16.3	"
			Ave. =	3.78	10.8	179.0	15.7	
4	Kam 60	16	41.6	6.80	14.34	150.0	15.6	Bond
5	"	16	41.6	6.28	14.67	148.0	15.4	"
6	"	16	41.6	8.12	16.00	160.0	16.6	"
			Ave. =	7.06	15.00	152.6	15.86	

X All specimens had spiral reinforcement 6 mm diameter mild steel at 25 mm pitch.

+ All specimens developed fine vertical cracks on all four faces and at failure bars pulled through freely.

TABLE (8)

Summary of Test Results

(Static, Repeated and Sustained Loading Tests)

Beam Mark	Type of Steel	Yield Point or 0.2% Proof Stress N/mm²	Mean Cube Strength of Concrete N/mm²	Calculated Loads (KN)		Test Max. Load P_t (KN)	Calculated Moments KN-mm x 10^2		Test Max. Moment M_t x 10^2 (KN-mm)	Ratio of Ultimate Load to Estimated Static Strength 7/6	Factor of Safety 7/5	Steel Stress at Failure N/mm²	Ratio 13/3	Mode of Failure
				Design £P_D	Ultimate ≠ P_u		Design M_D	Ultimate M_u						
1	2	3	4	5	6	7	8	9	10	11	12	13	14	15
A11	Mild Steel	317	32.4	25.0	55.4	63.00	190	422	480	1.14	2.52	367	1.16	Tension
A31[x]	"	317	52.7	25.0	58.6	62.00	190	446	470	1.06	2.48	317	1.0	"
A12	Unisteel 60	420	46.0	37.2	72.8	77.65	282	555	590	1.07	2.09	456	1.09	"
A32[x]	"	420	42.7	37.2	73.2	83.35	282	558	634	1.14	2.24	492	1.17	"
A13	Unisteel 80	650	41.4	46.6	105.3	110.85	354	804	843	1.05	2.38	696	1.07	"
A33[x]	"	650	48.9	46.6	108.7	104.85[+]	354	705	796[+]	-	2.25	-	-	"
A14	Kam 60	605	41.4	37.2	74.4	84.40	282	566	641	1.13	2.27	704	1.16	"
A34[x]	"	605	35.7	37.2	73.2	84.85	282	554	645	1.16	2.28	725	1.20	"
A15	Kam 90	870	42.7	51.0	101.8	110.85	387	775	843	1.09	2.18	983	1.12	"
B11	Mild Steel	317	47.5	42.0	94.5	104.85	319	720	796	1.11	2.50	359	1.13	"
B21‡	"	317	-	42.0	-	-	319	-	-	-	-	-	-	-
B12	Unisteel 60	438	35.5	46.6	94.3	104.00	354	719	790	1.10	2.23	514	1.17	"
B22‡	"	438	-	46.6	-	-	354	-	-	-	-	-	-	-
B23‡	Unisteel 80	650	-	46.6	-	-	354	-	-	-	-	-	-	-
B24‡	Kam 60	605	-	37.2	-	-	282	-	-	-	-	-	-	-
B15	Kam 90	845	36.5	33.2	59.9	68.00	252	456	516	1.14	2.05	973	1.15	"
B25‡	"	845	-	33.2	-	-	252	-	-	-	-	-	-	-
B16	C.P.S.W.	1380	37.6	42.5	88.5	94.85	323	675	721	1.07	2.24	1665	1.20	"
B17	P.S.W.	1515	37.6	41.4	84.8	64.00	314	646	486	0.76	1.55	1080	0.71	Bond
B18	P.S. Strand	1690	41.4	38.0	73.9	81.45	296	562	623	1.10	2.14	1760	1.04	Tension
B19	Bristrand 100	744	37.2	40.0	83.0	100.85	304	632	766	1.22	2.52	948	1.27	"
B_{st1}	Kam 60	605	39.1	62.0	123.0	126.00	282	562	576	1.02	2.03	627	1.04	"
B_{st2}	Unisteel 80	650	41.6	62.0	134.0	130.00	282	602	595	0.97	2.10	642	0.99	"

x Repeated Loading ‡ Sustained Loading

\+ Test stopped, beam sustains higher loads

£ M_D and P_D calculated in accordance with Draft Code.

≠ M_u and P_u calculated based on actual strength of materials.

TABLE (9)

Summary of Test Results

(Repeated Loading Tests)

Beam Mark	Type of Steel	Yield Stress or 0.2% Proof Stress N/mm^2	Mean Cube Strength of Concrete N/mm^2		Load Range[x] (KN)		Steel Stress Range N/mm^2		No. of Cycles x 10^6	Load for Failure in Subsequent Static Test (KN)
			At 28 days	At Test	Minimum	Maximum	Minimum	Maximum		
A31	Mild Steel	317	-	52.7	15	29	89	168	2.108	58.38
A32	Uni-Steel 60	420	-	42.7	19	39	113	229	3.597	79.50
A33	Uni-Steel 80	650	41.0	48.9	25	45	143.5	259	3.326	101.00+
A34	Kam 60	605	36.8	35.7	20	40	116	326	3.250	81.00

TABLE (10)

Summary of Test Results

(Sustained Loading Tests)

Beam Mark	Type of Steel	Yield Stress or 0.2% Proof Stress N/mm^2	Mean Cube Strength of Concrete N/mm^2 28 days	Sustained Load[x] (KN)	Initial Stress N/mm^2		Duration (days)
					Steel	Concrete	
B21	Mild Steel	317	42.0	51.0	175	19.0	623
B22	Uni-steel 60	438	47.4	51.0	224	22.2	520
B23	Uni-steel 80	650	35.5	49.0	289	21.0	623
B24	Kam 60	605	38.8	37.2	301	19.0	553
B25	Kam 90	845	-	33.5	460.5	22.4	553

x Applied Load + Self Weight

\+ Sustains higher load

TABLE (11)

Cracking of Reinforced Concrete (Static Loading Tests)

Beam Mark	Steel Stress (N/mm^2) at		Remaining Crack Width x 10^{-2} mm						Design Load Crack Width x 10^{-2} mm								No. of cracks under		Average Spacing
			Maximum				Average		Maximum					Average					
			Measurement at																
			Bottom Edge		Steel Level		Bottom Edge	Steel Level	Bottom Edge		Steel Level			Bottom Edge	Steel Level				
	Design Load	Zero Live Load	Measured	Calculated ‡	Measured	Calculated ‡	Measured	Measured	Measured	Calculated ≠ Draft Code	Measured	Calculated ≠ Draft Code	Proposed x	Measured	Measured			Design Load	Zero Live Load	
A11	180	29	10	3.6	6	0.70	5.28	1.72	18	10.7	10	5.38	8.20	10.40	8.30			11	11	132
A12	243	29	6	5.3	3	1.94	1.11	0.27	20	12.6	11	6.33	11.00	11.50	6.90			15	5	90
A13	298	29	8	6.8	4	2.96	3.44	0.93	30	20.7	12	10.20	14.50	17.40	9.20			16	12	86
A14	342	40	6	7.9	2	3.77	2.36	0.77	20	20.8	11	10.70	16.00	12.60	6.79			17	13	91
A15	417	40	6	6.6	3	5.15	2.60	0.74	22	27.4	12	14.00	18.00	12.60	7.20			17	15	93
B11	143	7	3	2.7	1	0.93	1.73	0.30	12	10.2	6	4.80	7.30	8.48	2.20			13	11	114
B12	224	21	6	4.8	1	1.59	5.00	1.00	20	20.4	11	9.65	10.60	11.50	4.70			14	3	108
B15	462	67	10	11.0	6	6.00	-	-	32	25.4	23	13.60	20.00	16.90	8.86			14	12	102
B16	678	68	16	16.7	11	10.00	7.15	3.84	60	45.0	40	21.40	50.00	35.00	21.60			12	10	128
B17+	760	83	30	17.4	18	11.50	18.78	12.40	100	57.4	70	26.90	55.00	73.20	45.60			7	7	195
B19	384	39	10	9.0	3	4.55	6.12	1.42	32	28.0	18	13.00	27.00	19.90	10.15			13	12	108

\+ Bond slip failure

≠ $W = 2.3Ce_t$

‡ $\Delta W_s = 5.28C\,(f_s - 138) \times 10^{-6}$; $\Delta W_b = 5.0C\,(f_s - 41.4) \times 10^{-6}$

x $W_{(max)_1} = RC\,(f_s - \frac{K_s}{p})$

TABLE (12)

Effect of Loading Cycles on Deflection

Beam Mark	Design Load P_D (KN)	Deflection at P_D (mm)	2nd cycle Maximum Load P_s (KN)	Deflection at P_s (mm)	Remaining Deflection at the end of 1st cycle (mm)	Remaining Deflection at the end of 2nd cycle (mm)	Ratio 5/2 x 100	Ratio 6/4 x 100	Deflection at P_D at 2nd cycle (ascending) (mm)	Deflection at P_D at 2nd cycle (descending) (mm)	Deflection at P_D at 3rd cycle (ascending) (mm)	Total Deflection at Design Load+ (mm)				Ratio 14/12	Ratio 15/13
												Calculated		Observed			
												1st Cycle	2nd Cycle	1st Cycle	2nd Cycle		
	1	2	3	4	5	6	7	8	9	10	11	12	13	14	15	16	17
A11	25	9.80	32	12.95	2.24	2.66	22.8	20.6	10.04	10.60	10.92	10.20	11.41	10.40	10.64	1.02	0.93
A31	25	8.85	-	-	3.04	-	34.3	-	-	-	-	8.90	-	9.45	-	1.06	-
B11	42	12.00	49	14.25	2.70	2.92	22.7	20.5	11.59	12.52	12.33	14.85	15.99	12.50	12.59	0.84	0.79
A12	37	14.80	48	20.16	3.57	4.60	25.4	22.8	15.19	15.89	15.79	13.76	14.90	15.32	15.71	1.11	1.05
A32	37	11.75	-	-	2.26	-	19.2	-	-	-	-	17.70	-	12.25	-	0.69	-
B12	46	15.20	60	20.00	3.41	4.19	22.4	21.0	15.27	17.01	16.66	16.59	16.98	15.68	15.75	0.94	0.93
A13	46	19.25	60	25.60	3.79	4.70	19.7	18.4	19.54	21.32	21.49	17.23	18.04	19.74	20.03	1.14	1.12
A33	46	17.25	-	-	3.45	-	20.0	-	-	-	-	20.77	-	17.70	-	0.85	-
A14	37	16.25	56	26.20	3.71	5.08	22.8	19.4	16,51	19.34	19.14	16.93	18.25	16.93	17.19	1.00	0.94
A34	37	17.20	-	-	4.08	-	23.7	-	-	-	-	18.18	-	17.98	-	0.99	-
A15	51	24.20	66	34.89	4.62	6.47	19.1	18.6	24.70	28.46	28.09	26.09	27.15	24.80	25.30	0.95	0.93
B15	33	24.30	38	29.75	6.29	7.21	25.8	24.0	25.25	28.46	27.73	26.19	29.40	24.90	25.85	0.95	0.88
B16	42	35.50	55	48.00	8.68	10.24	24.5	21.4	36.42	-	-	37.40	40.27	36.00	36.92	0.96	0.92
B17	42	45.00	55	73.00	16.98	21.21	37.7[x]	29.0	48.42	-	-	38.63	41.37	45.55	48.97	1.18	1.19
B19	40	23.25	50	31.25	6.50	8.00	28.0	25.6	25.25	28.58	27.10	24.61	36.10	23.75	25.75	0.96	0.99

x Bond slip failure

\+ Includes deflection under dead weight

TABLE (13)

Effect of Steel Stress on Deflection

Steel Stress N/mm^2	Span/Deflection Ratio									
	A11	A12	A13	A14	A15	B11	B12	B15	B16	B19
50	1830	2170	2030	3800	3800	1450	1830	5700	5700	5700
100	730	780	748	1580	1430	600	720	1760	3040	1520
200	324	338	333	490	475	280	300	520	530	400
300		217	214	290	285		191	304	292	235
400			154	205	199			216	204	158
500				159	156			166	156	121
600					123			130	127	96
700									104	78
800									86	
900									75	

TABLE (14)

Effect of High Tensile Steel on the Ultimate Strength of Concrete

Group	Beam Mark	Type of Steel	% Steel	Working Load (KN) A	Concrete Compressive Strain x 10^{-5} at A	% Ultimate+ Load B	Concrete Compressive Strain x 10^{-5} at B	Mean Strain at yield point or 0.2% proof stress in steel %	Depth of Neutral Axis (mm)
A	A11	Mild Steel	1.44	25	48	86	116.5	0.16	95
	A12	Unisteel 60	1.44	38	72	83	128.5	0.22	109
	A13	Unisteel 80	1.44	47	91	79	186.5	0.53	102
	A14	Kam 60	1.01	37	72	88	162.5	0.29	103
	A15	Kam 90	1.01	47	94	89	245.0	0.63	97
B	B11	Mild Steel	2.580	42	62	90	198.5	0.16	108
	B12	Unisteel 60	1.960	42	78	91	179.5	0.47	120
	B16	C.P.S. Wire	0.598	42	119	90	278.0	0.89	74
	B17	P.P.S. Wire	0.522	42	130	93	195.0	0.92	62
	B18	P.S. Strand	0.395	42	135	85	241.5	1.90	57
	B19	Bristrand 100	1.09	42	112	78	179.5	0.60	82

+ Maximum load at which strain measurement was stopped.

TABLE (15)

Comparison of Crack Width at the Level of the Reinforcement

Under Static, Sustained and Repeated Design Load (mm)

Beam Mark	Steel Type	Comparable Static Tests Instant-aneous	Sustained Load		Repeated Load		Ratio 5/4	Ratio 7/6
			Instant-aneous	Final+	Instant-aneous	Final		
1	2	3	4	5	6	7	8	9
A31	Mild Steel	0.10			0.08	0.12x		1.50
B21	"	0.06	0.06	0.10			1.67	
A32	Unisteel 60	0.11			0.08	0.11		1.38
B22	"	0.11	0.09	0.11			1.22	
A33	Unisteel 80	0.12			0.09	0.12x		1.33
B23	"	0.12	0.10	0.16			1.60	
A34	Kam 60	0.11			0.12	0.18x		1.50
B24	"	0.11	0.08	0.11			1.37	
B25	Kam 90	0.23	0.20	0.29			1.45	

TABLE (16)

Comparison of Deflection under Static, Sustained and Repeated Design Load

Beam Mark	Steel Type	Deflection (mm)					Ratio 5/4	Ratio 7/6
		Static Load Instant-aneous	Sustained Load		Repeated Load			
			Instant-aneous	Final+	Instant-aneous	Final		
1	2	3	4	5	6	7	8	9
A31	Mild Steel	10.22			8.82	11.70x		1.33
B21	"	11.06	13.54	30.00			2.22	
A32	Unisteel 60	14.78			10.68	14.07		1.32
B22	"	15.53	14.78	28.50			1.93	
A33	Unisteel 80	19.40			14.80	18.00x		1.22
B23	"	19.40	17.25	30.90			1.79	
A34	Kam 60	17.11			17.48	21.50x		1.23
B24	"	17.11	15.17	27.00			1.78	
B25	Kam 90	21.17	23.33	36.60			1.57	

+ x Values extrapolated for 1000 days duration for sustained loading and 3.5 million repetitions in the case of repeated load tests

TABLE (17)

Comparison of Deflections (Sustained Loading Tests)

Type of Steel	Instant-aneous Deflection (mm)	H.T.S. / M.S. [x]	After 6 months (inelastic)	H.T.S. / M.S.	Total Deflection After 6 months	H.T.S. / M.S.	After 1 year (inelastic)	H.T.S. / M.S.	Total Deflection after 1 year	H.T.S. / M.S.
Mild Steel	13.54	1.00	10.46	1.00	24.00	1.00	13.63	1.00	27.17	1.00
Unisteel 60	14.78	1.09	9.00	0.860	23.78	0.99	11.53	0.845	26.31	0.969
Unisteel 80	17.25	1.27	9.34	0.894	26.59	1.11	11.49	0.842	28.74	1.060
Kam 60	15.17	1.12	8.35	0.798	23.52	0.98	9.76	0.717	24.93	0.917
Kam 90	23.33	1.72	8.67	0.830	32.00	1.33	10.49	0.77	33.82	1.247

x H.T.S. High Tensile Steel M.S. Mild Steel Deflection as ratio of Mild Steel

TABLE 18

Time-Dependent Deflection

Beam Mark	% Steel	Design[+] Load (KN)	Design Steel Stress (N/mm^2)	Mean Neutral[‡] Axis Depth (mm)		Creep Coeff-icient (C_c)	Shrinkage $e_{sh} \times 10^{-6}$	Instantaneous Deflection (mm)		Deflection After One Year (mm)		
				Meas-ured	Calc-ulated[x]			Meas-ured	Proposed[o] Method	Meas-ured	Calc-[x] ulated	Proposed[o] Method
B21	2.580	51.0	175	160	161	2.66	135	13.54	14.77	26.77	21.95	29.1
B22	1.960	51.0	224	145	147	2.45	193	14.78	15.47	25.82	22.80	27.4
B23	1.440	49.0	289	140	134	2.29	110	17.25	19.77	28.25	23.46	32.6
B24	1.010	37.2	301	128	118	2.29	120	15.17	17.77	24.93	20.46	29.0
B25	0.564	33.5	460.5	96	96	2.15	66	23.33	24.62	33.82	28.14	35.8

+ Total working load (including self weight and the arrangement's weight)

‡ Neutral axis of stress

x Calculated according to Pauw and Meyer using "Effective" modulus § 2.2.6 $U_w = 41.4 N/mm^2$, $E_s = 200\ KN/mm^2$, $E_c = 4/\sqrt{U_w}$

o Calculated according to Chapter 9 and 10 (using multipliers for time-dependent deflections Fig. 101)

TABLE (19)

Recovery of Deflection

(Sustained Loading Tests)

Beam Mark	Loading			Unloading							
	Instant-aneous Live-Load Deflection (mm)	Long-term Deflection (mm)	Total Measured Deflection (mm)	Duration (days)	Instant-aneous Recovery (mm)	Additional Recovery				Total Recovery (mm)	Residual Deflection (mm)
						After 1 day (mm)	After 5 days (mm)	After 14 days (mm)	After 28 days (mm)		
B22	14.30	12.01	26.31	520	12.14	0.35	0.59	-	-	12.73	13.58
B24	14.75	10.83	25.58	553	12.17	0.27	0.43	0.70	0.84	13.01	12.57
B25	22.83	11.72	34.55	553	18.64	0.29	0.49	0.80	1.08	19.72	14.83

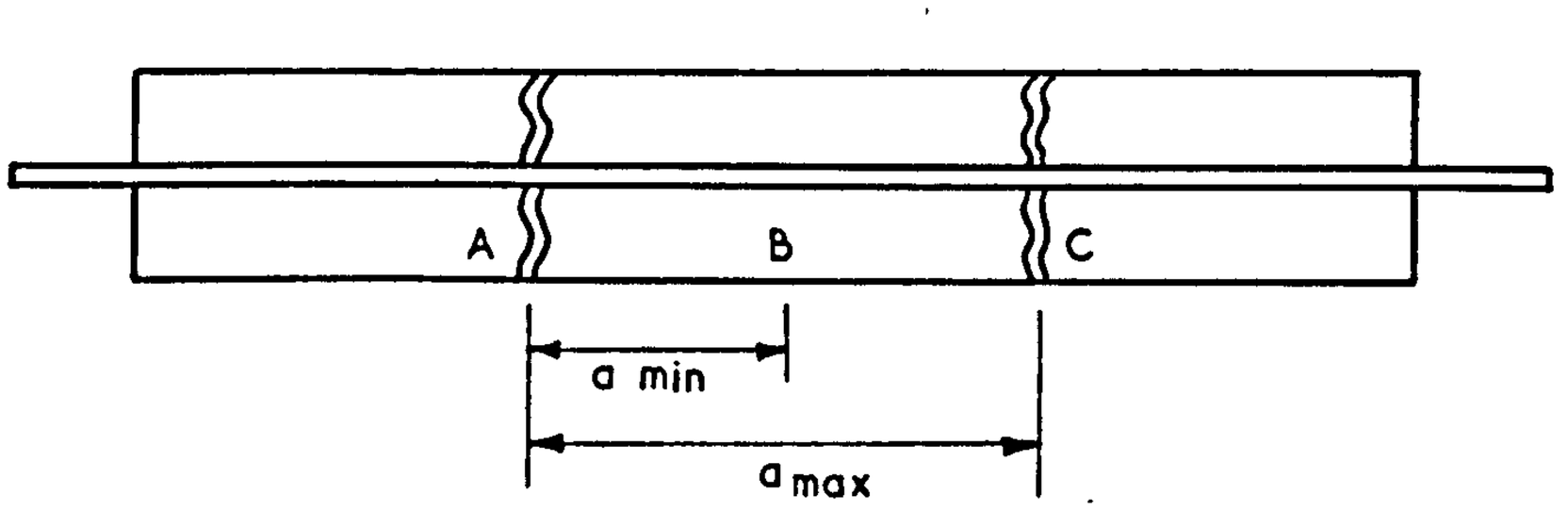

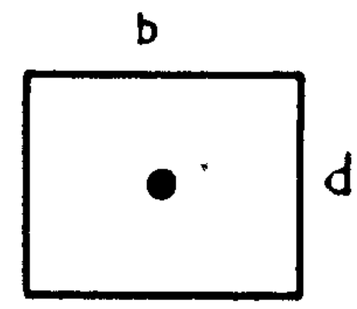

$A_e = b\,d$

(a) TENSION SPECIMEN

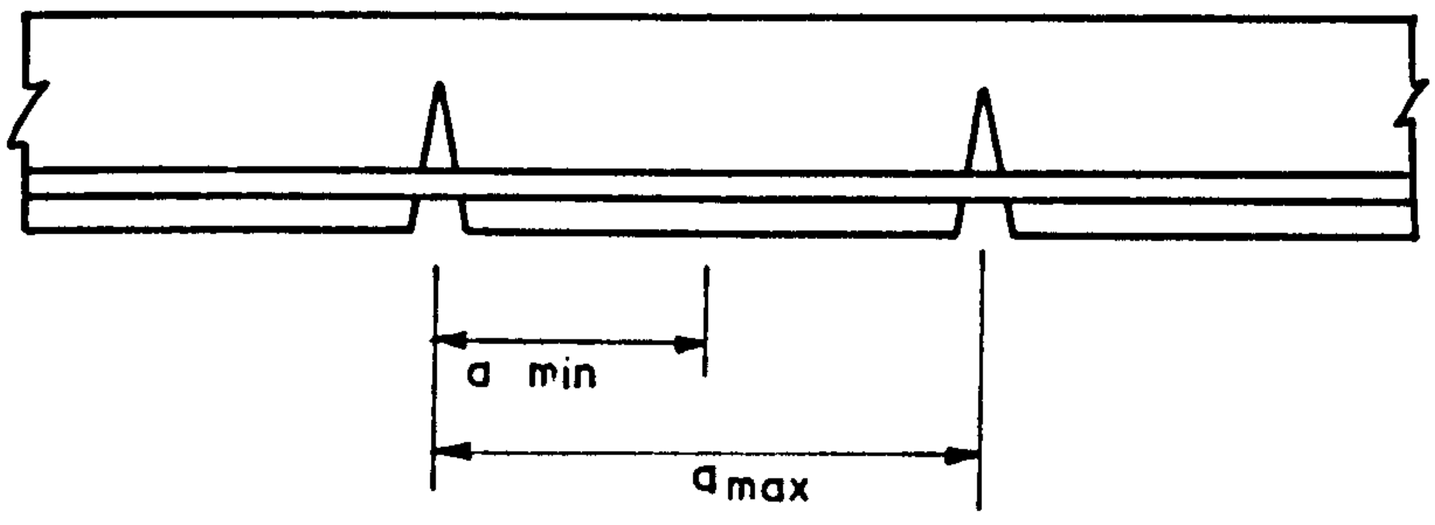

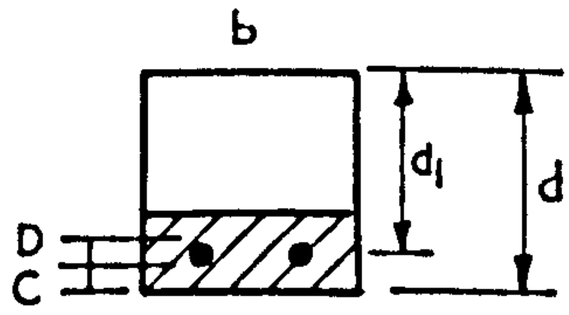

$A_e = b(2C + D)$

(b) FLEXURAL SPECIMEN

FIG. (1) MECHANISM OF CRACKING.

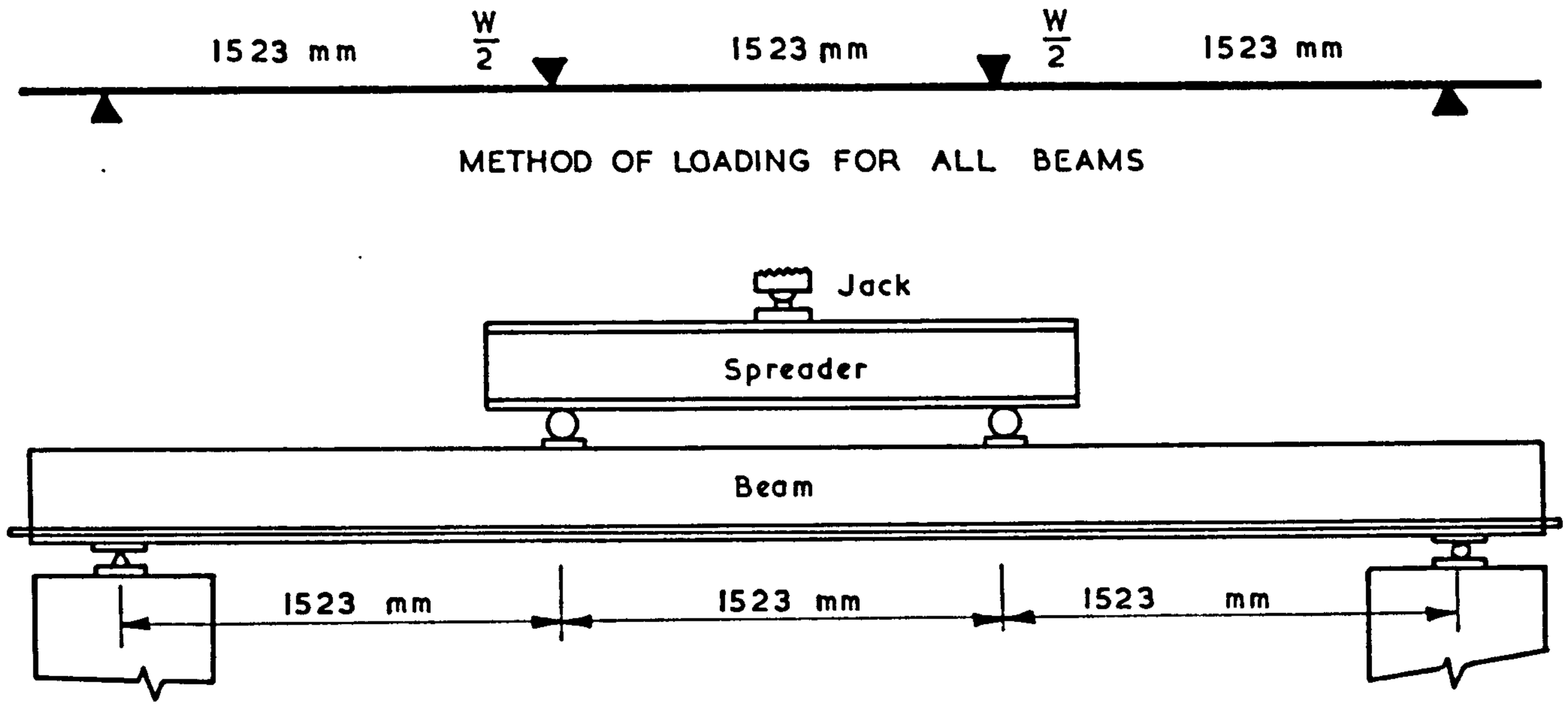

FIG. (2) TEST LOADING ARRANGEMENT FOR STATIC AND FATIGUE TESTS

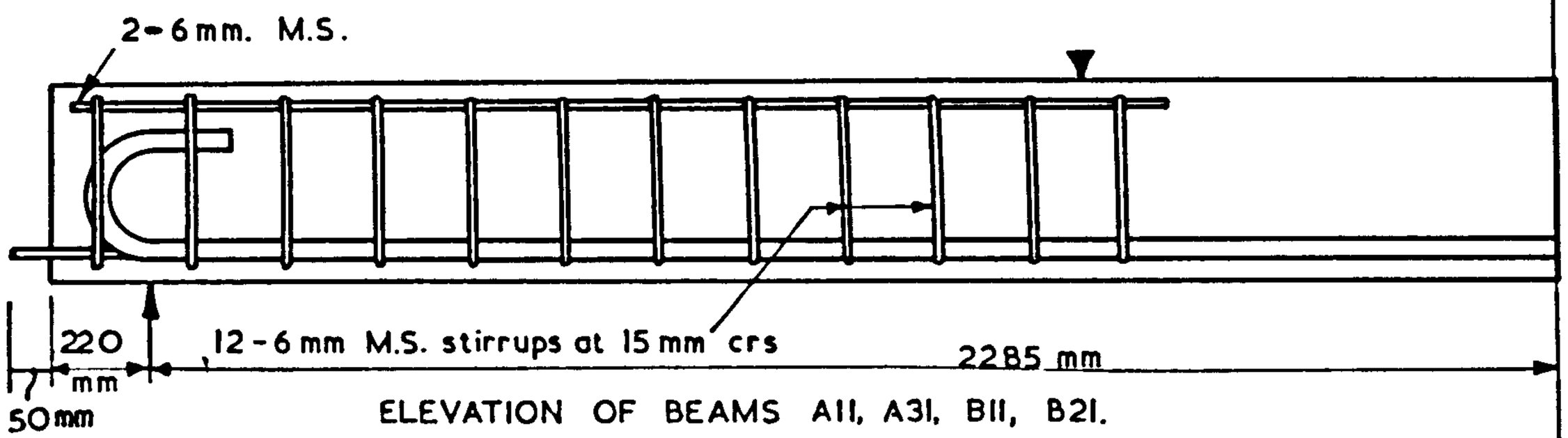

ELEVATION OF BEAMS A11, A31, B11, B21.

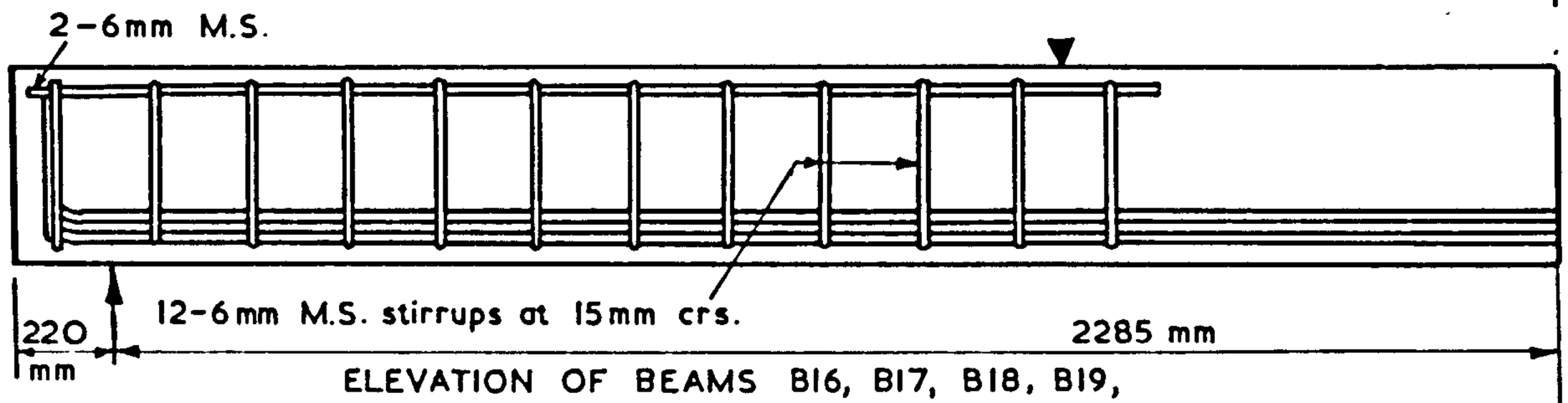

ELEVATION OF BEAMS B16, B17, B18, B19,

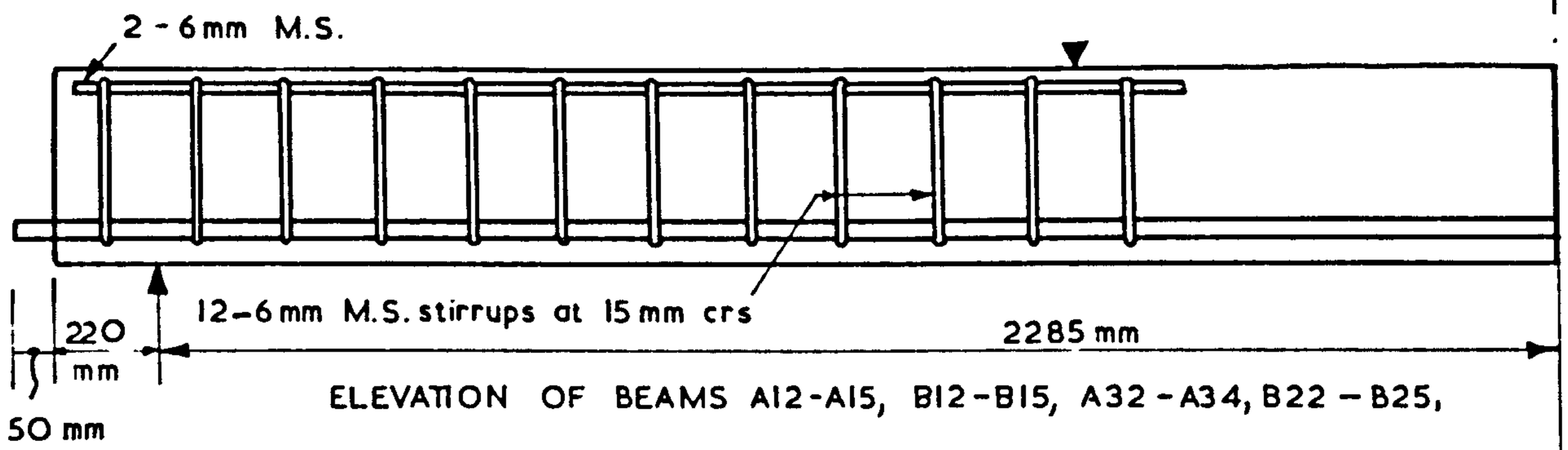

ELEVATION OF BEAMS A12-A15, B12-B15, A32-A34, B22-B25,

FIG. (3) DETAILS OF TEST BEAMS

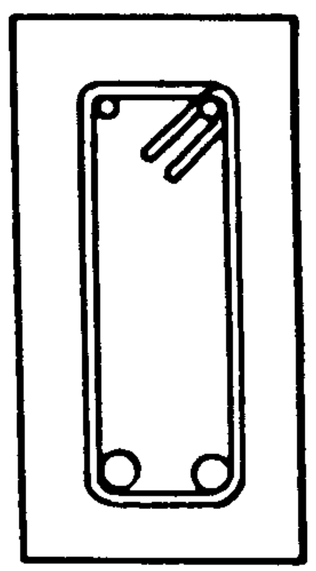

Two 19mm dia. bars
BEAMS A11, A12, A13
A31, A33
B23.

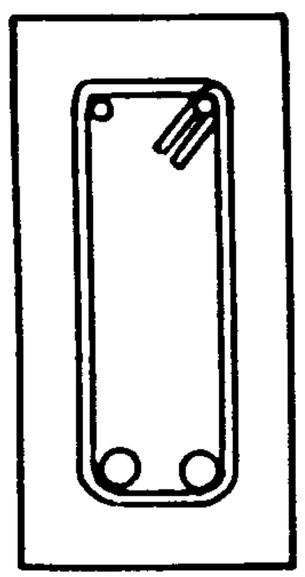

Two 25 mm dia. bars
BEAMS B11, B21

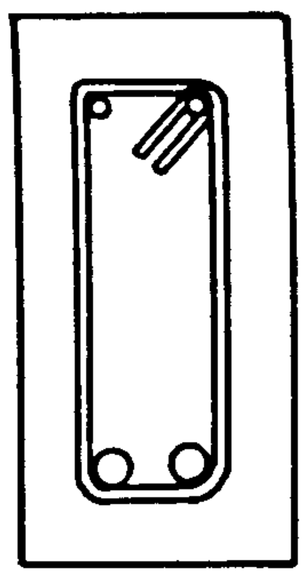

Two 22mm dia. bars
BEAMS B12, B22

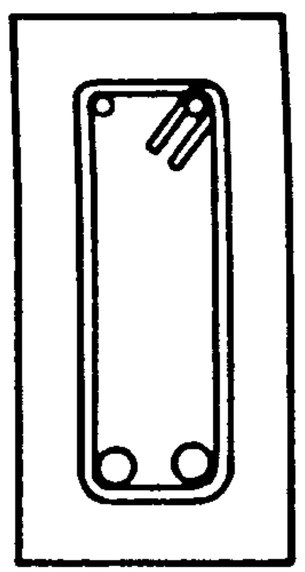

Two 16 mm dia. bars
BEAMS A14, A15
B24, A34
B_{st1}, Bst2

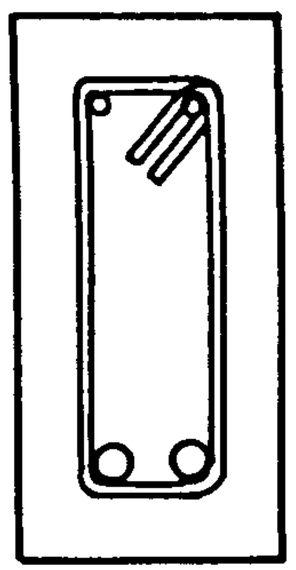

Two 12mm dia. bars
BEAMS B15, B25

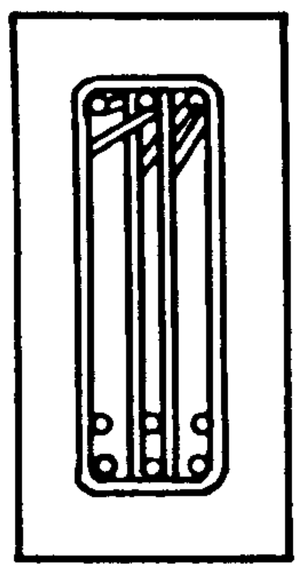

Six 7mm dia. crimped wires
BEAM, B16

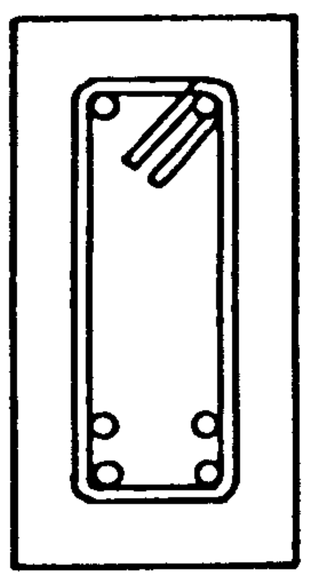

Four 8 mm dia. plain wires
BEAM B17

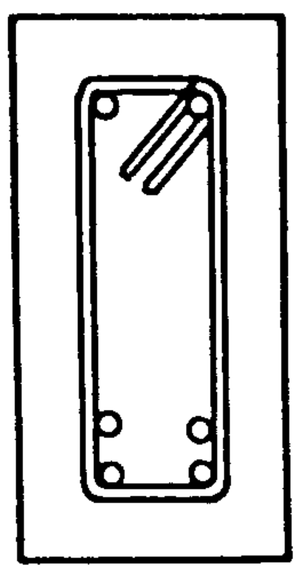

Four 7·94 mm dia. strand
BEAM B18

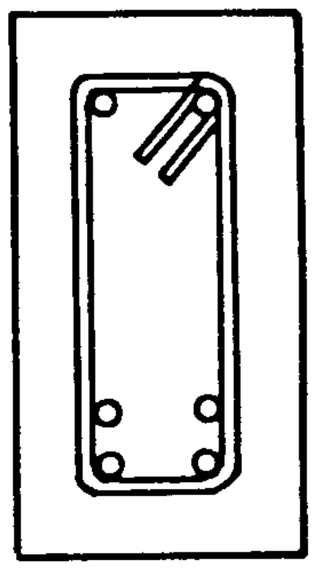

Four 14 mm dia. Bristrand
BEAM B19

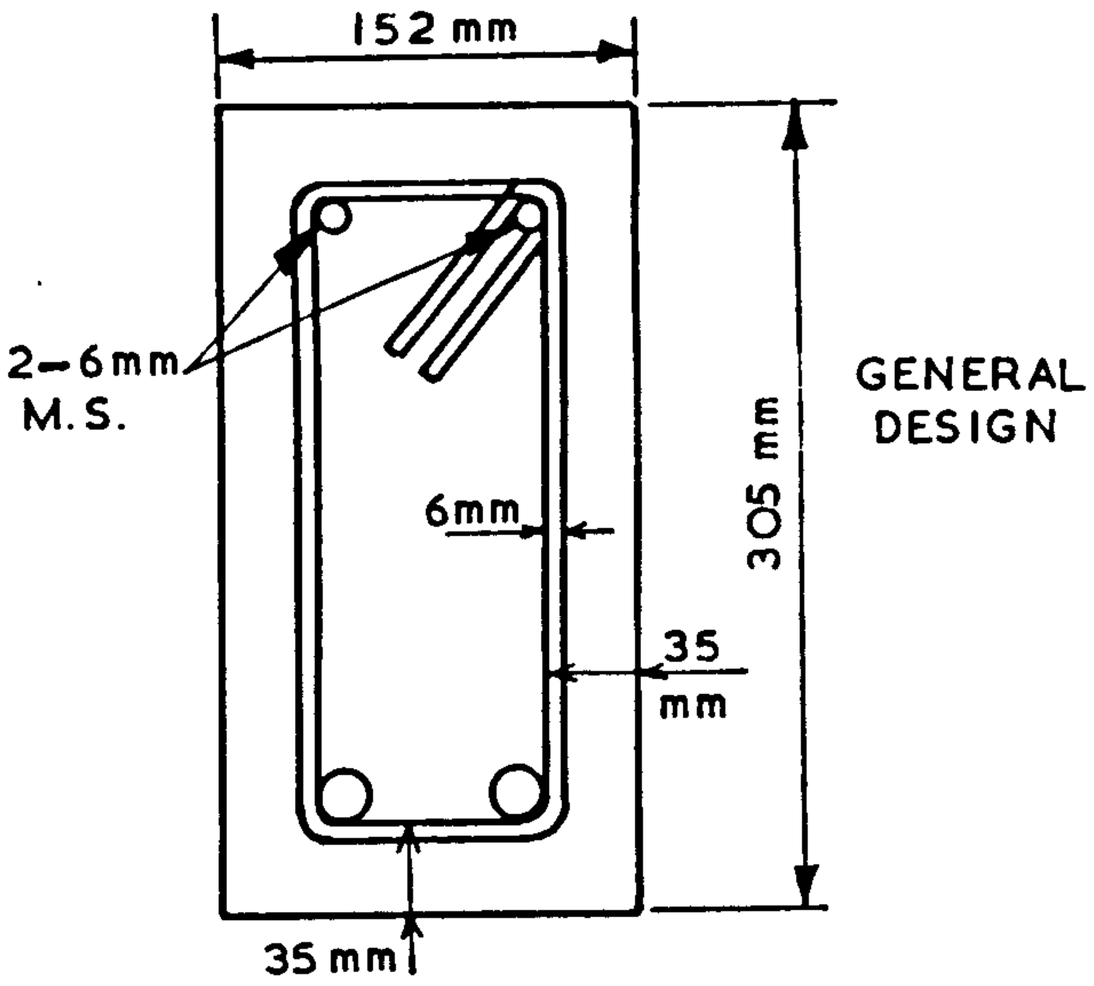

FIG. (4) SECTION – DIMENSIONS FOR ALL BEAMS

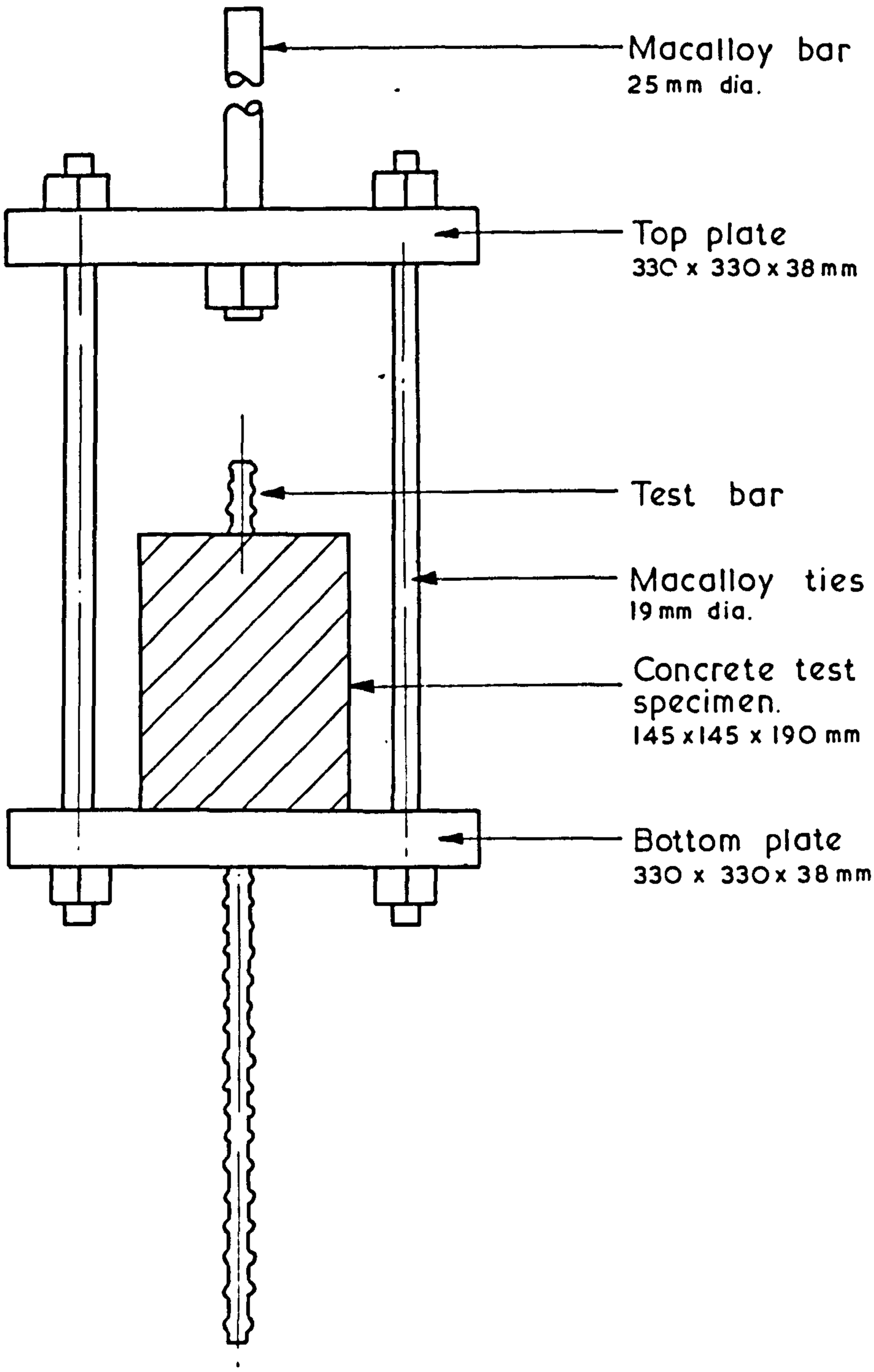

FIG. (5) PULL-OUT TEST ARRANGEMENT
(BOND TEST)

FIG. (6) STRESS–STRAIN CURVES FOR STEEL.

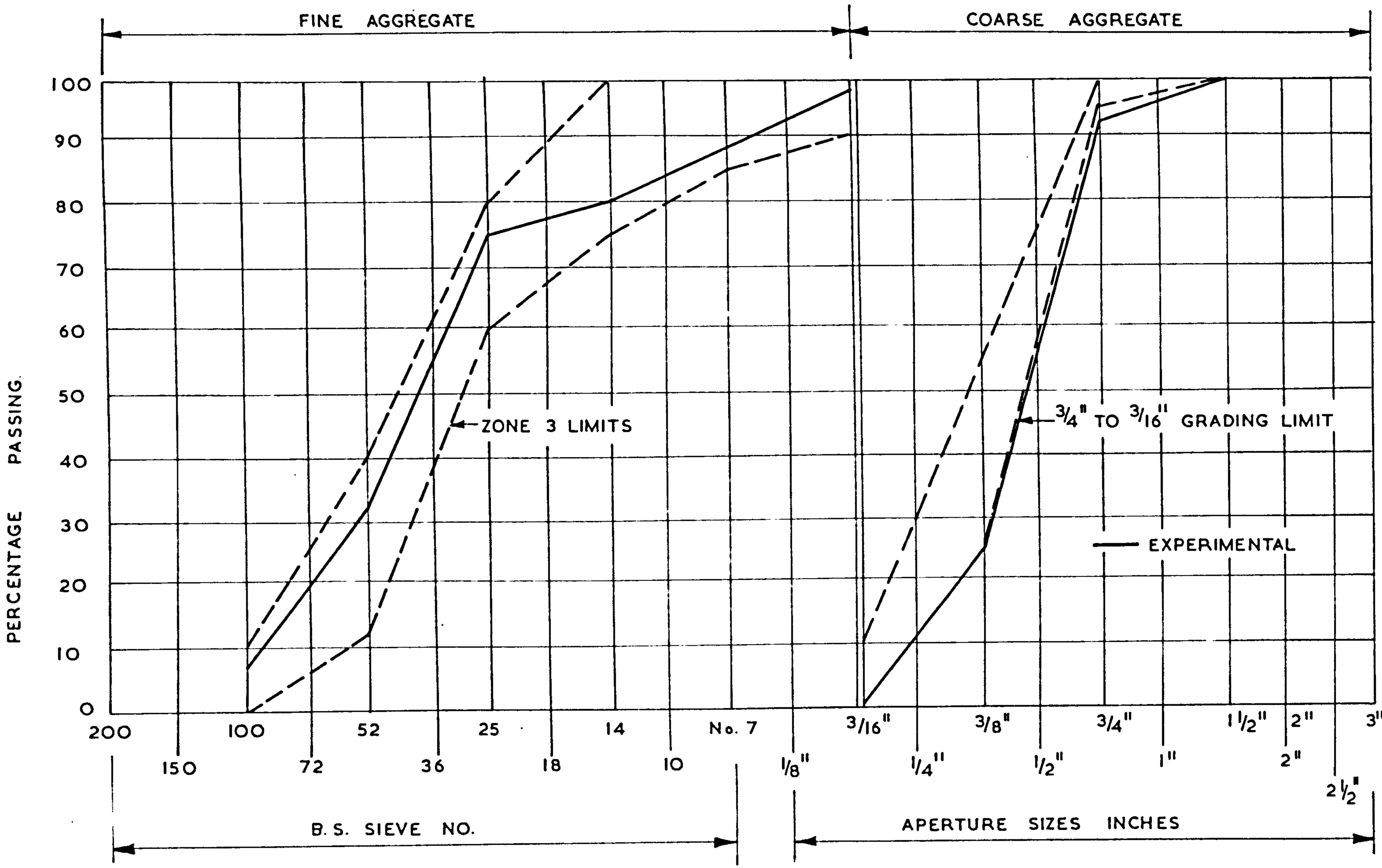

FIG. (7) GRADING OF AGGREGATES

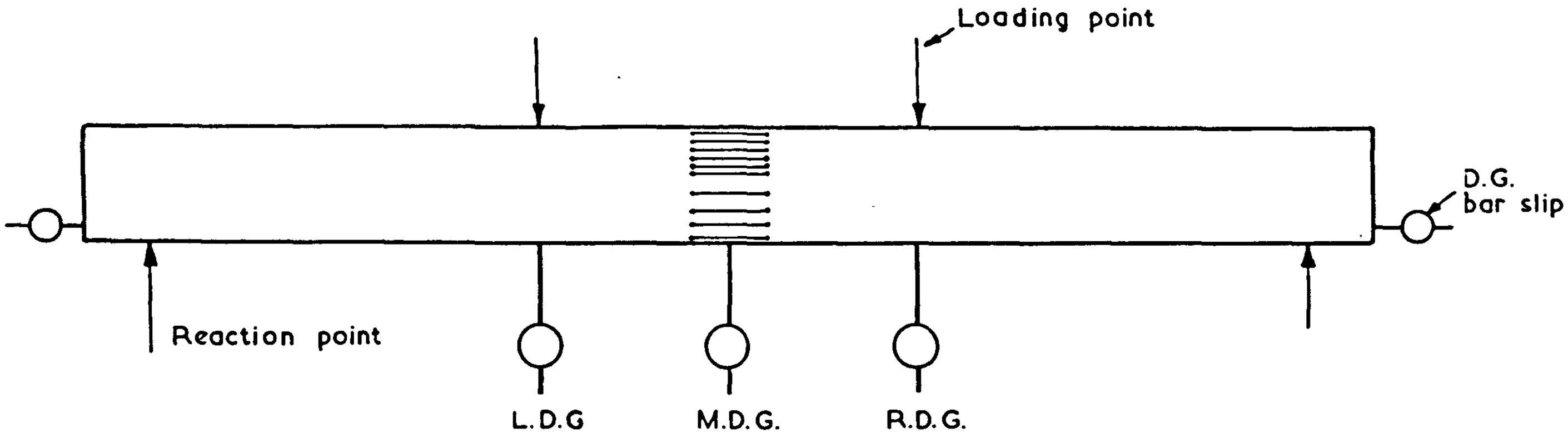

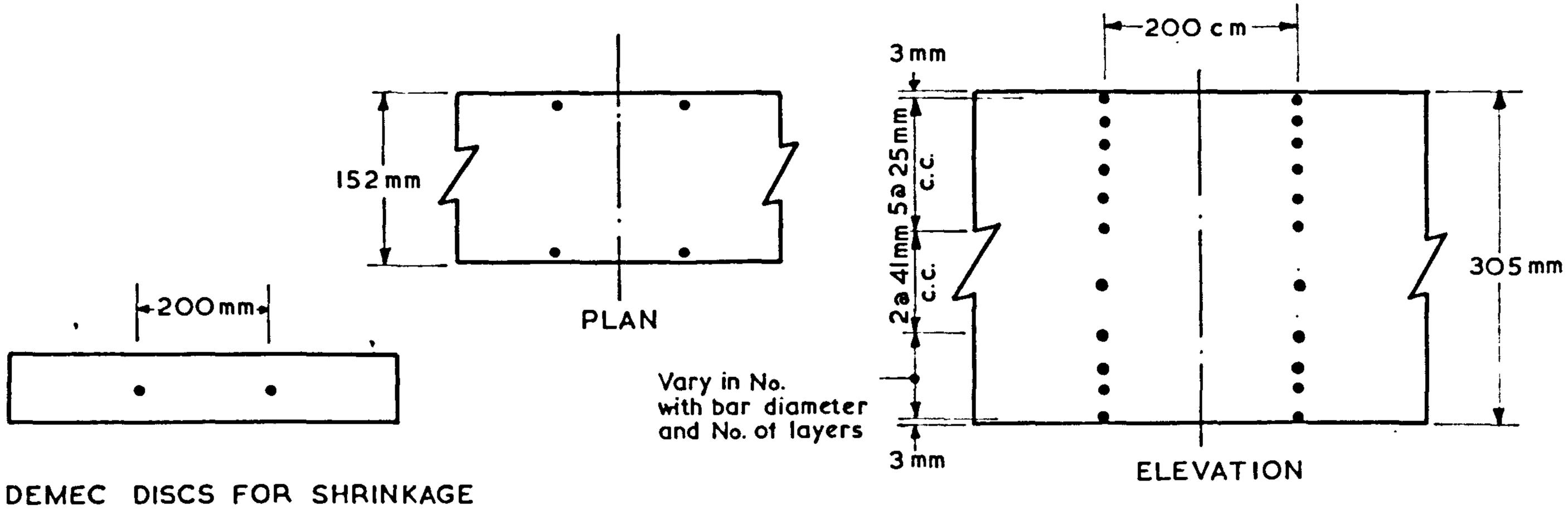

FIG. (8) GENERAL LAYOUT OF INSTRUMENTATION.

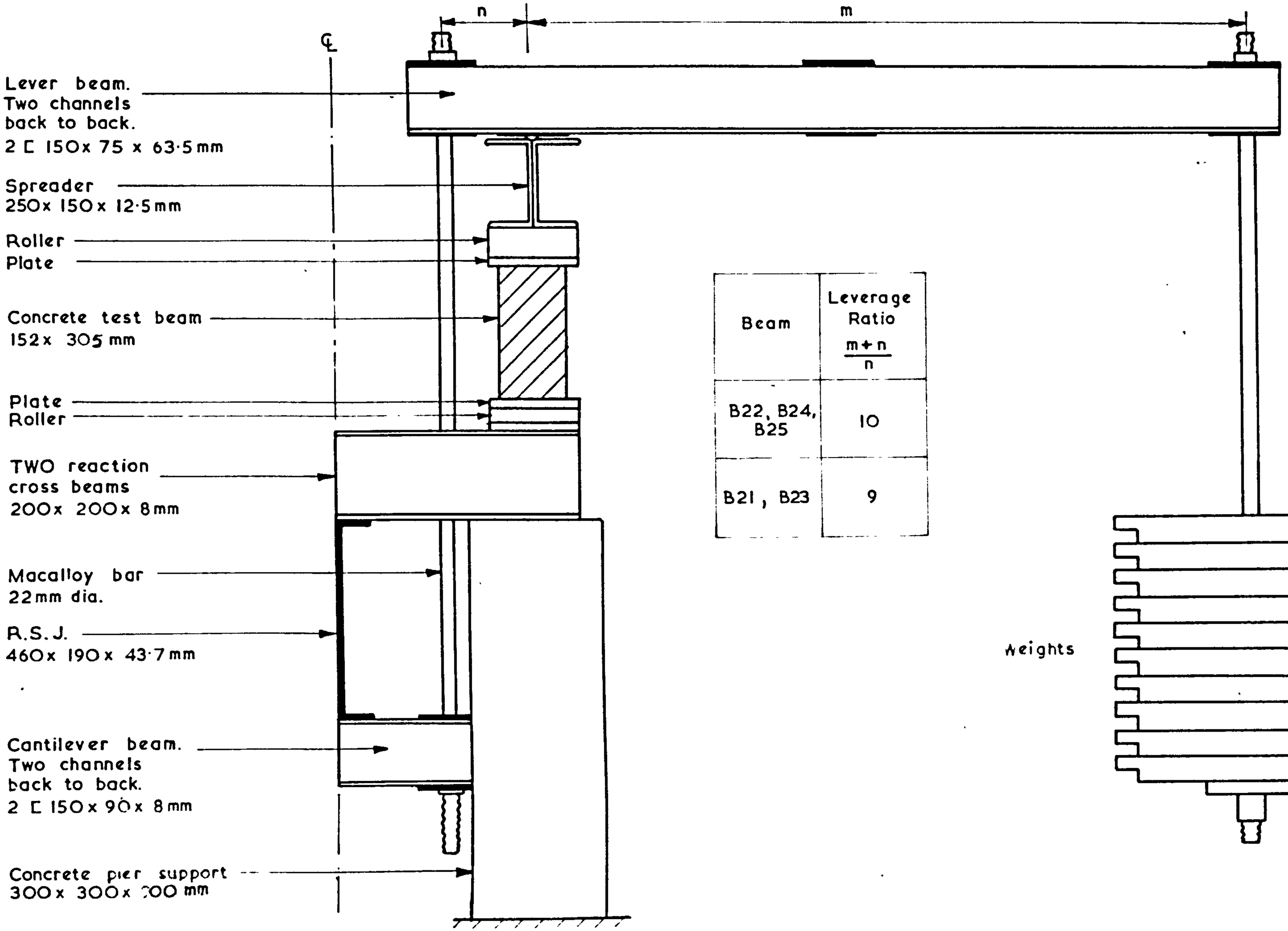

Beam	Leverage Ratio $\frac{m+n}{n}$
B22, B24, B25	10
B21, B23	9

Weights

FIG. (9) LEVER ARRANGEMENT FOR SUSTAINED LOADING TESTS

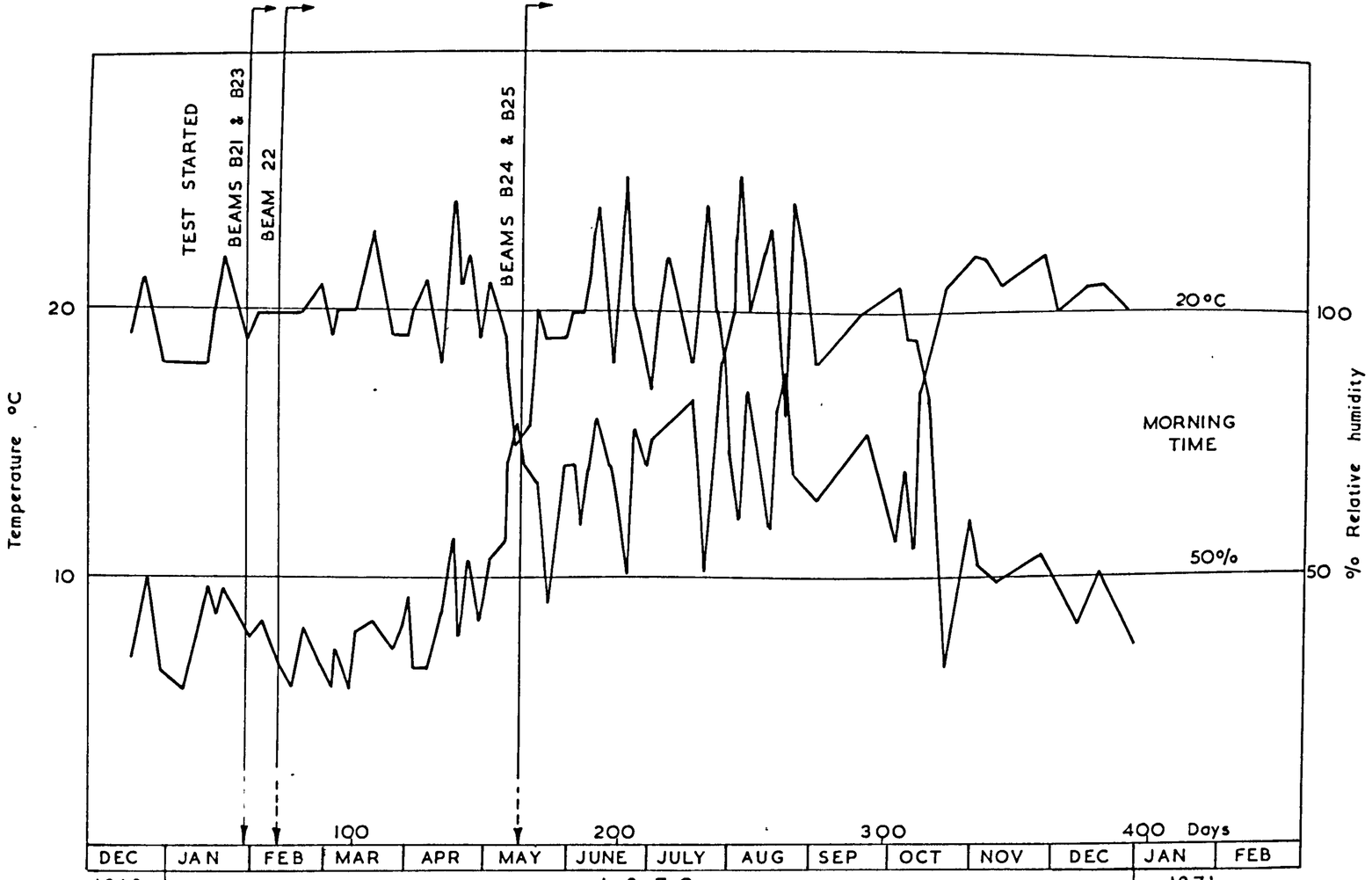

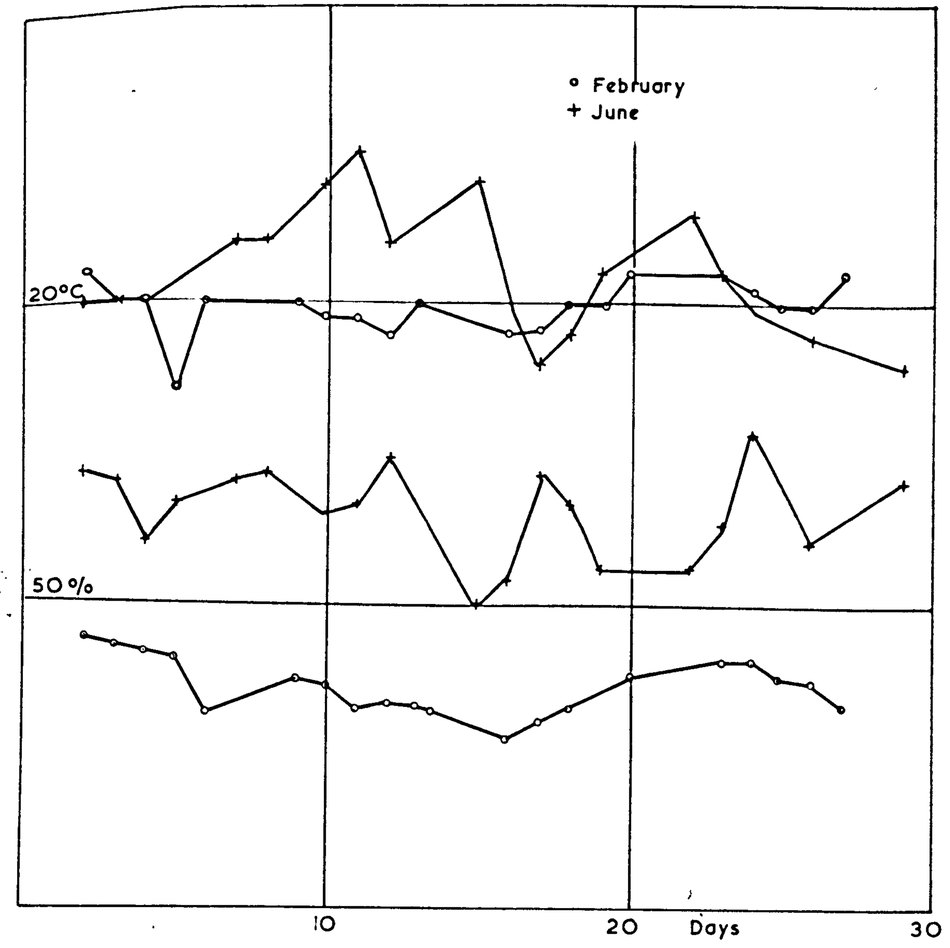

FIG (10) VARIATION OF TEMPERATURE AND RELATIVE HUMIDITY WITH TIME.

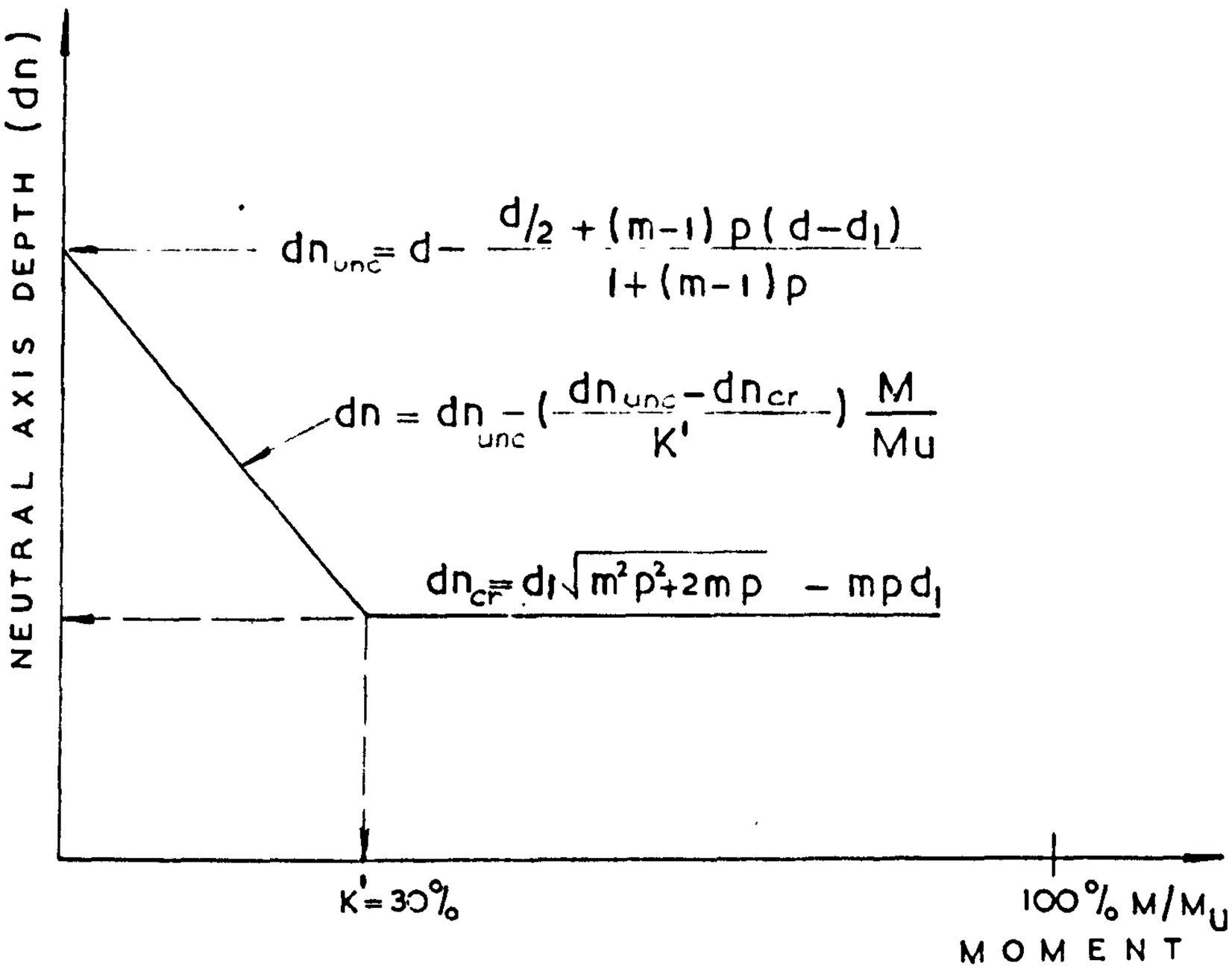

FIG.(11) BILINEAR RELATIONSHIP BETWEEN NEUTRAL AXIS DEPTH & MOMENT

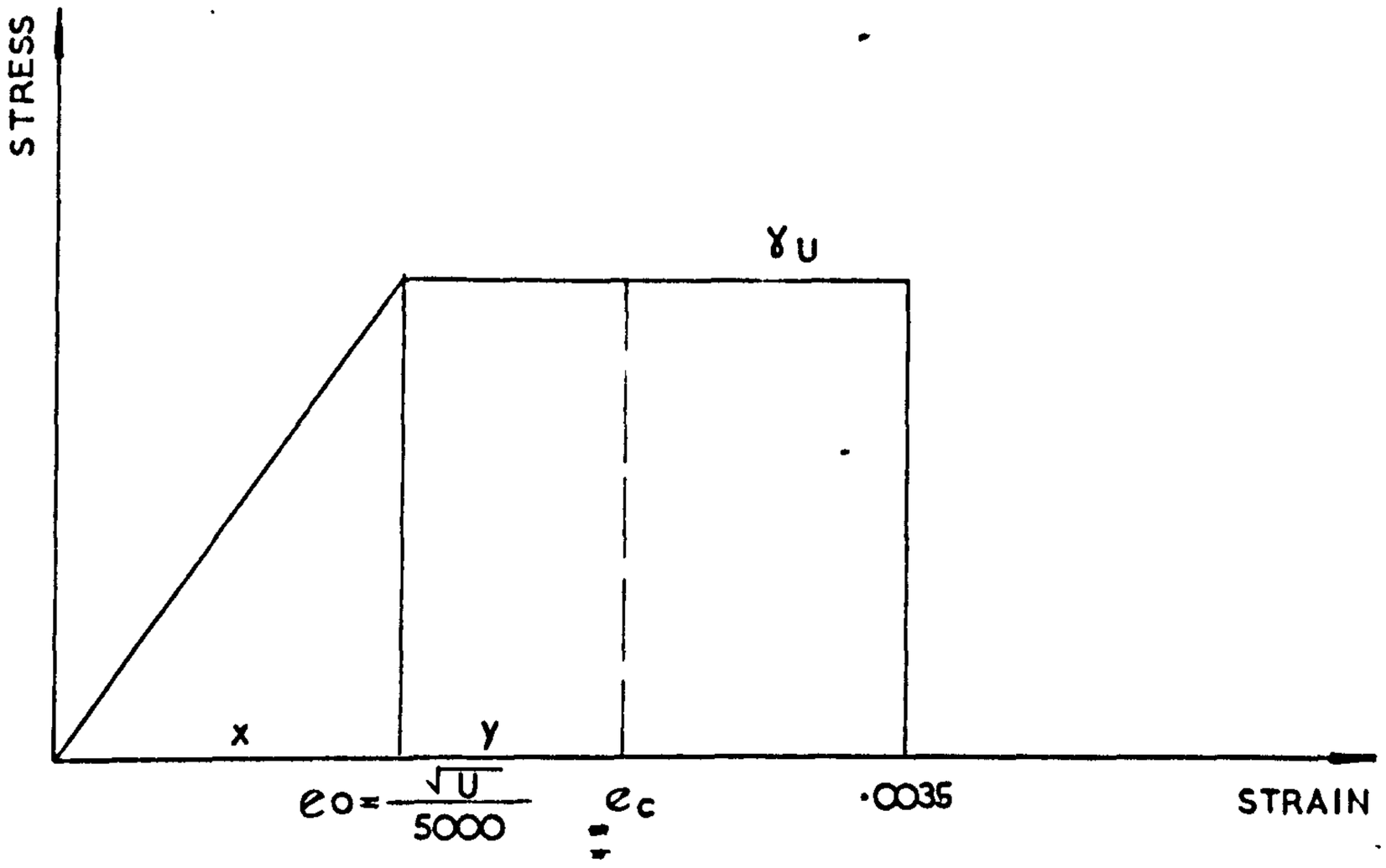

FIG.(12) DESIGN STRESS CURVE FOR CONCRETE

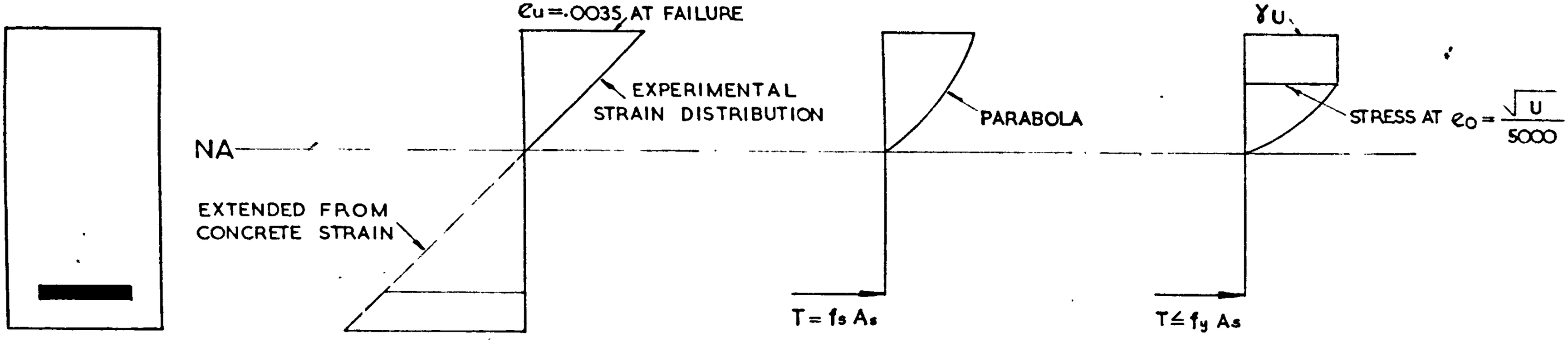

(a) BEAM SECTION (b) STRAIN DISTRIBUTION (c) STRESS DISTRIBUTION AT WORKING LOAD (d) STRESS DISTRIBUTION BEAM APPROACHING FAILURE

FIG (13) CALCULATION OF STRESSES (USING EXPERIMENTAL CONCRETE STRAIN MEASUREMENT)
STATIC LOAD

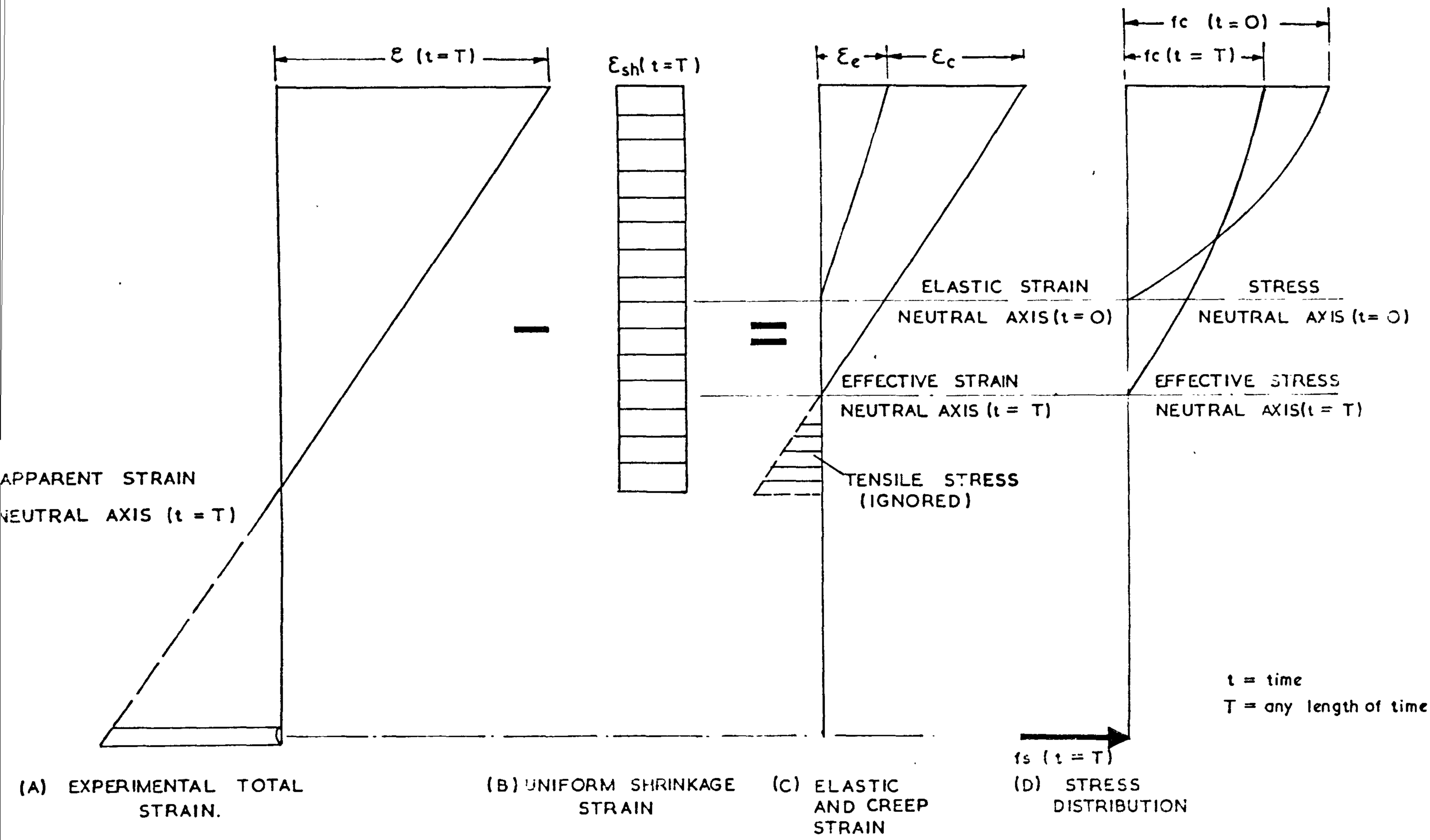

FIG. (14) CALCULATION OF STRESS (USING EXPERIMENTAL STRAIN) SUSTAINED AND REPEATED LOADS.

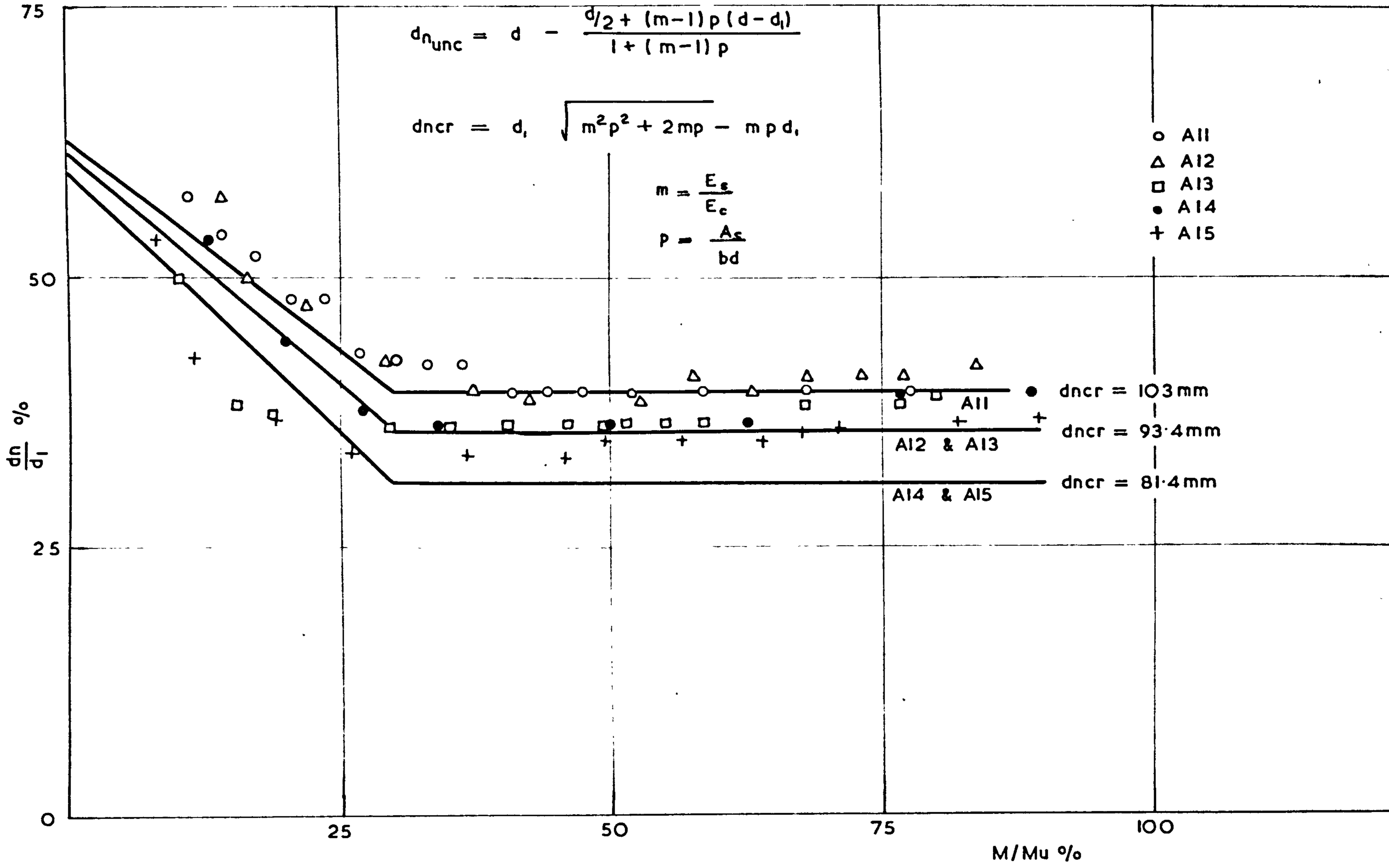

FIG. (15) VARIATION OF THE NEUTRAL AXIS DEPTH WITH MOMENT (STATIC LOAD)

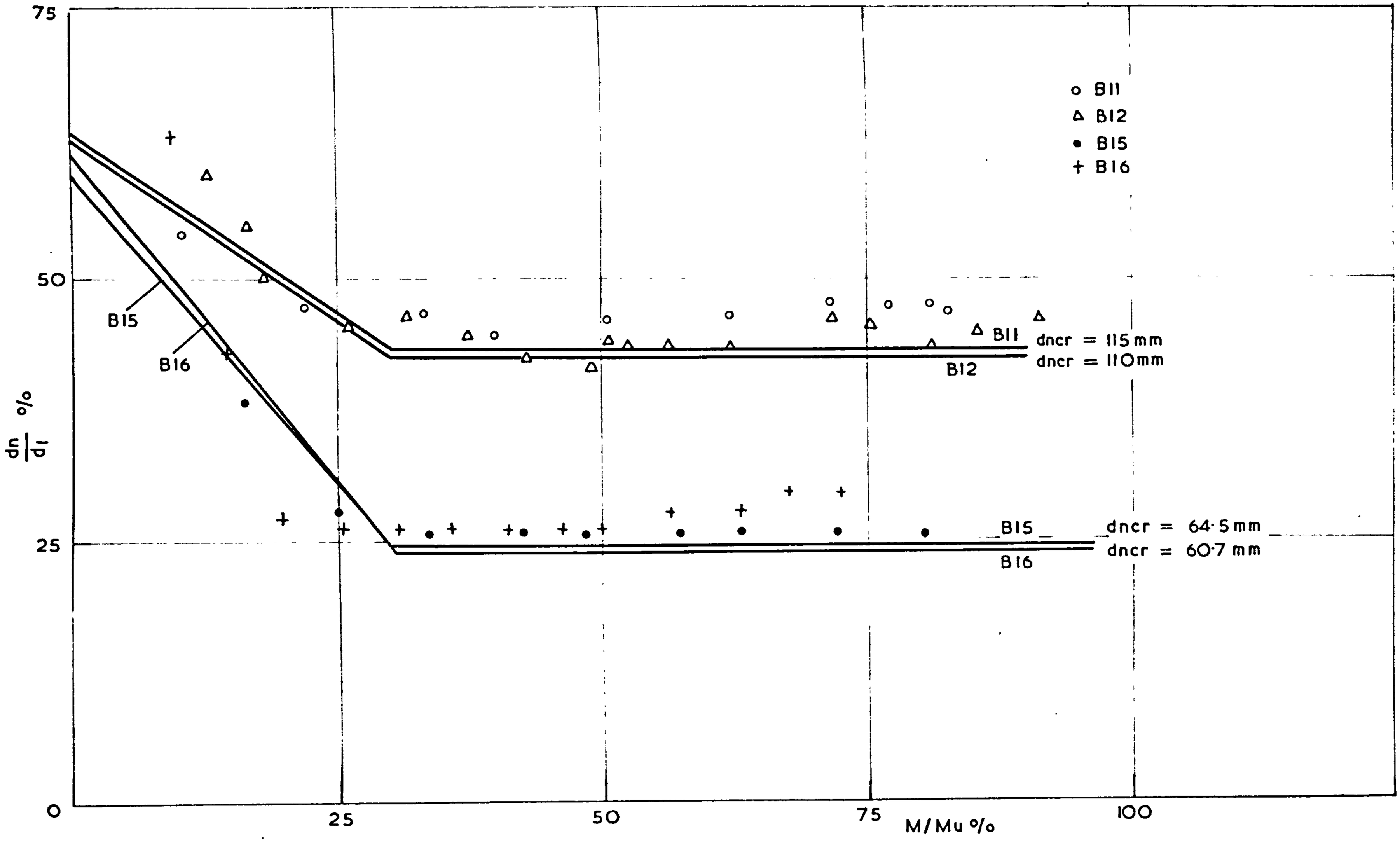

FIG. (16) VARIATION OF THE NEUTRAL AXIS DEPTH WITH MOMENT (STATIC LOAD)

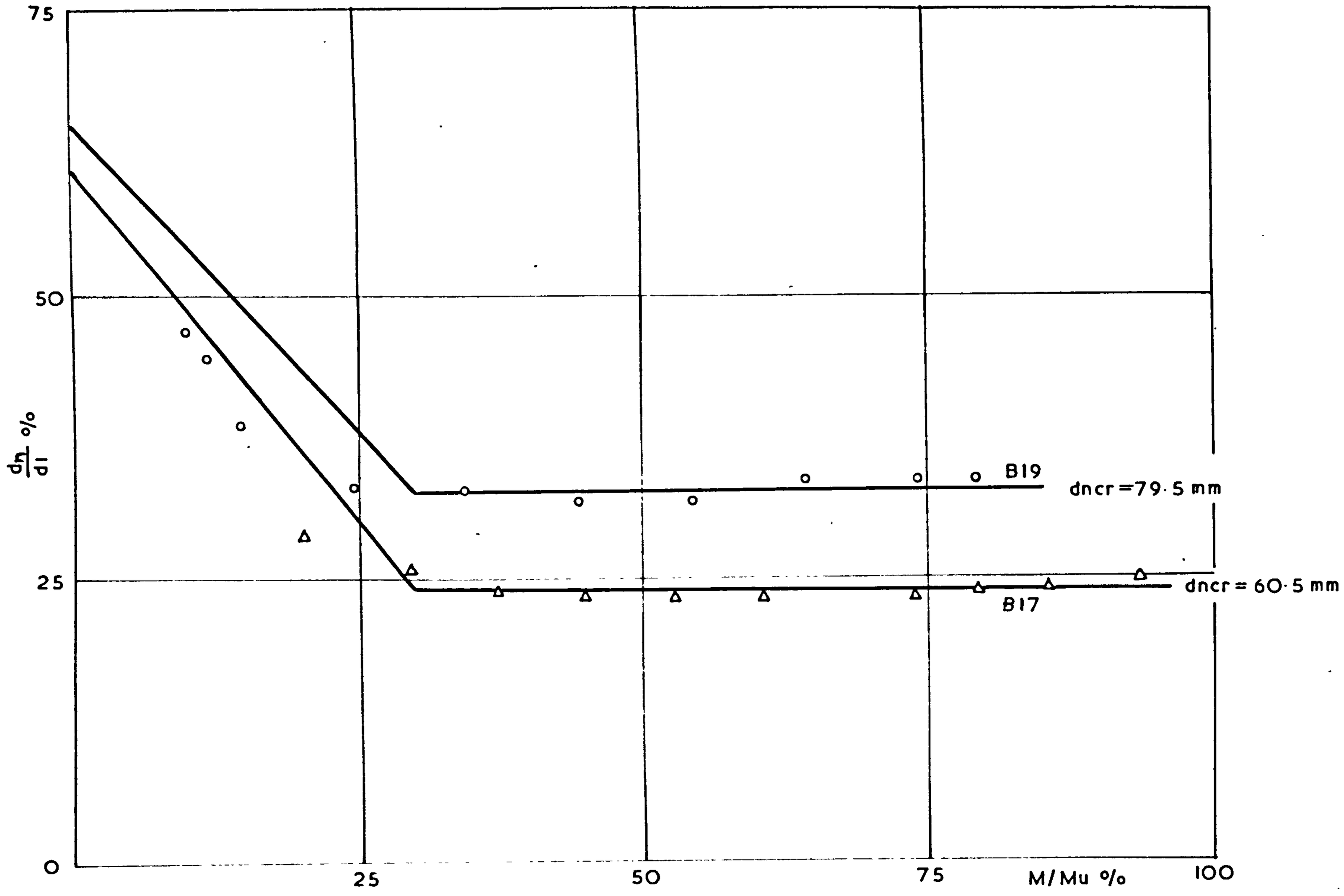

FIG. (17) VARIATION OF THE NEUTRAL AXIS DEPTH WITH MOMENT (STATIC LOAD)

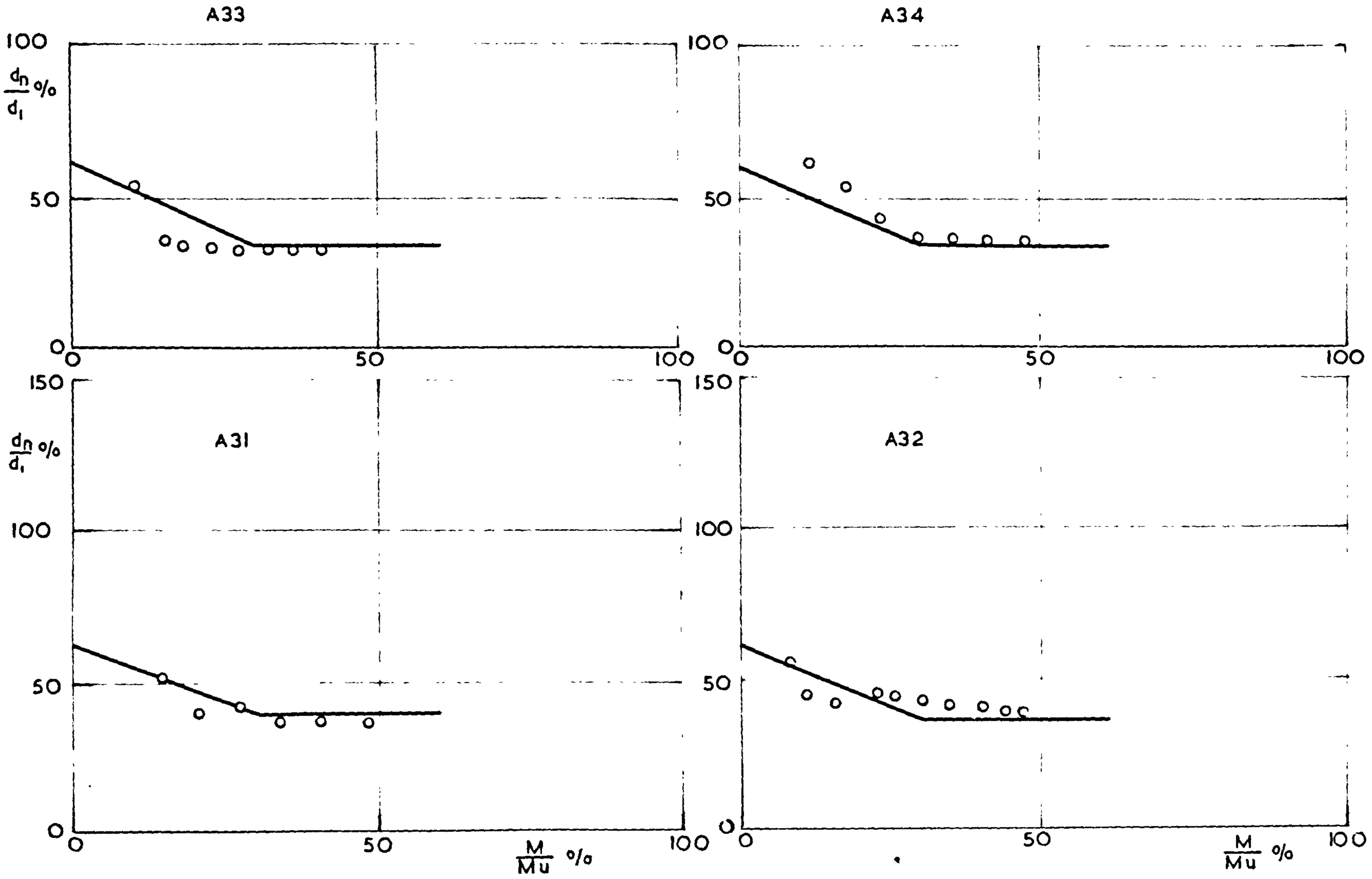

FIG. (18) VARIATION OF NEUTRAL AXIS DEPTH WITH MOMENT (STATIC LOAD)

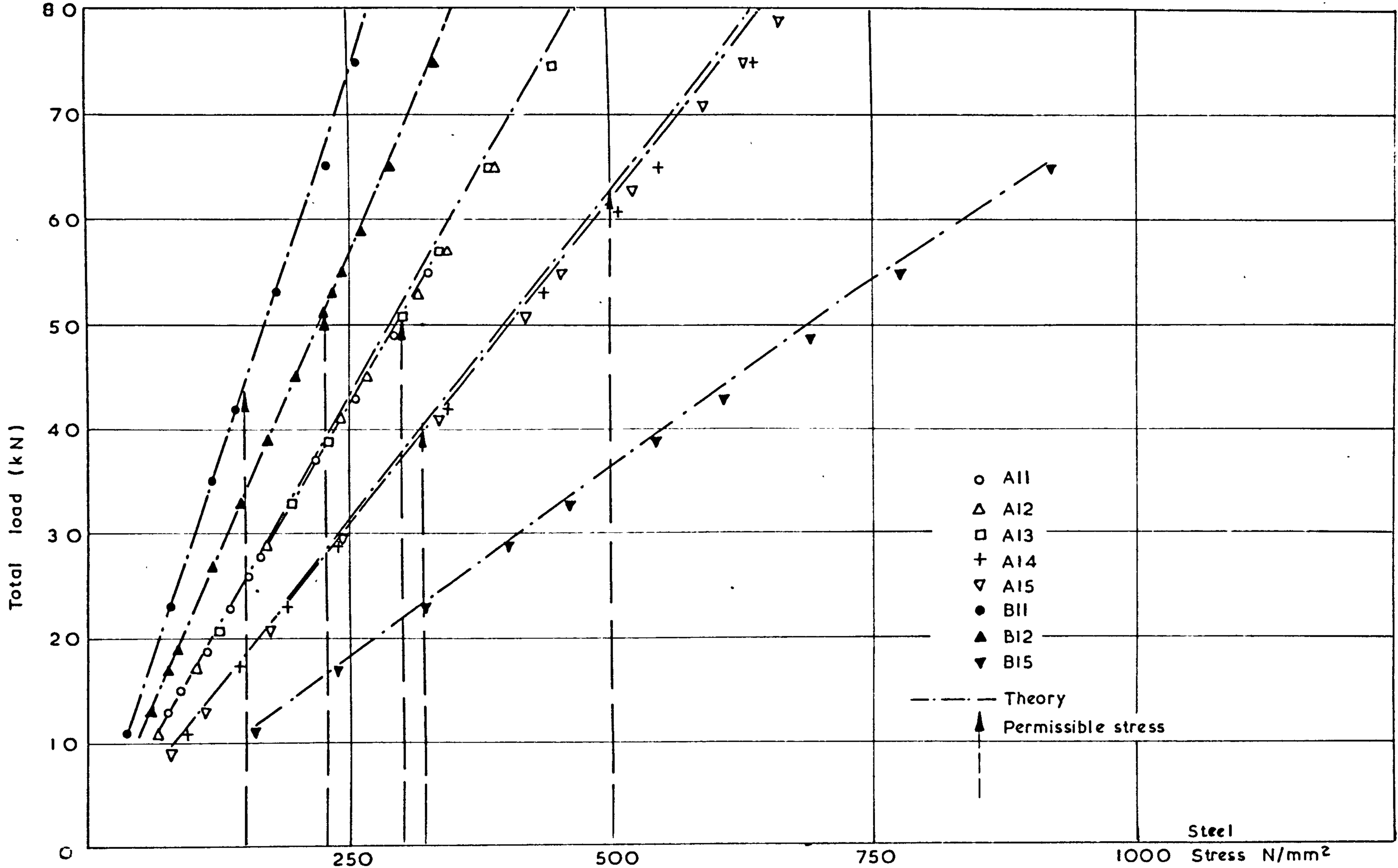

FIG. (19) LOAD – STRESS CURVES (STATIC LOAD) PLAIN AND DEFORMED BARS

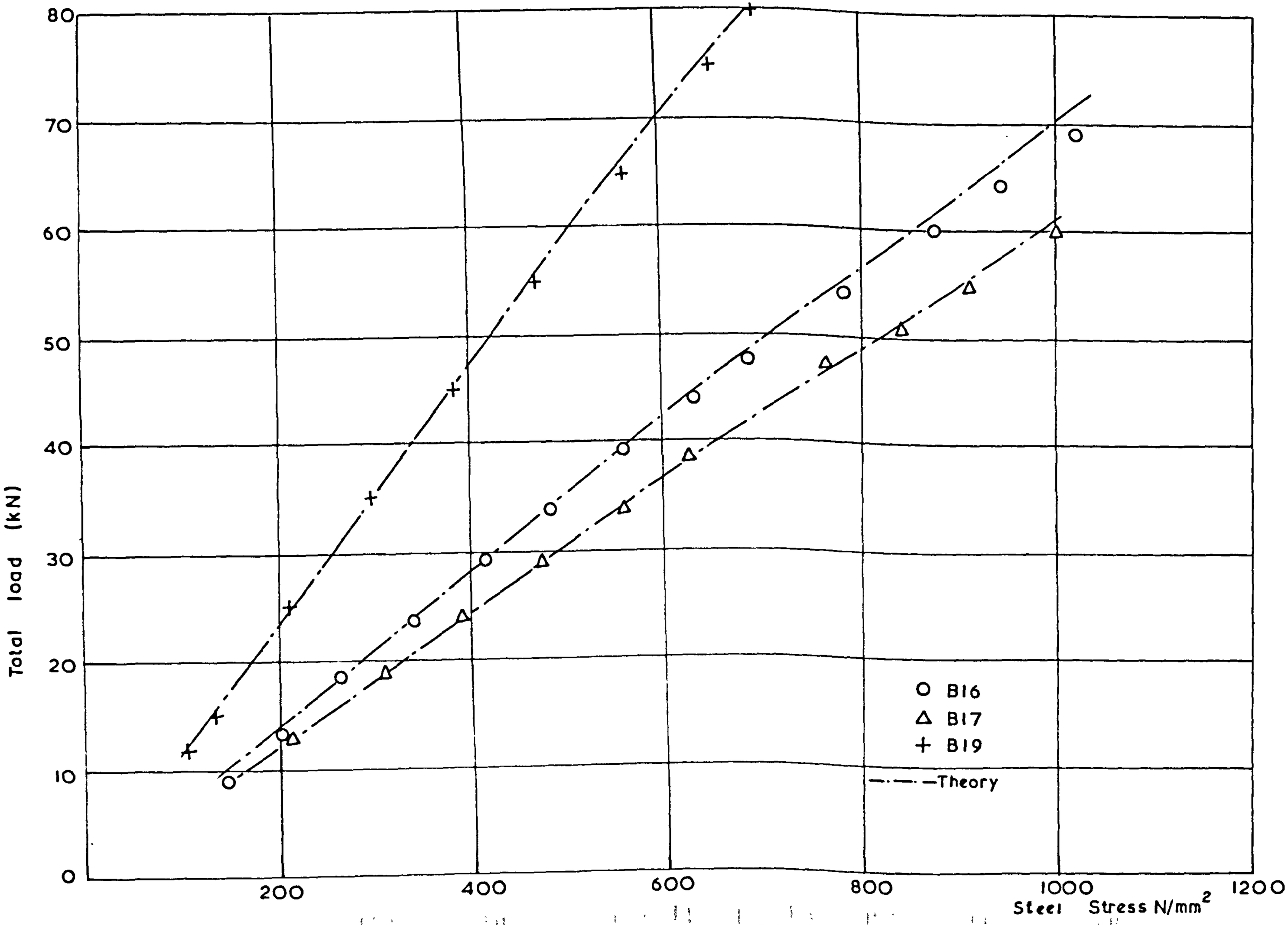

FIG. (20.) LOAD-STRESS CURVES (STATIC LOAD) WIRES AND STRANDS.

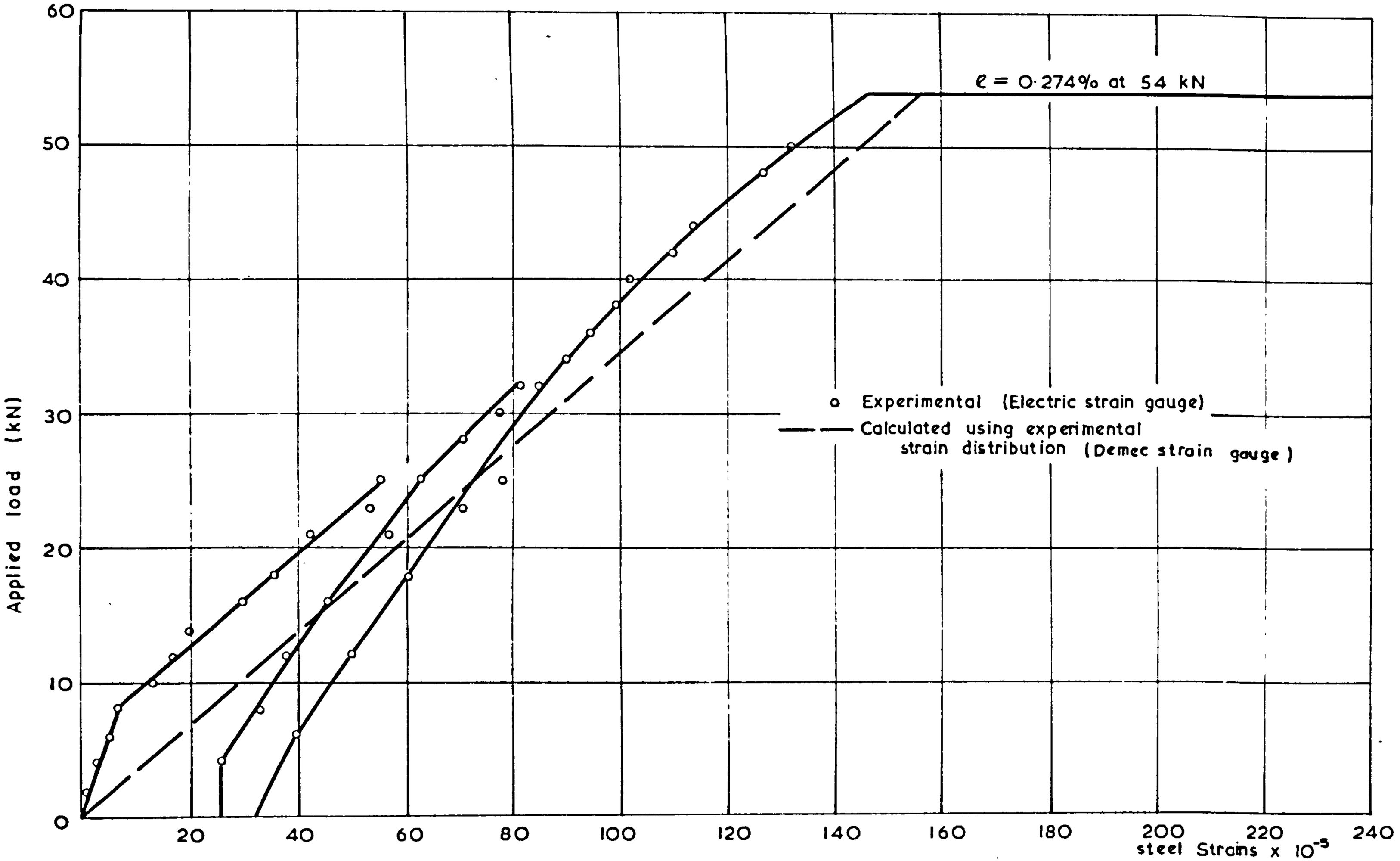

FIG. (21) LOAD — STRAIN CURVES. (STATIC LOAD.) BEAM AII

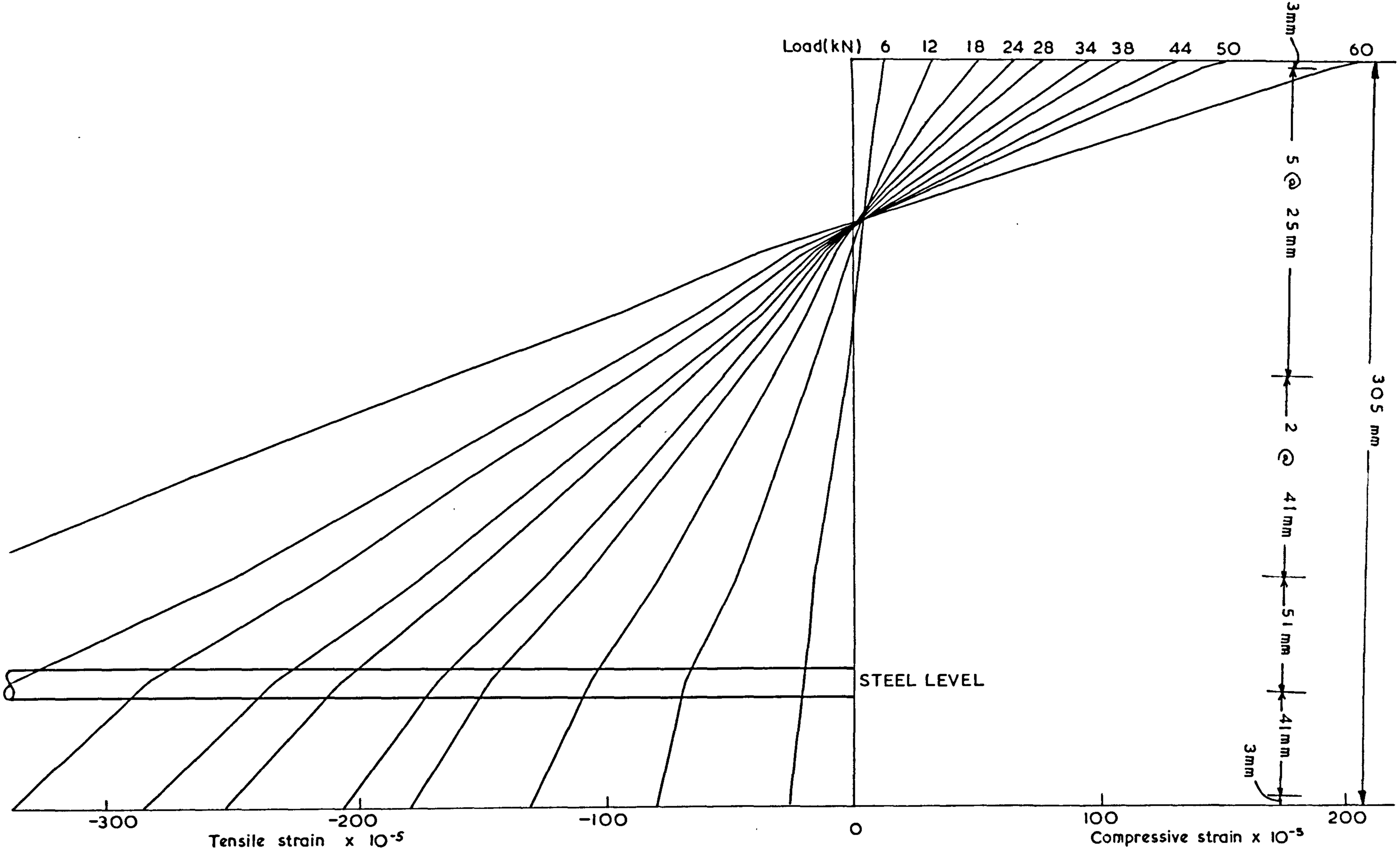

FIG. (22) TYPICAL STRAIN DISTRIBUTION (STATIC LOAD) BEAM B15

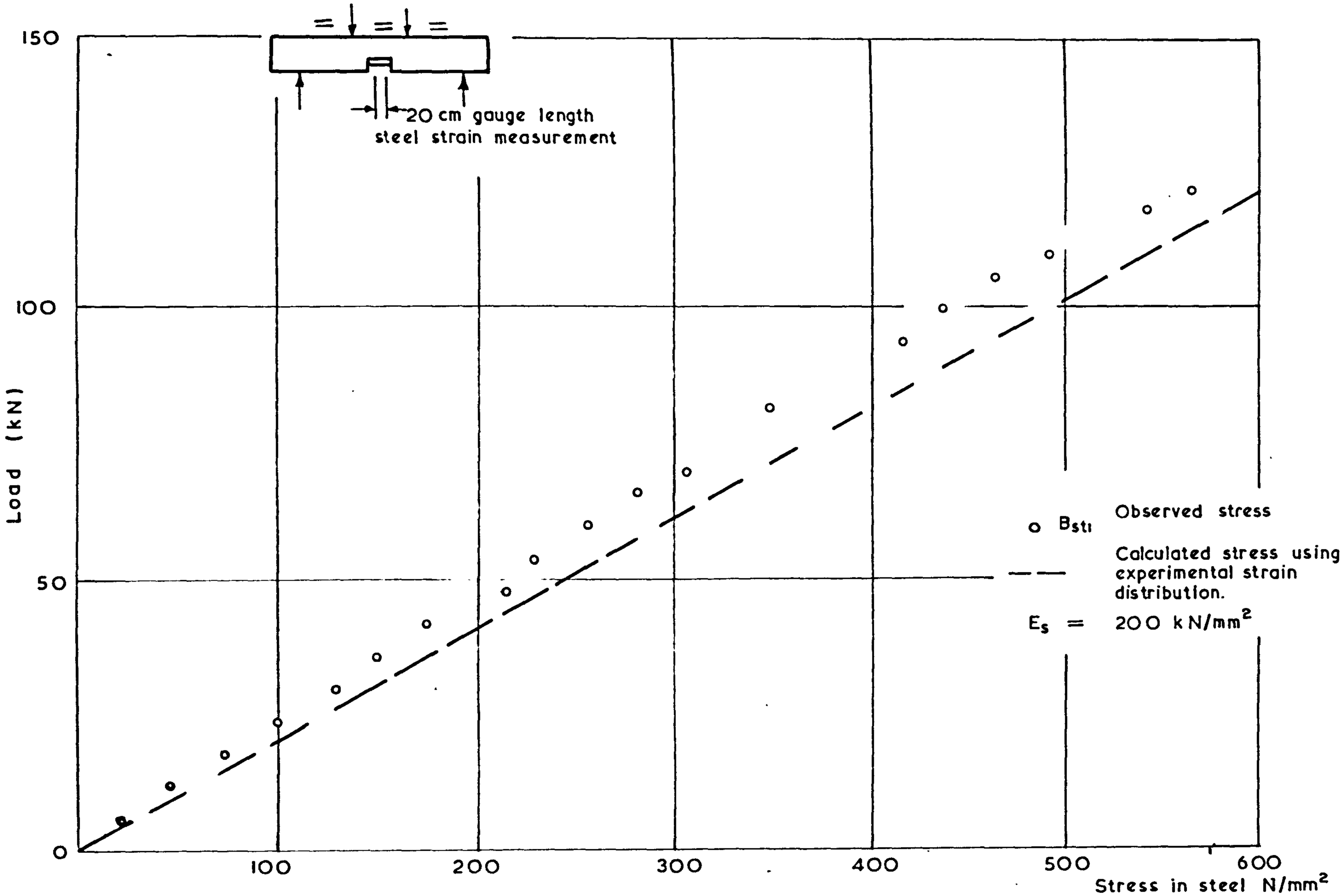

FIG. (23) LOAD–STRESS CURVE FOR "EXPOSED STEEL" BEAM

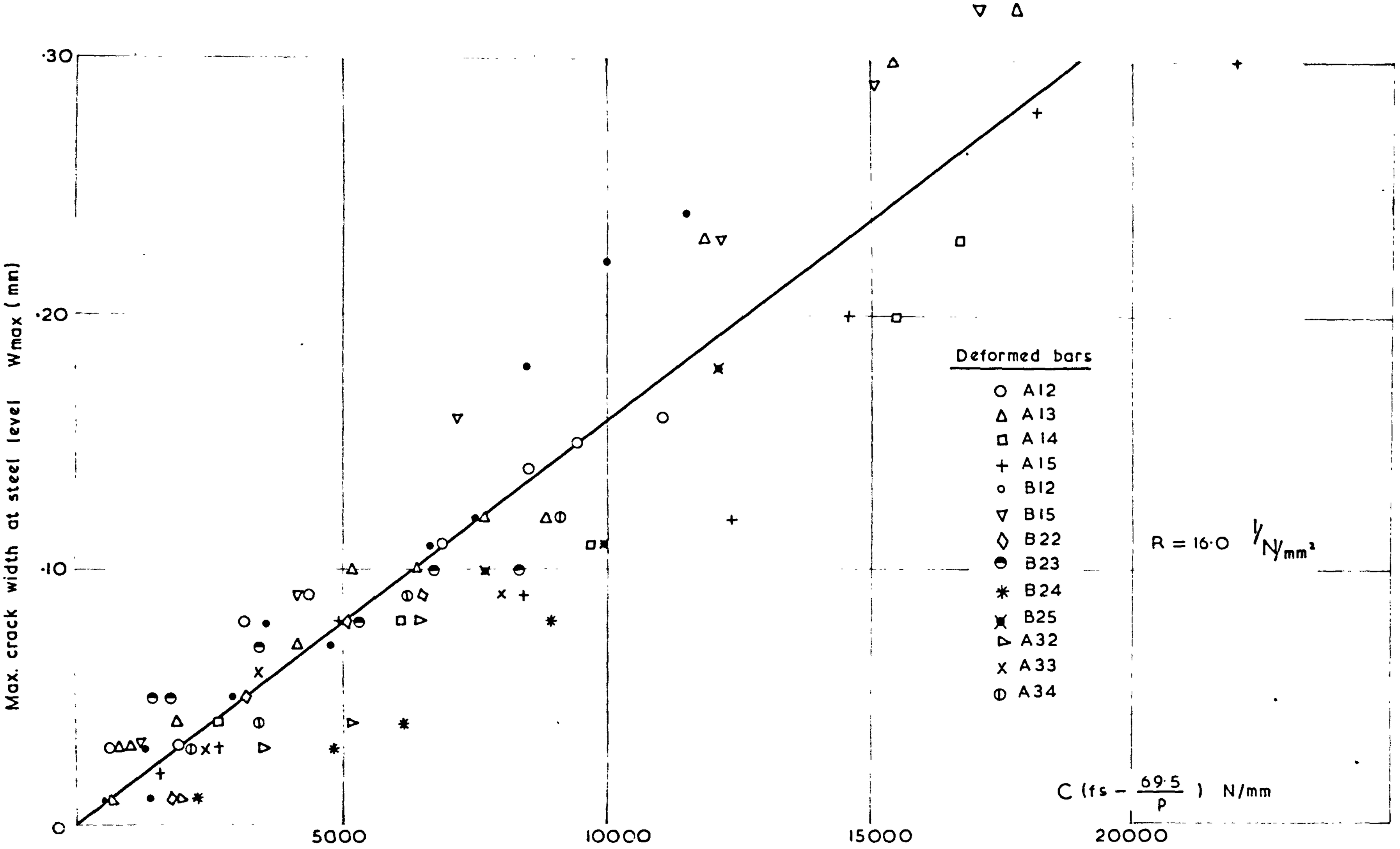

FIG. (24) CRACK WIDTH FORMULA (VIRGIN CYCLES)

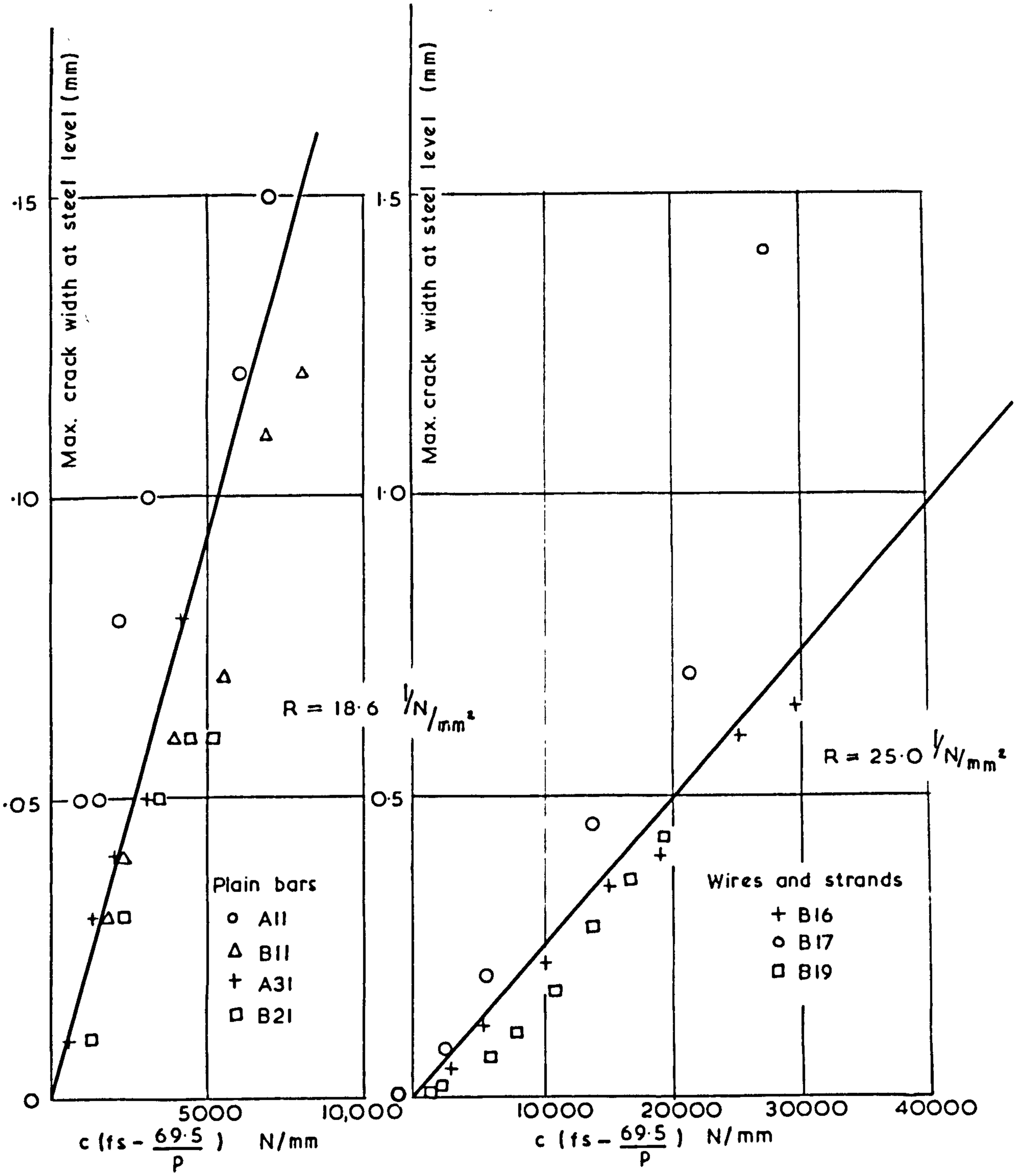

FIG (25) CRACK WIDTH 'FORMULA (VIRGIN CYCLES)

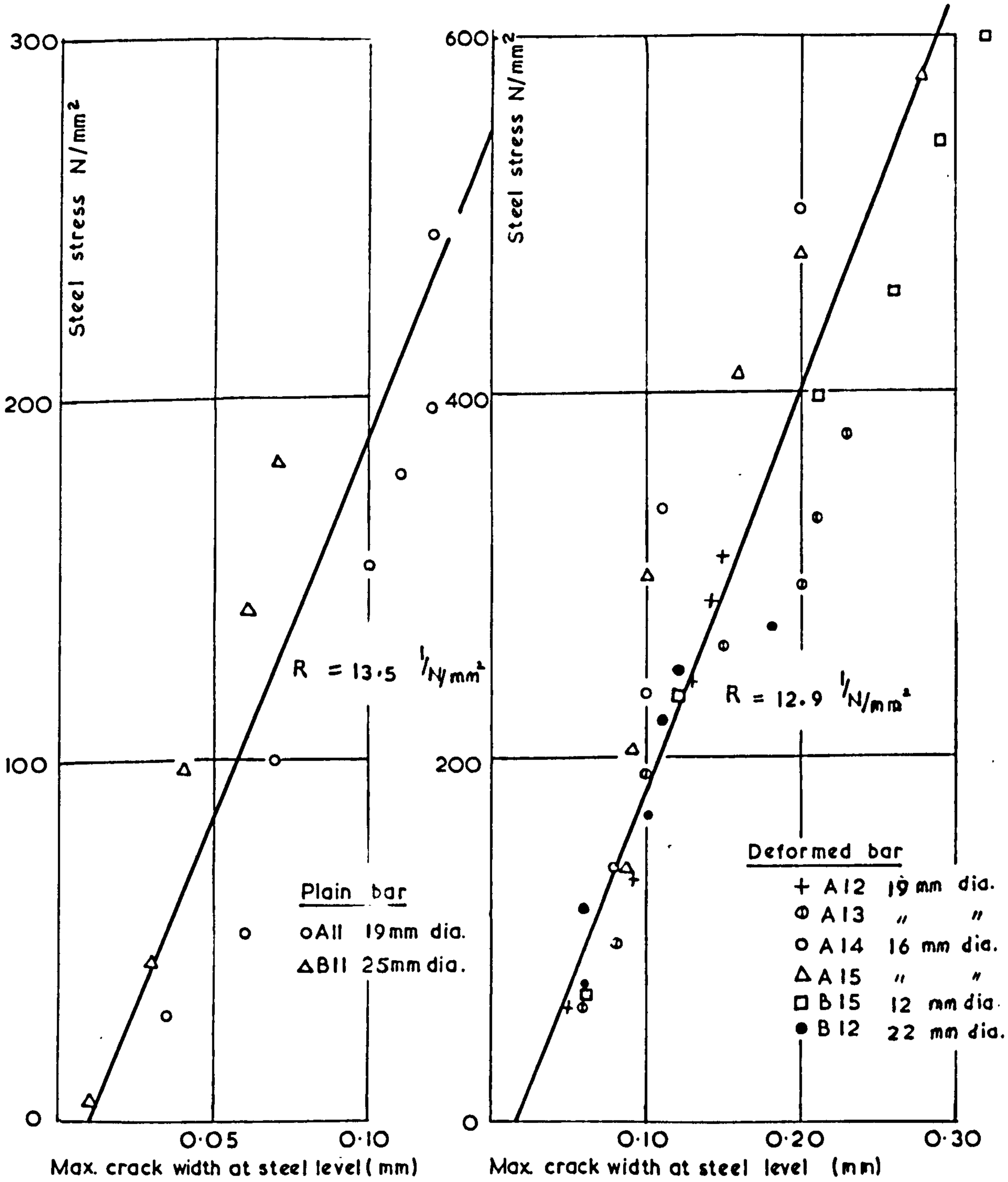

FIG.(26) STEEL STRESS — CRACK WIDTH RELATIONSHIP
(STATIC LOAD — SECOND CYCLE.)

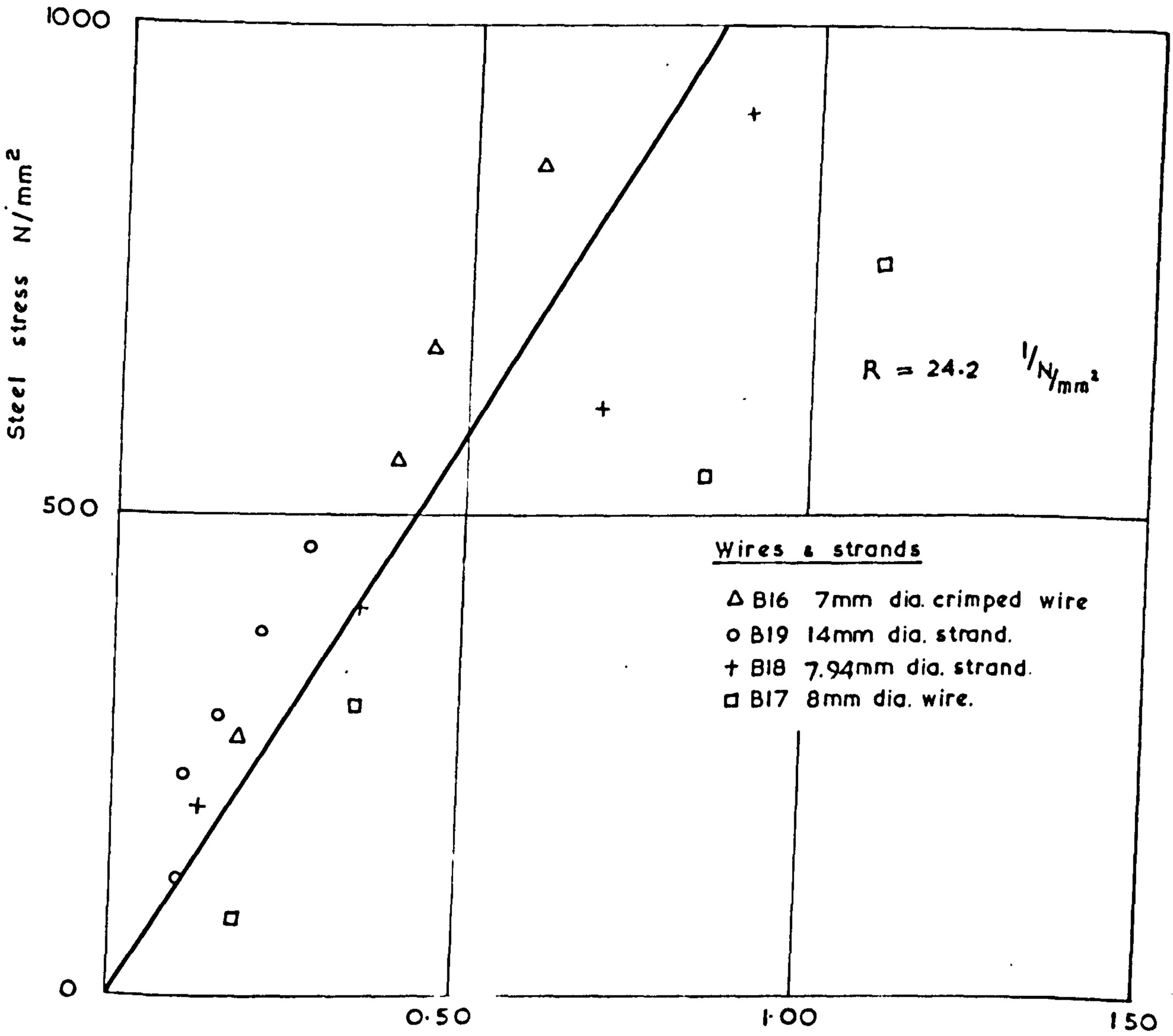

FIG. (27) STEEL STRESS — CRACK WIDTH RELATIONSHIP
(STATIC LOAD — SECOND CYCLE.)

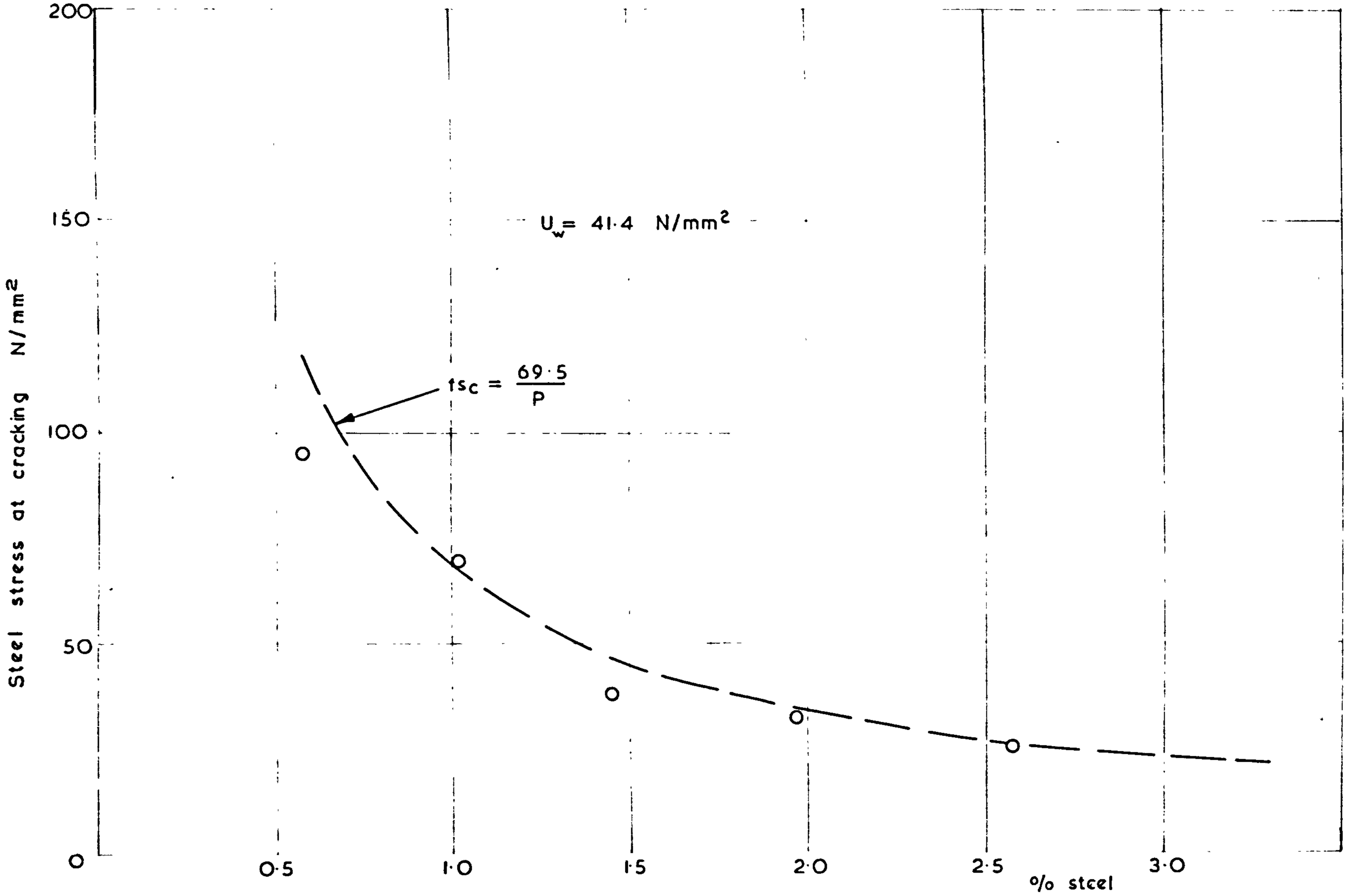

FIG(28) STEEL STRESS – PERCENTAGE STEEL RELATIONSHIP

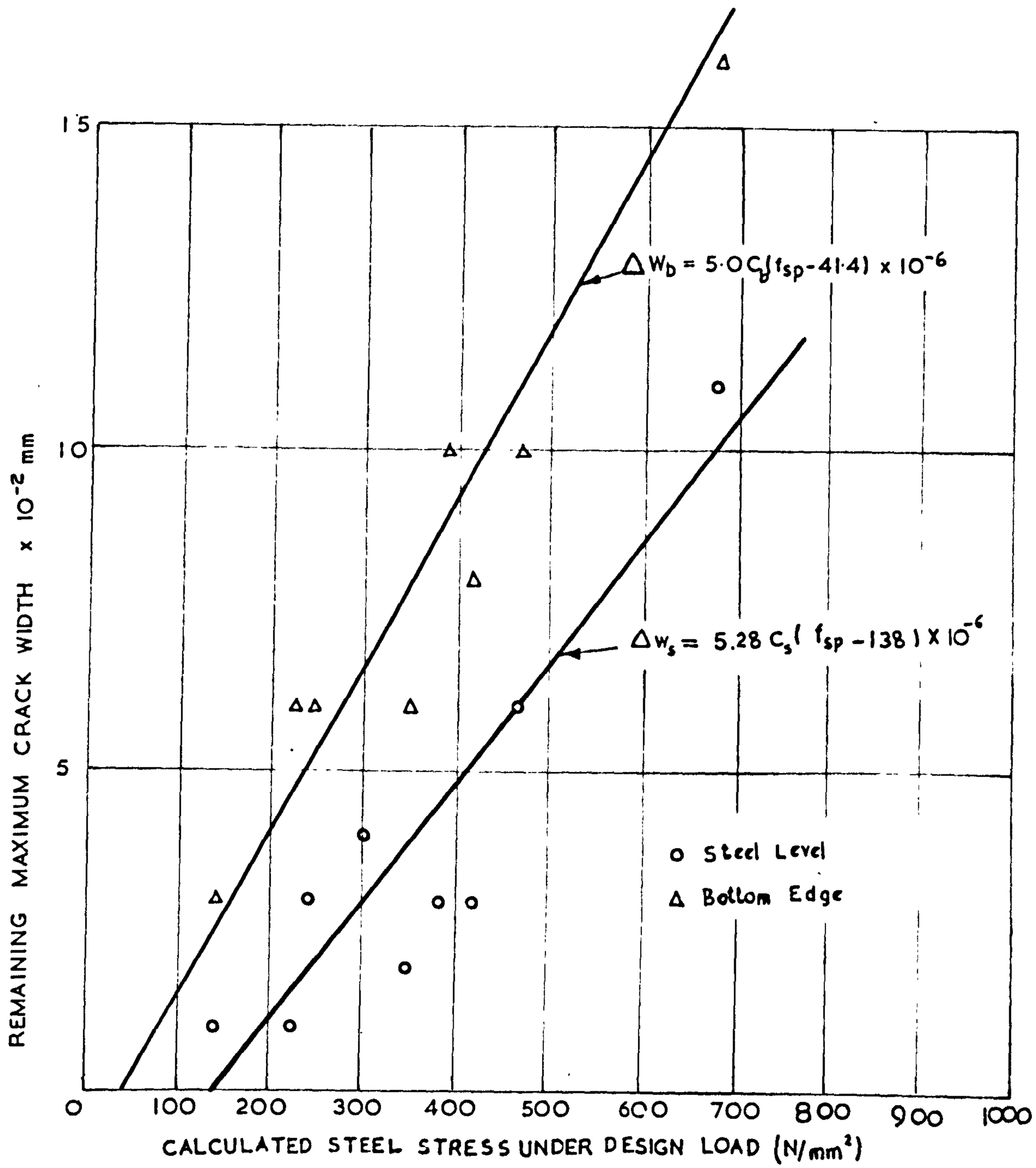

FIG.(29) STEEL STRESS – REMAINING CRACK WIDTH RELATIONSHIP (STATIC LOAD)

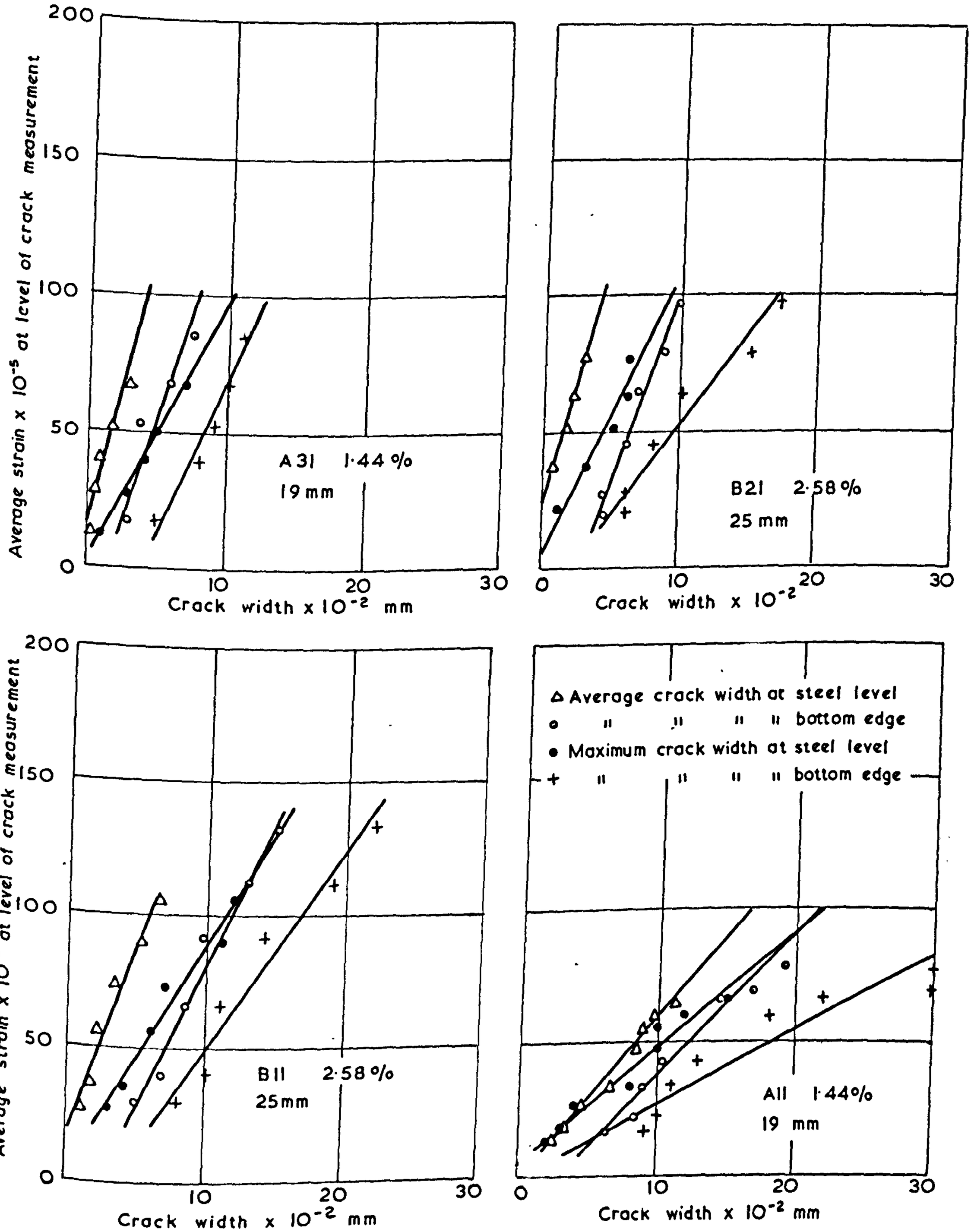

FIG.(30) AVERAGE CONCRETE STRAIN V.S. CRACK WIDTH (STATIC LOAD) PLAIN M.S. BAR.

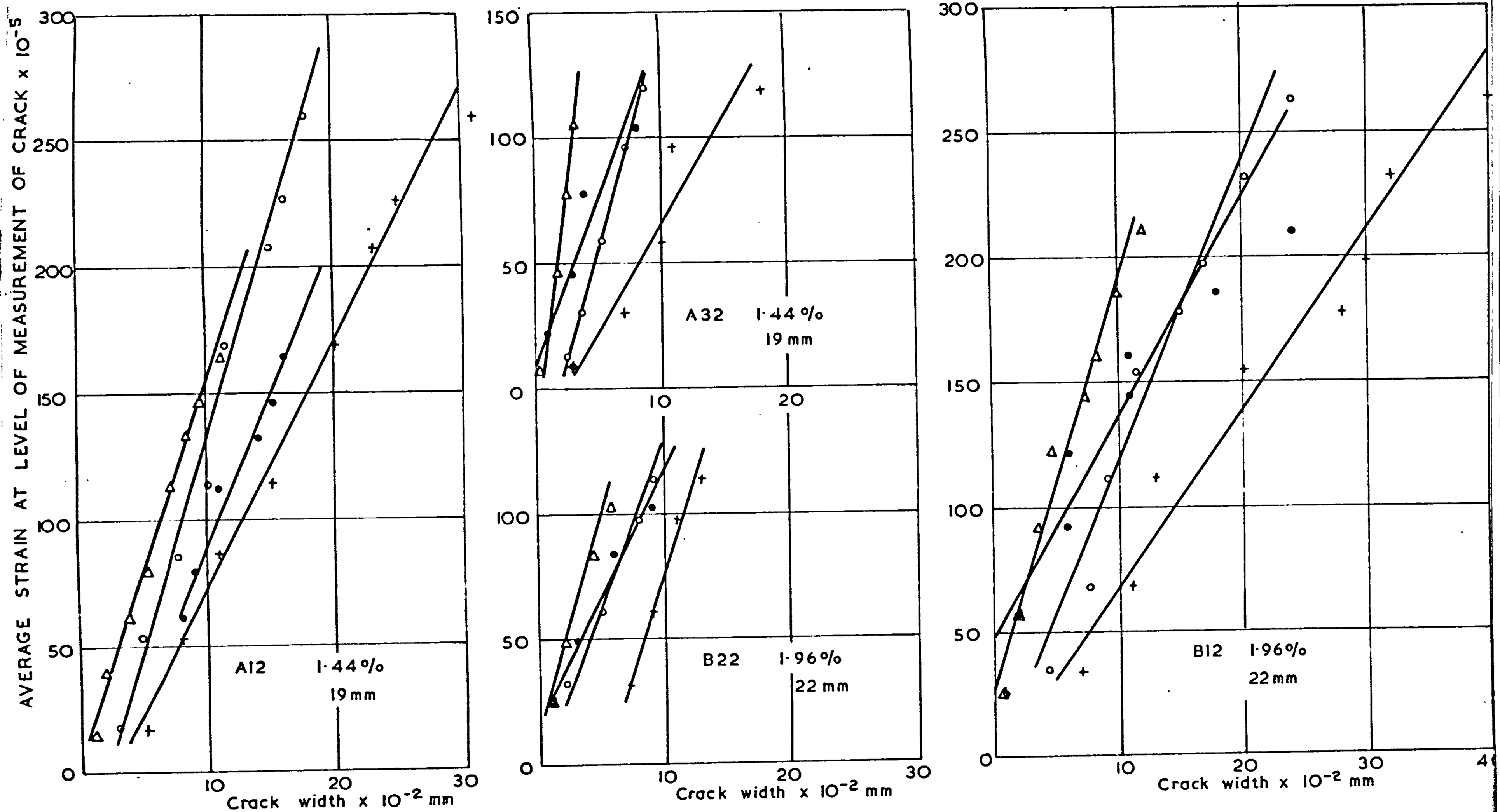

FIG. (31) AVERAGE CONCRETE STRAIN V.S. CRACK WIDTH (STATIC LOAD) DEFORMED H.T.S. BAR.

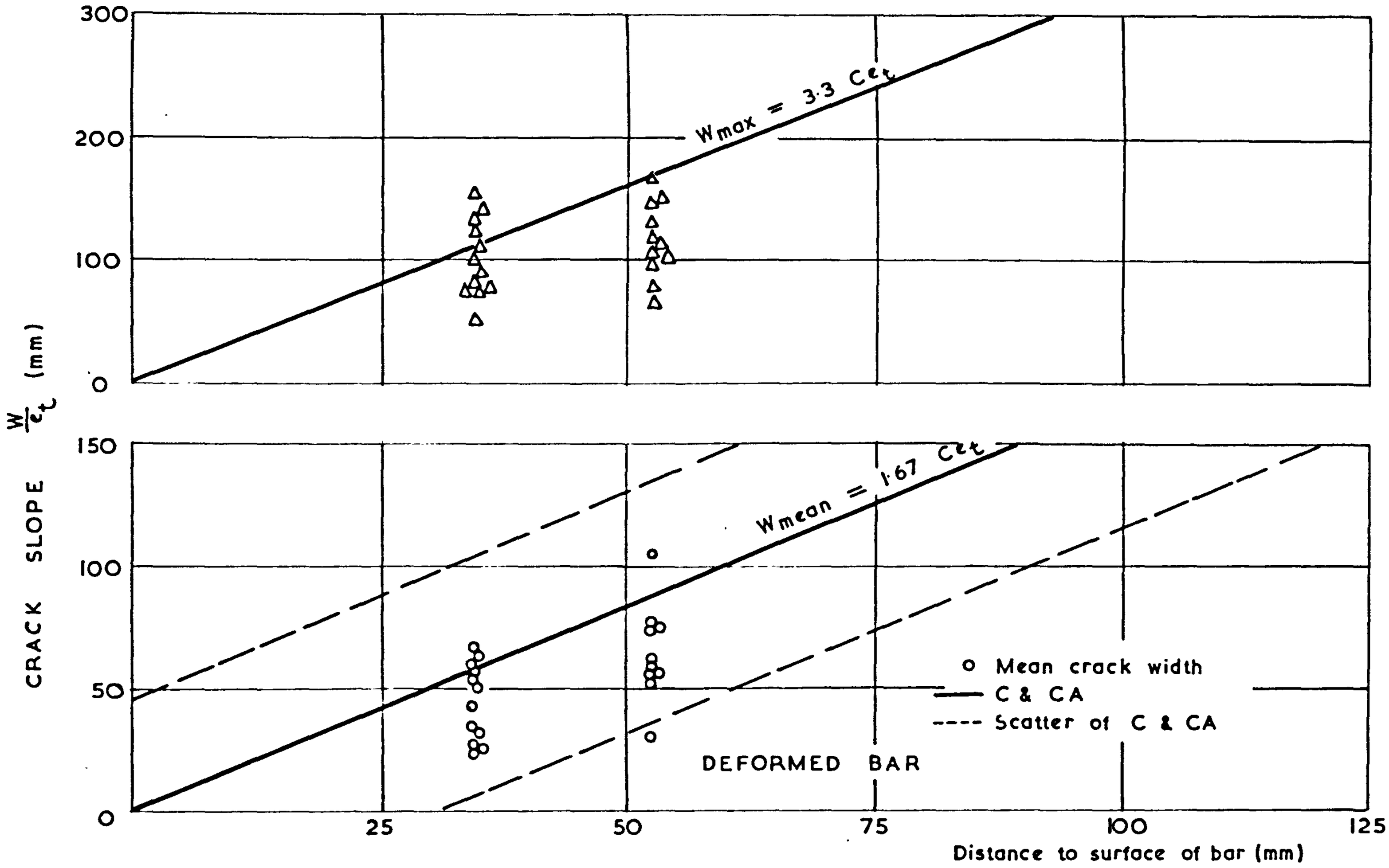

FIG. (32) RELATIONSHIP BETWEEN CRACK SLOPE W/e_t AND DISTANCE TO SURFACE OF BAR (STATIC LOAD – FIRST CYCLE)

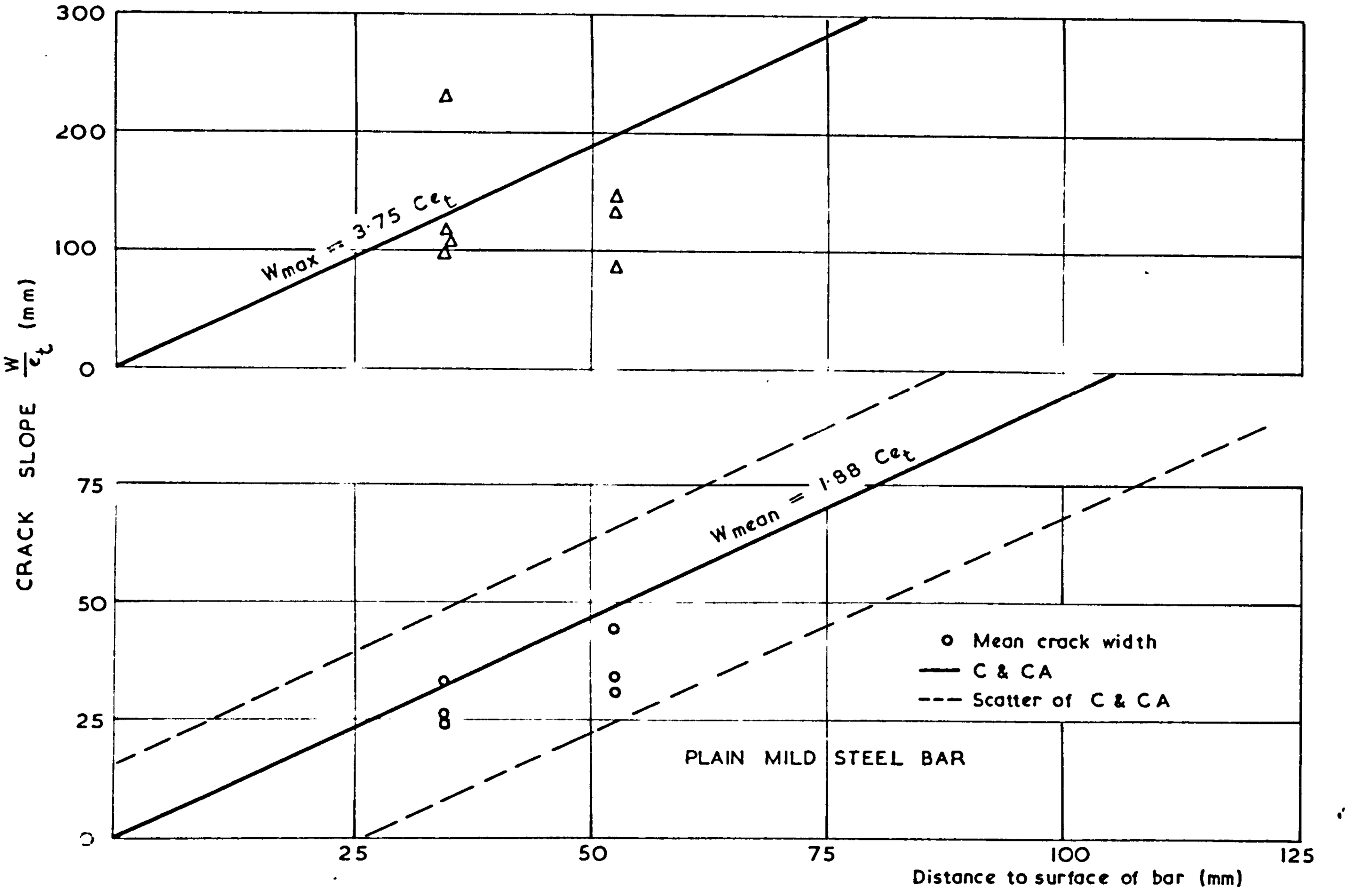

FIG. (33) RELATIONSHIP BETWEEN CRACK SLOPE W/e_t AND DISTANCE TO SURFACE OF BAR (STATIC LOAD - FIRST CYCLE.)

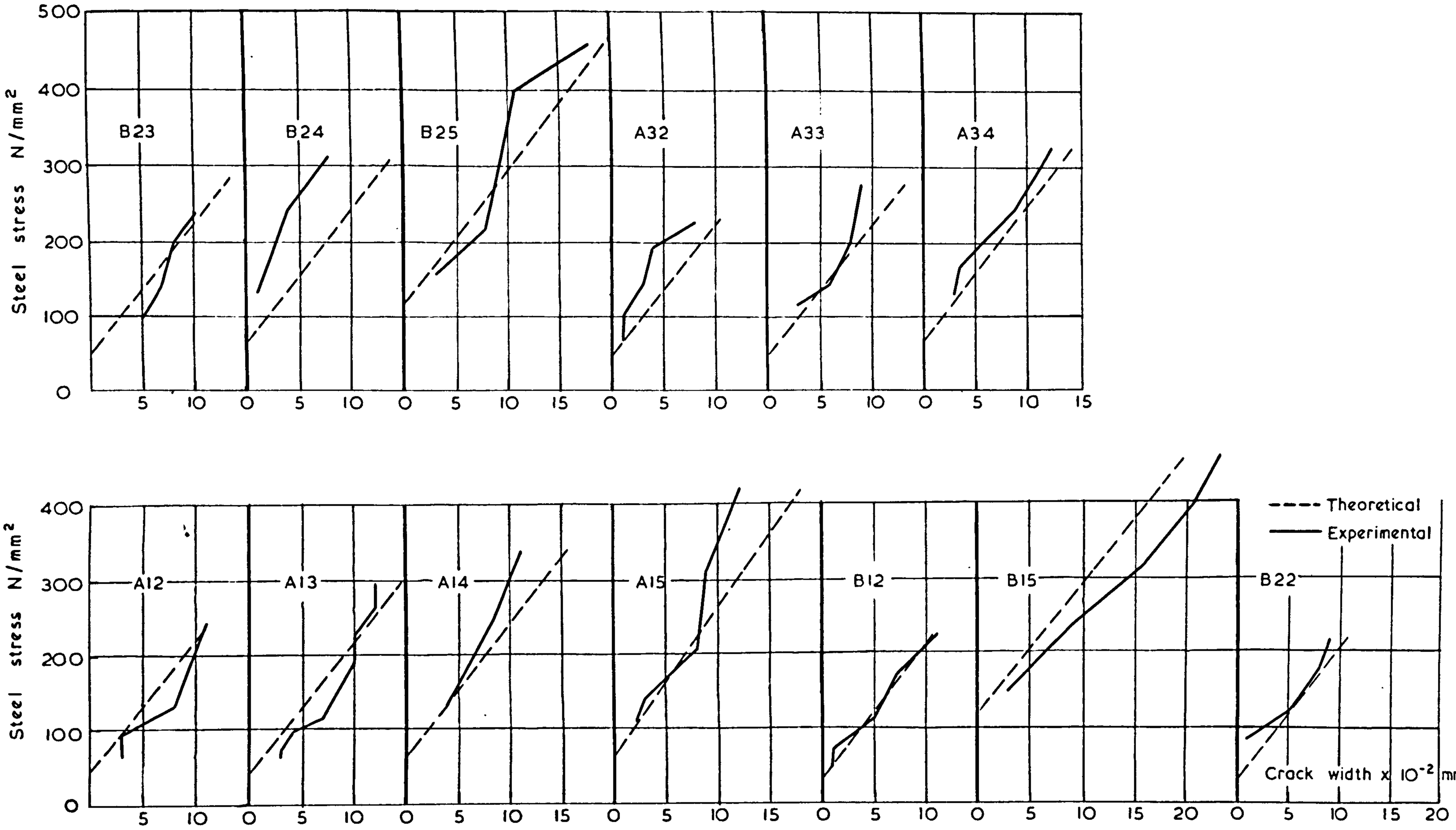

FIG. (34) STEEL STRESS - CRACK WIDTH RELATIONSHIP (STATIC LOAD - FIRST CYCLE) DEFORMED BARS

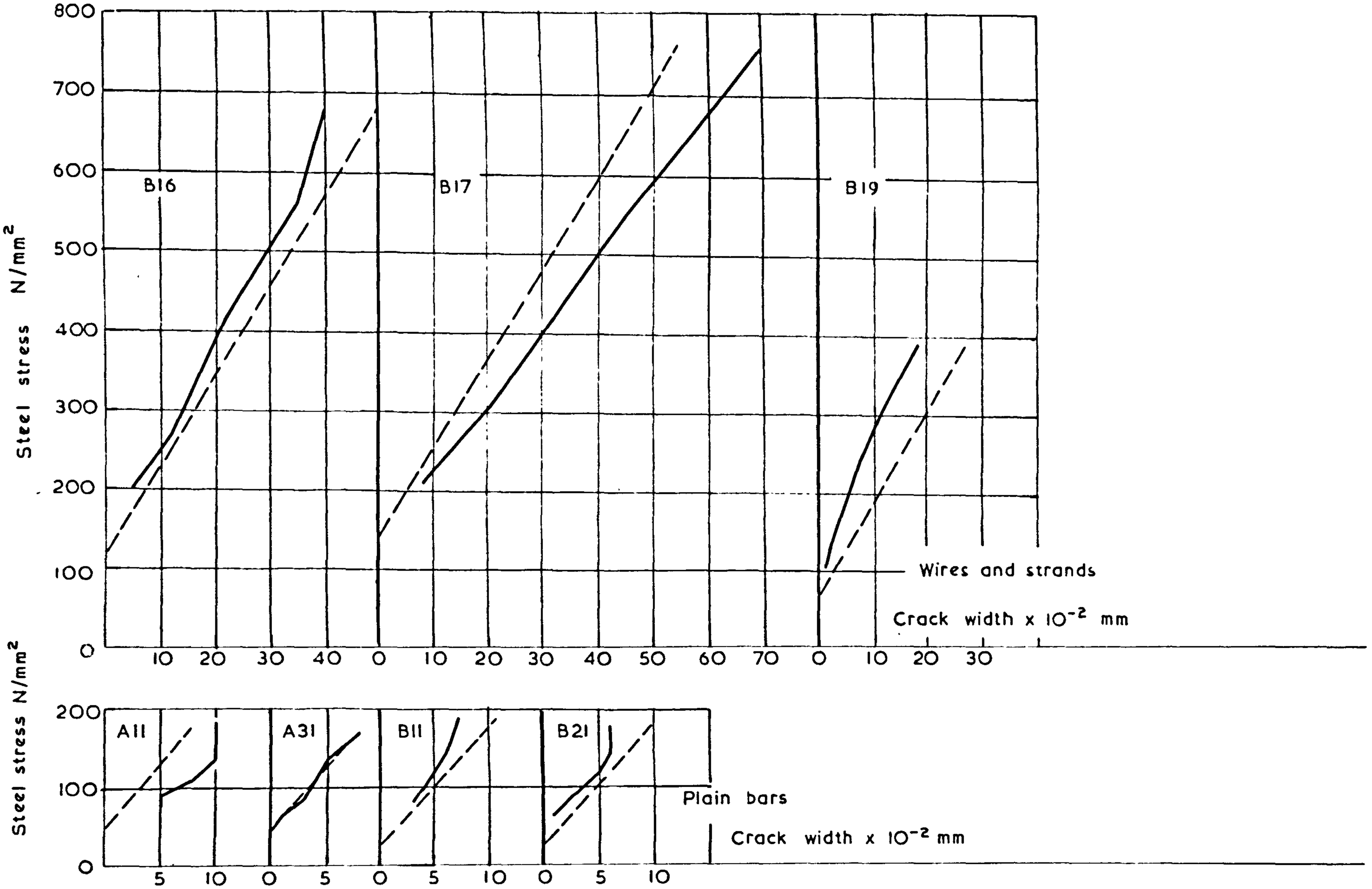

FIG. (35) STEEL STRESS – CRACK WIDTH RELATIONSHIP (STATIC LOAD – FIRST CYCLE) PLAIN BARS AND WIRES AND STRANDS.

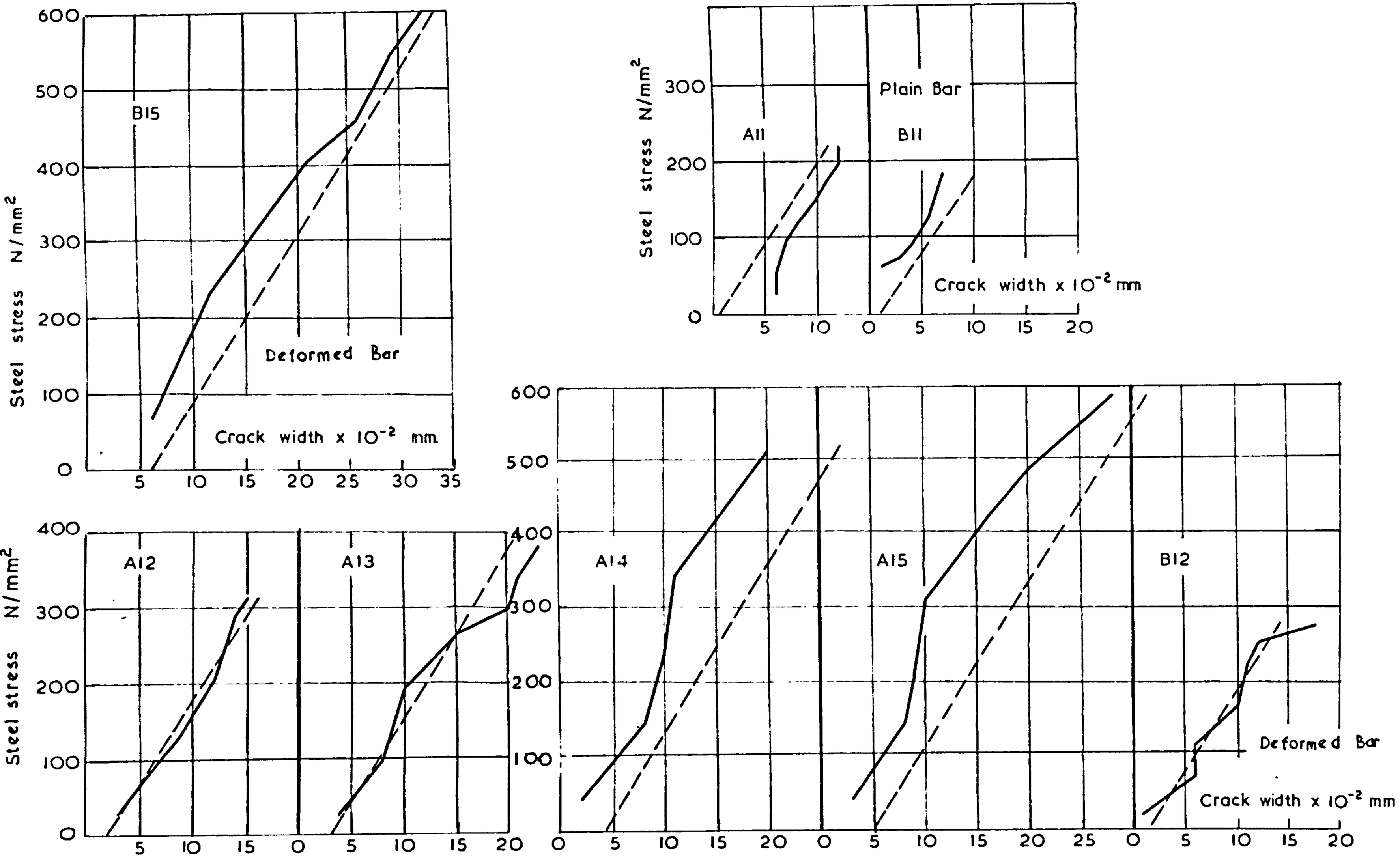

FIG.(36) STEEL STRESS – CRACK WIDTH RELATIONSHIP (STATIC LOAD – SECOND CYCLE) DEFORMED AND PLAIN BARS.

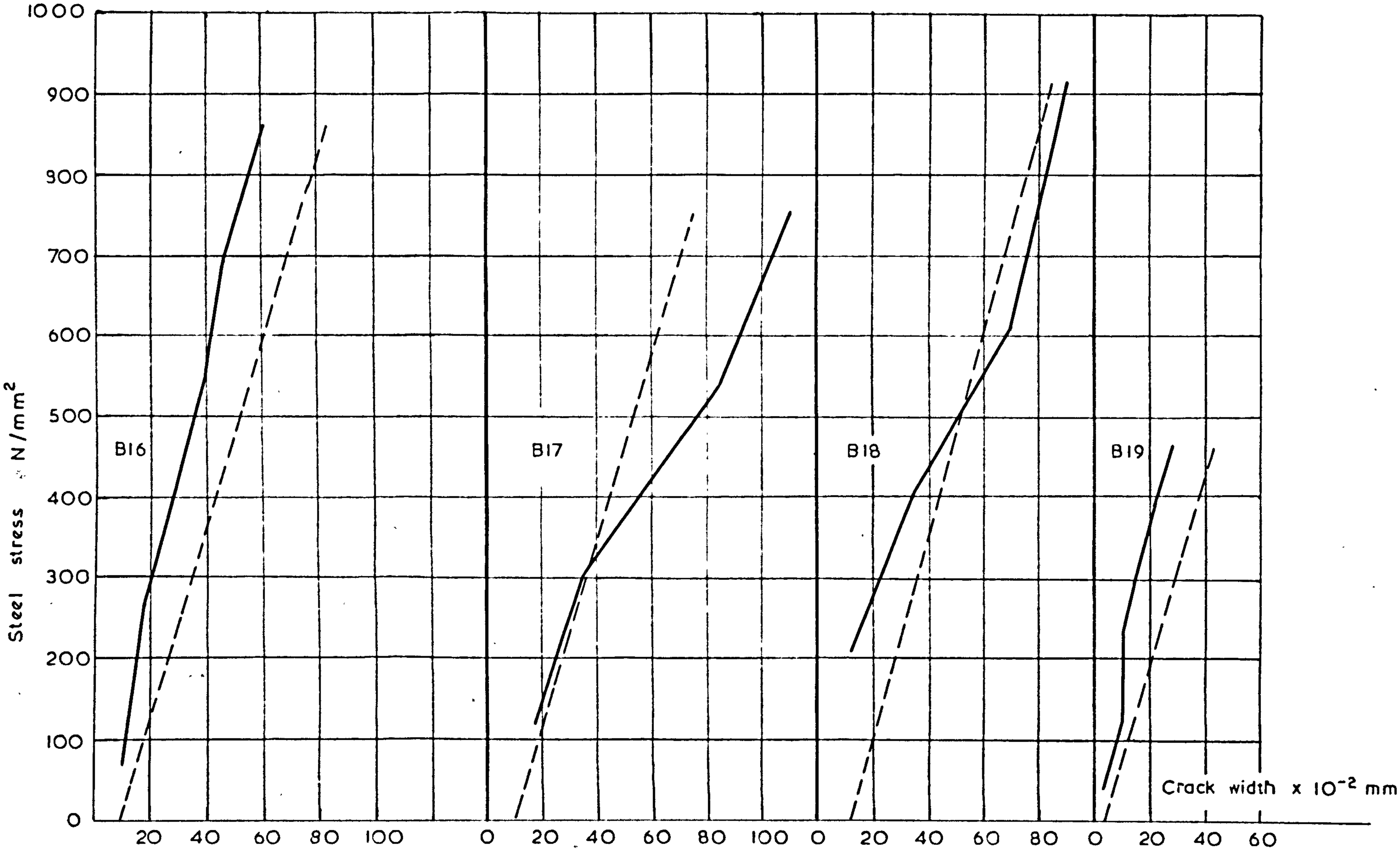

FIG.(37) STEEL STRESS — CRACK WIDTH RELATIONSHIP (STATIC LOAD — SECOND CYCLE) WIRES AND STRANDS.

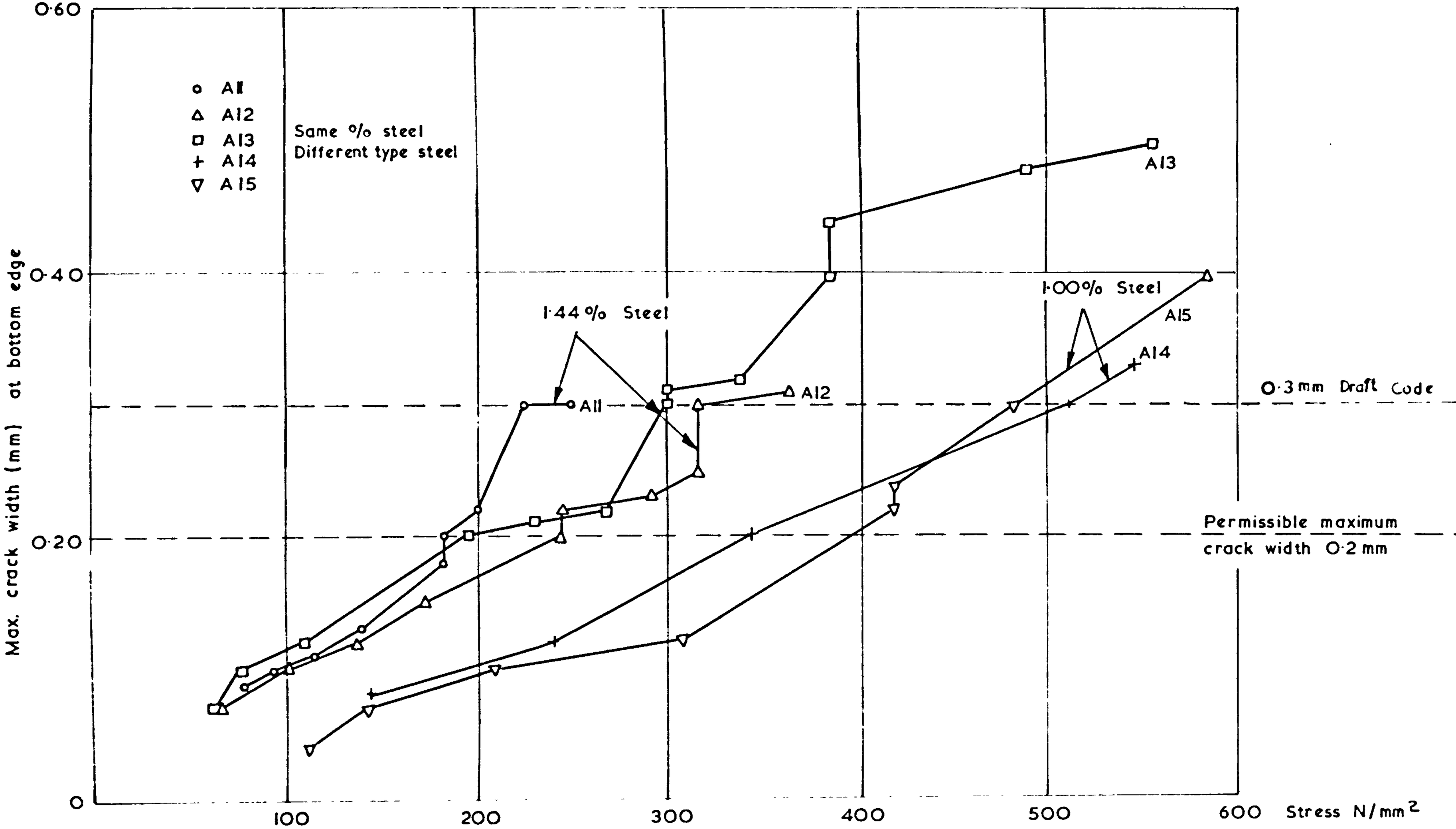

FIG.(38) STEEL STRESS — MAXIMUM CRACK WIDTH (VIRGIN CYCLE — STATIC LOAD)

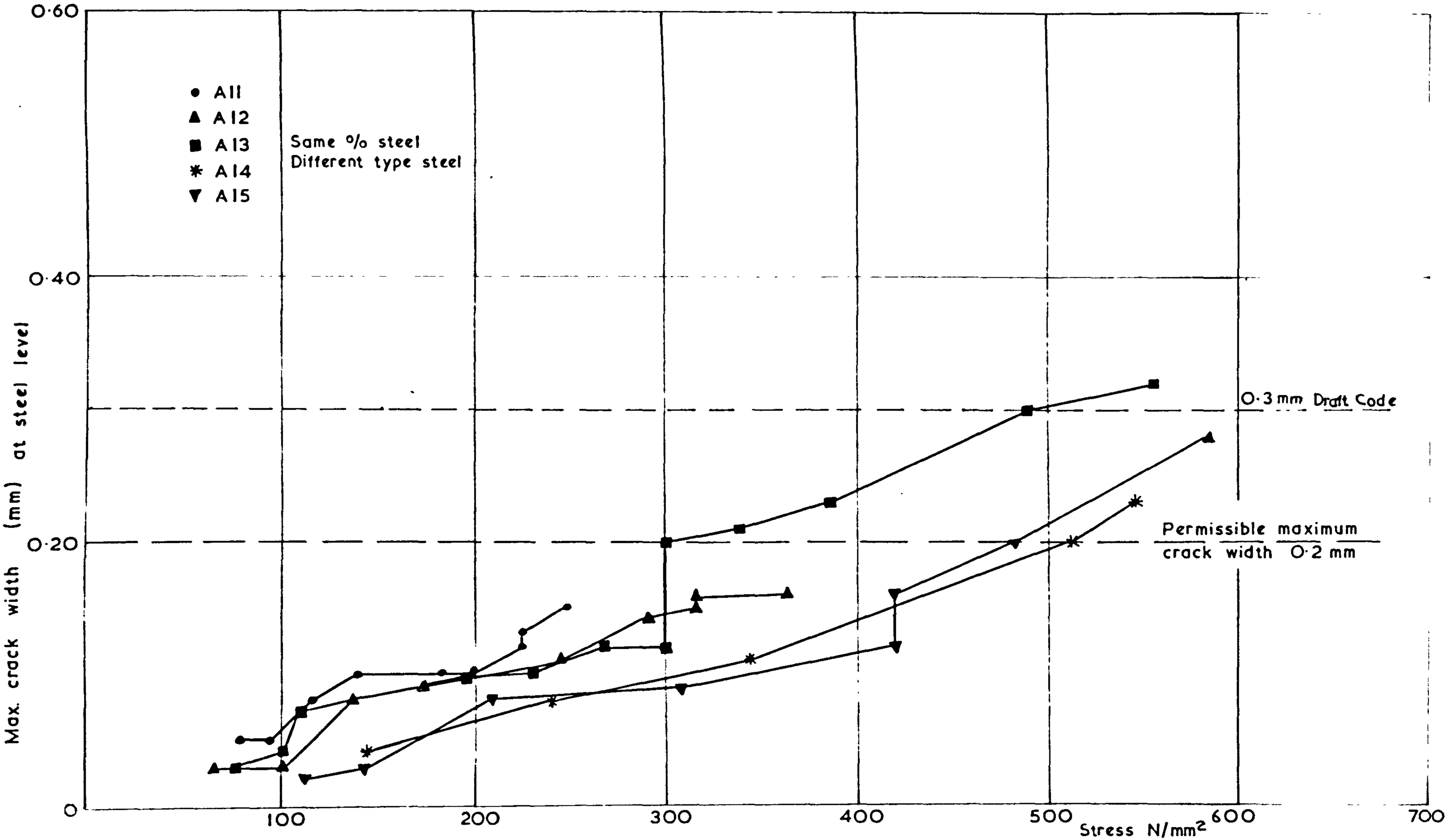

FIG. (39) STEEL STRESS - MAXIMUM CRACK WIDTH (VIRGIN CYCLE - STATIC LOAD)

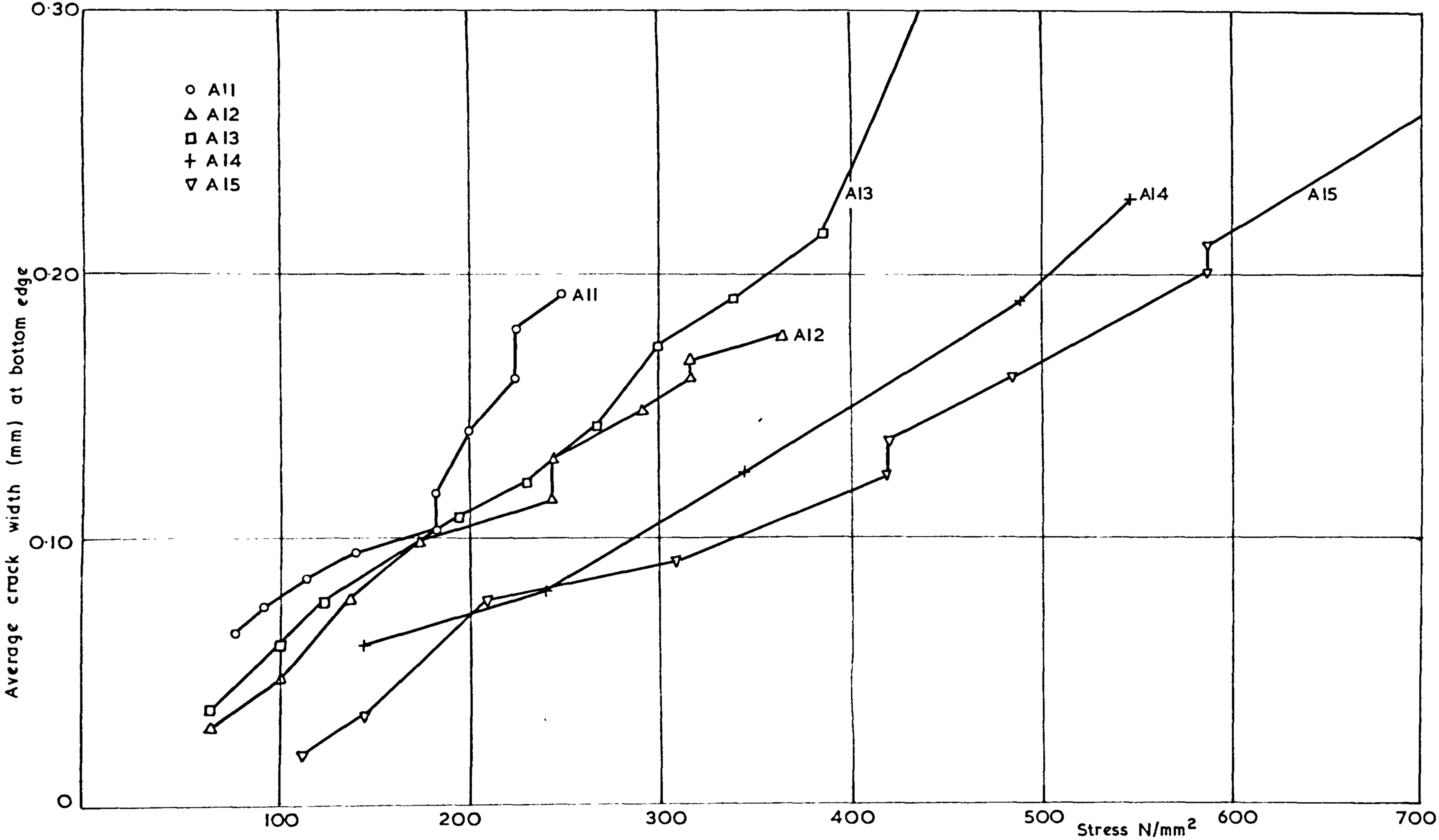

FIG. (40) STEEL STRESS – AVERAGE CRACK WIDTH (VIRGIN CYCLE – STATIC LOAD)

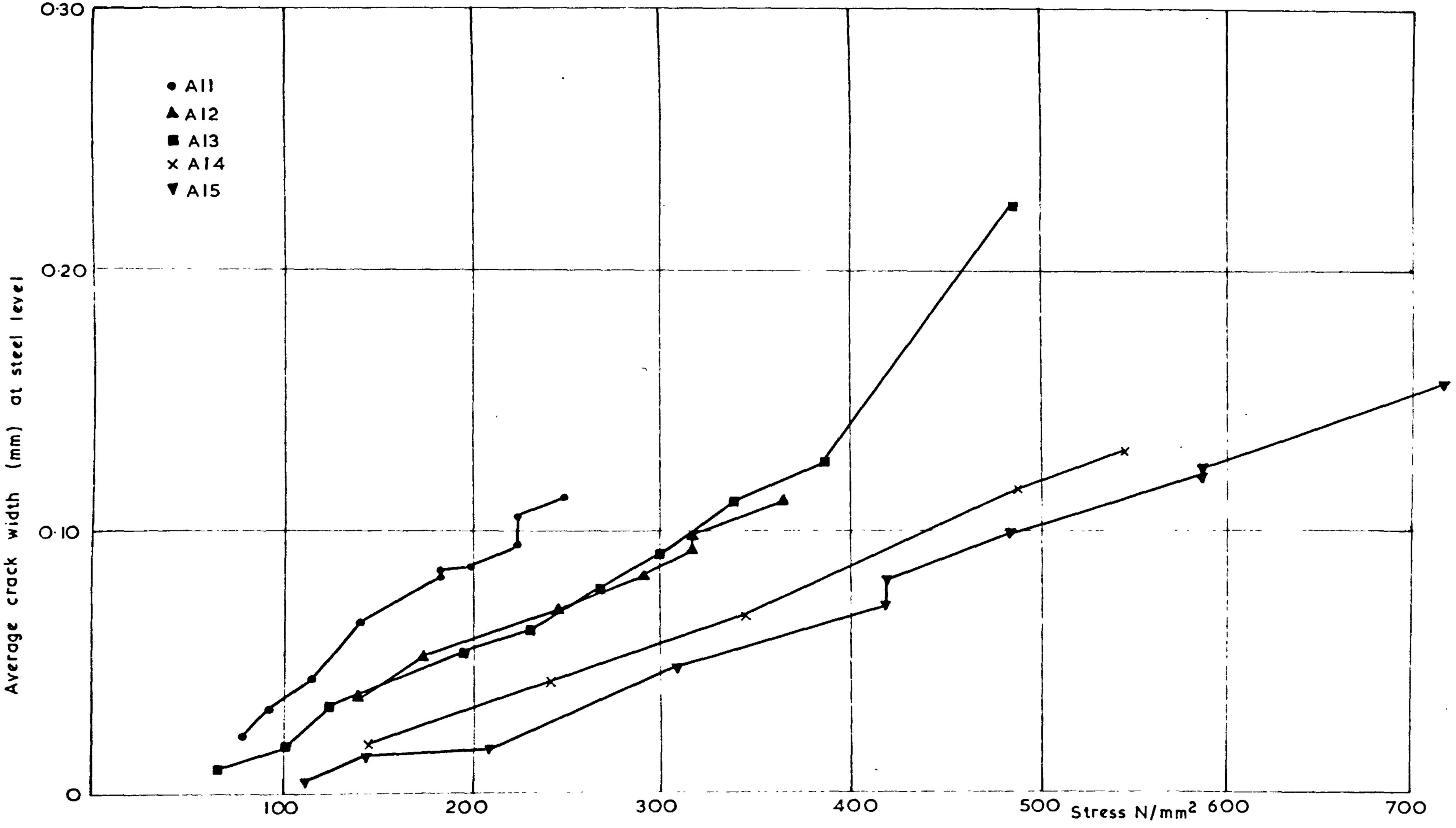

FIG. (41) STEEL STRESS — AVERAGE CRACK WIDTH (VIRGIN CYCLE — STATIC LOAD)

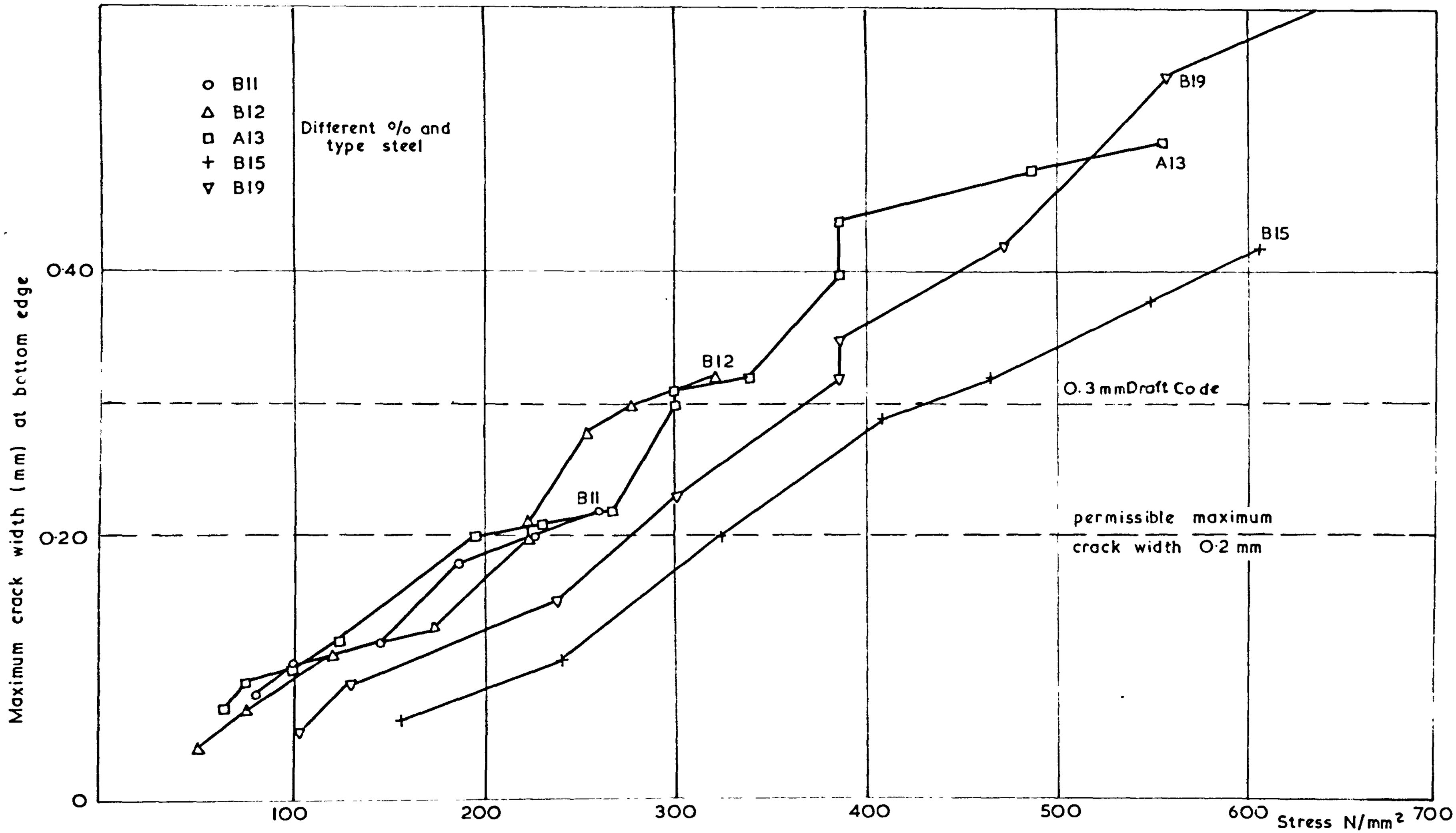

FIG. (42) STEEL STRESS - MAXIMUM CRACK WIDTH (VIRGIN CYCLE - STATIC LOAD)

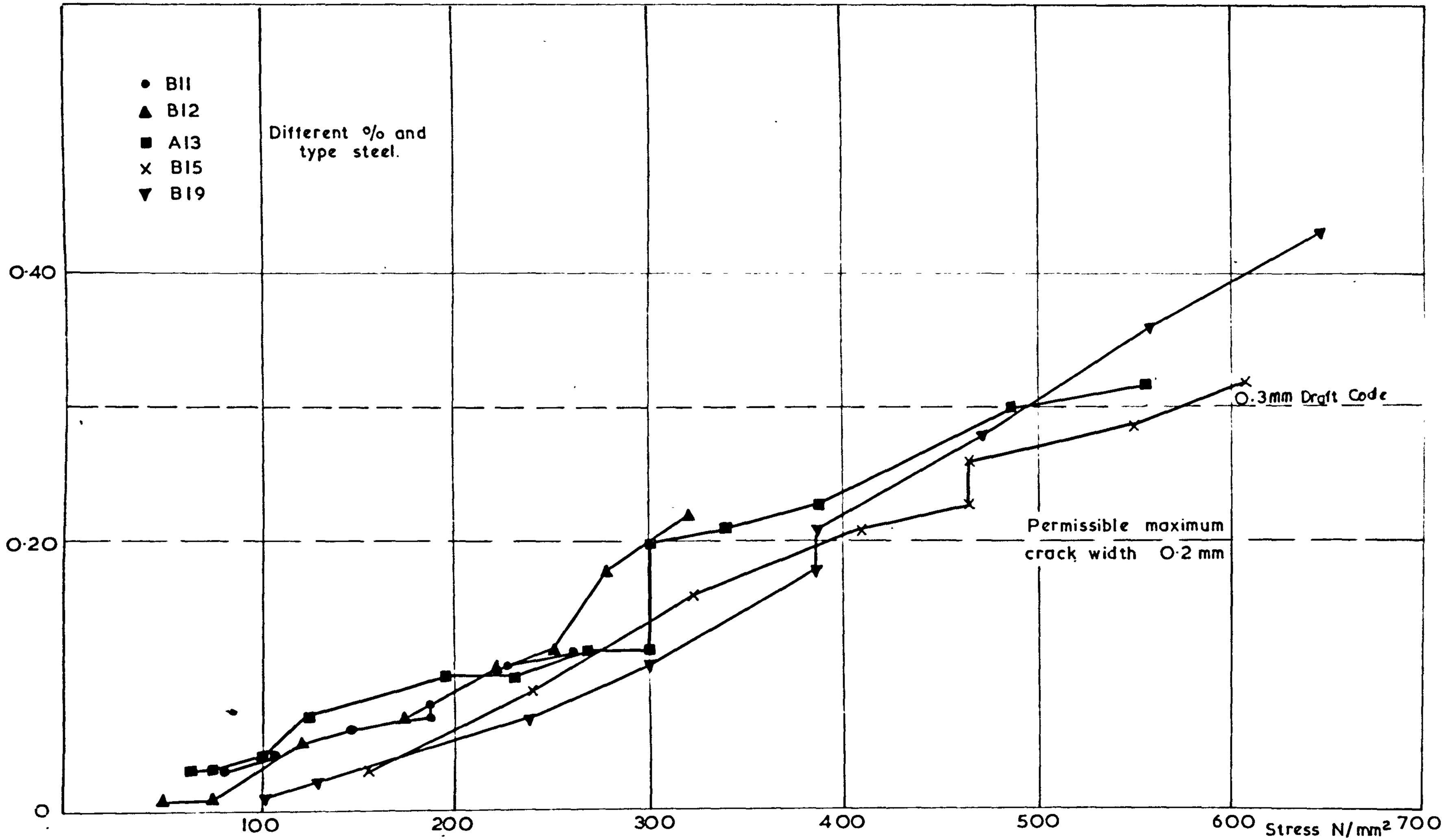

FIG.(43) STEEL STRESS – MAXIMUM CRACK WIDTH (VIRGIN CYCLE – STATIC LOAD.)

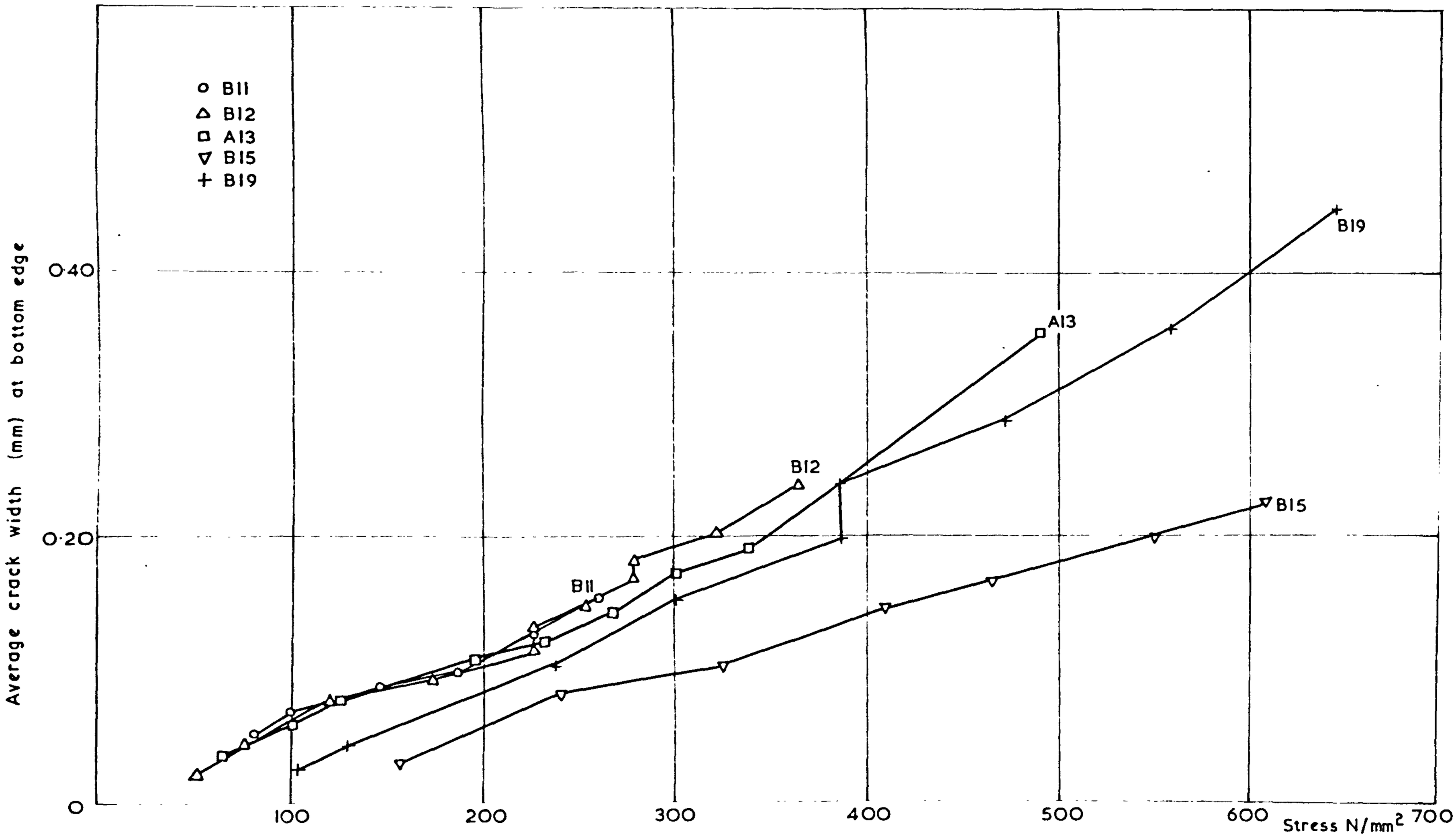

FIG.(44) STEEL STRESS – AVERAGE CRACK WIDTH (VIRGIN CYCLE – STATIC LOAD)

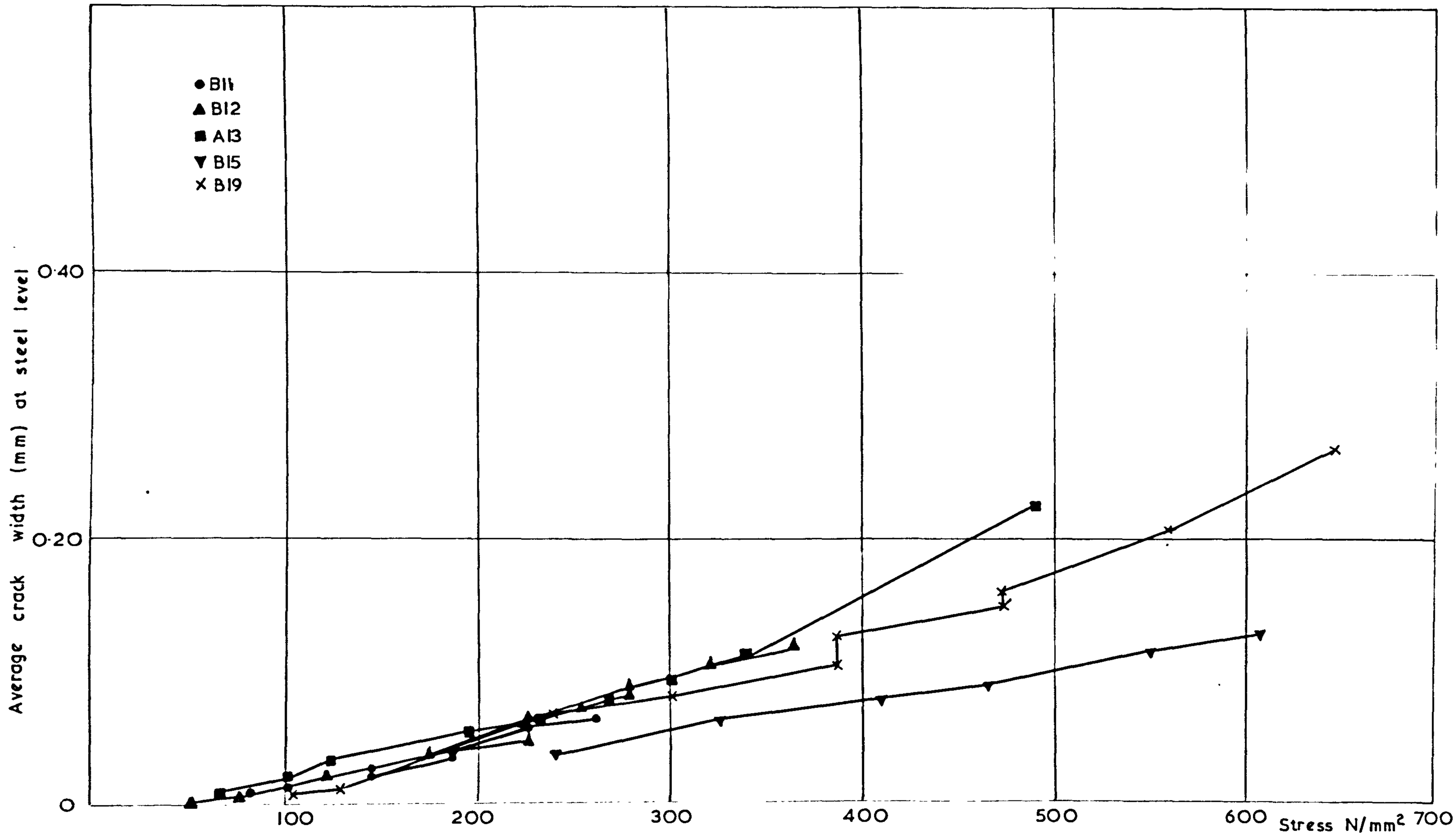

FIG. (45) STEEL STRESS – AVERAGE CRACK WIDTH (VIRGIN CYCLE – STATIC LOAD)

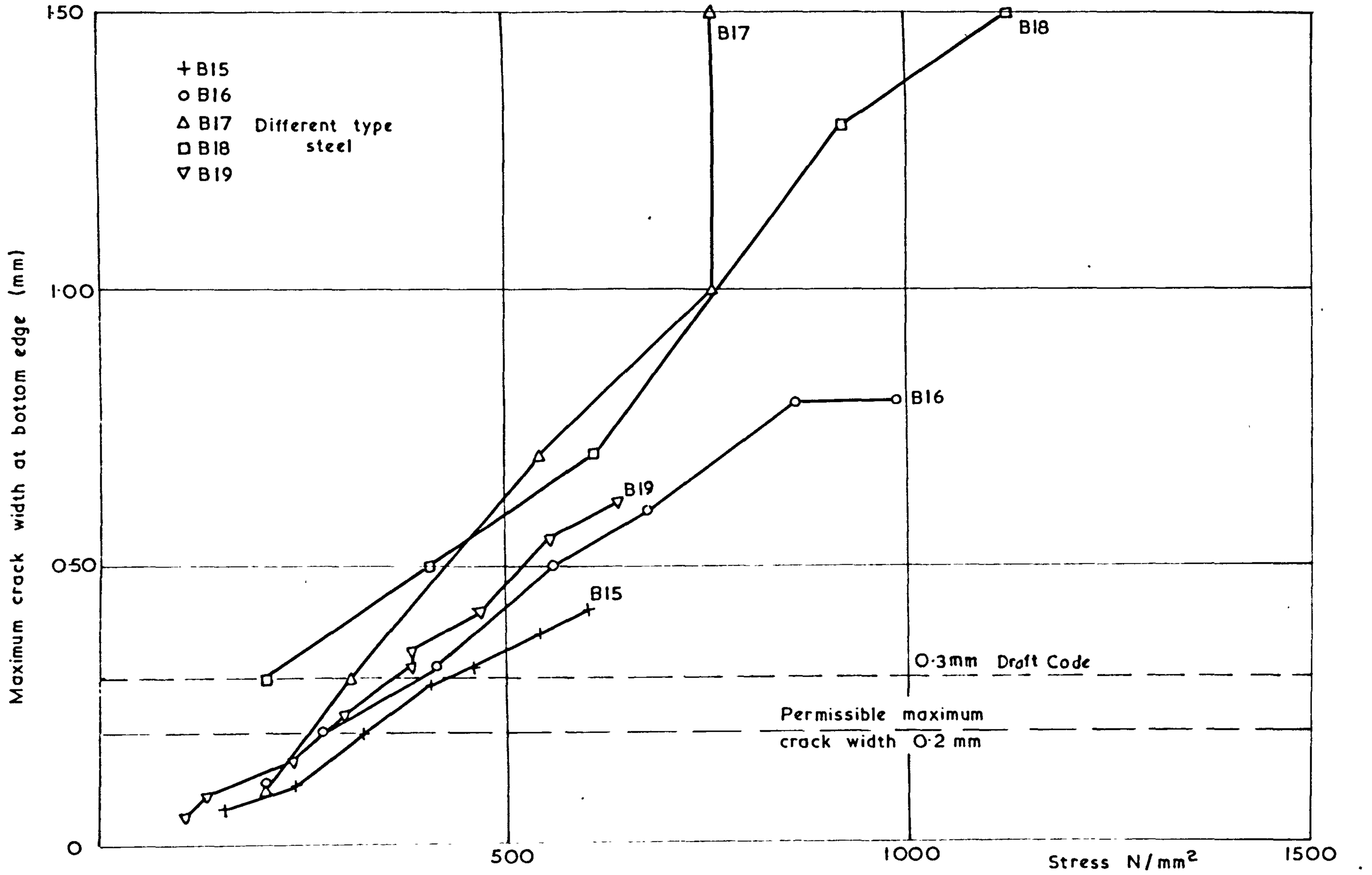

FIG.(46) STEEL STRESS – MAXIMUM CRACK WIDTH (VIRGIN CYCLE – STATIC LOAD)

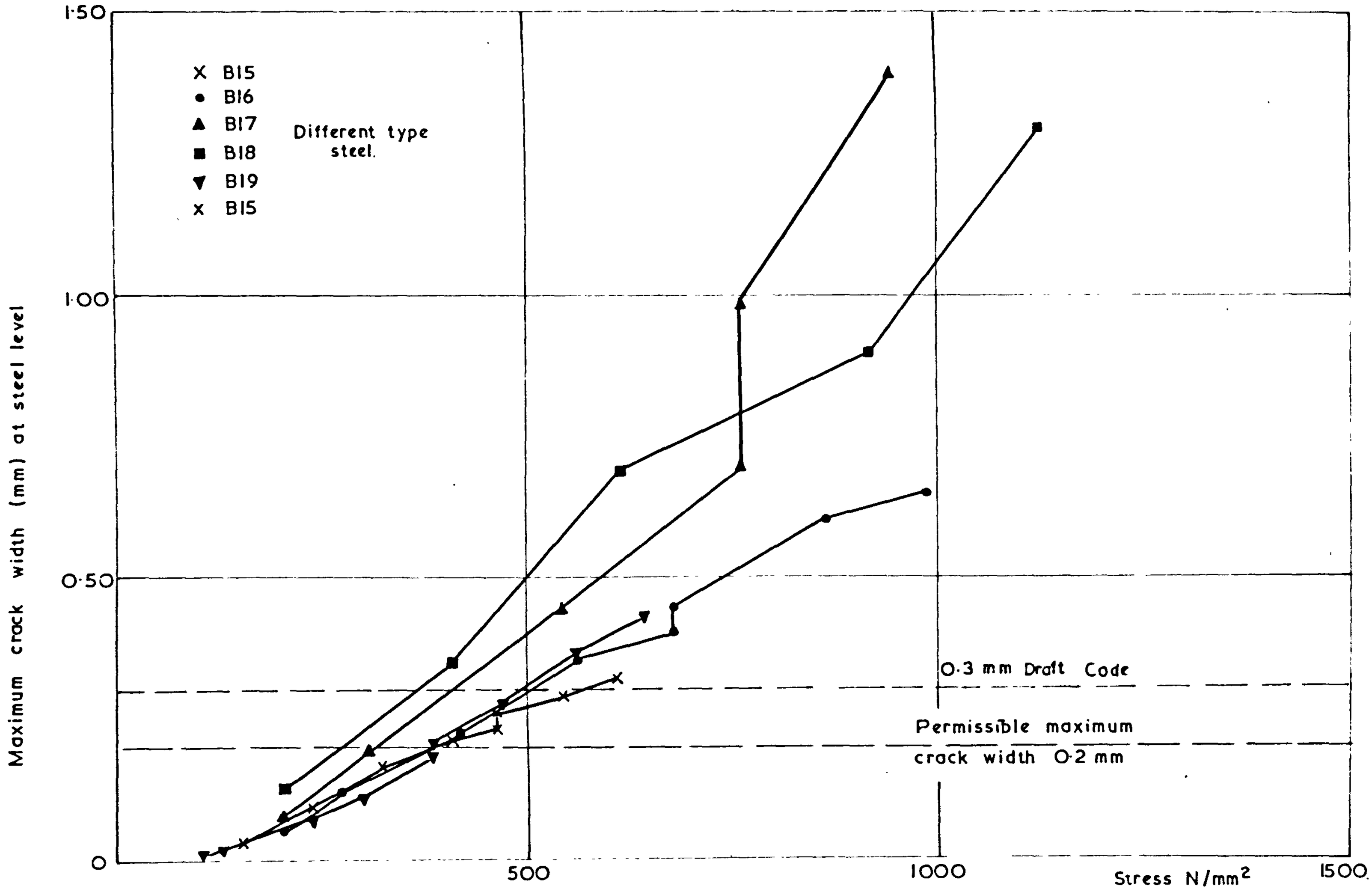

FIG.(47) STEEL STRESS – MAXIMUM CRACK WIDTH (VIRGIN CYCLE – STATIC LOAD.)

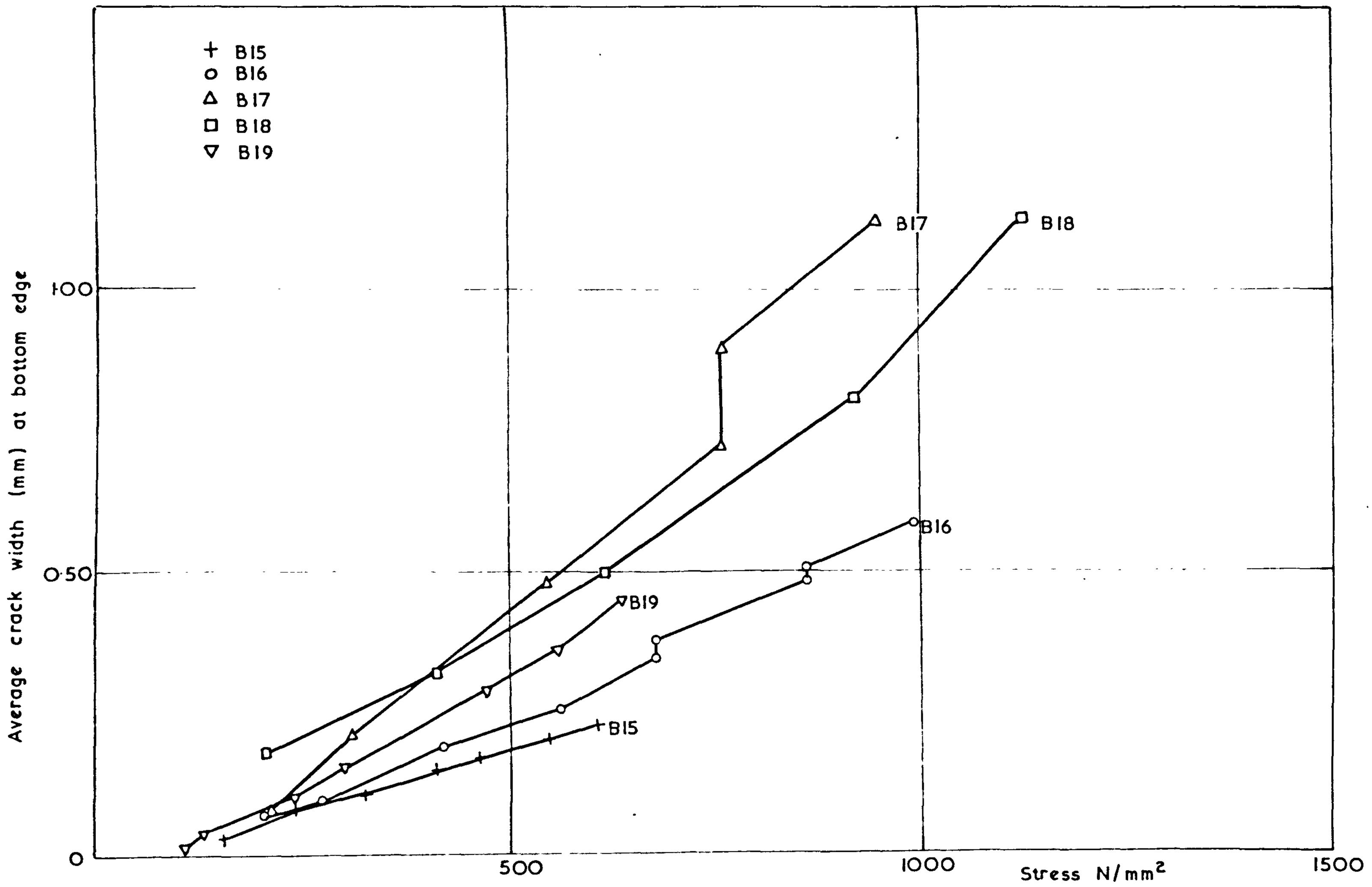

FIG.(48) STEEL STRESS — AVERAGE CRACK WIDTH (VIRGIN CYCLE—STATIC LOAD)

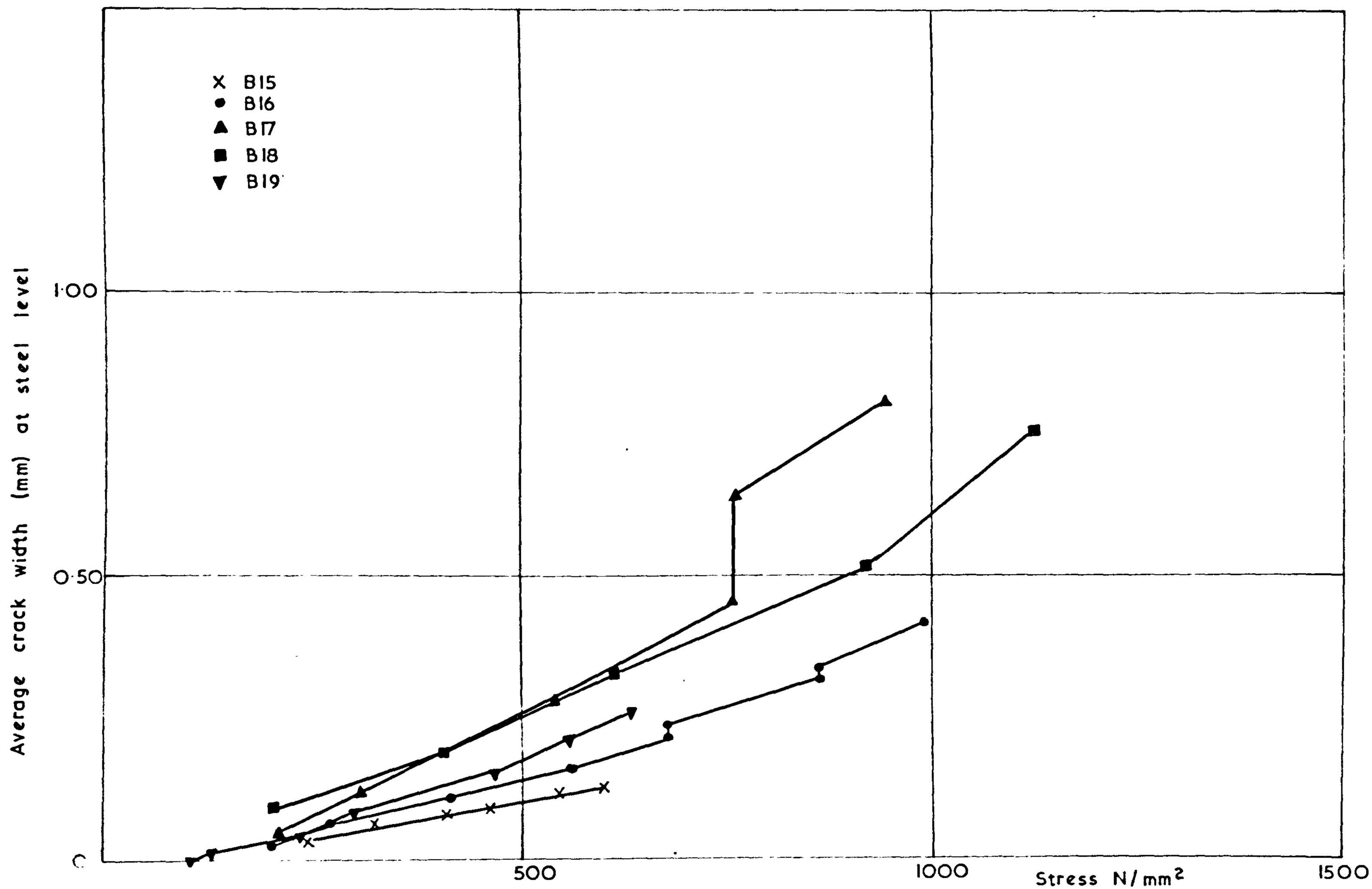

FIG. (49) STEEL STRESS – AVERAGE CRACK WIDTH (VIRGIN CYCLE – STATIC LOAD)

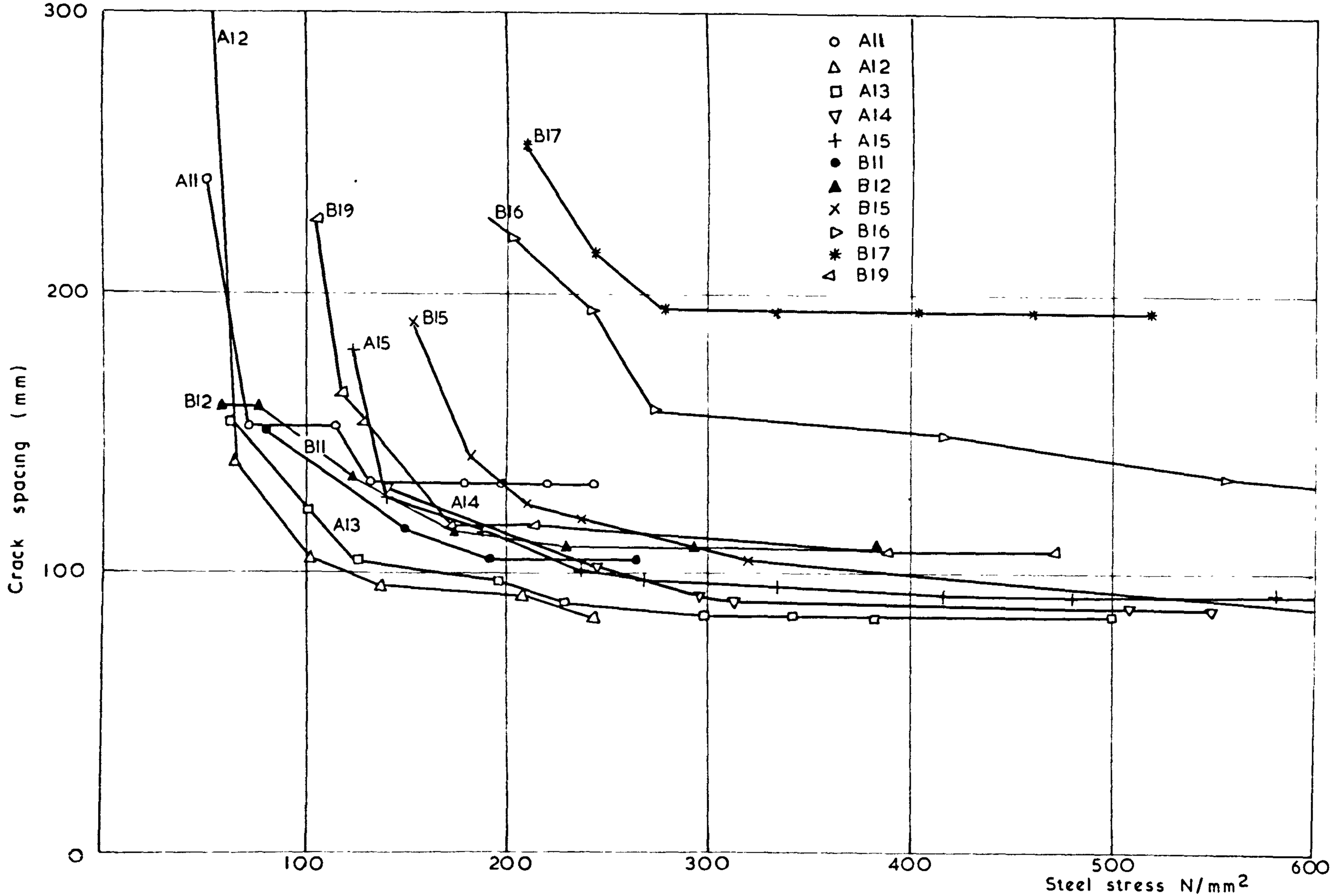

FIG(50) STEEL STRESS CRACK SPACING CURVES (STATIC LOAD)

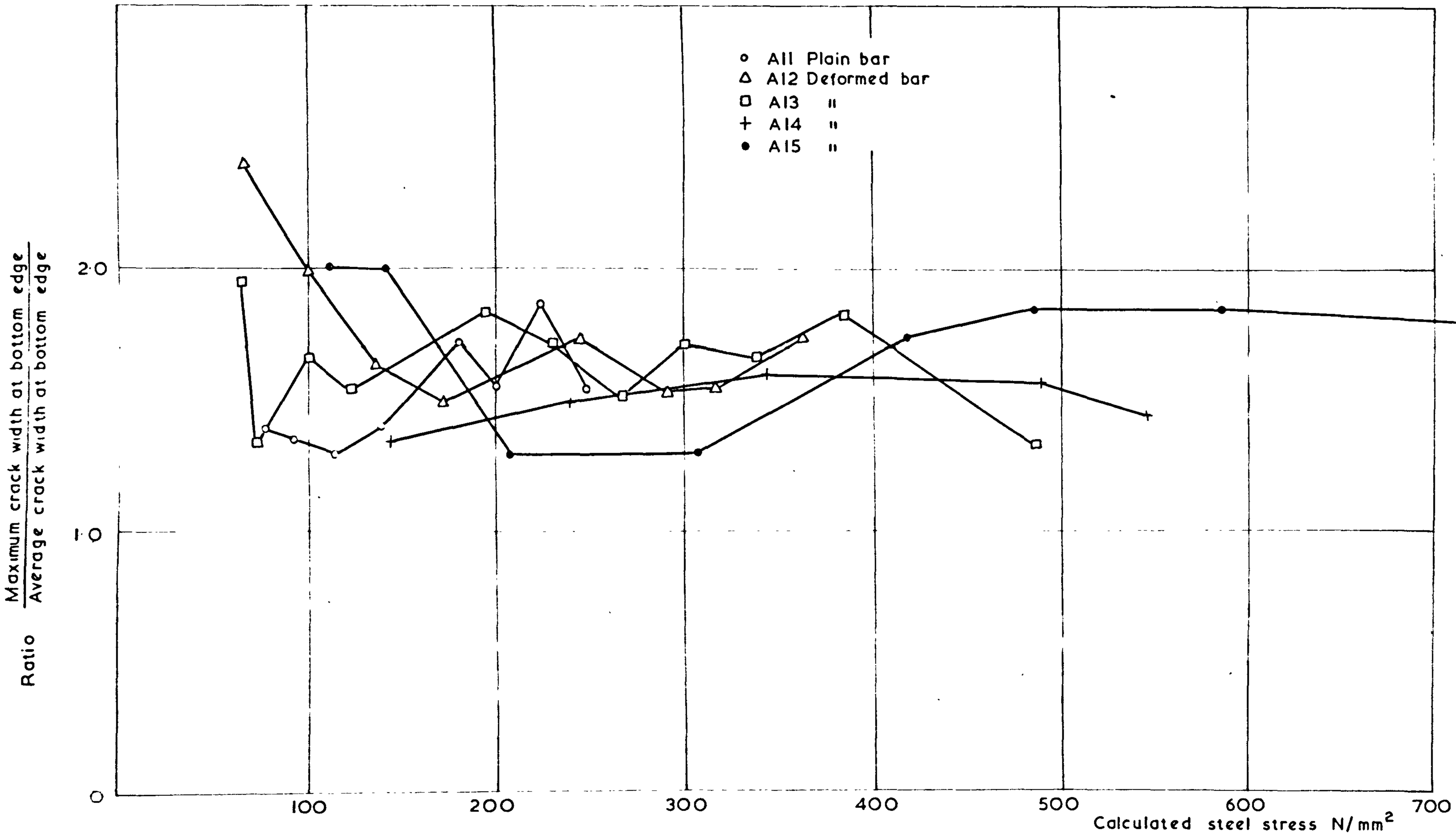

FIG. (51) RELATIONSHIP BETWEEN RATIO OF MAXIMUM TO AVERAGE CRACK WIDTHS AND STEEL STRESS (STATIC LOAD – VIRGIN CYCLE)

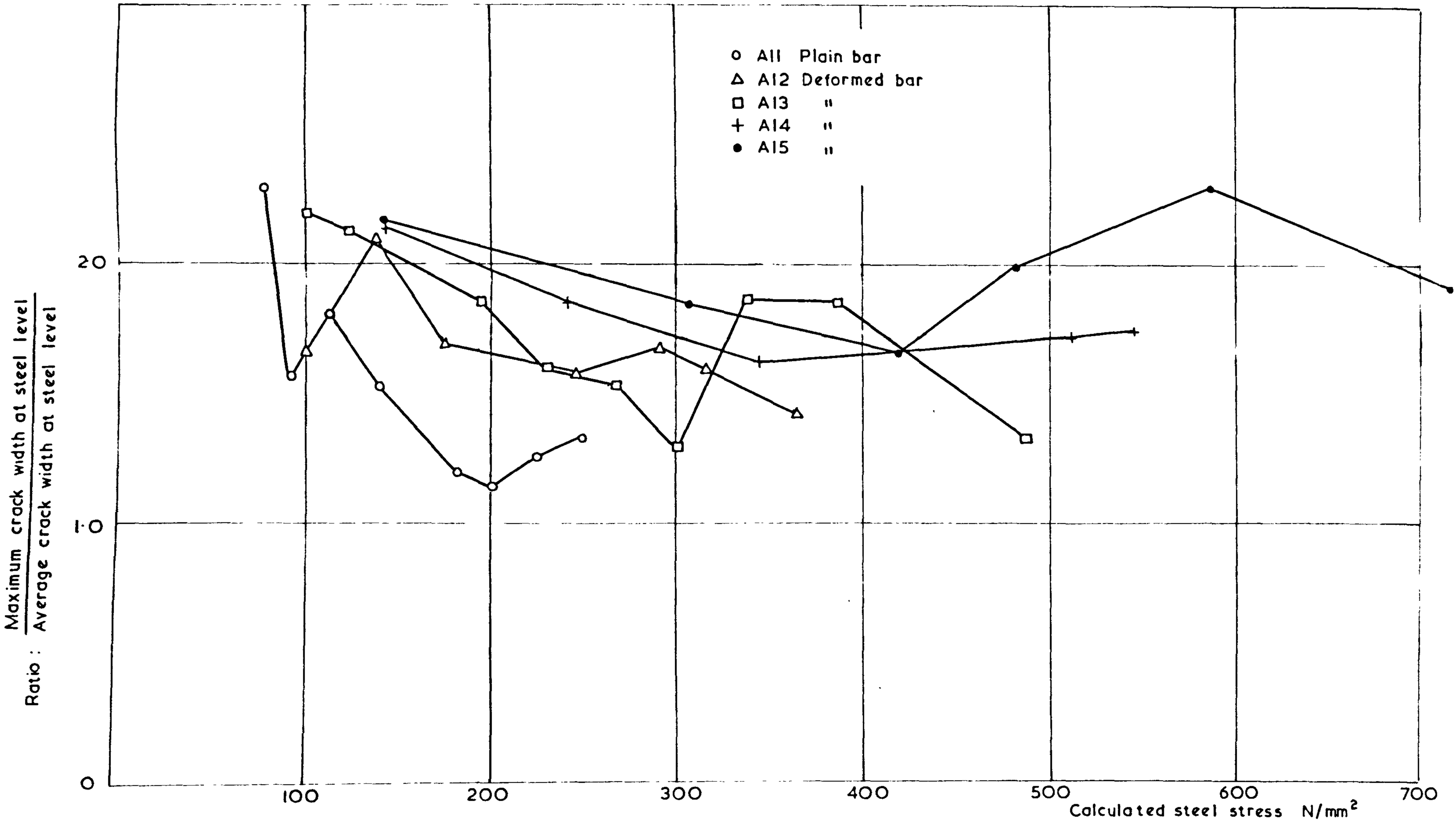

FIG.(5 2) RELATIONSHIP BETWEEN RATIO OF MAXIMUM TO AVERAGE CRACK WIDTHS AND STEEL STRESS (STATIC LOAD – VIRGIN CYCLE)

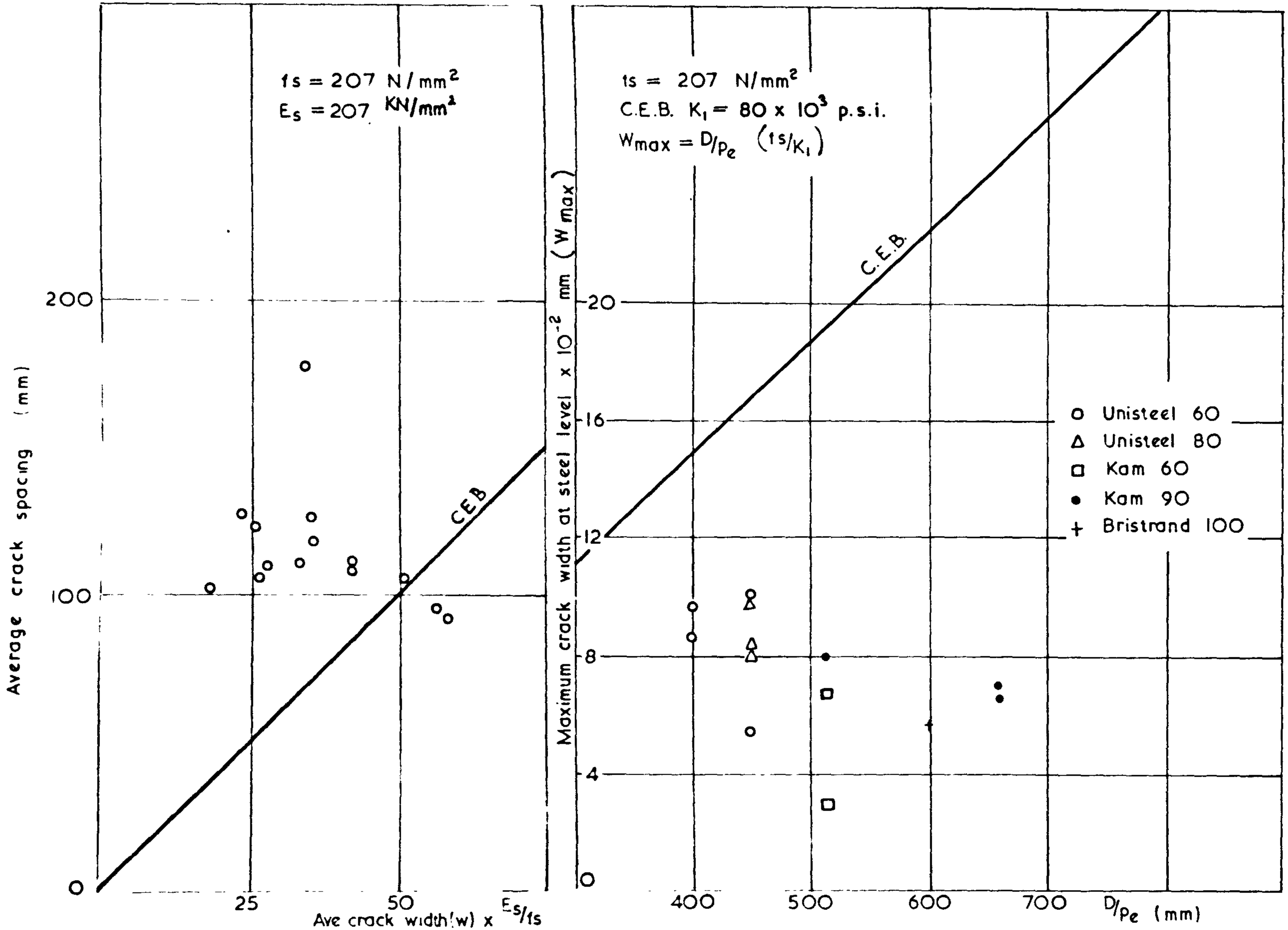

FIG 54. RELATIONSHIP BETWEEN CRACK SPACING AND CRACK WIDTH.

FIG 53 RELATIONSHIP BETWEEN CRACK WIDTH AND D/P_e

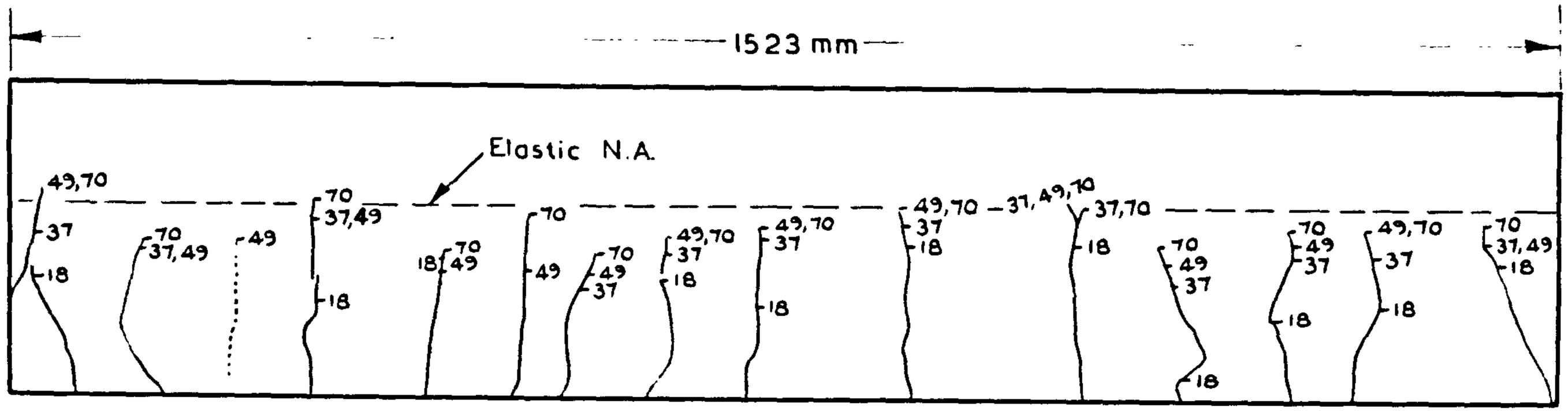

B11

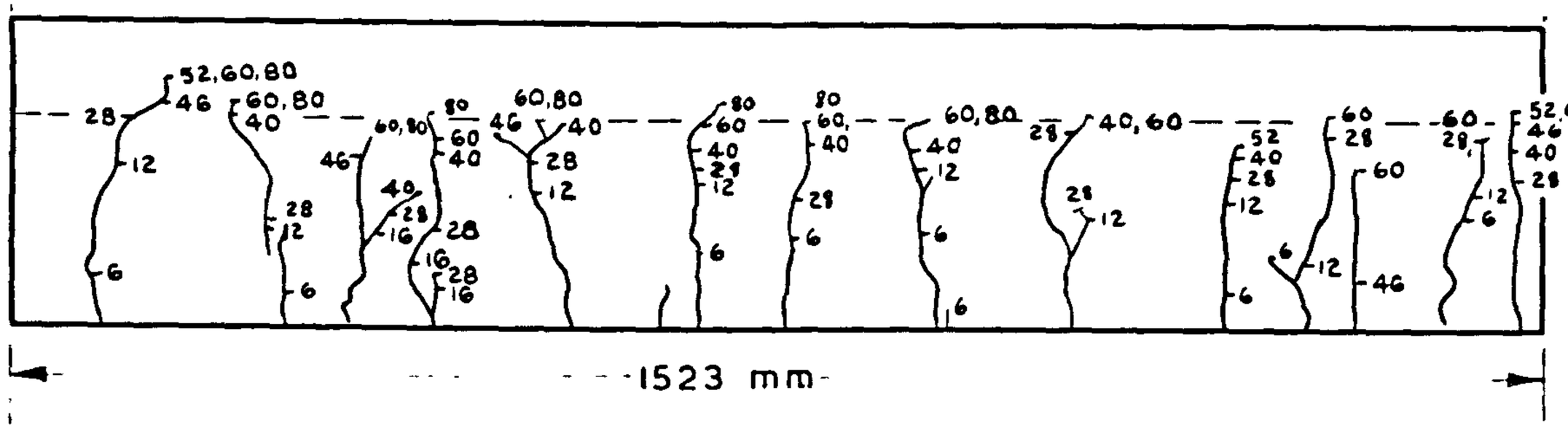

A13

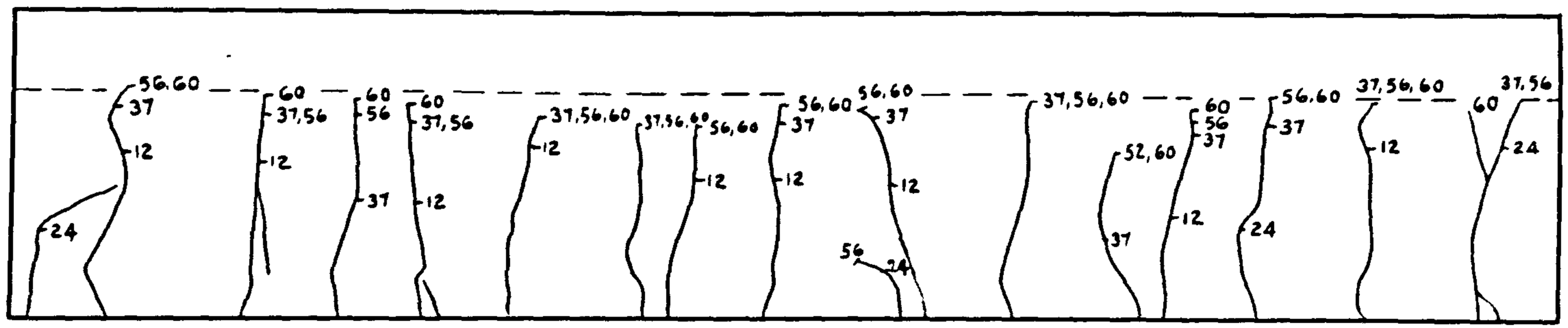

A14

FIG. (55) CRACKING PATTERNS (STATIC LOAD)

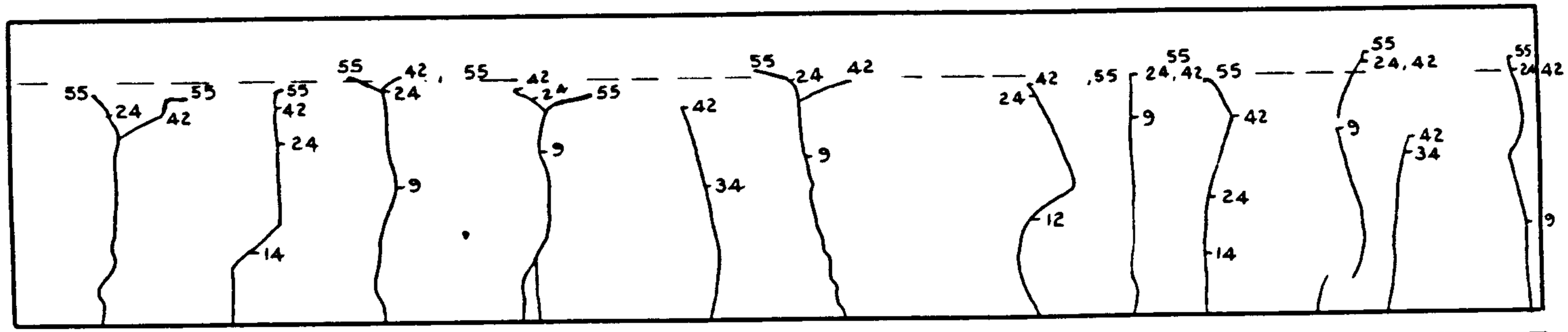

B16

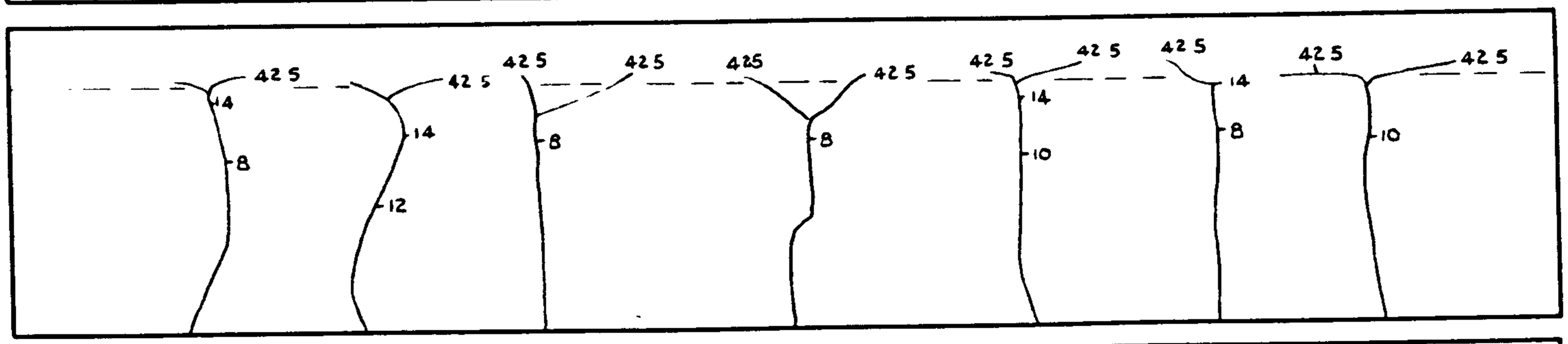

B17

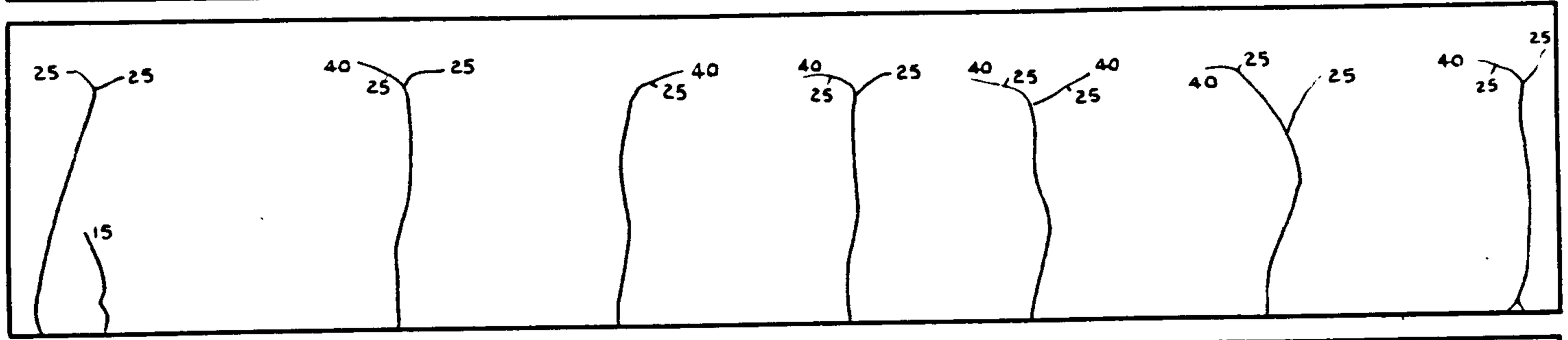

B18

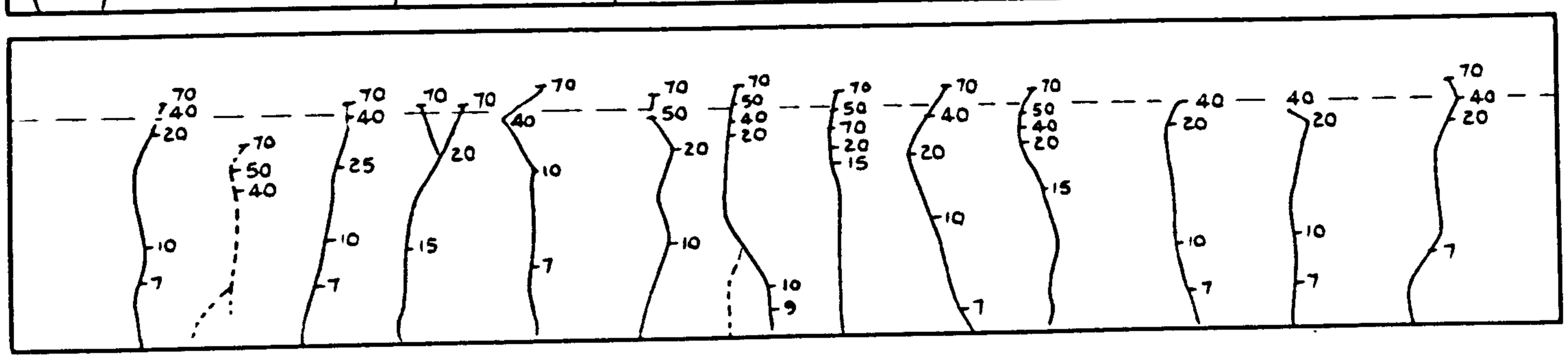

B19

FIG (56) CRACKING PATTERNS (STATIC LOAD)

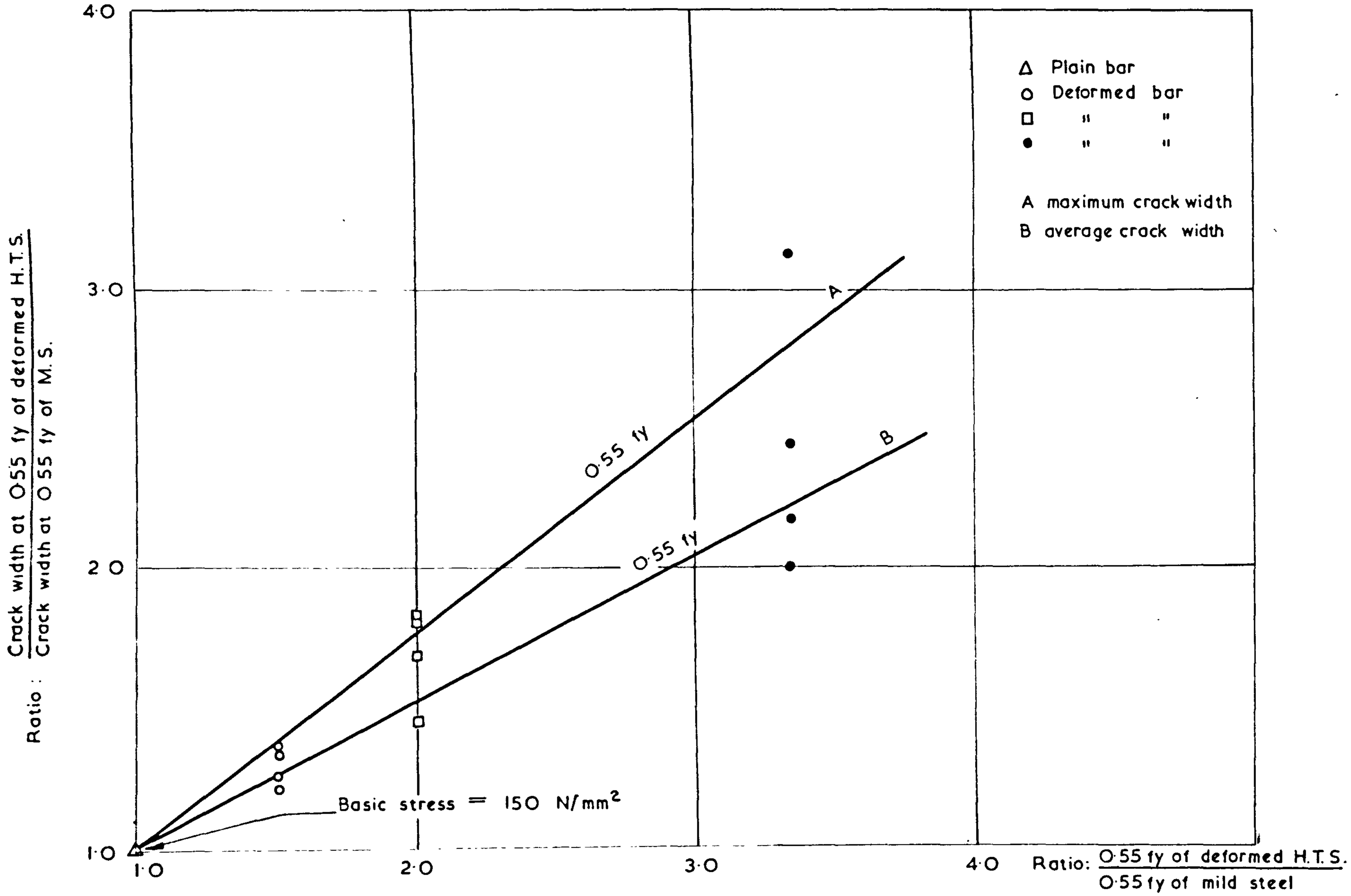

FIG (57) COMPARISON OF CRACK WIDTHS BETWEEN PLAIN AND DEFORMED BARS

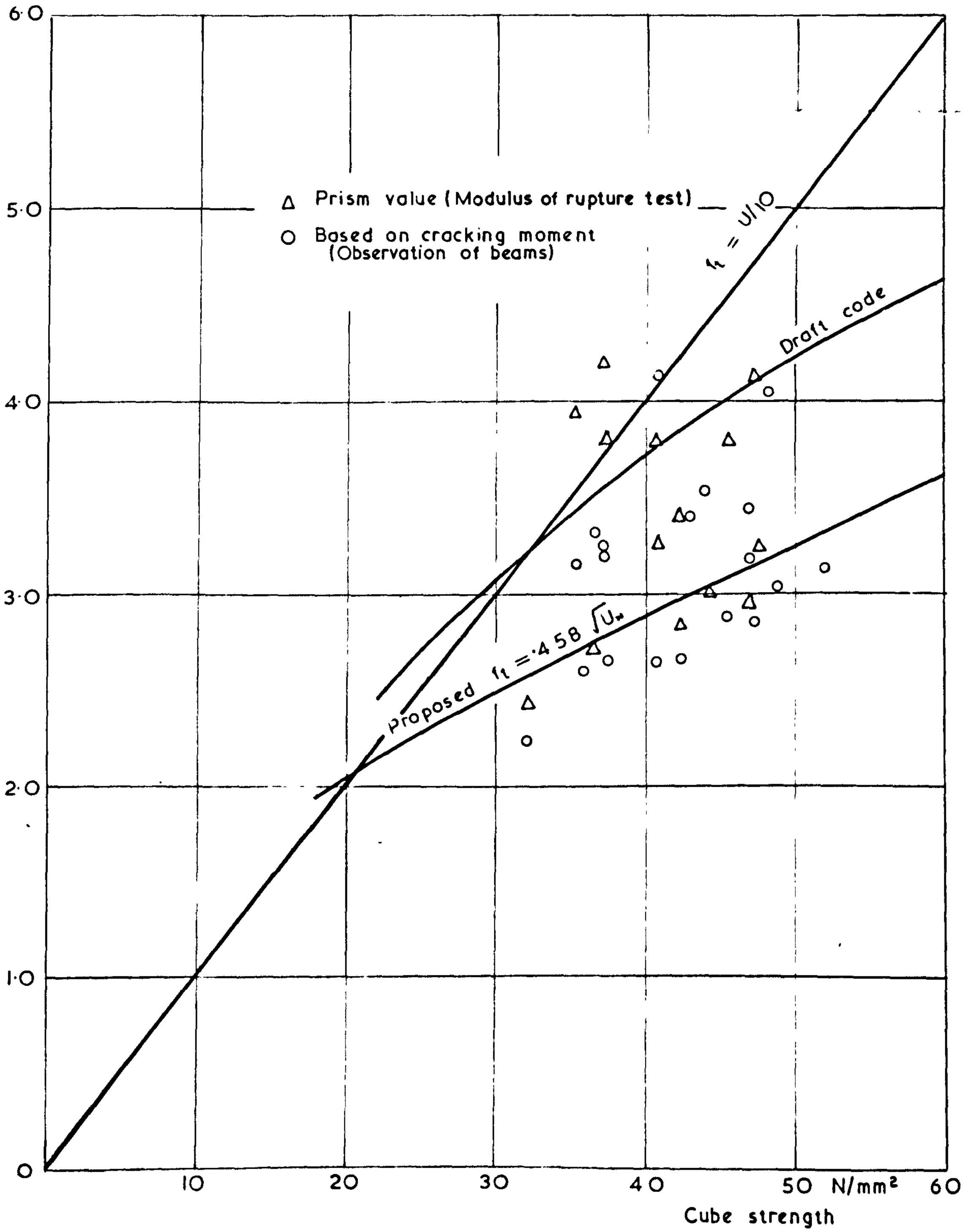

FIG. (58) CUBE STRENGTH — MODULUS OF RUPTURE. CURVES FOR CONCRETE

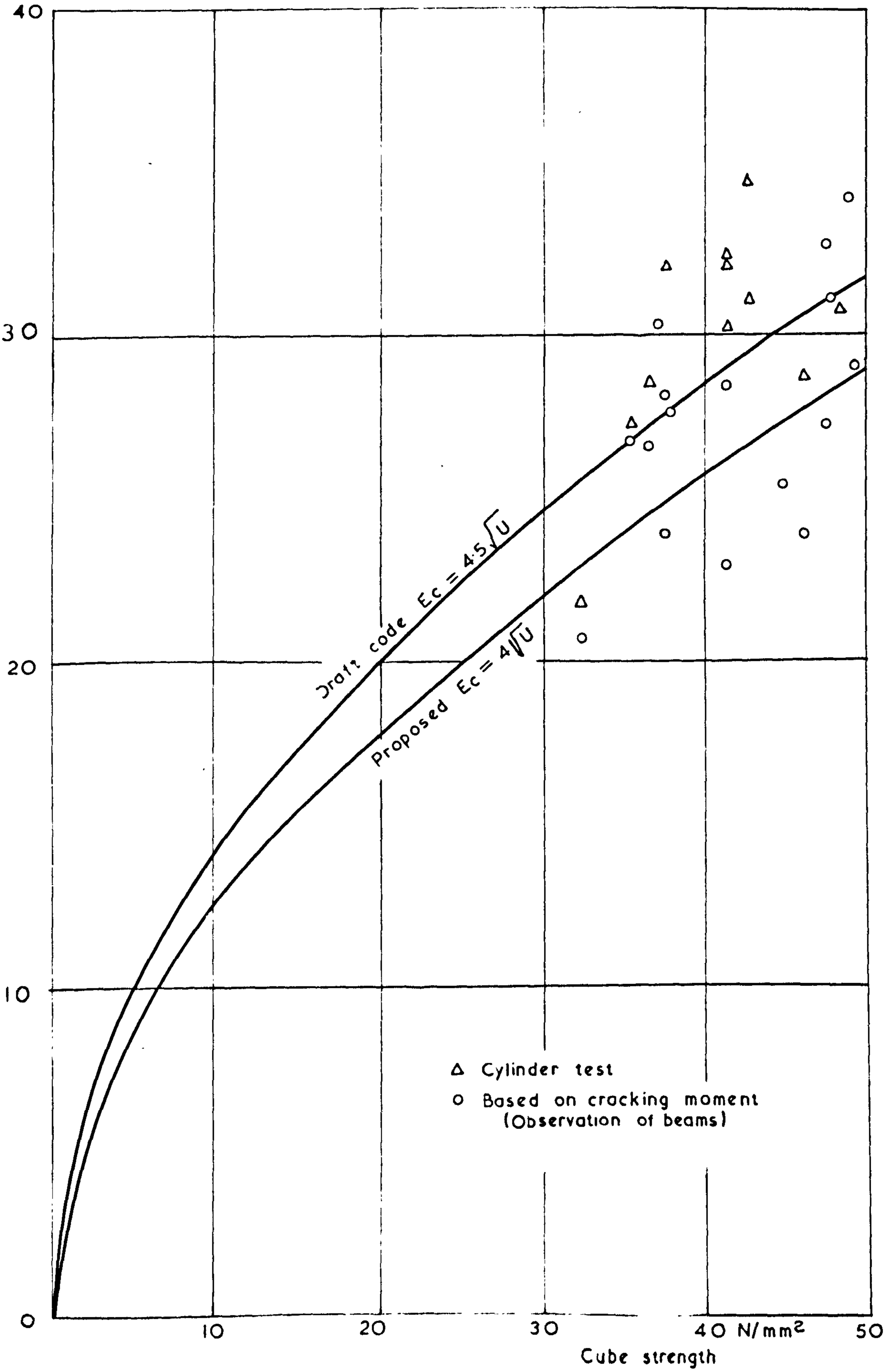

FIG.(59) CUBE STRENGTH – MODULUS OF ELASTICITY CURVES FOR CONCRETE

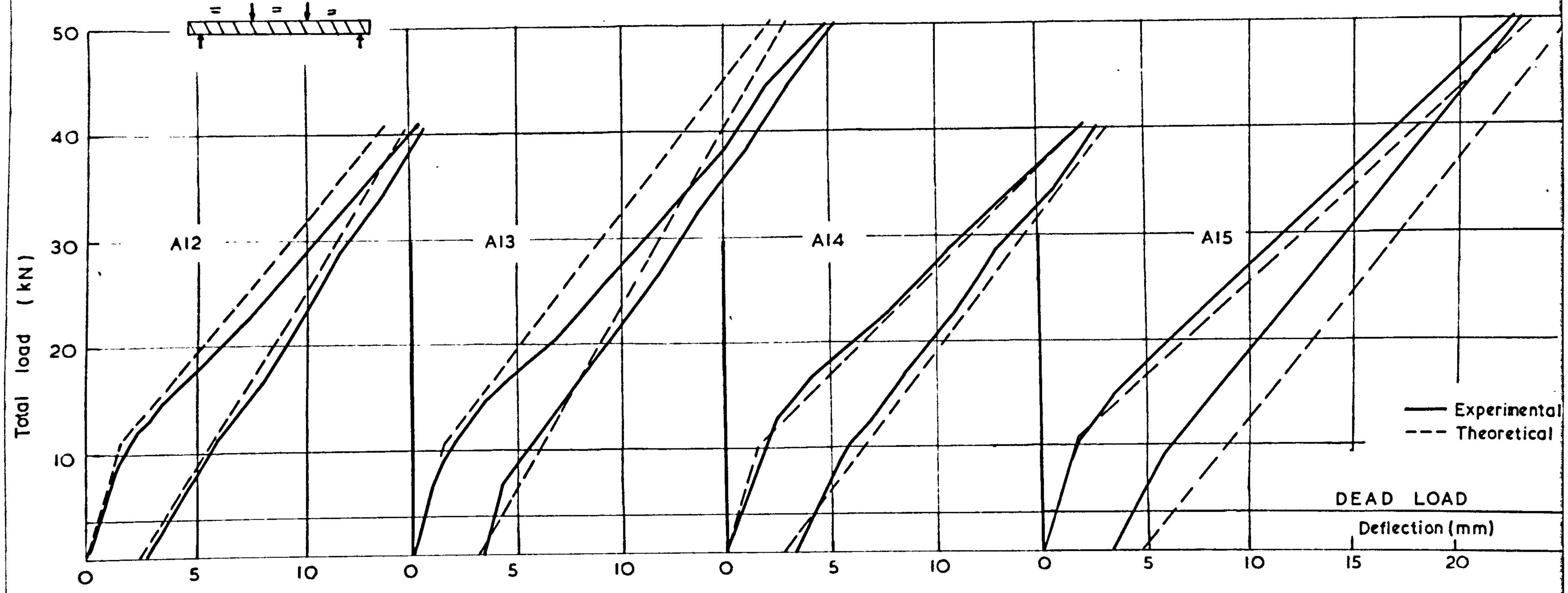

FIG.(60) LOAD – DEFLECTION CURVES (STATIC LOAD – FIRST AND SECOND CYCLES) DEFORMED BARS.

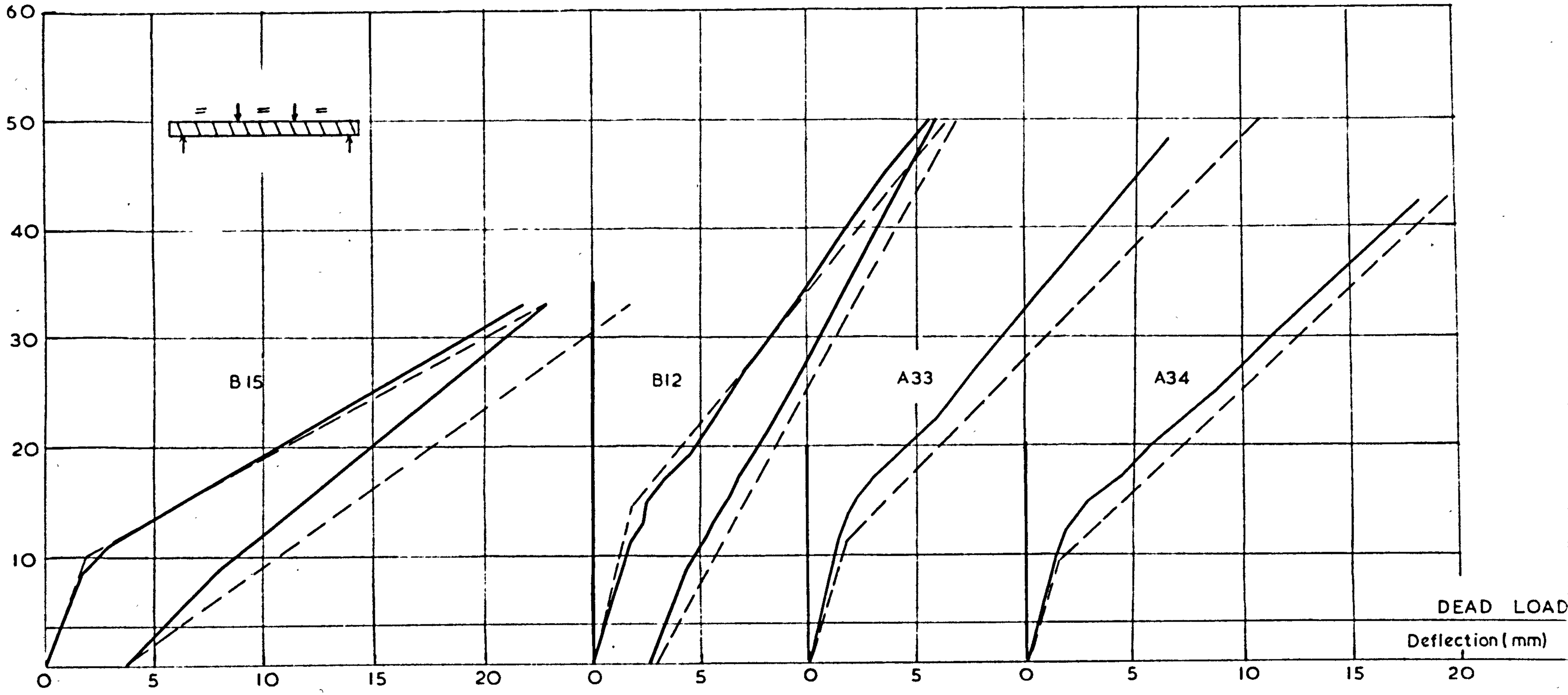

FIG.(61) LOAD-DEFLECTION CURVES (STATIC LOAD- FIRST & SECOND CYCLES) DEFORMED BARS.

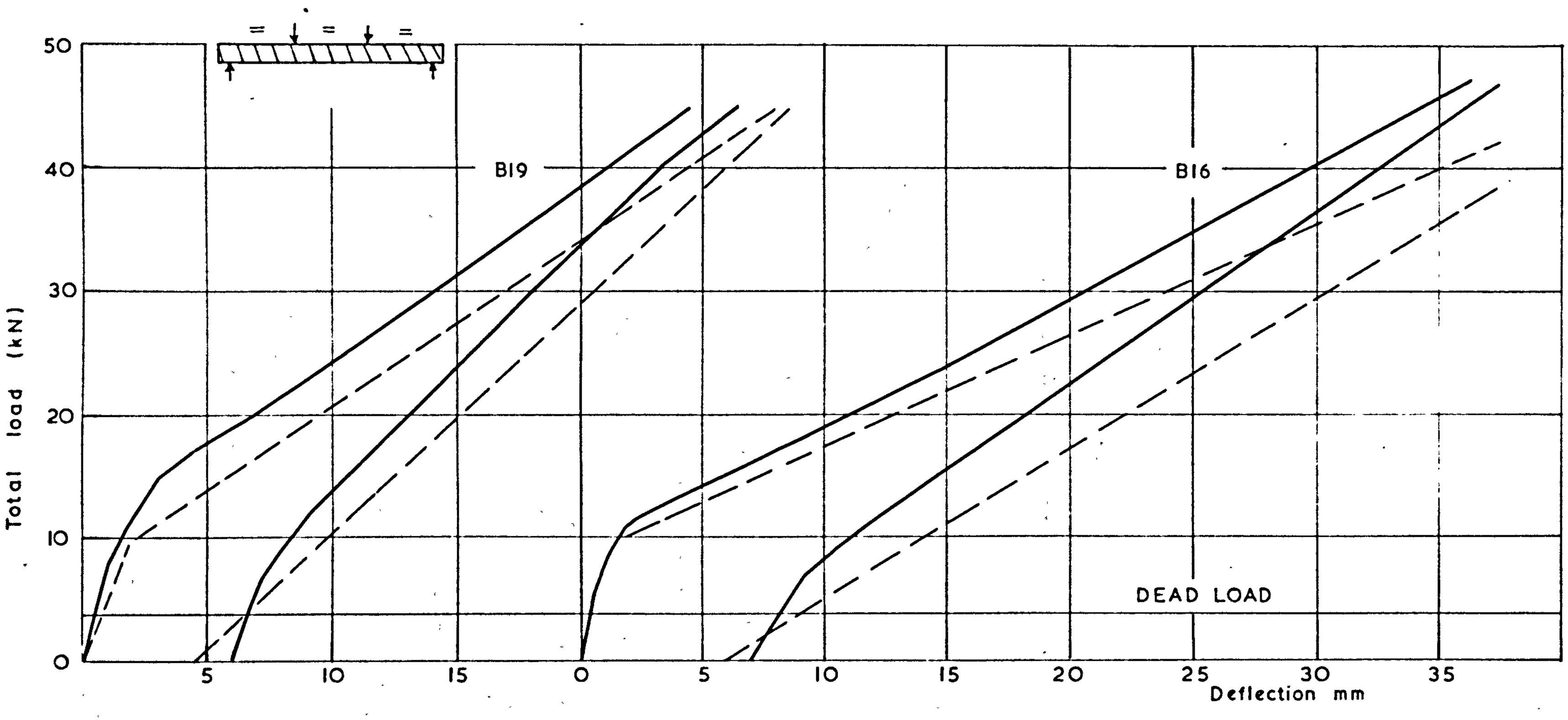

FIG.(62) LOAD – DEFLECTION CURVES (STATIC LOAD – FIRST AND SECOND CYCLES) WIRES AND STRANDS

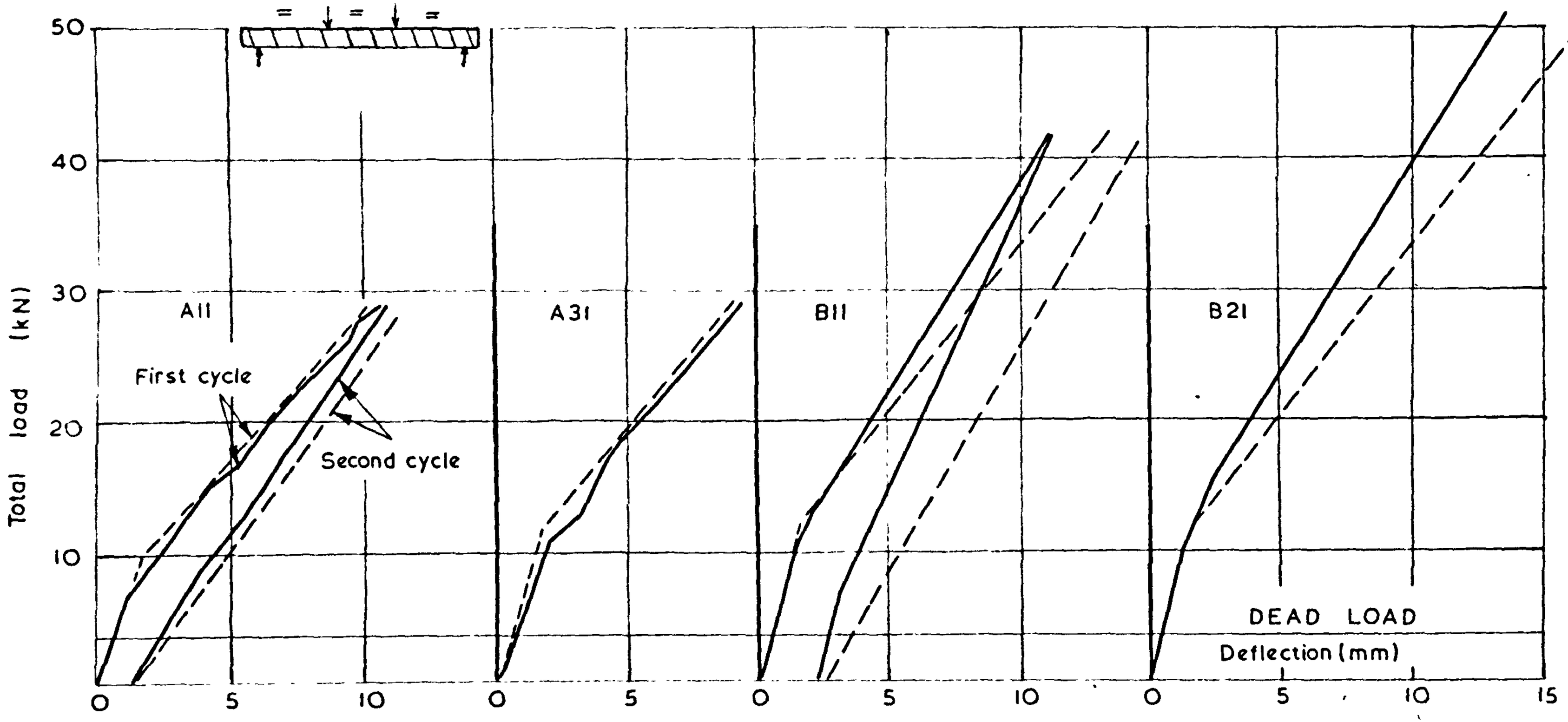

FIG. (63) LOAD-DEFLECTION CURVES (STATIC LOAD) PLAIN BARS

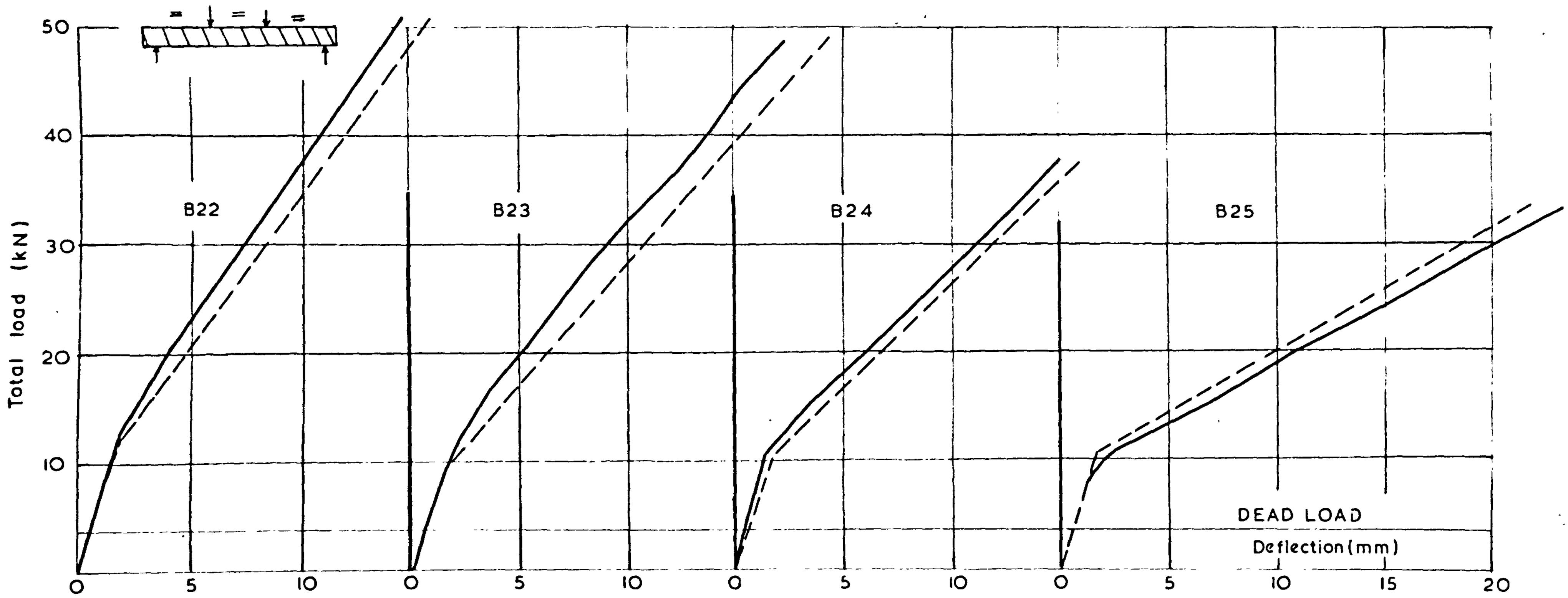

FIG. (64) LOAD-DEFLECTION CURVES (STATIC LOAD-FIRST CYCLE) DEFORMED BARS.

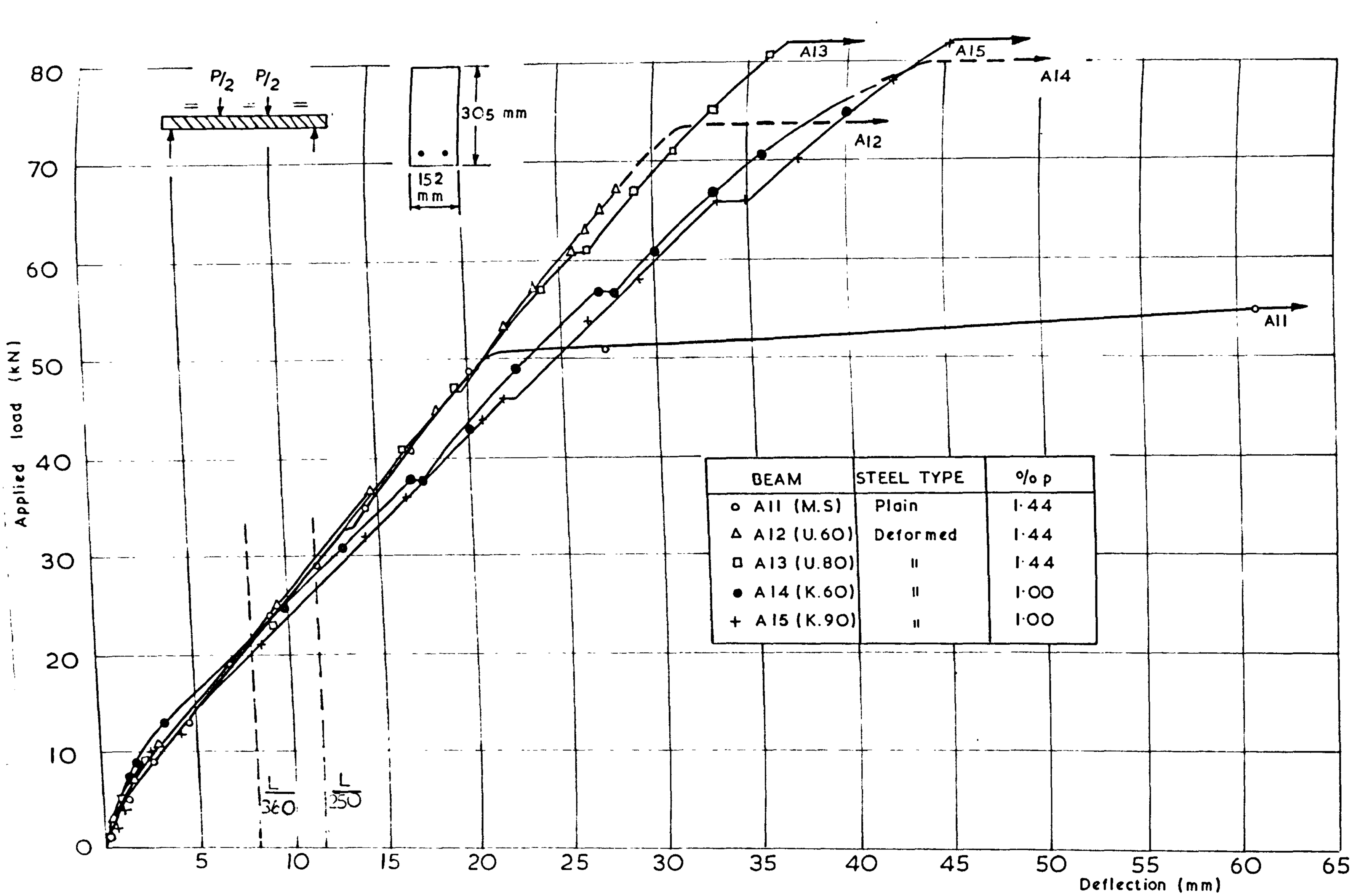

BEAM	STEEL TYPE	% p
o A11 (M.S)	Plain	1·44
Δ A12 (U.60)	Deformed	1·44
□ A13 (U.80)	〃	1·44
● A14 (K.60)	〃	1·00
+ A15 (K.90)	〃	1·00

FIG.(65) LOAD–DEFLECTION CURVES (STATIC LOAD — VIRGIN CYCLES.)

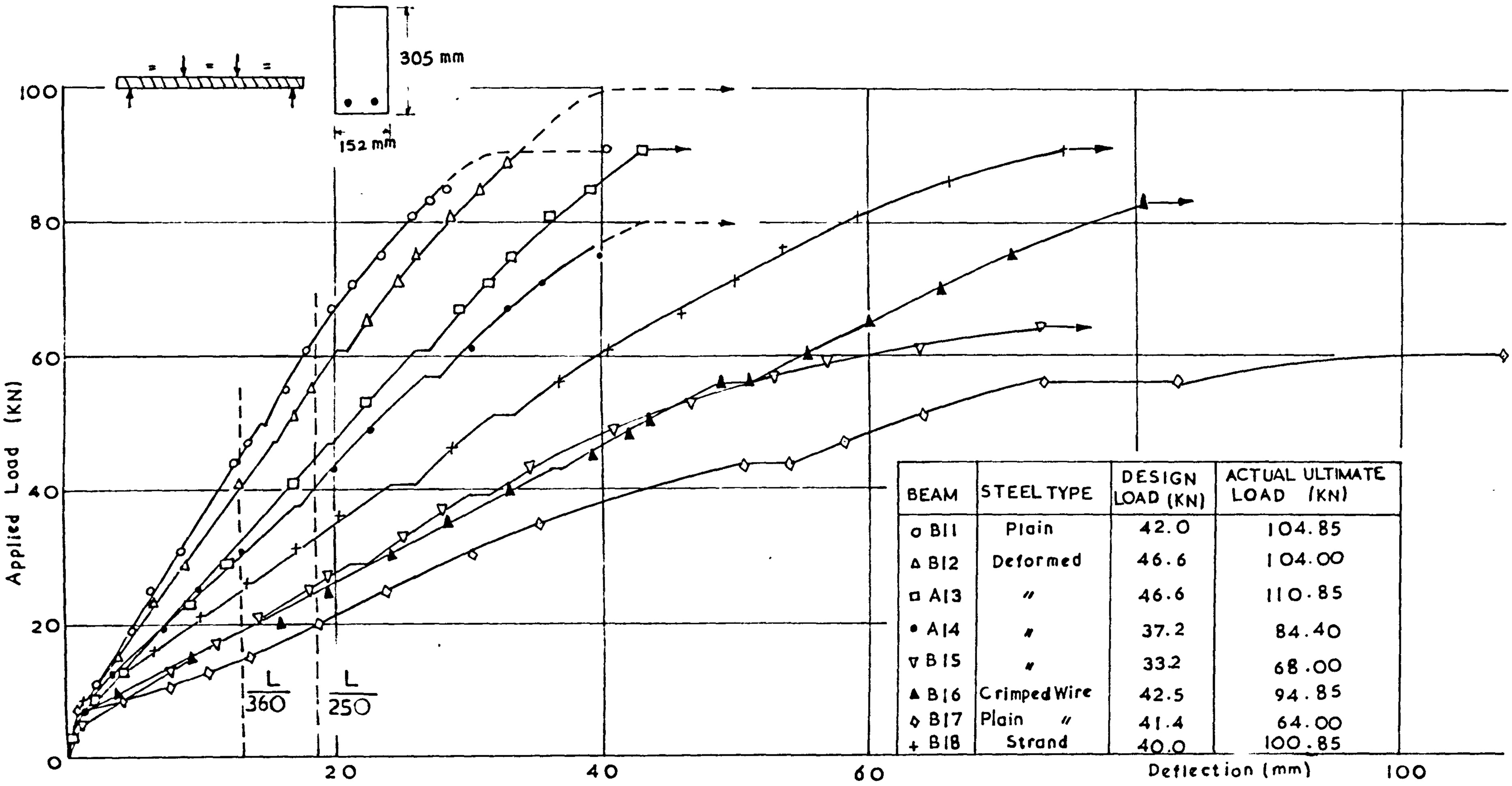

BEAM	STEEL TYPE	DESIGN LOAD (KN)	ACTUAL ULTIMATE LOAD (KN)
o B11	Plain	42.0	104.85
Δ B12	Deformed	46.6	104.00
□ A13	〃	46.6	110.85
• A14	〃	37.2	84.40
▽ B15	〃	33.2	68.00
▲ B16	Crimped Wire	42.5	94.85
◇ B17	Plain 〃	41.4	64.00
+ B18	Strand	40.0	100.85

FIG (66) LOAD–DEFLECTION CURVES (STATIC LOAD VIRGIN CYCLES)

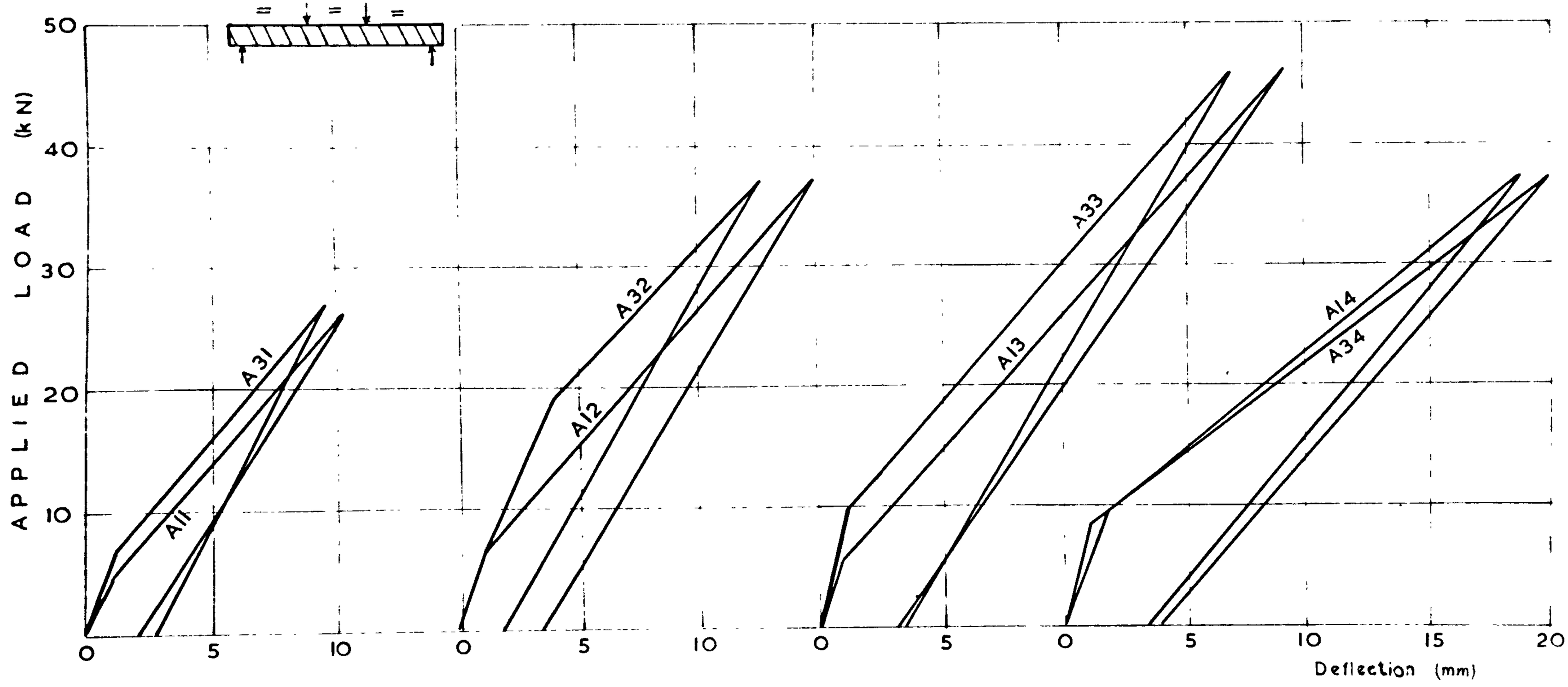

FIG.(67) LOAD-DEFLECTION CURVES FIRST & SECOND CYCLES (DUPLICATE BEAMS)

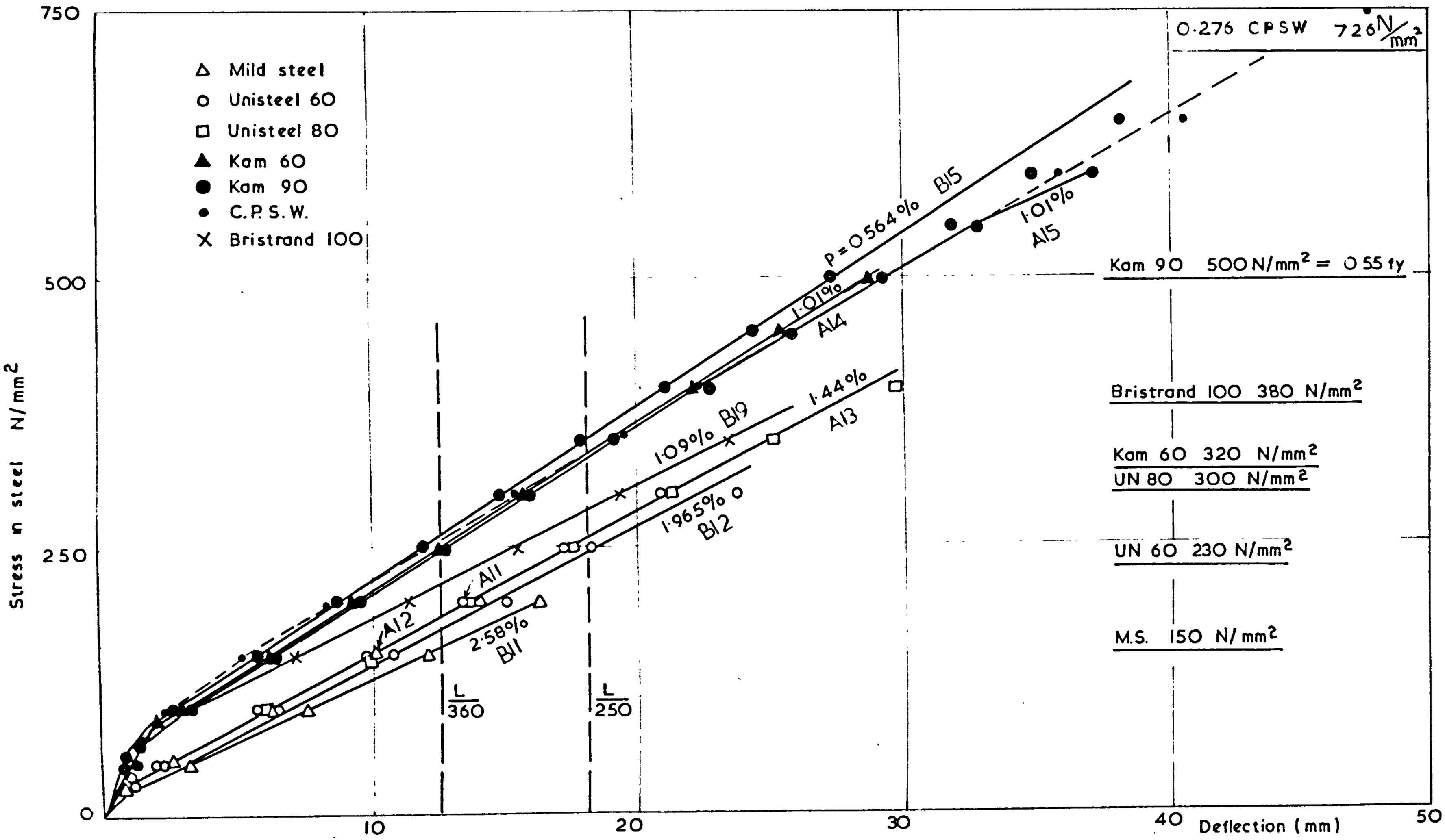

FIG. (68) STEEL STRESS–DEFLECTION CURVES (STATIC LOAD – VIRGIN CYCLES)

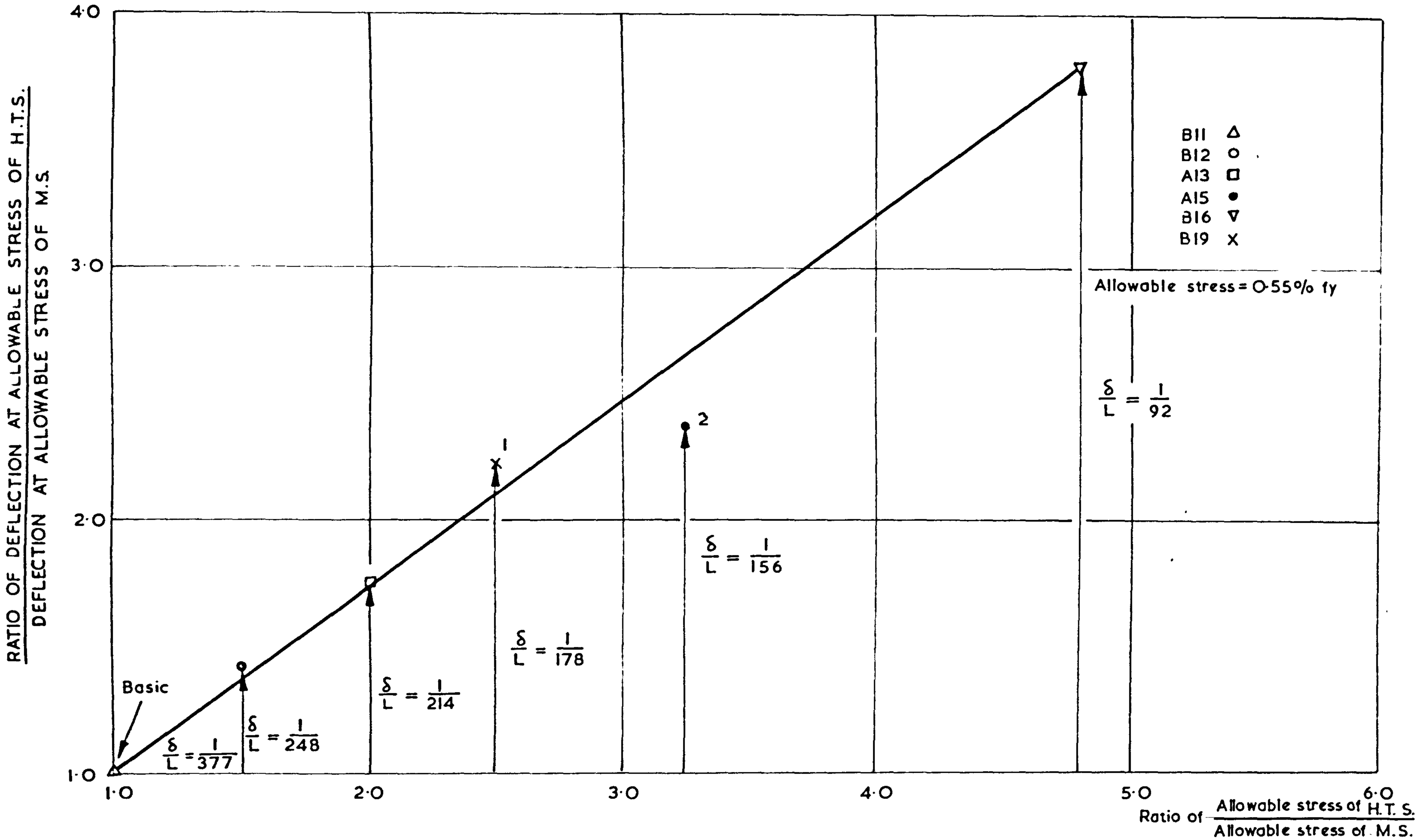

FIG.(69) EFFECT OF HIGH TENSILE STEEL (H.T.S.) ON DEFLECTION.

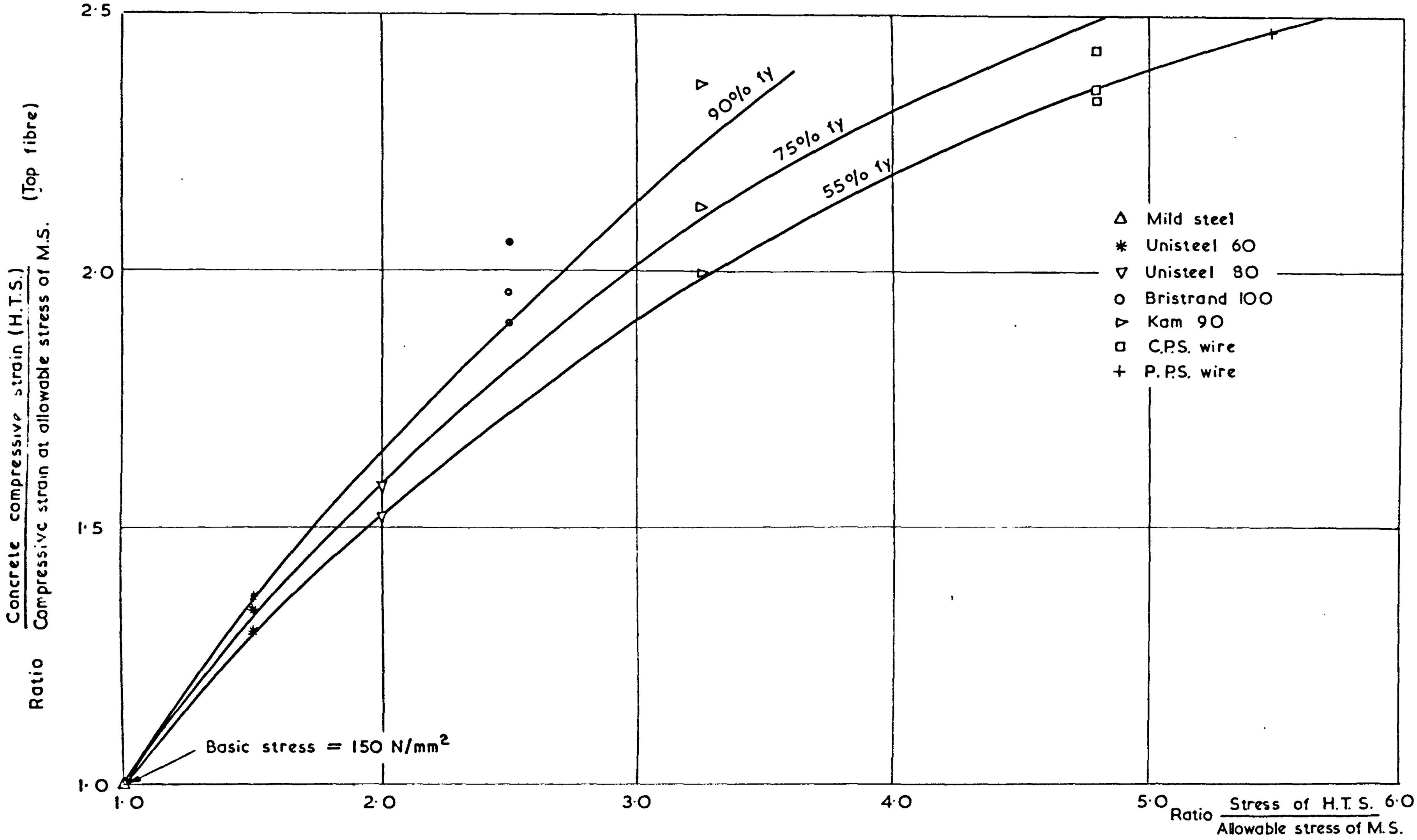

FIG. (70) EFFECT OF HIGH TENSILE STEEL ON STRAIN OF CONCRETE

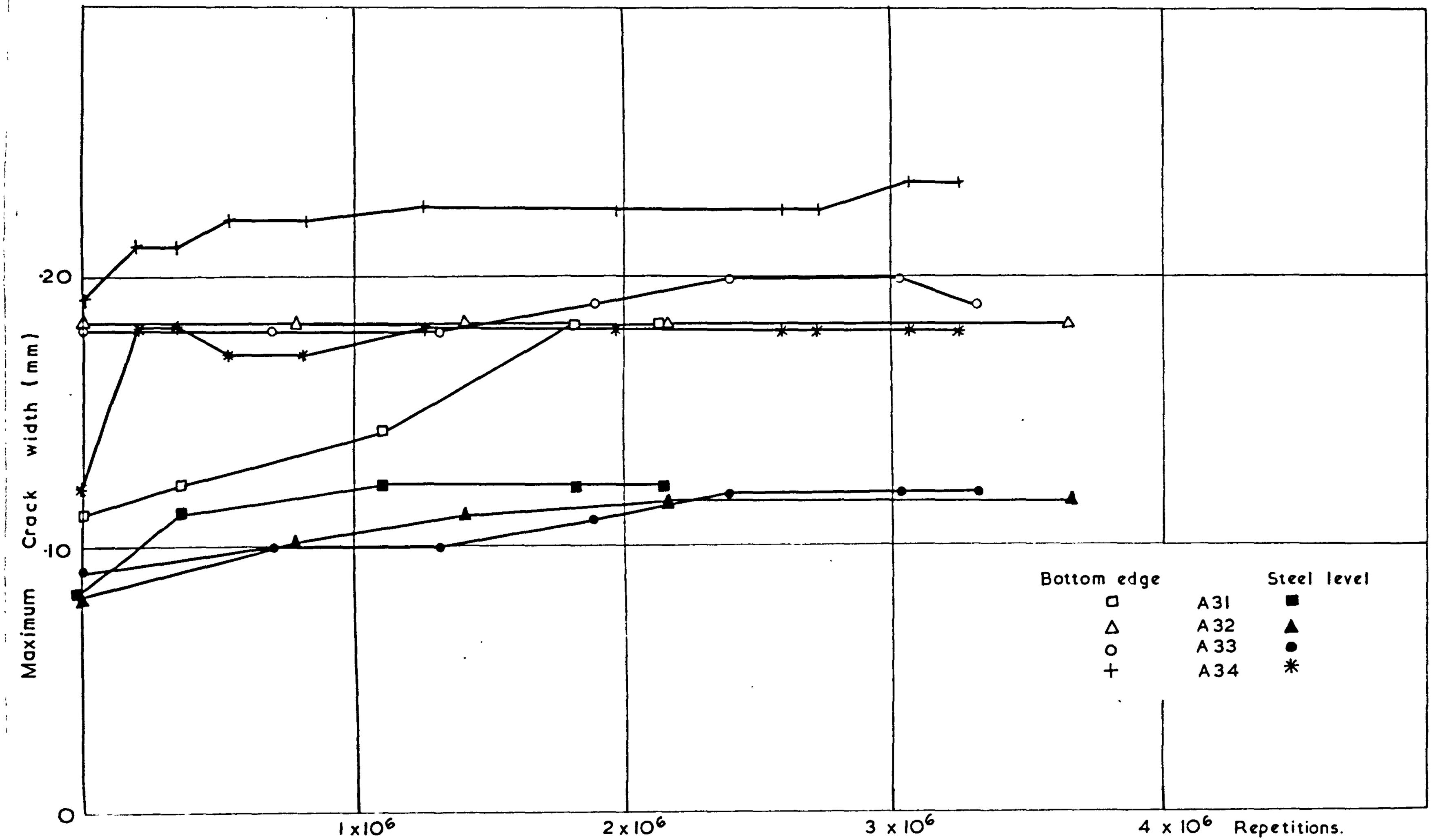

FIG.(71) VARIATION IN CRACK WIDTH UNDER REPEATED LOADING.

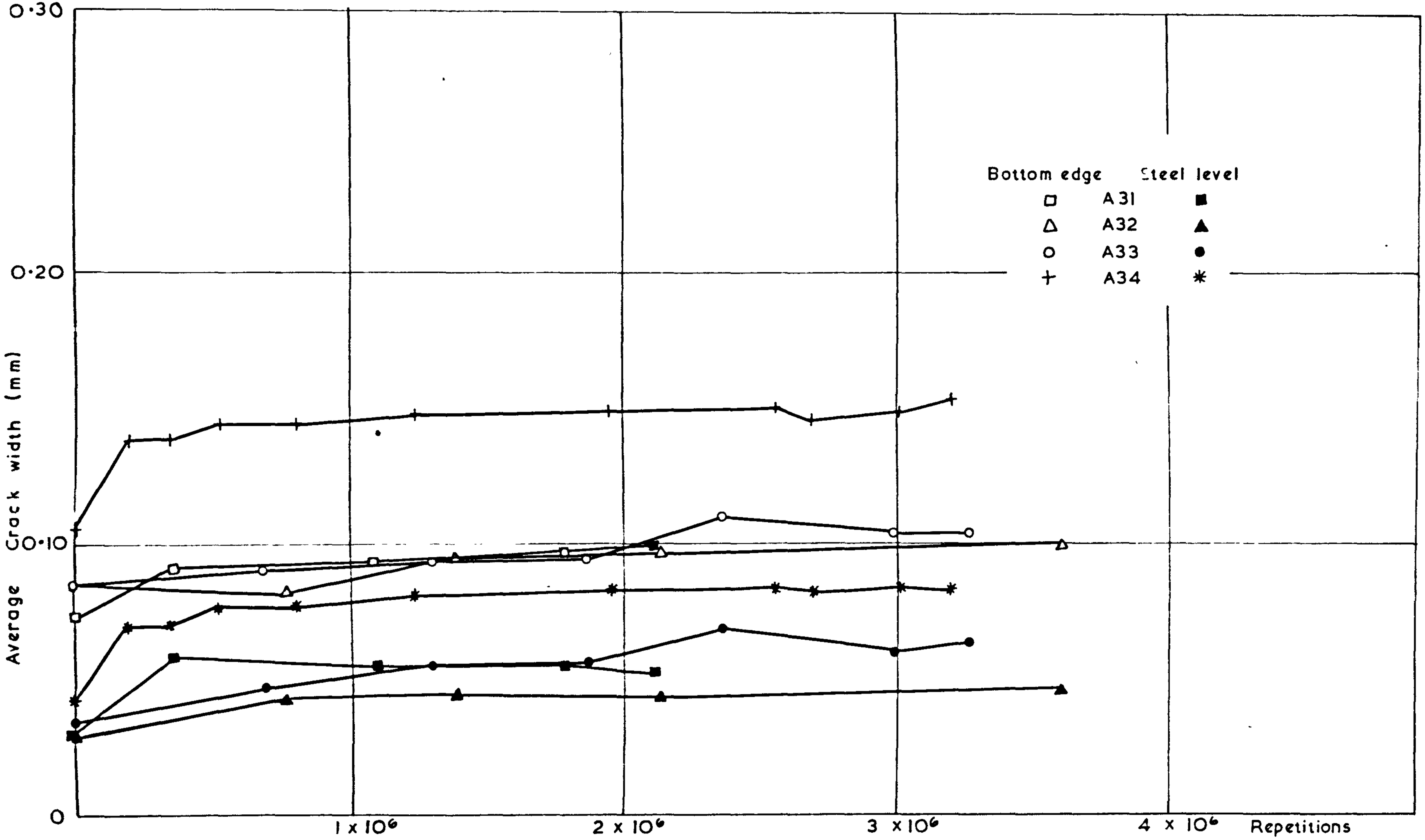

FIG.(72) VARIATION IN CRACK WIDTH UNDER REPEATED LOADING.

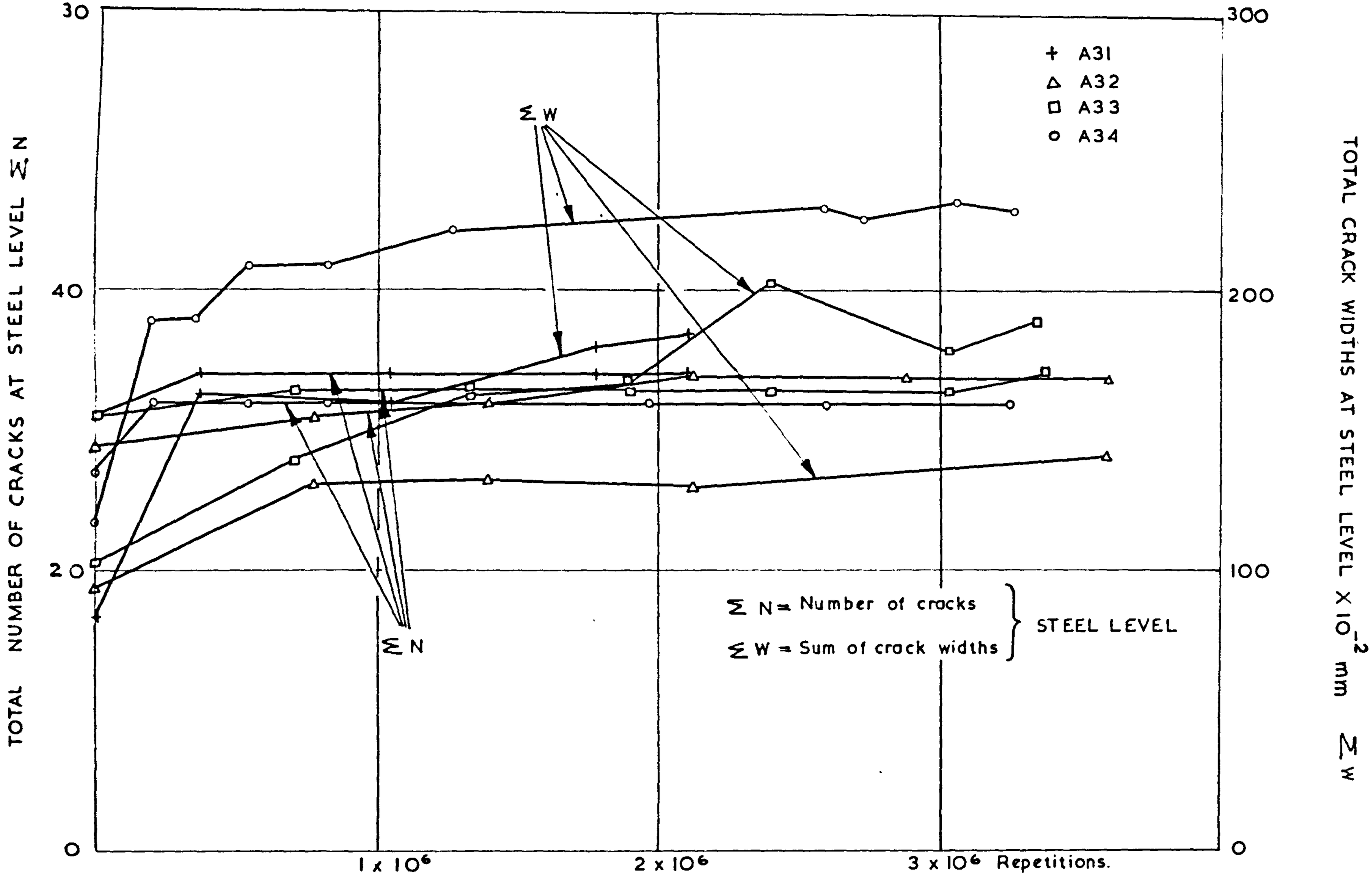

FIG. (73) EFFECT OF REPEATED LOADING ON CRACKING.

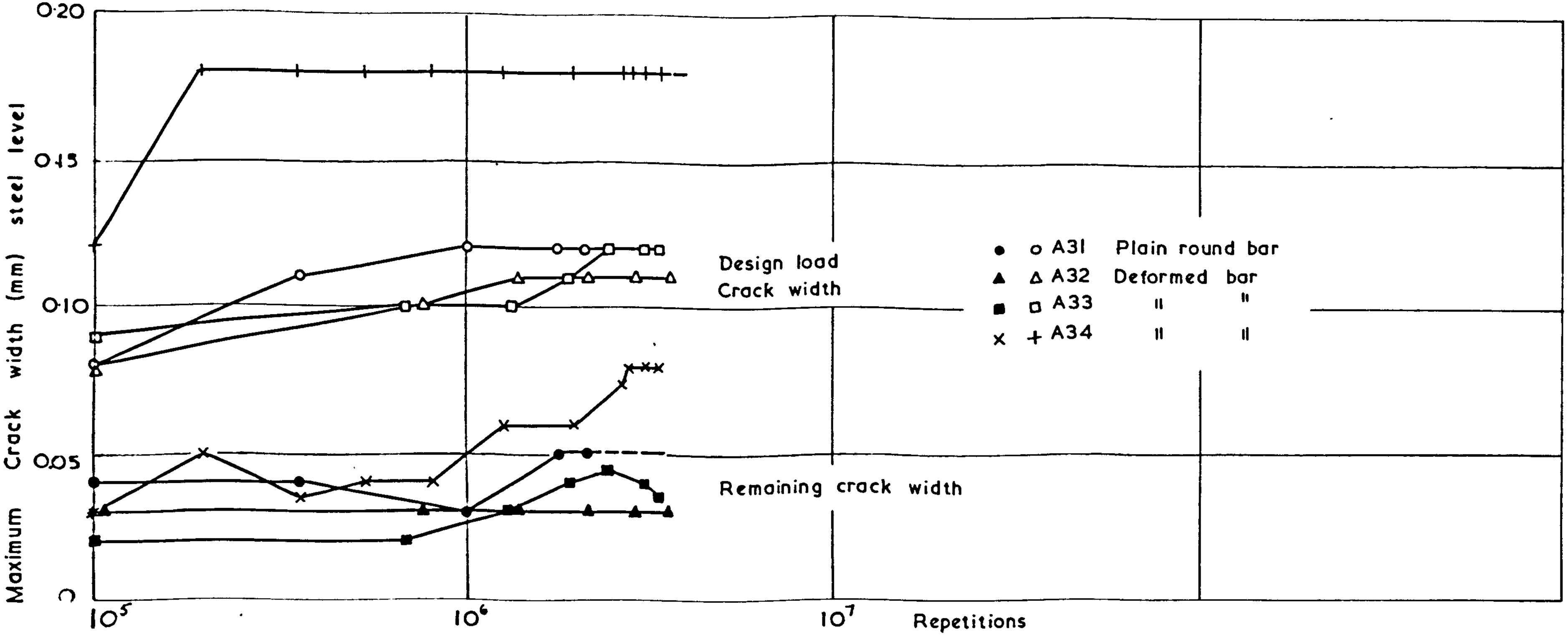

FIG.(74) INCREASE IN CRACK WIDTH UNDER REPEATED LOADING.

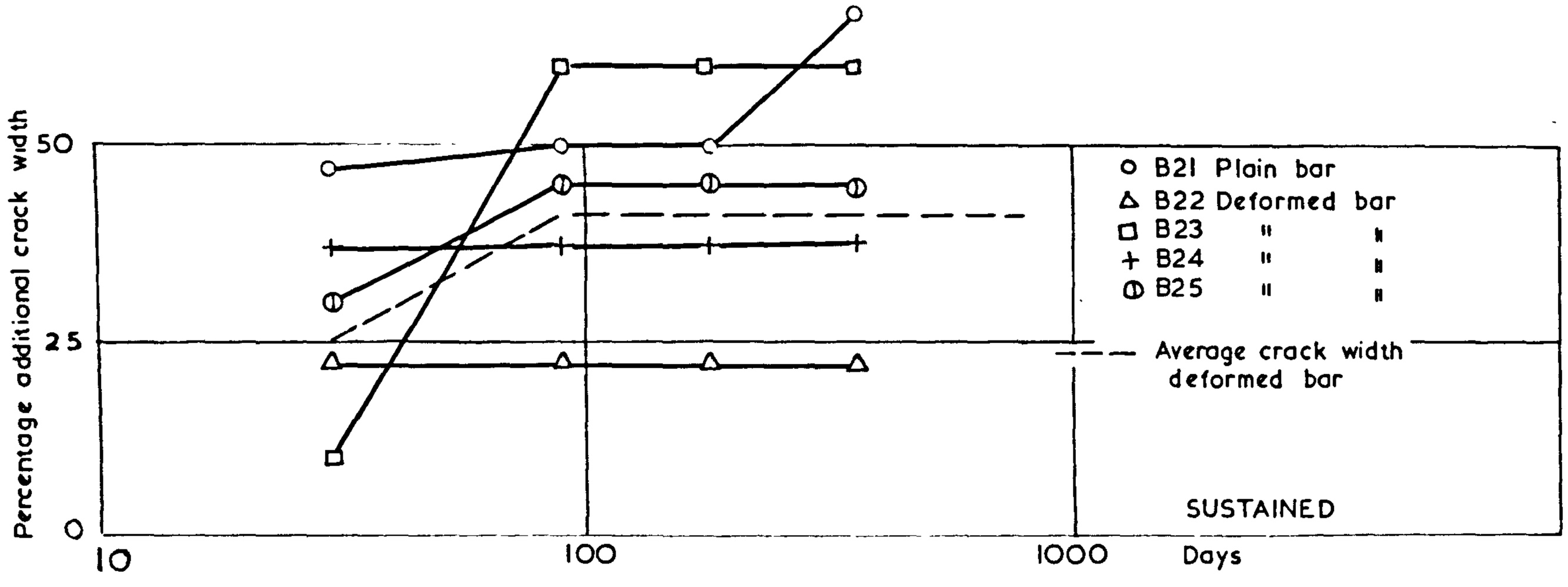

FIG.(75) ADDITIONAL CRACK WIDTH UNDER SUSTAINED AND REPEATED LOADING.

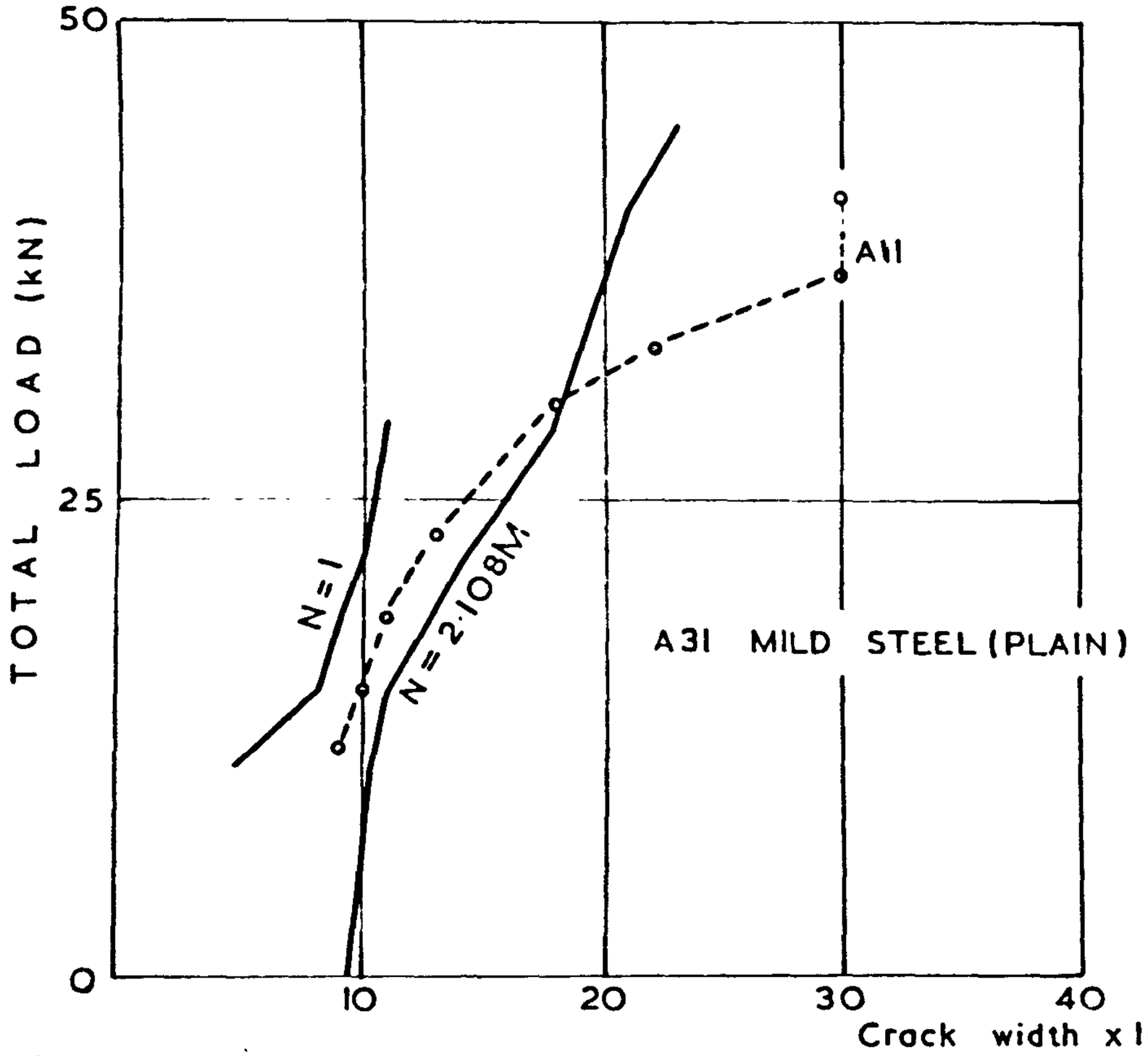

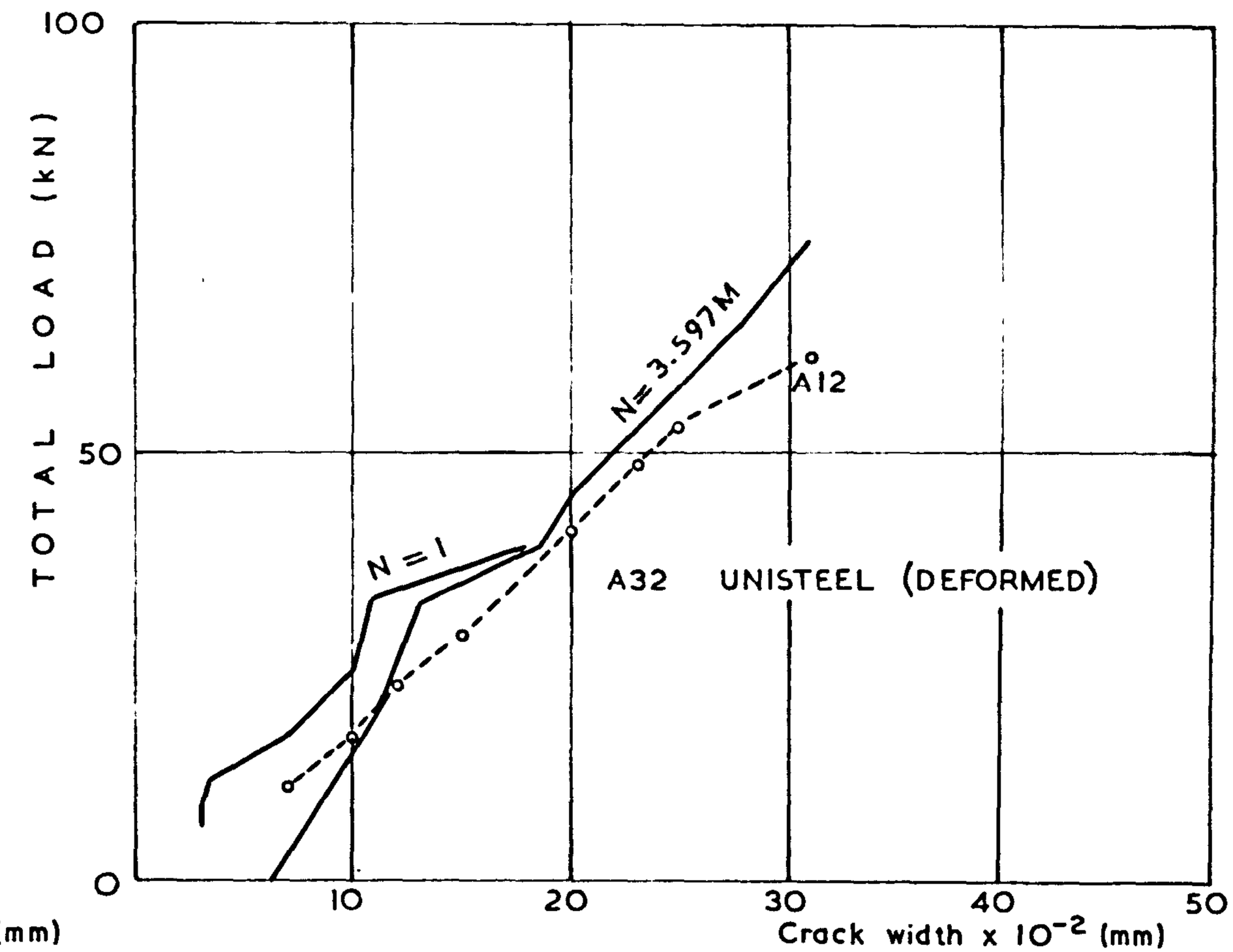

FIG. (76) COMPARISON OF STATIC AND REPEATED LOADING BEAMS. (CRACKS AT STEEL LEVEL)

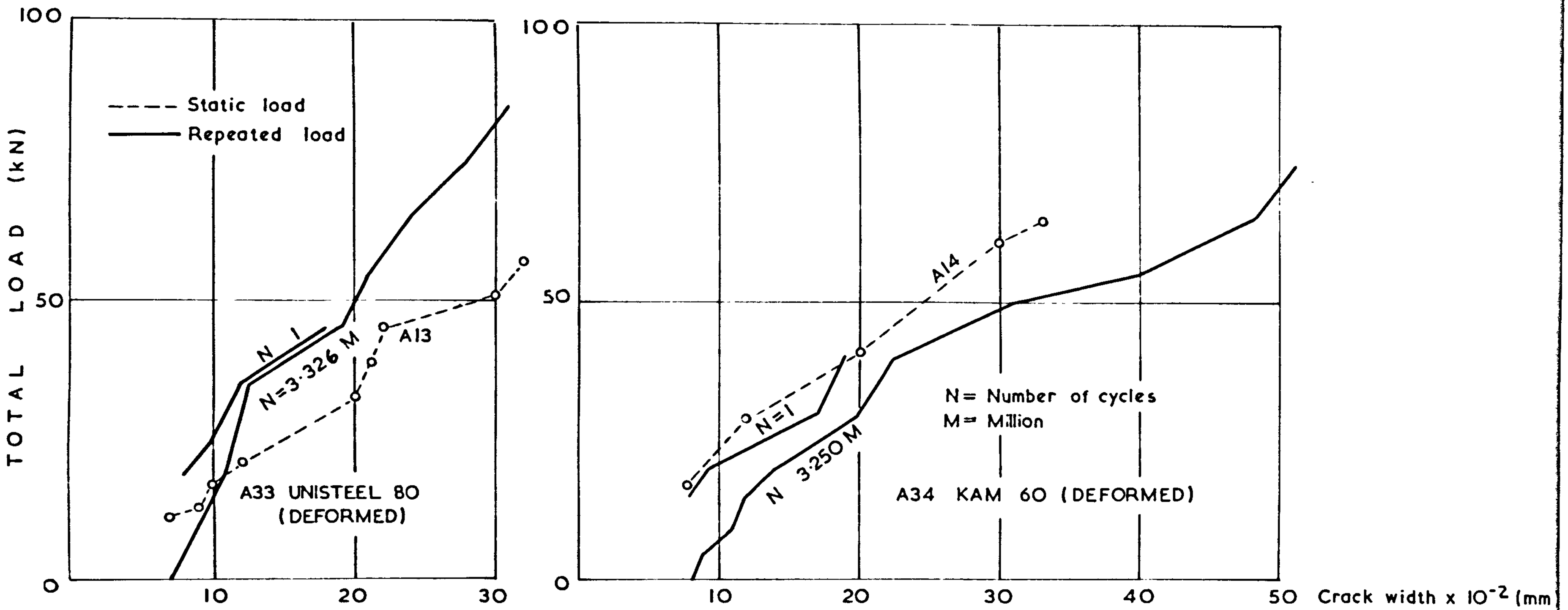

FIG. (77) COMPARISON OF STATIC AND REPEATED LOADING BEAMS (CRACKS AT STEEL LEVEL)

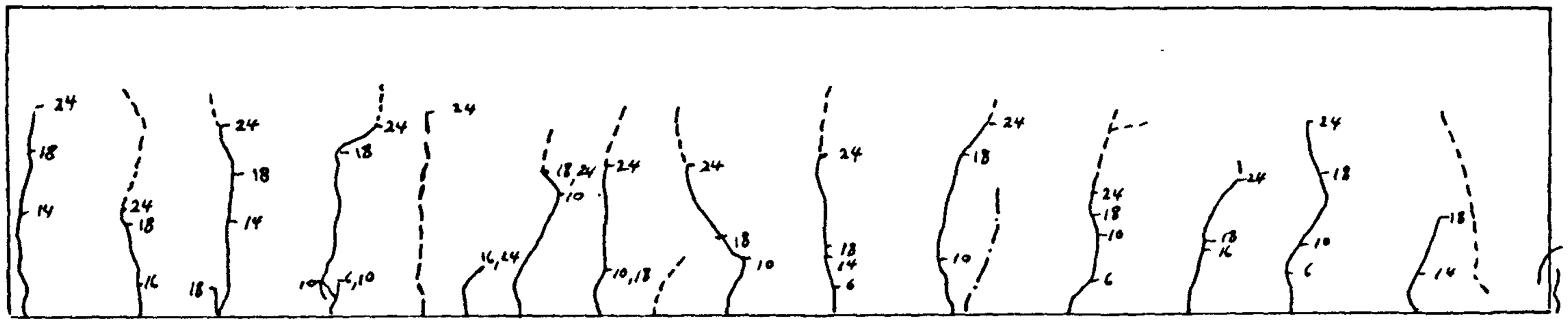

BEAM A31

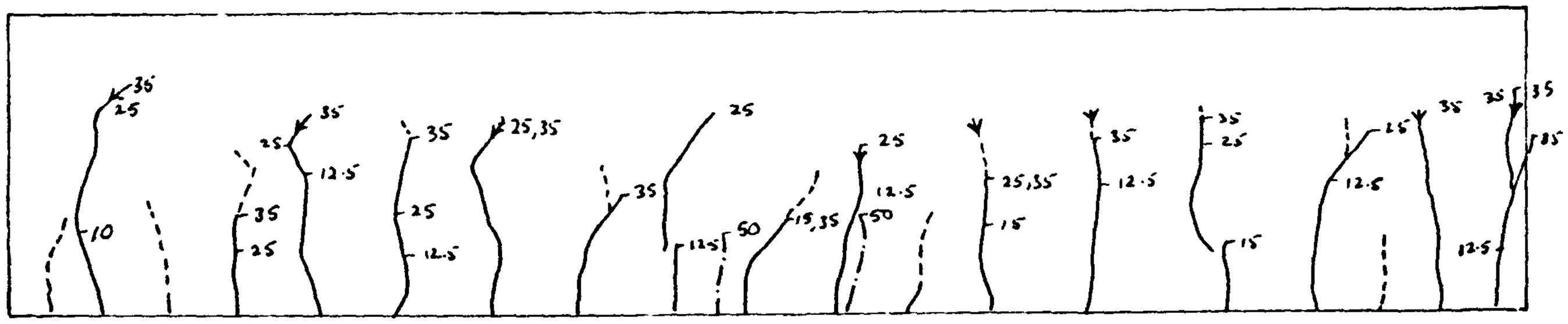

BEAM A34

——— Before Repeated Loading

– – – – – After 350,000 cycles (A31) & 3,250,000 cycles (A34)

—·—·— Near Failure

⟶ Shortening of Cracking Length

Figures on Cracks Indicate Load in (KN)

FIG(78) CRACKING PATTERN(UNDER REPEATED LOADING)

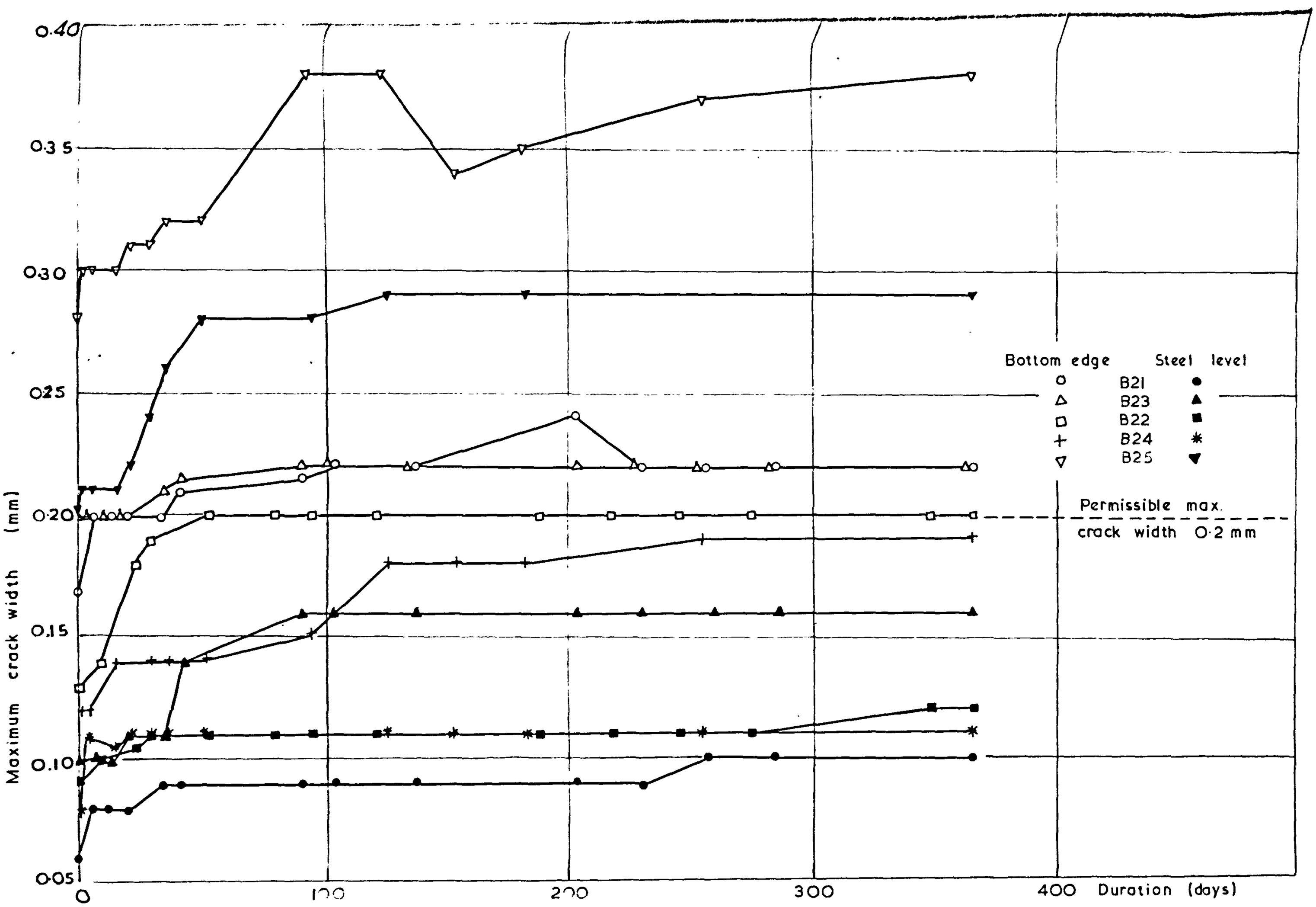

FIG. (79) VARIATION IN CRACK WIDTH UNDER SUSTAINED LOADING.

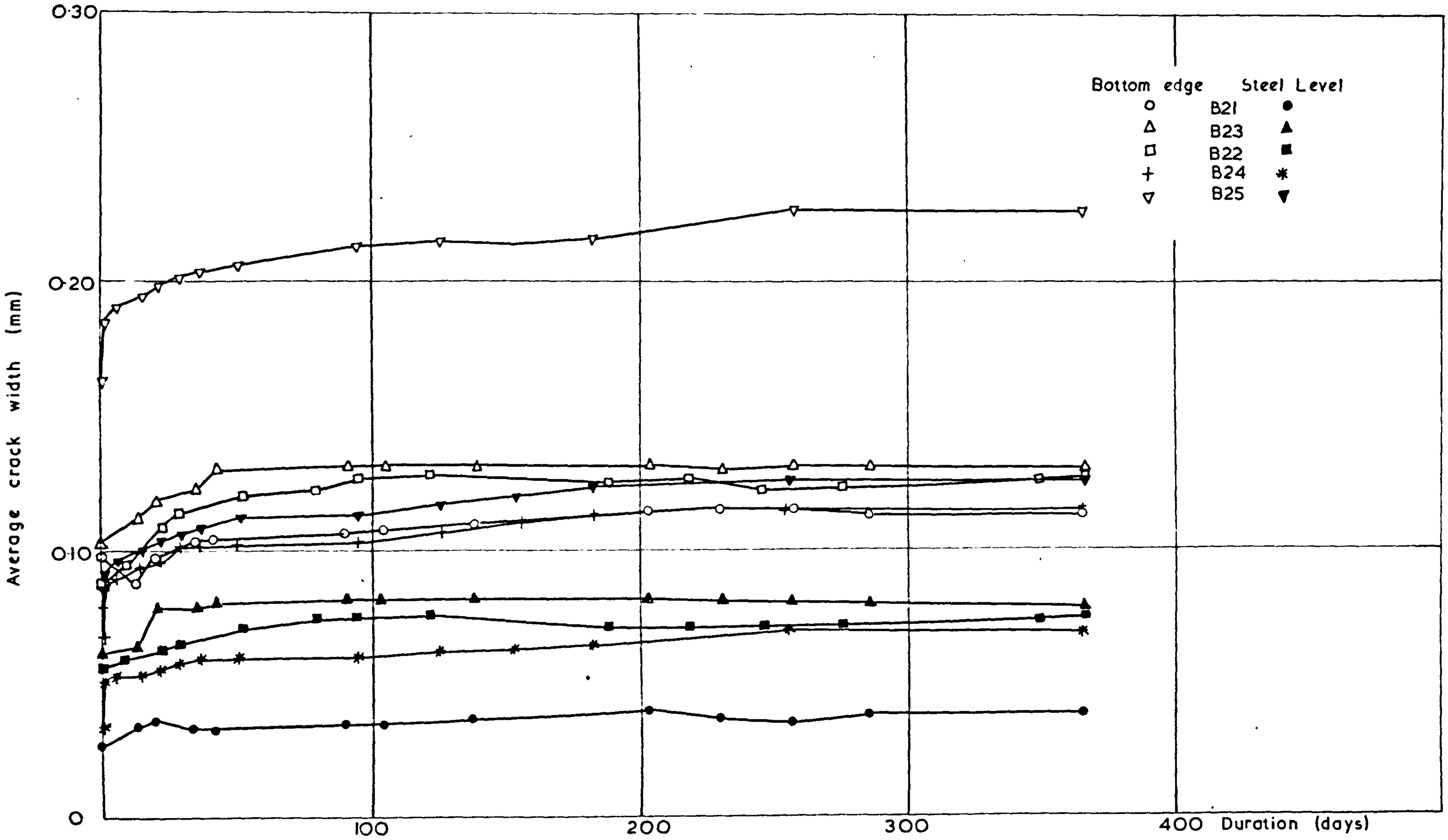

FIG.(8.1) VARIATION IN CRACK WIDTH UNDER SUSTAINED LOADING.

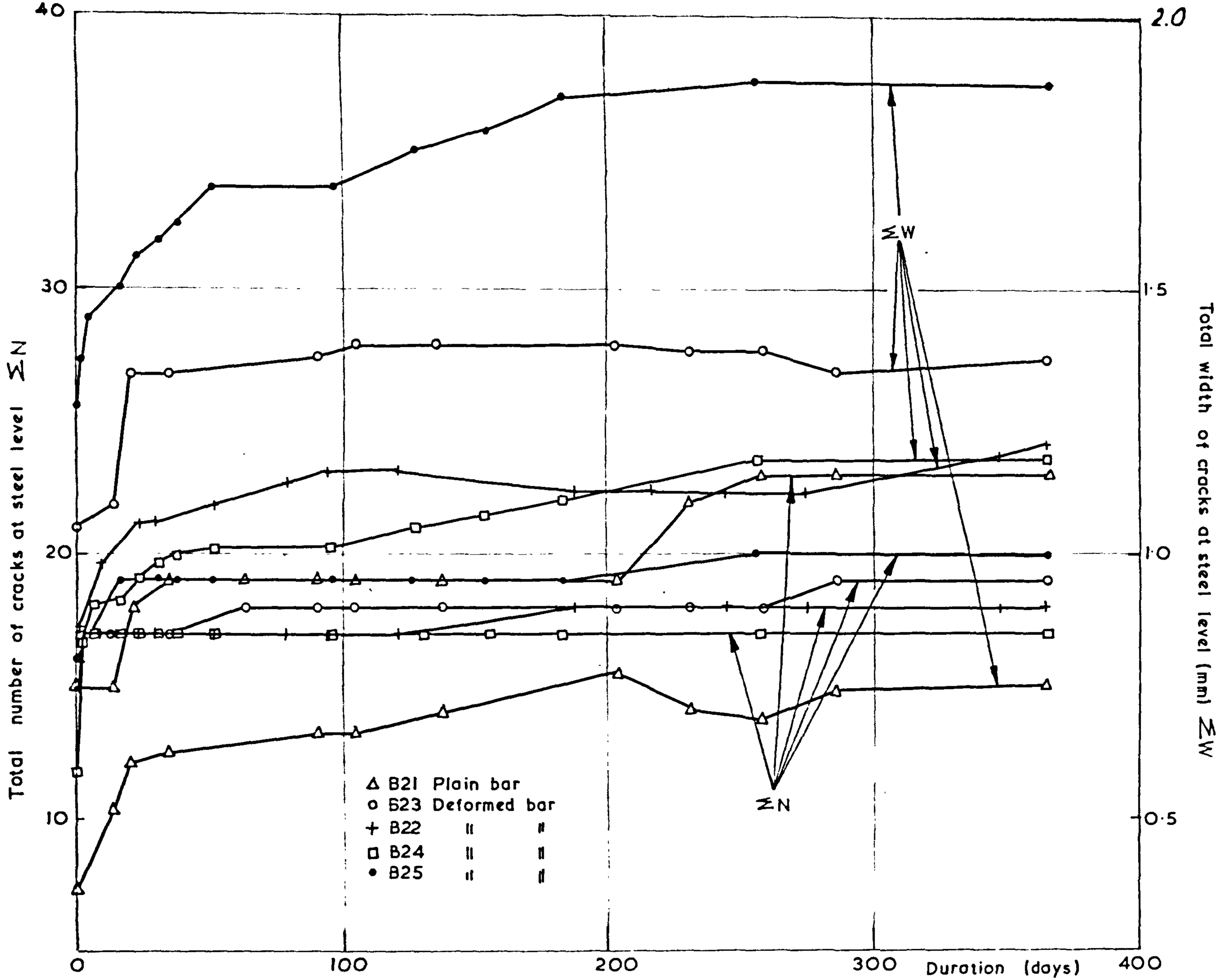

FIG.(81) EFFECT OF SUSTAINED LOADING ON CRACKING

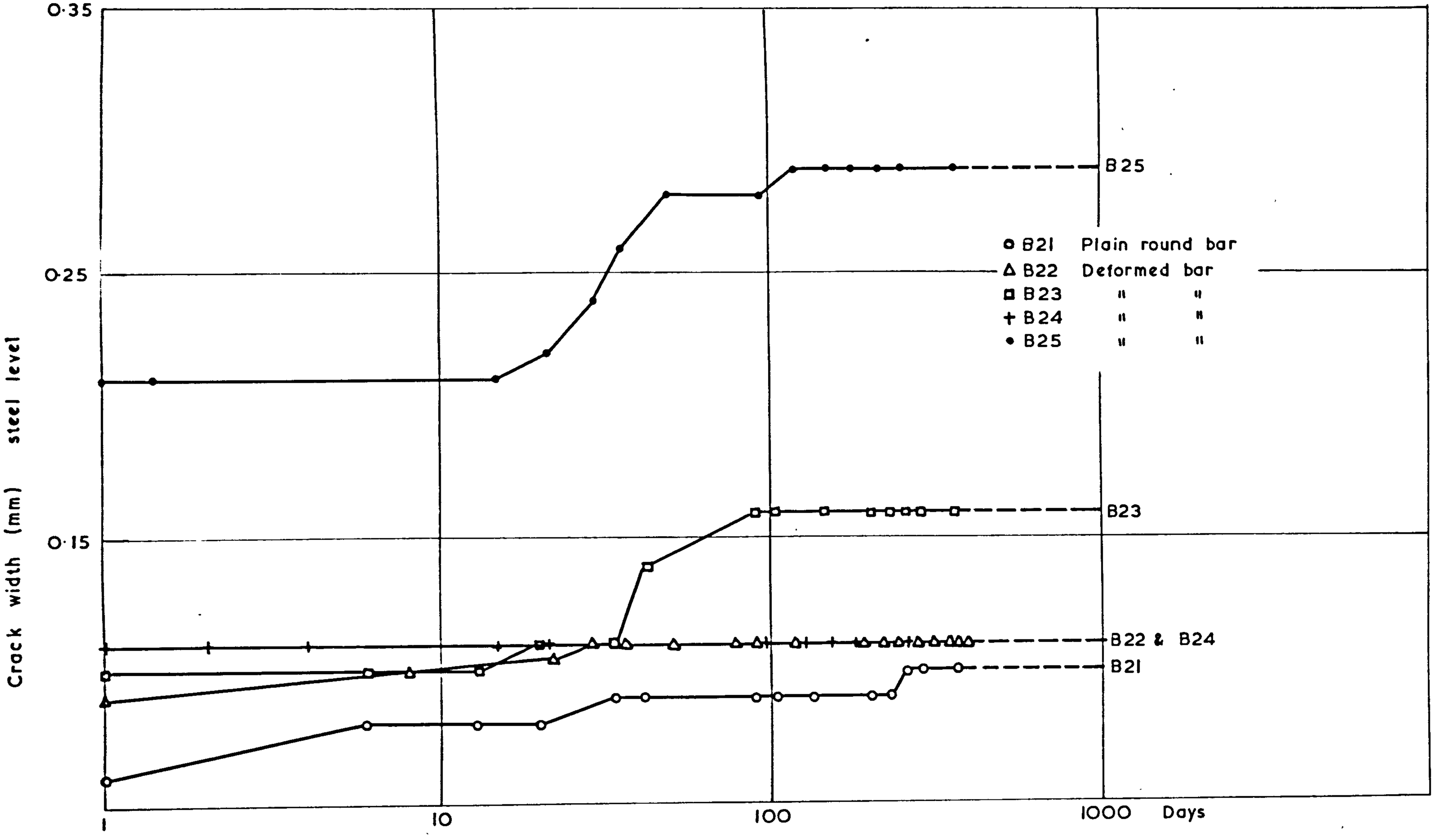

FIG. (8 2) INCREASE IN CRACK WIDTH UNDER SUSTAINED LOADING.

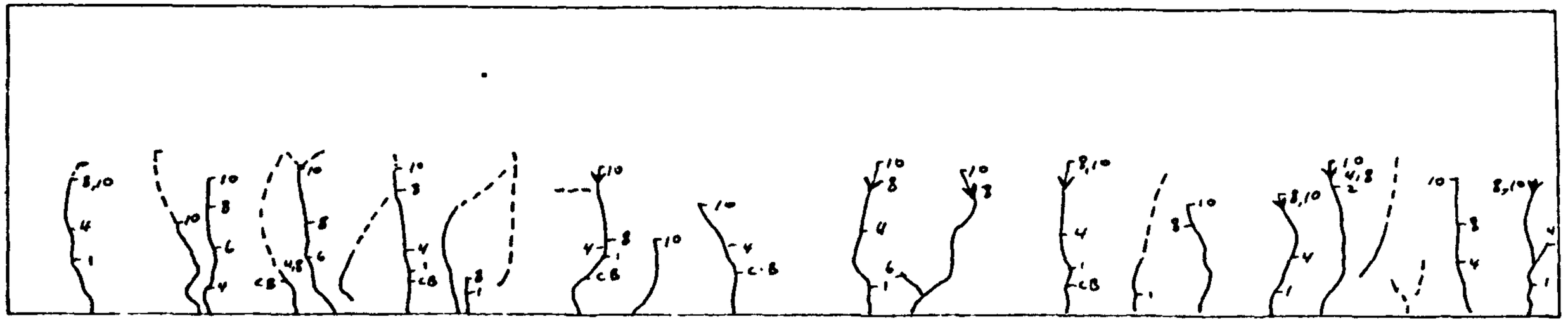

BEAM B21

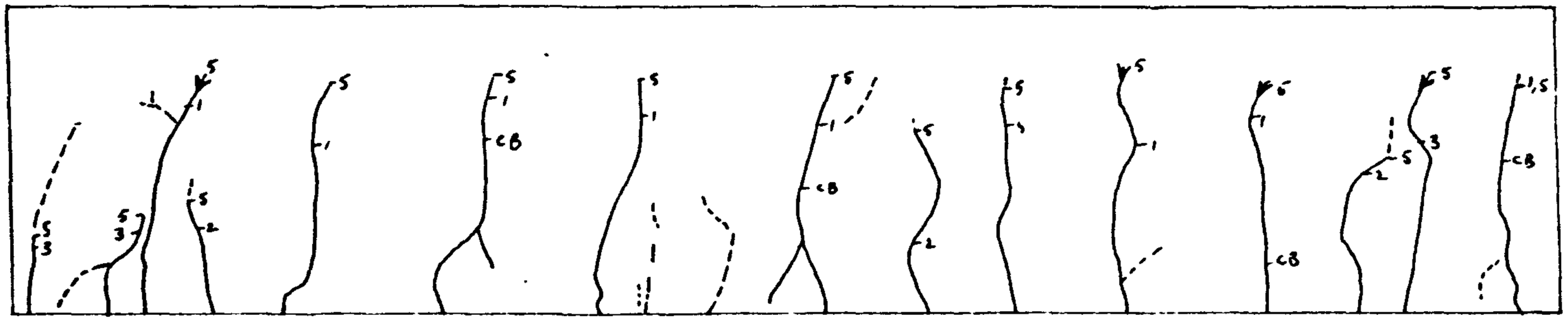

BEAM B25

——— Original Crack

– – – – – New Crack Formation

——→ Shortening of Crack Length

C.B. Weight of Sustained Loading Arrangement

Figures on Cracks Indicate Load (KN)

FIG (83) CRACKING PATTERN (UNDER SUSTAINED LOADING)
ONE YEAR

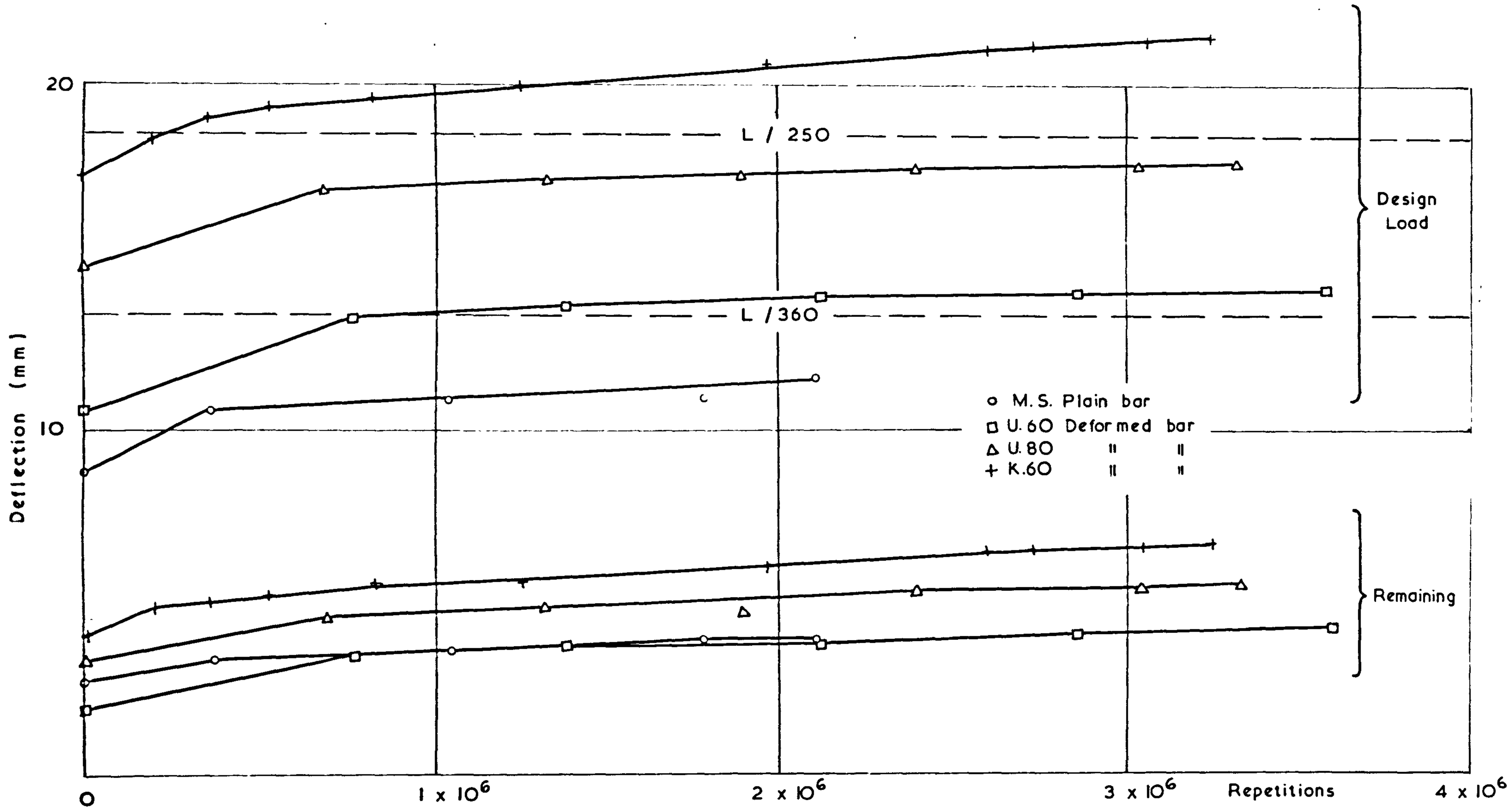

FIG. (84) INCREASE IN DEFLECTION UNDER REPEATED LOADING.

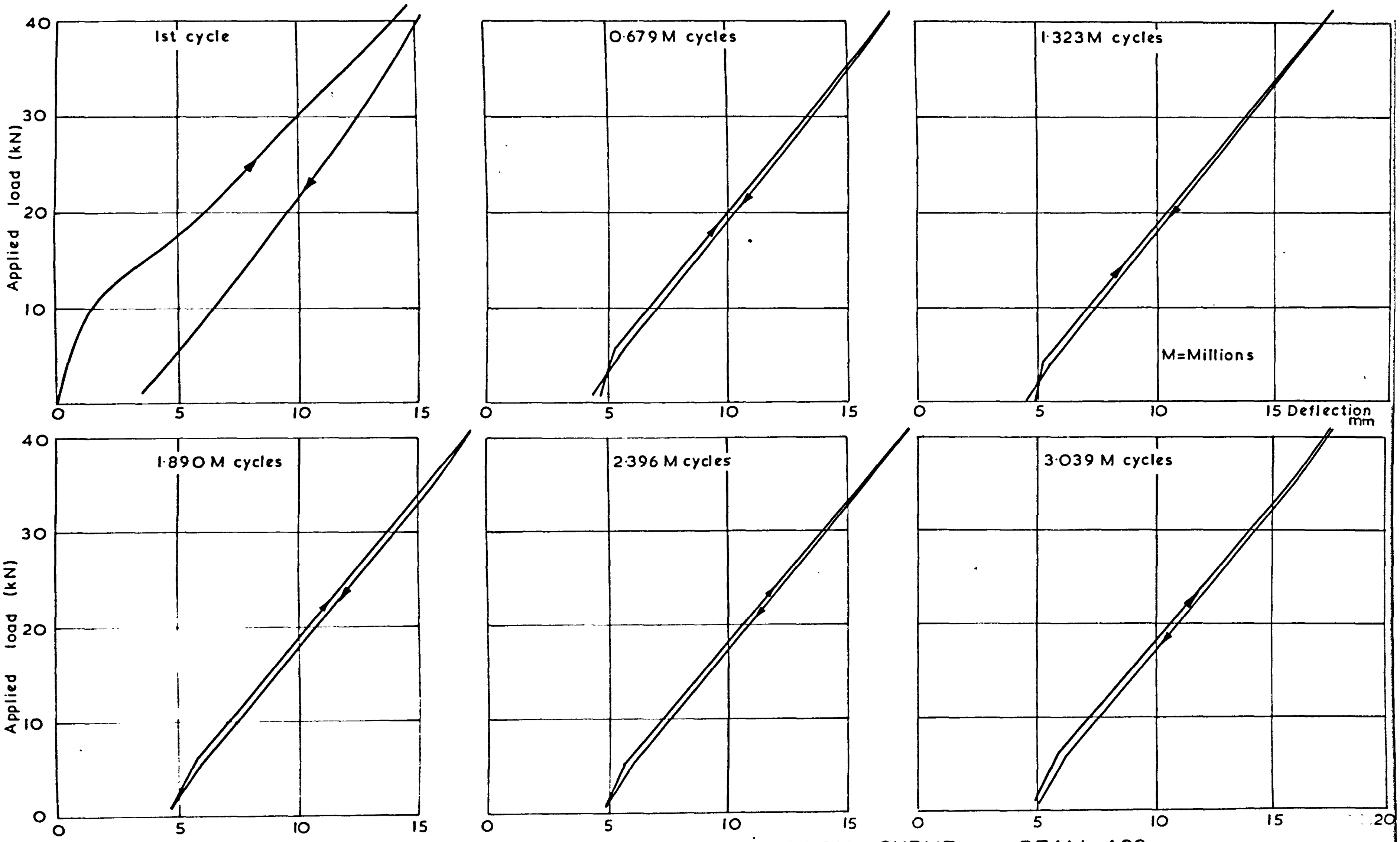

FIG. 85 EFFECT OF REPEATED LOADING ON LOAD-DEFLECTION CURVE BEAM A33.

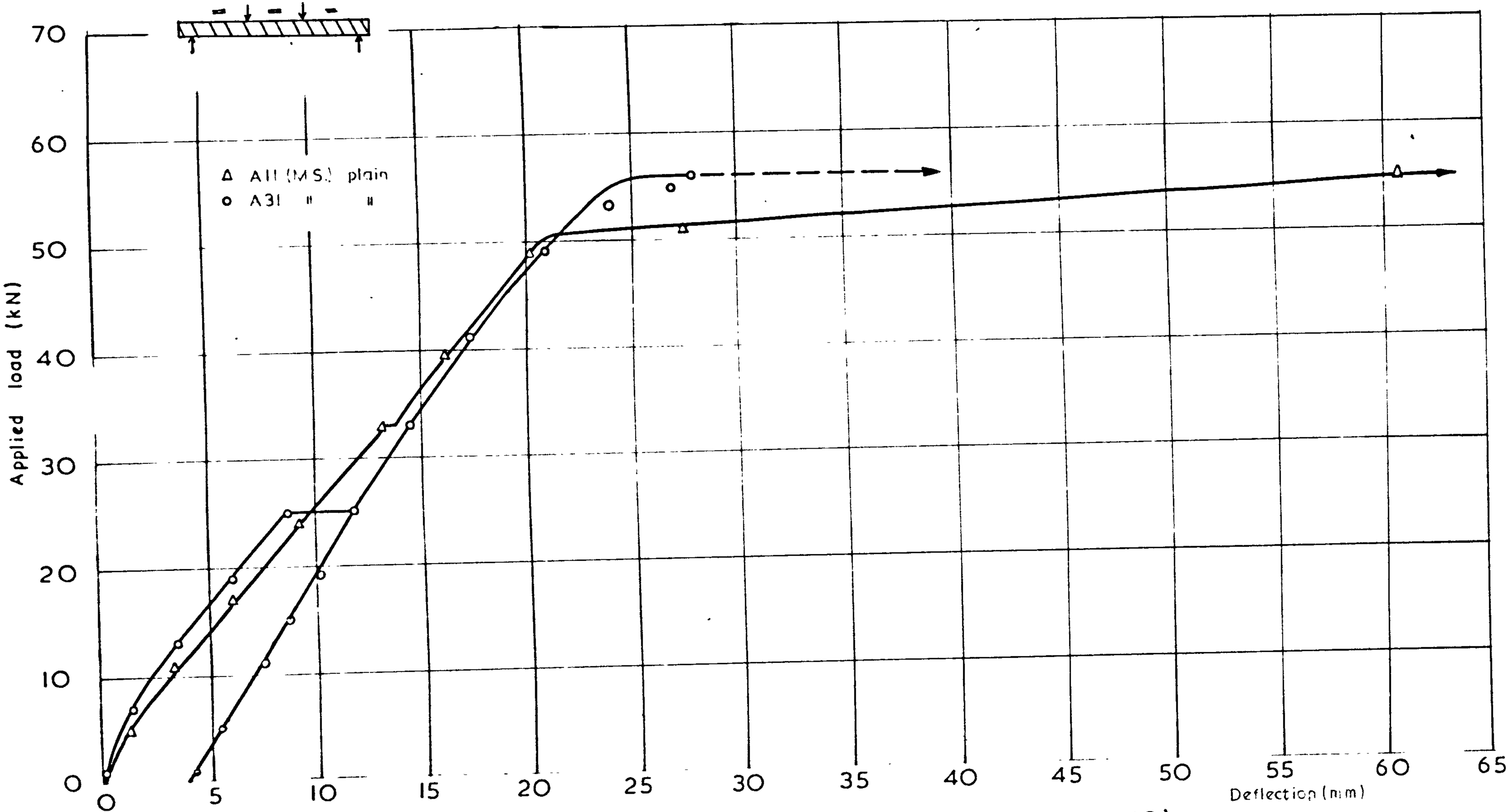

FIG. (86.) LOAD – DEFLECTION CURVE (REPEATED LOADING)

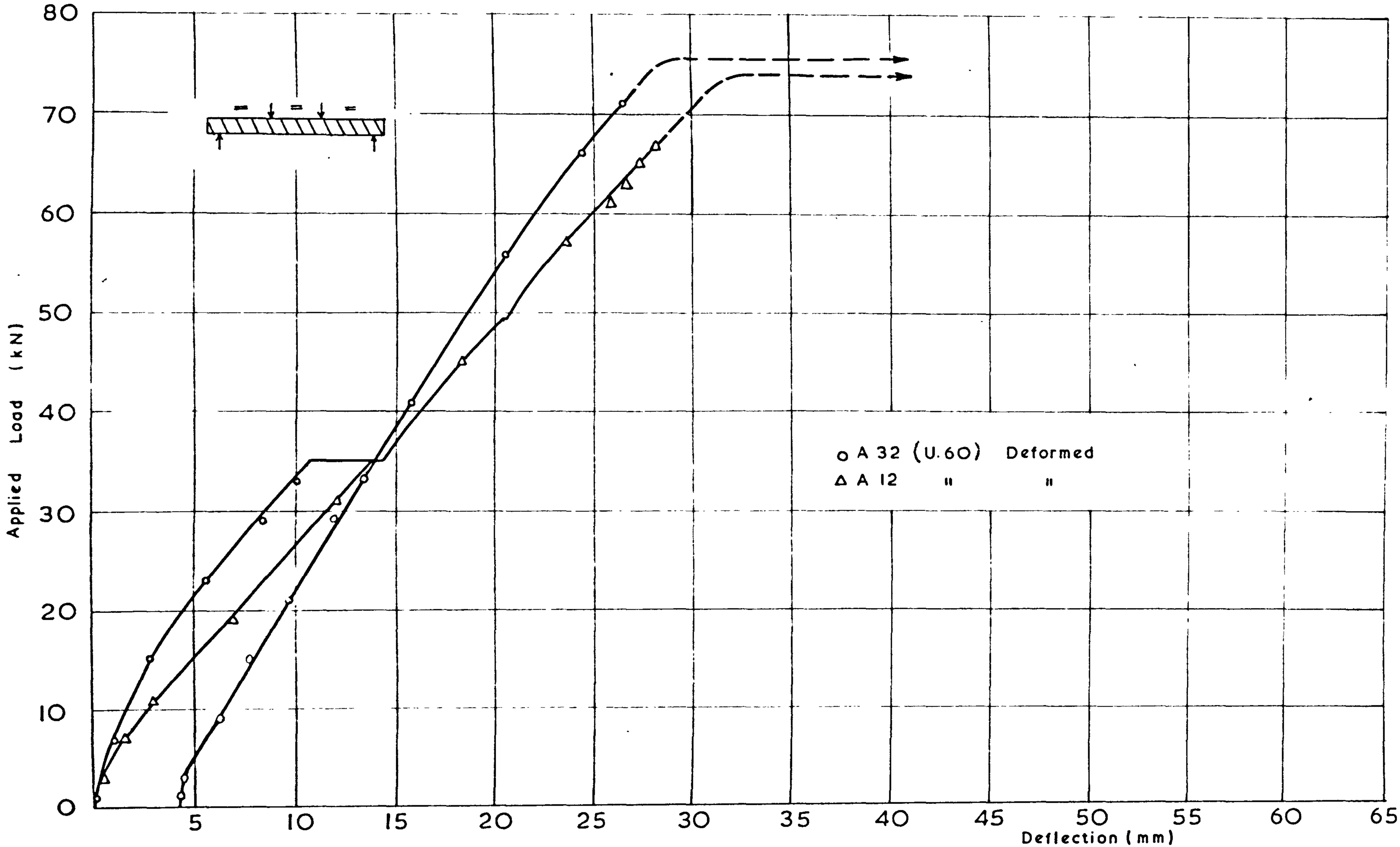

FIG.(8 7) LOAD—DEFLECTION CURVE (REPEATED LOADING)

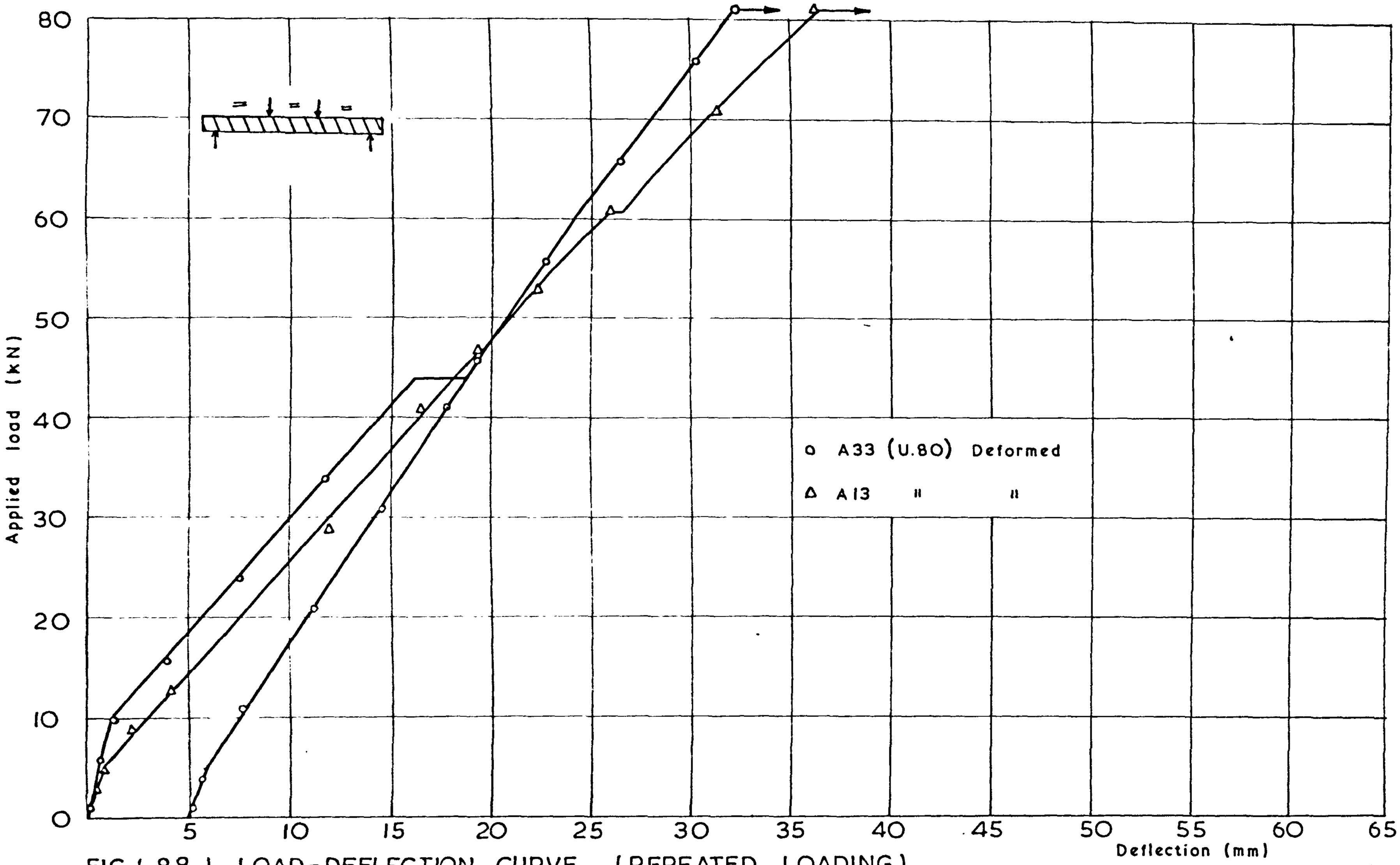

FIG. (88) LOAD-DEFLECTION CURVE (REPEATED LOADING)

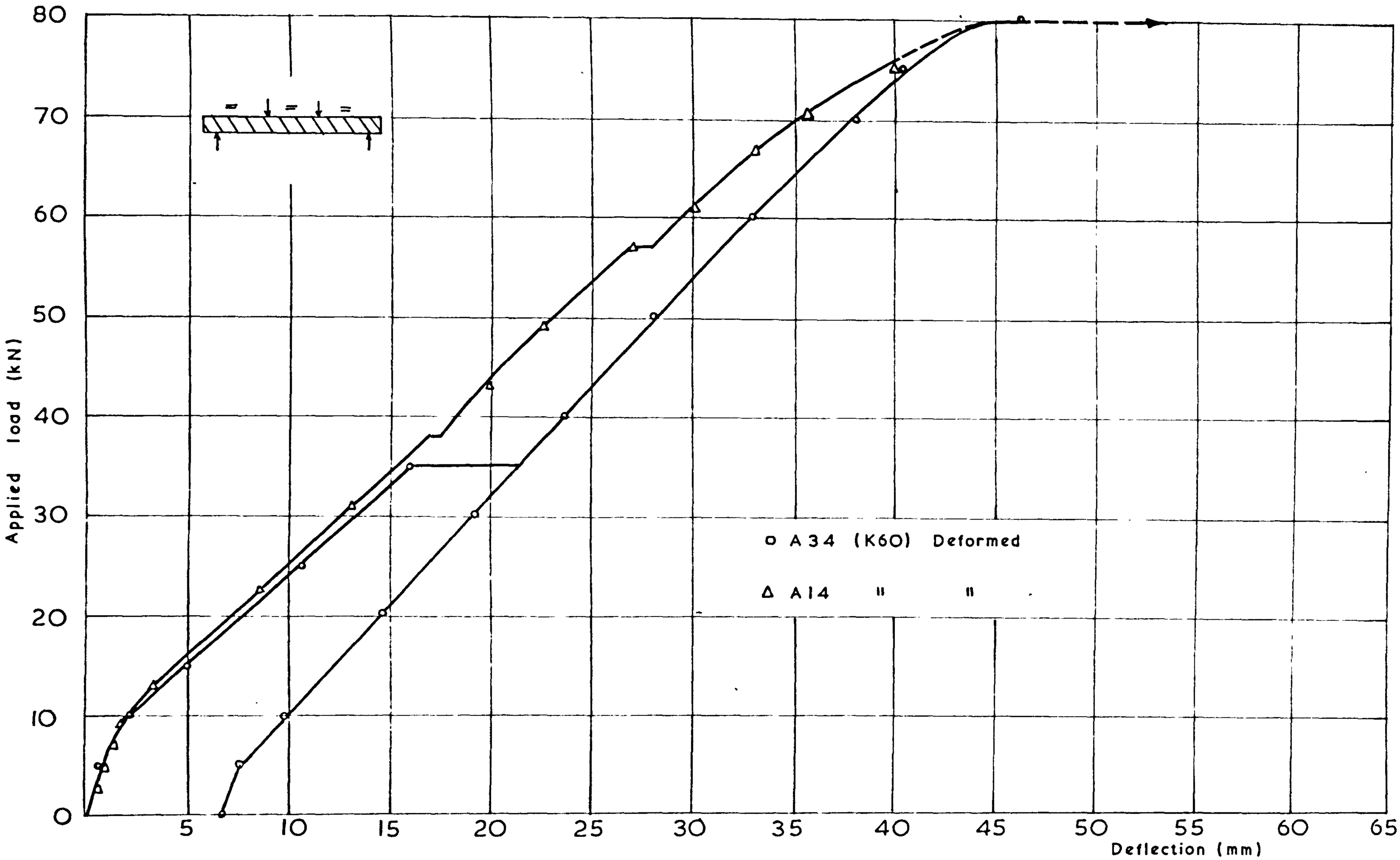

FIG. (89) LOAD- DEFLECTION CURVE (REPEATED LOADING)

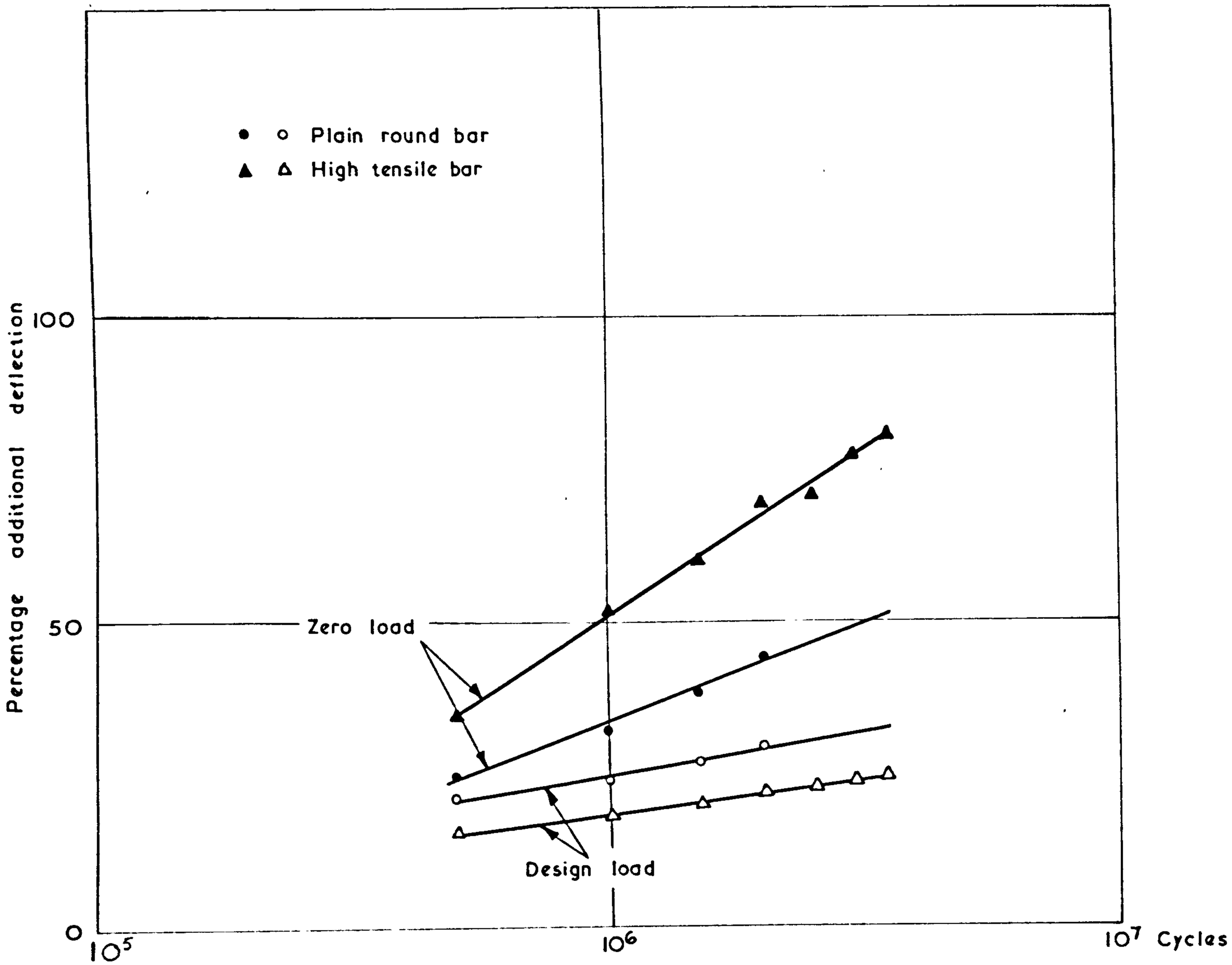

FIG(90) ADDITIONAL DEFLECTION (REPEATED LOADING)

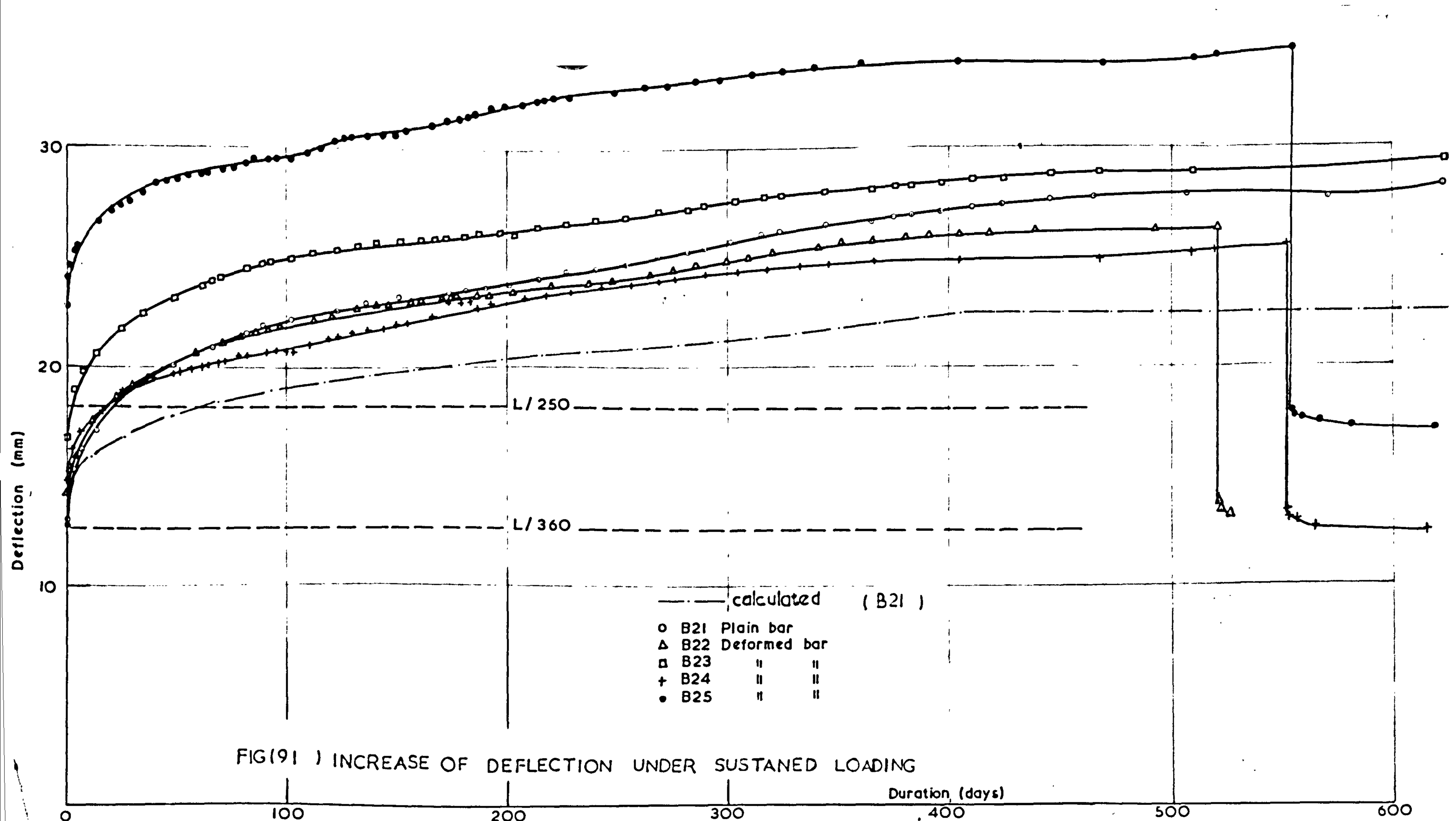

FIG(91) INCREASE OF DEFLECTION UNDER SUSTANED LOADING

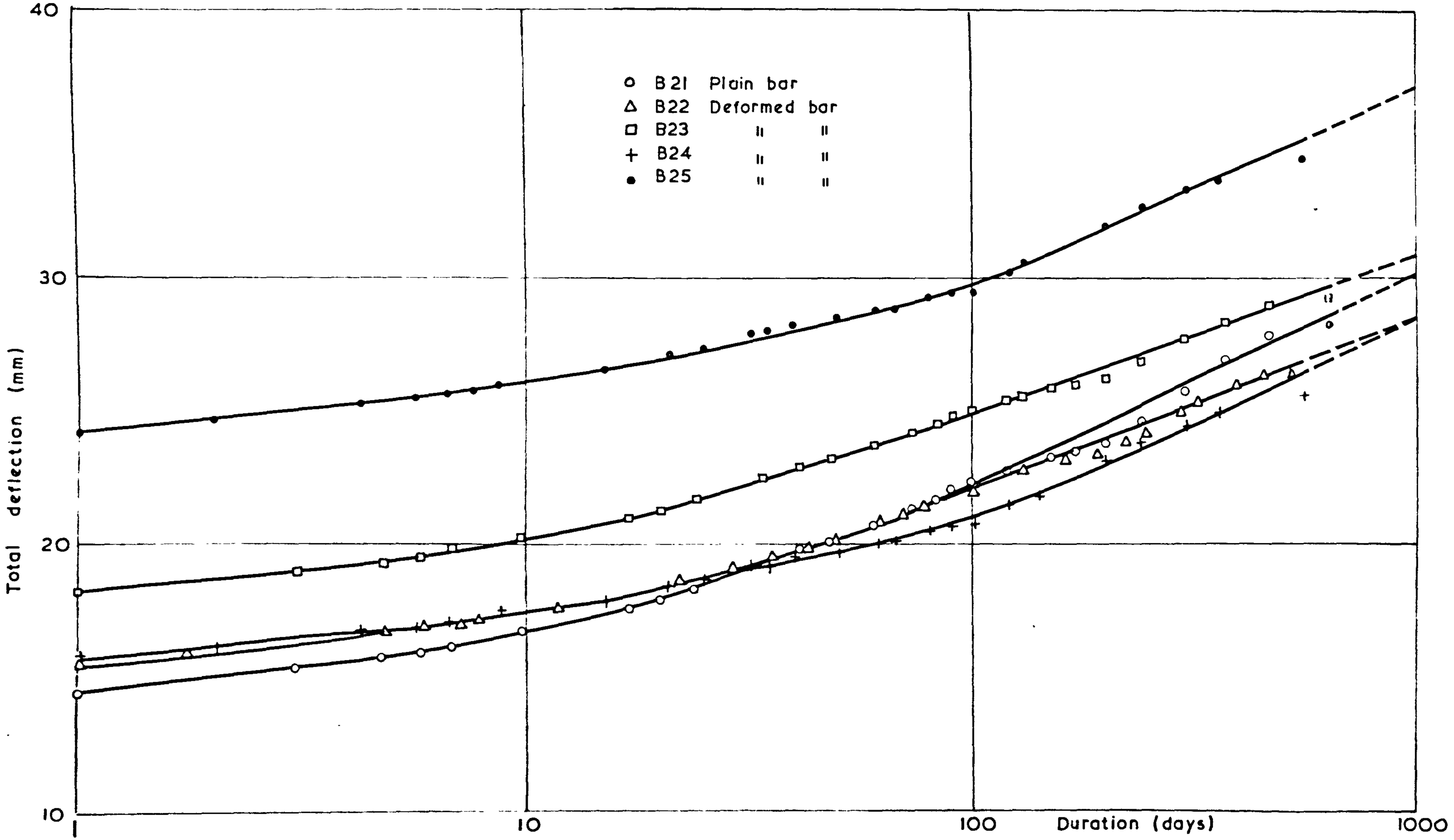

FIG. (92) INCREASE IN DEFLECTION UNDER SUSTAINED LOADING.

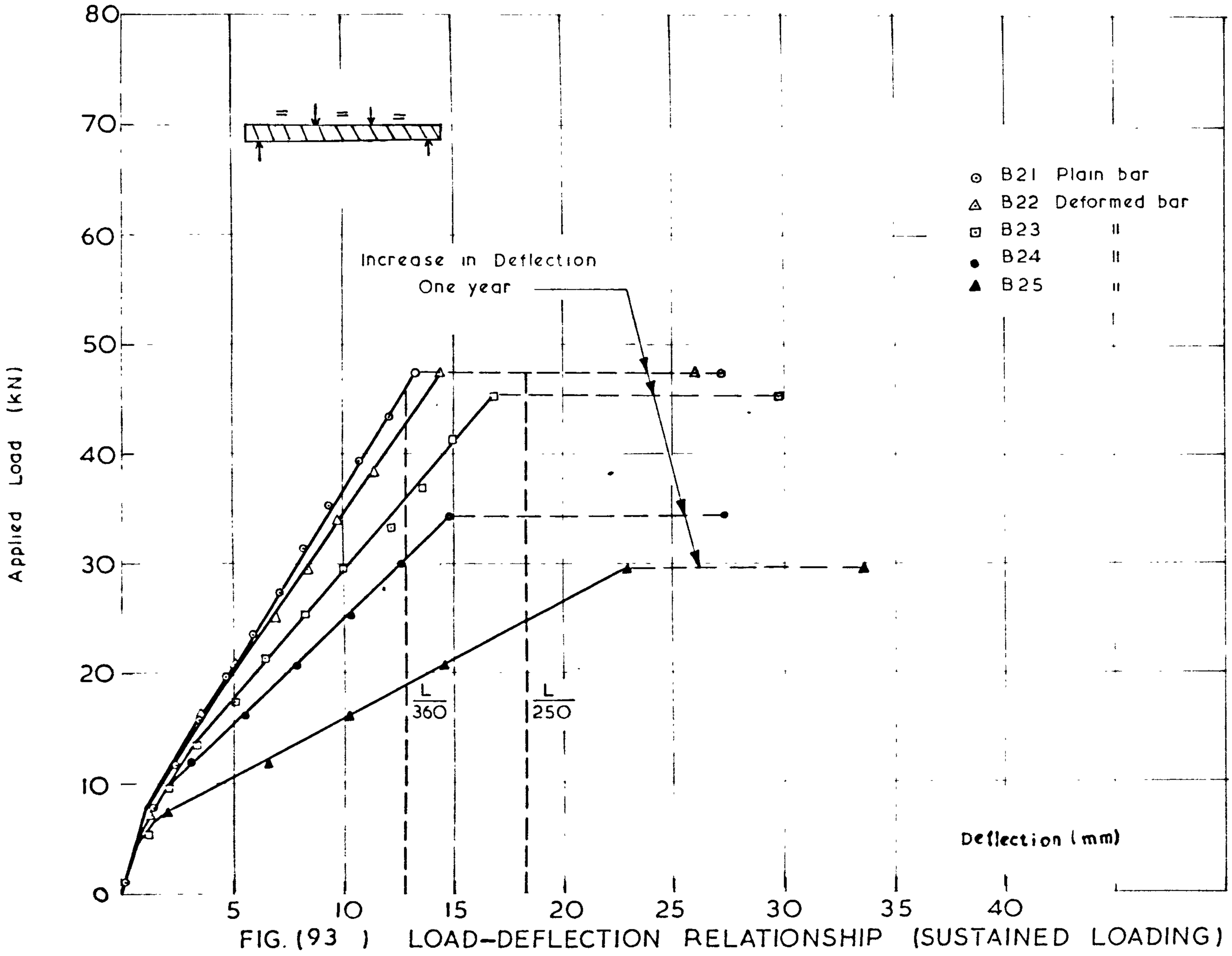

FIG. (93) LOAD–DEFLECTION RELATIONSHIP (SUSTAINED LOADING)

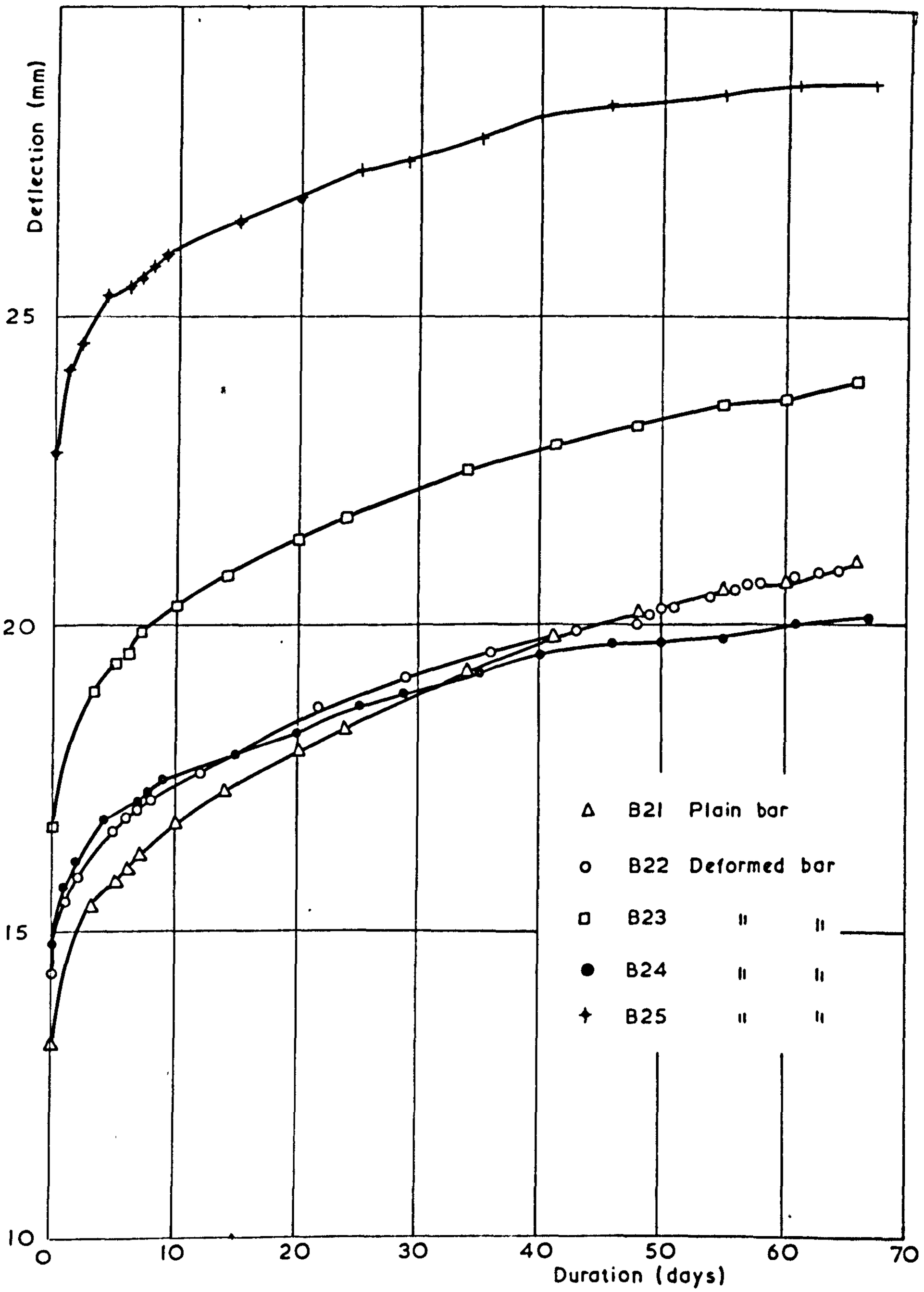

FIG. (94) COMPARISON OF DEFLECTION UNDER SUSTAINED LOADING.

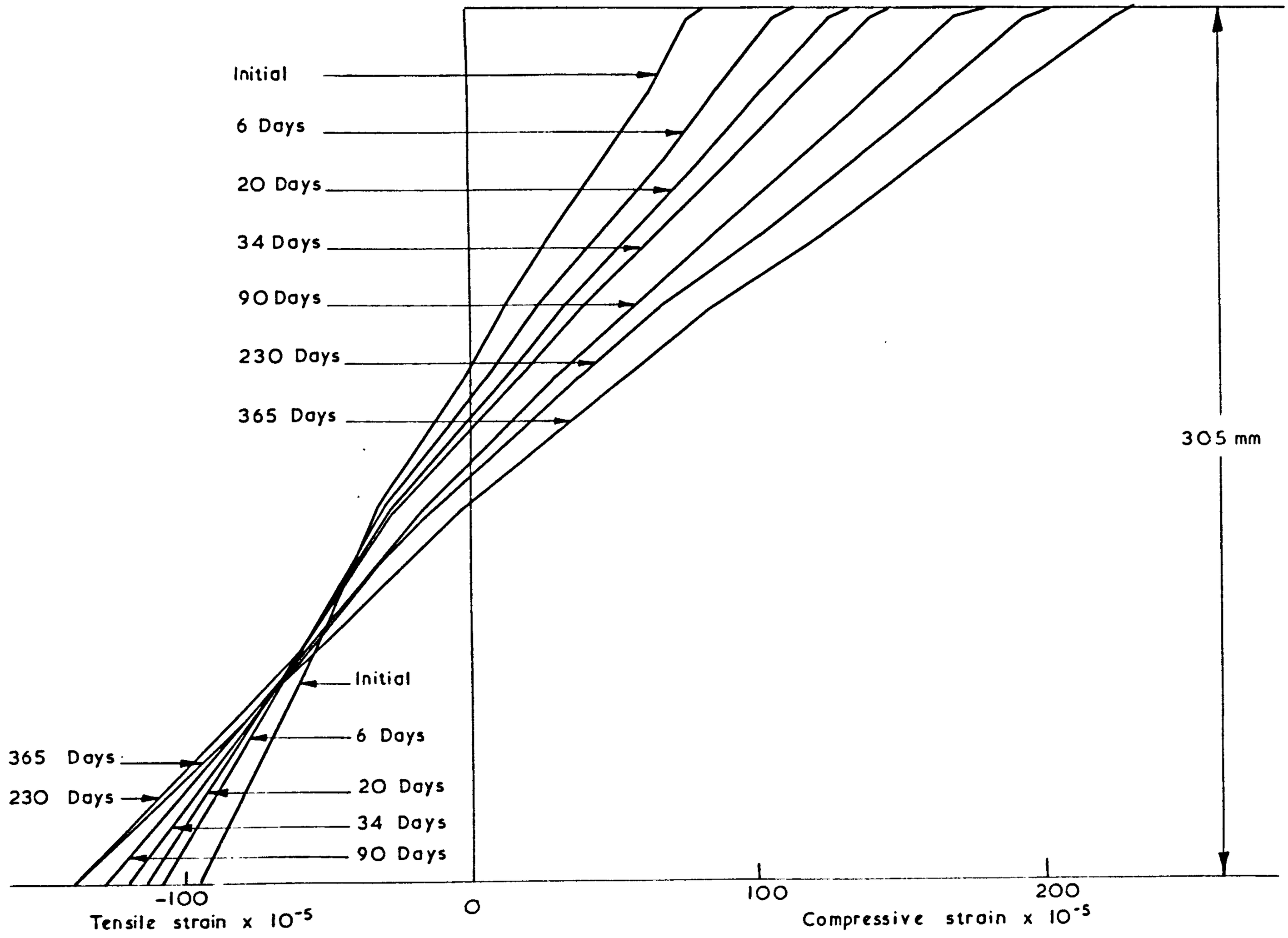

FIG.(95) VARIATION OF STRAIN DISTRIBUTION WITH TIME (SUSTAINED LOAD) BEAM B21

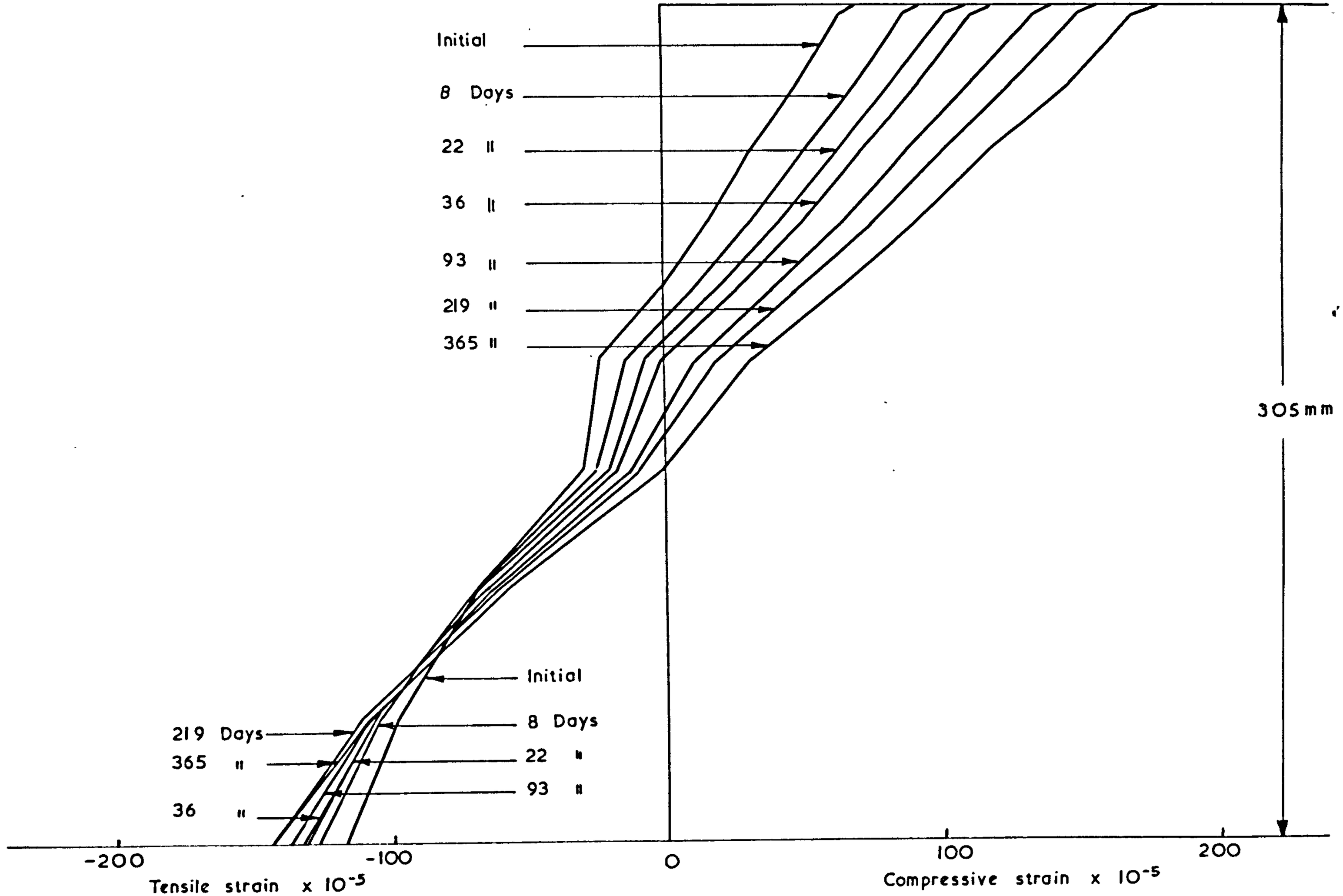

FIG. (96) VARIATION OF STRAIN DISTRIBUTION WITH TIME (SUSTAINED LOAD) BEAM B22

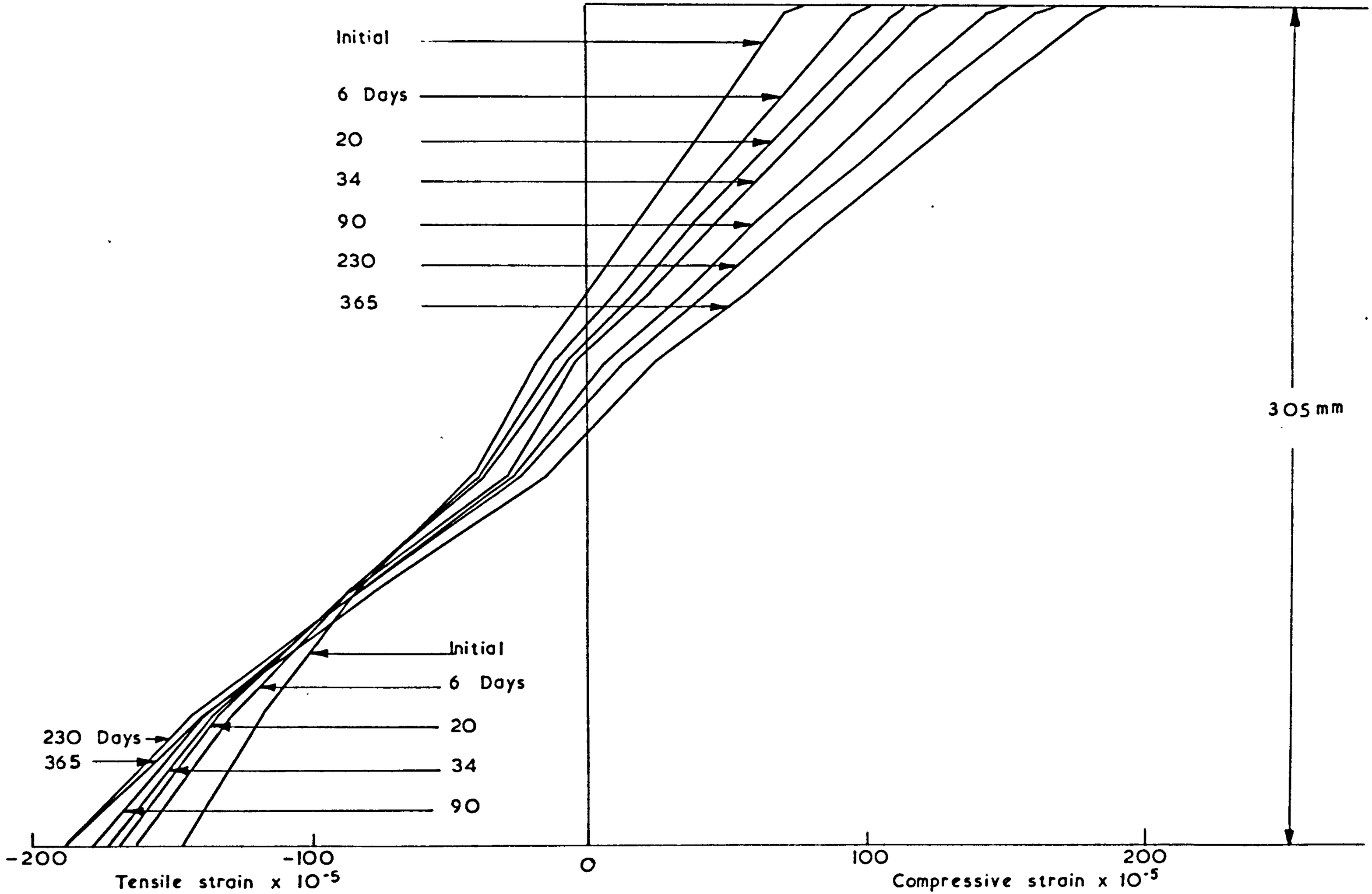

FIG. (97) VARIATION OF STRAIN DISTRIBUTION WITH TIME (SUSTAINED LOAD) BEAM B23

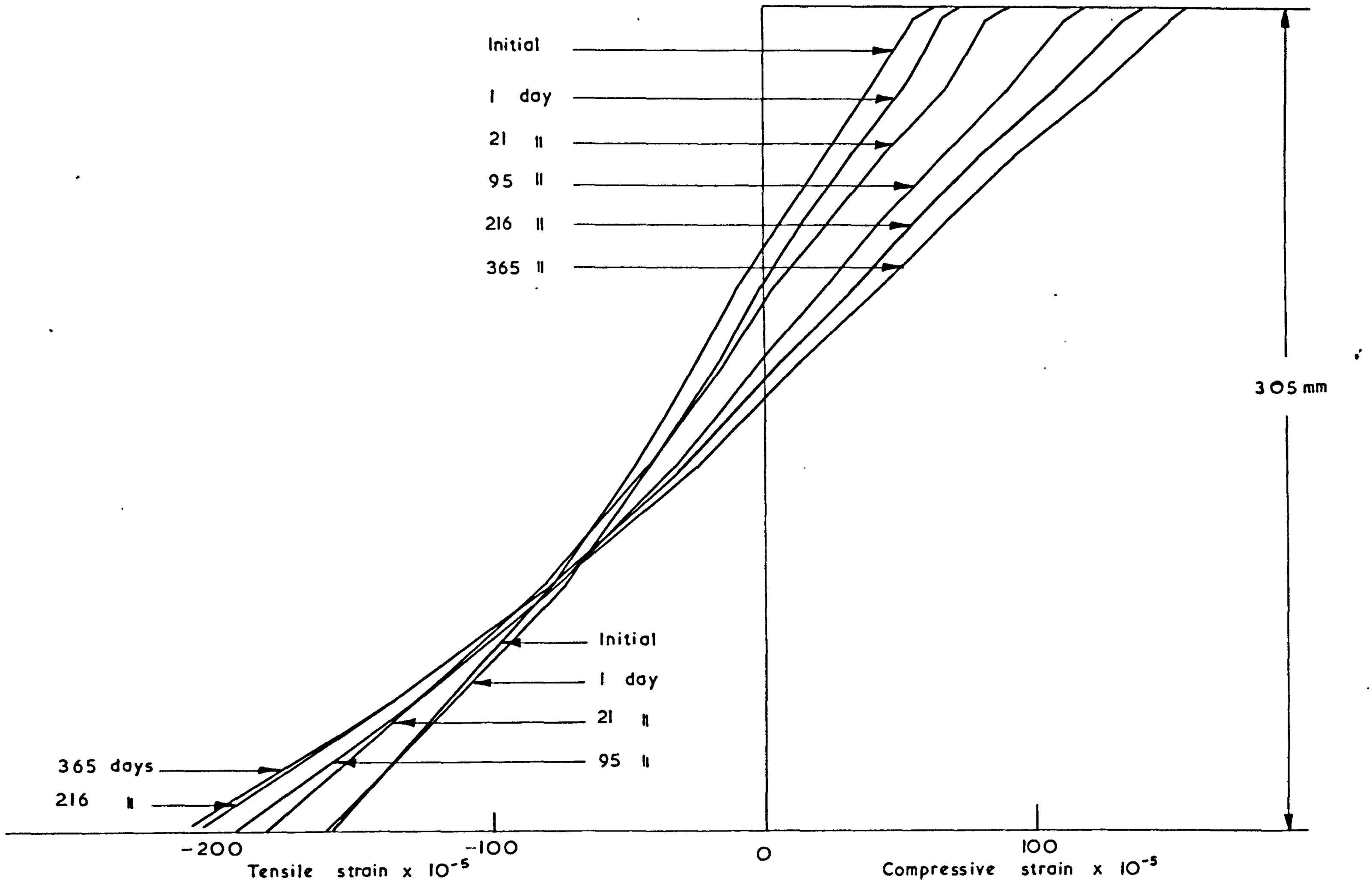

FIG. (98) VARIATION OF STRAIN DISTRIBUTION WITH TIME (SUSTAINED LOAD) BEAM B24

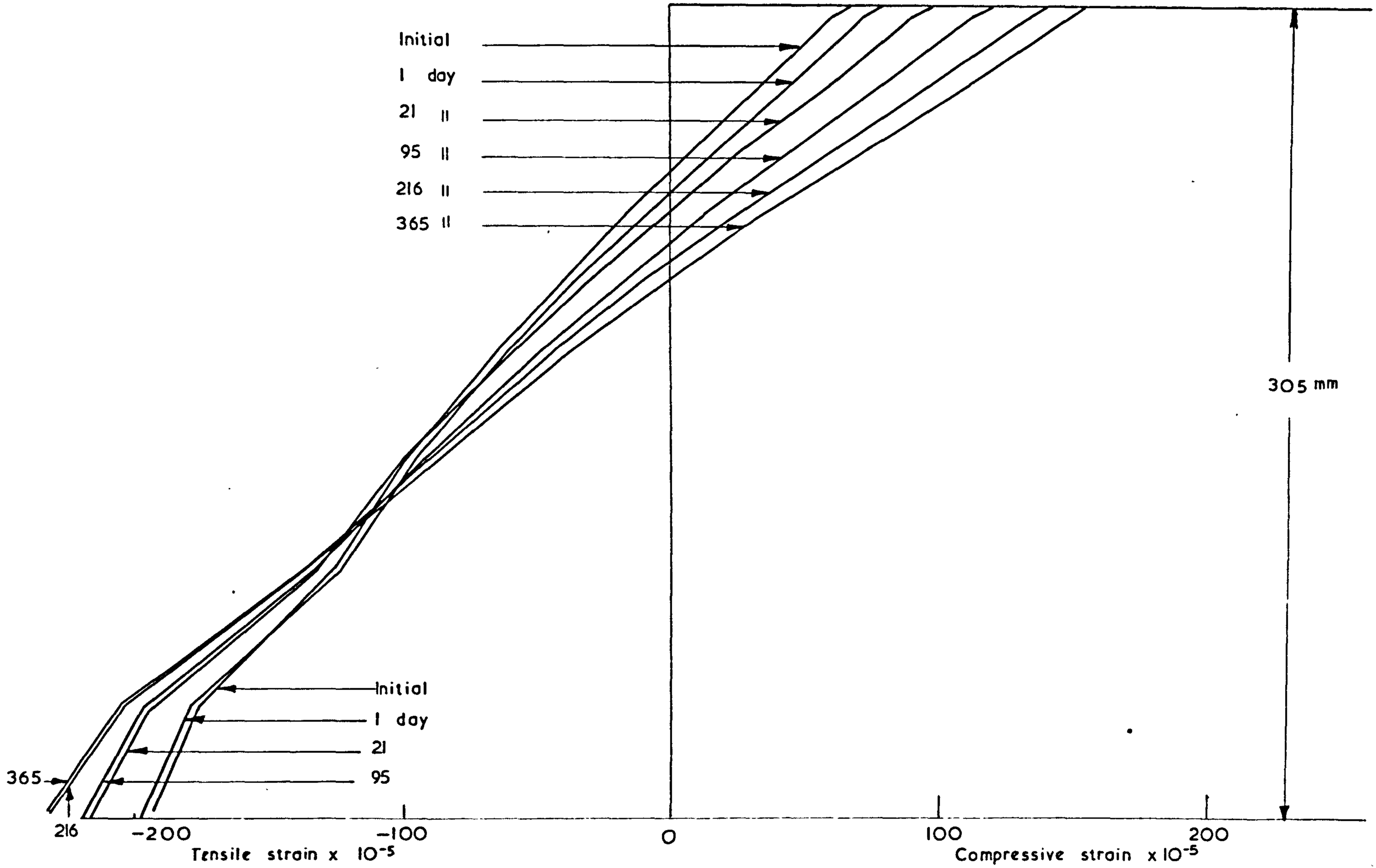

FIG. (99) VARIATION OF STRAIN DISTRIBUTION WITH TIME (SUSTAINED LOAD) BEAM B25

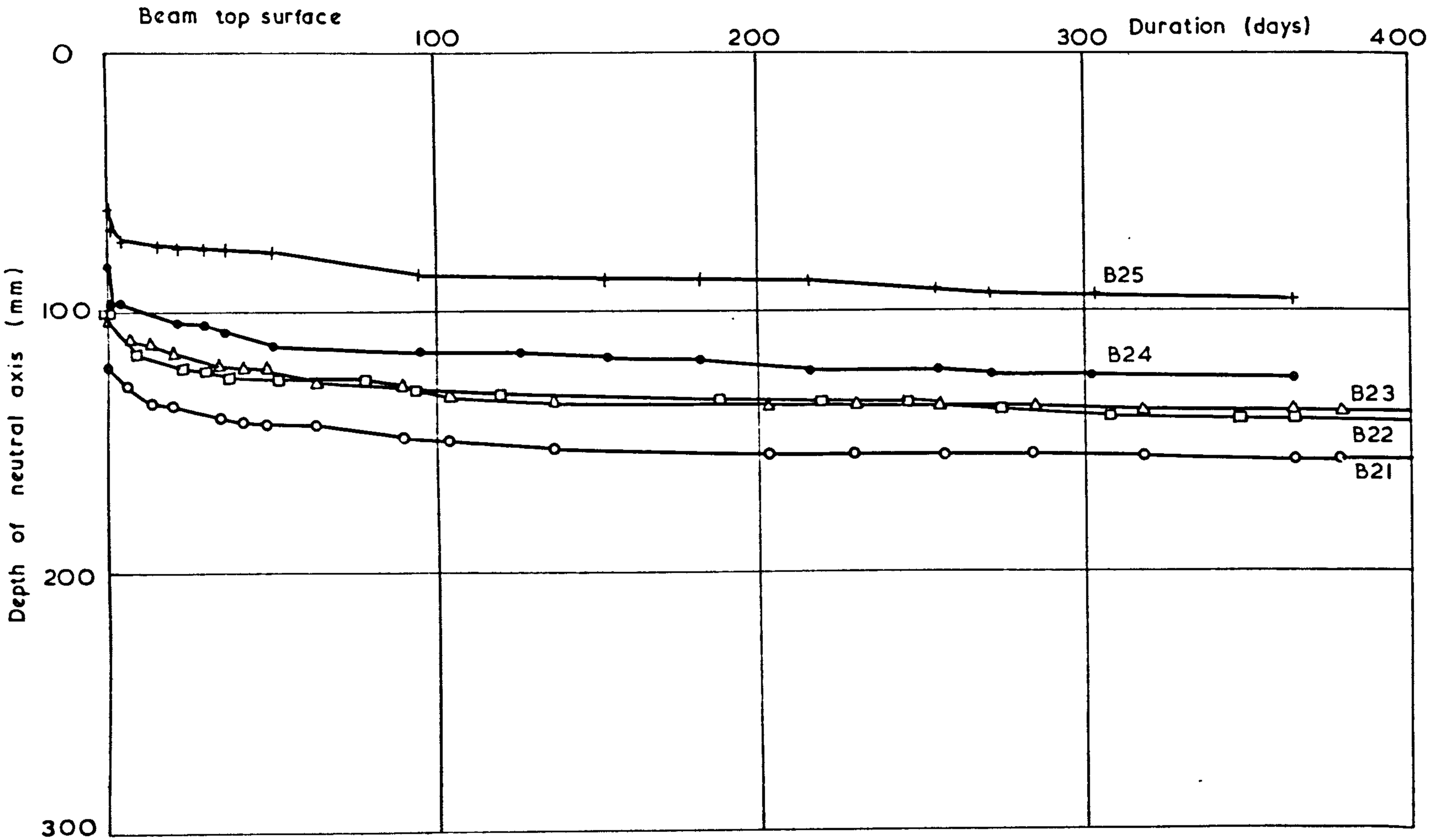

FIG (100) VARIATION OF NEUTRAL AXIS DEPTH WITH TIME (SUSTAINED LOAD)

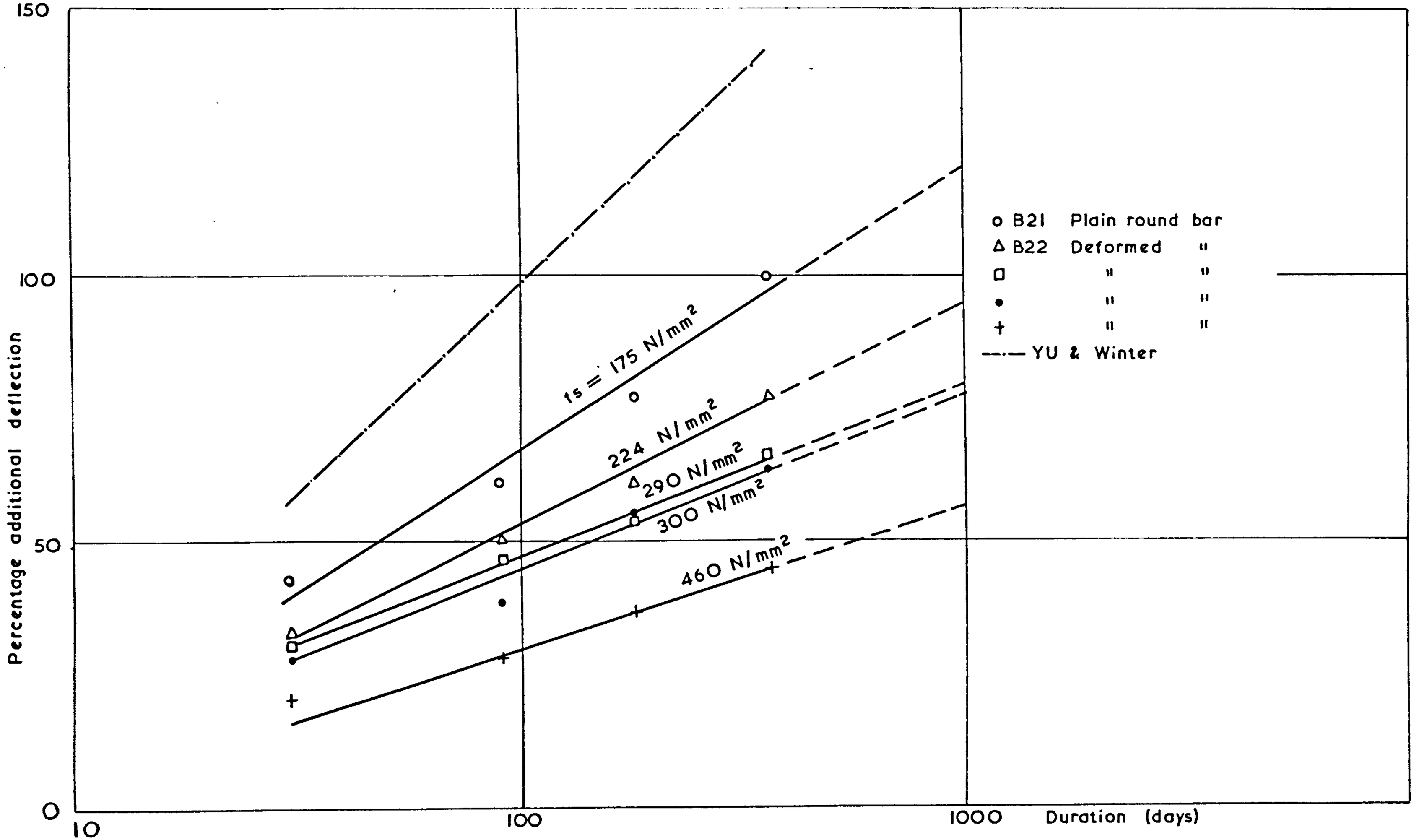

FIG (101) ADDITIONAL DEFLECTION (CREEP AND SHRINKAGE)

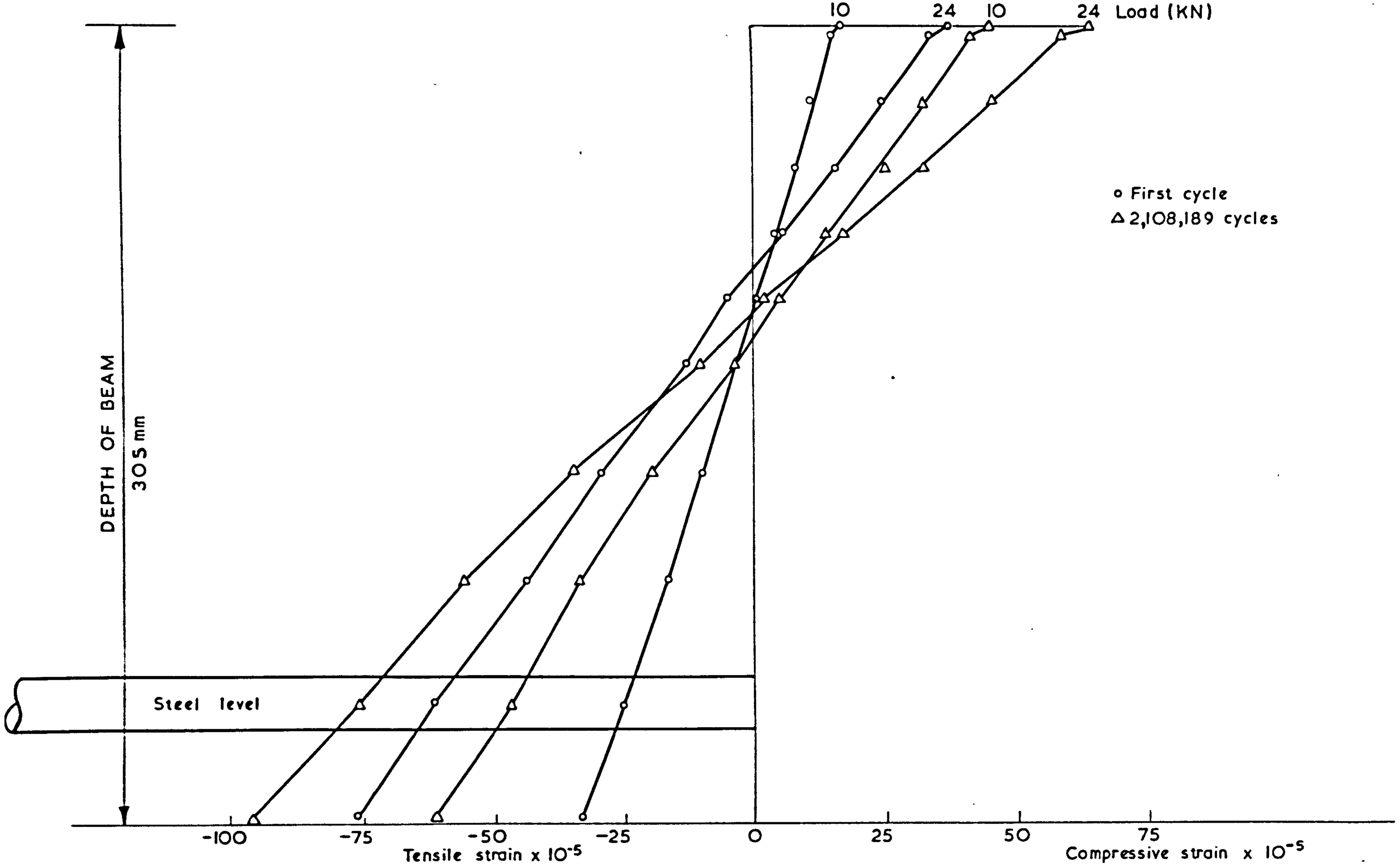

FIG. (102) STRAIN DISTRIBUTION (REPEATED LOAD) BEAM A31

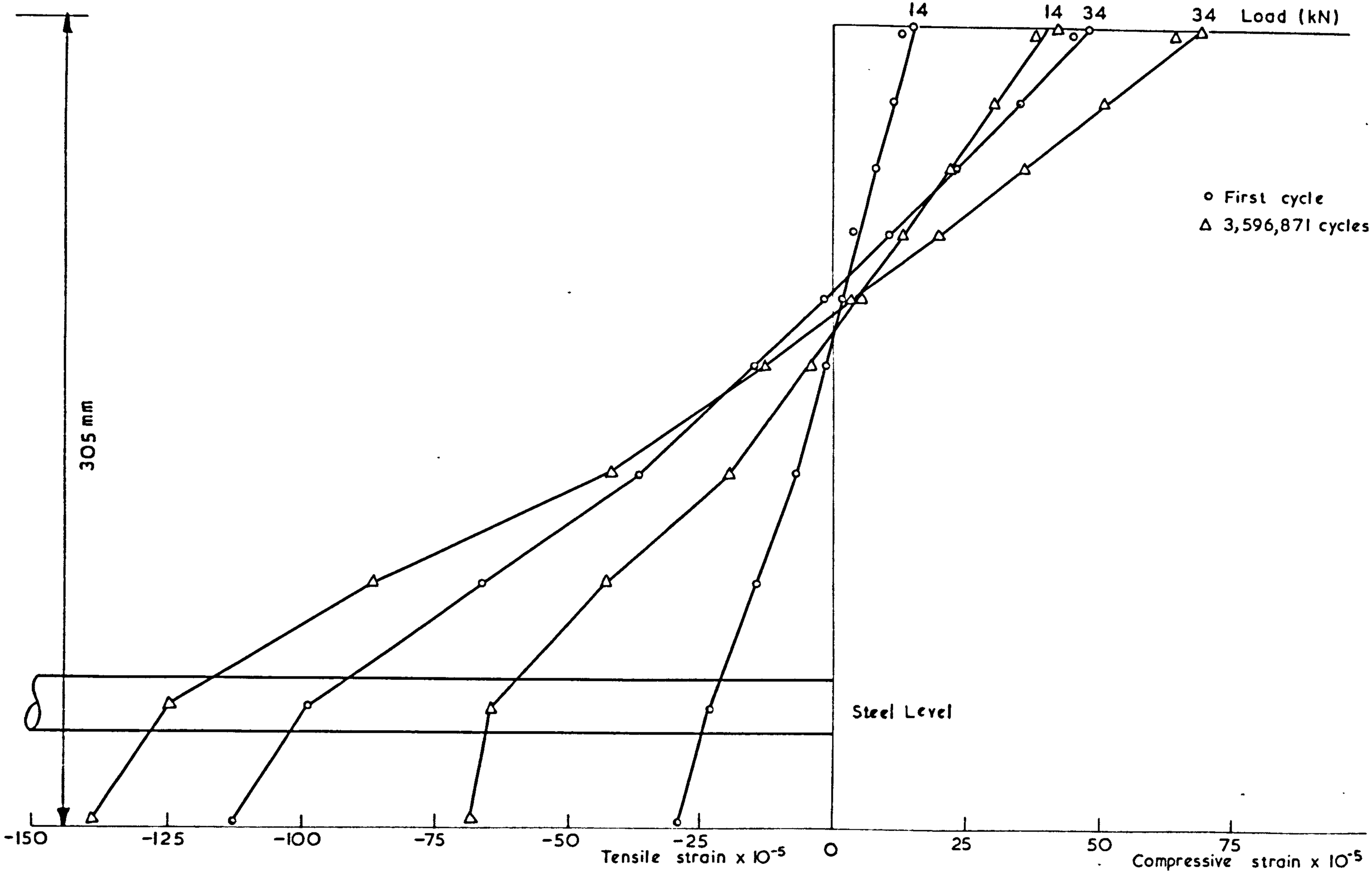

FIG. (103) STRAIN DISTRIBUTION (REPEATED LOAD) BEAM A32

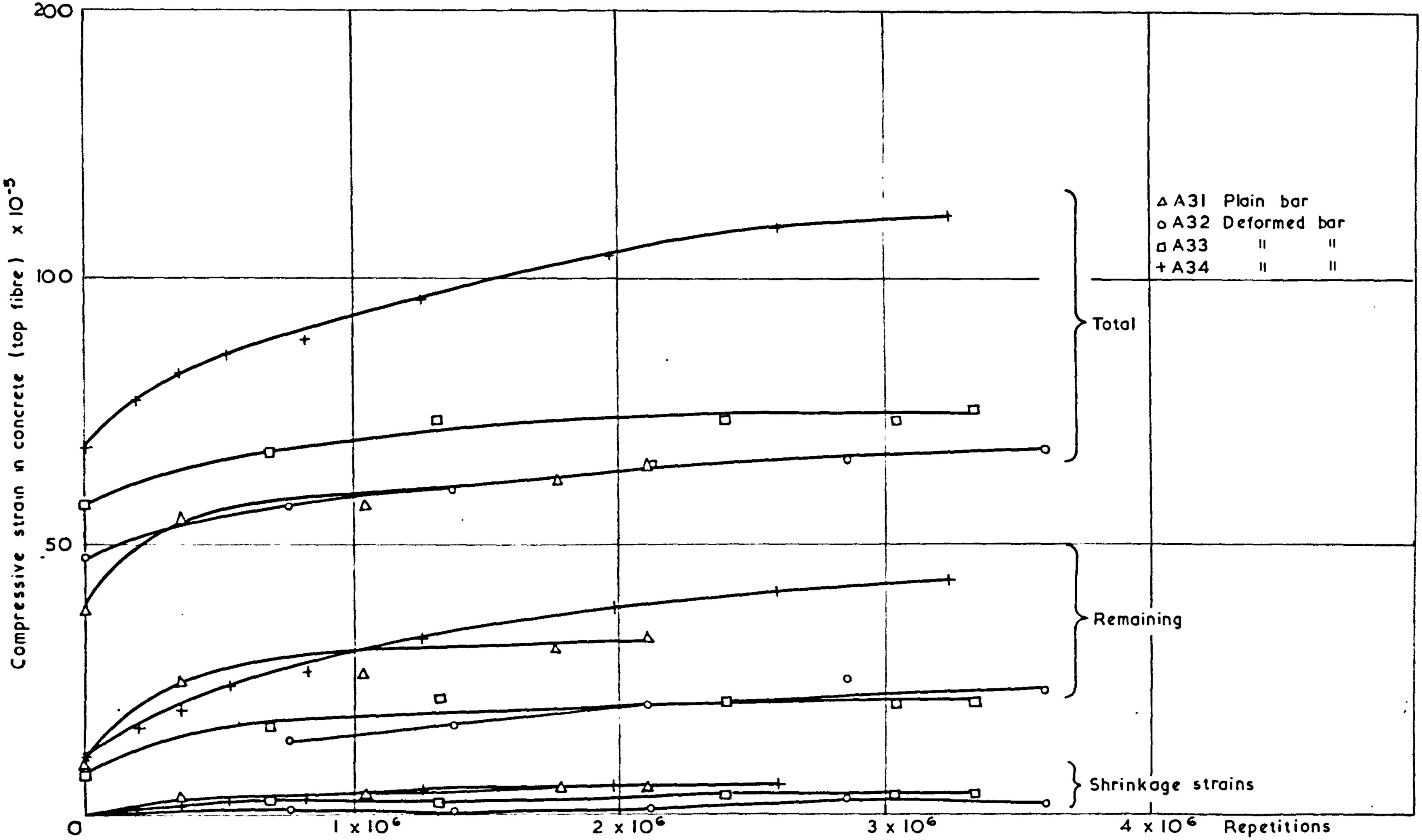

FIG.(104) VARIATION OF CONCRETE STRAIN WITH REPETITIONS

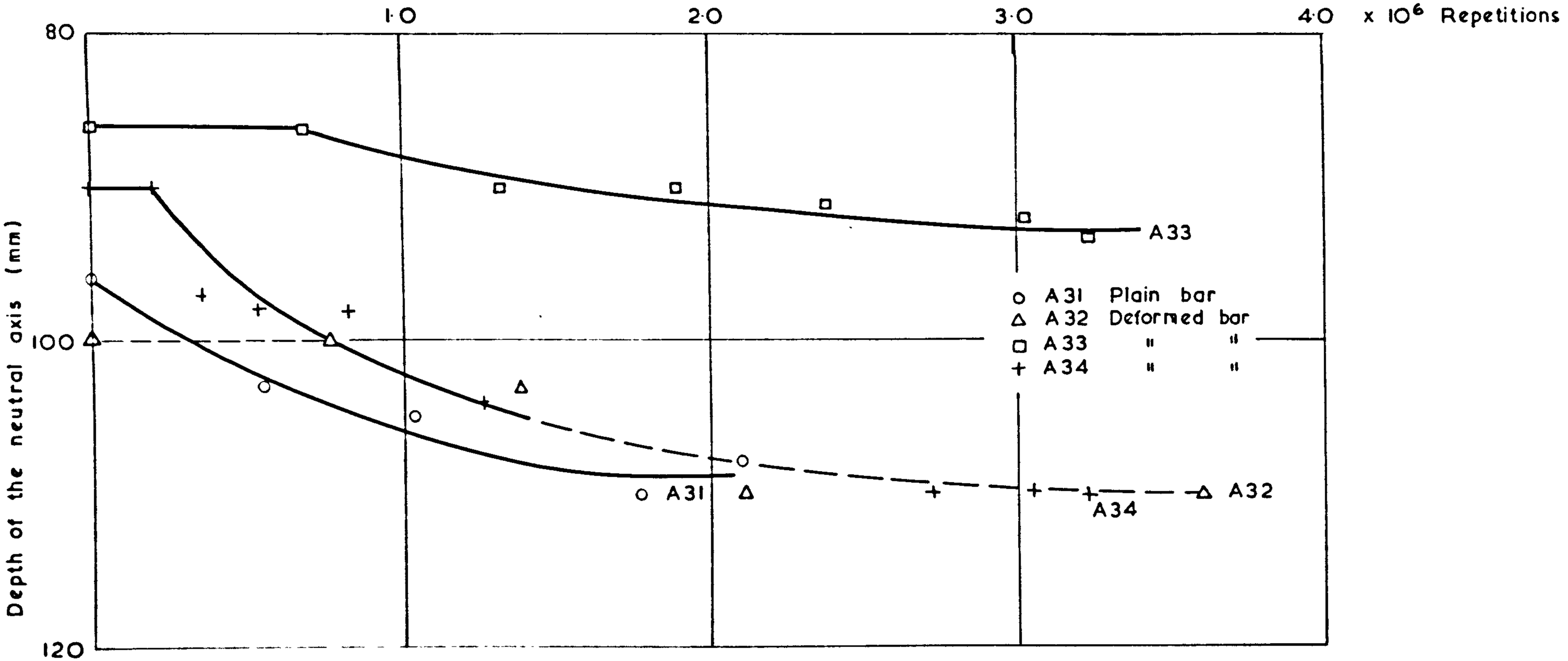

FIG (105) EFFECT OF REPEATED LOAD ON THE NEUTRAL AXIS POSITION

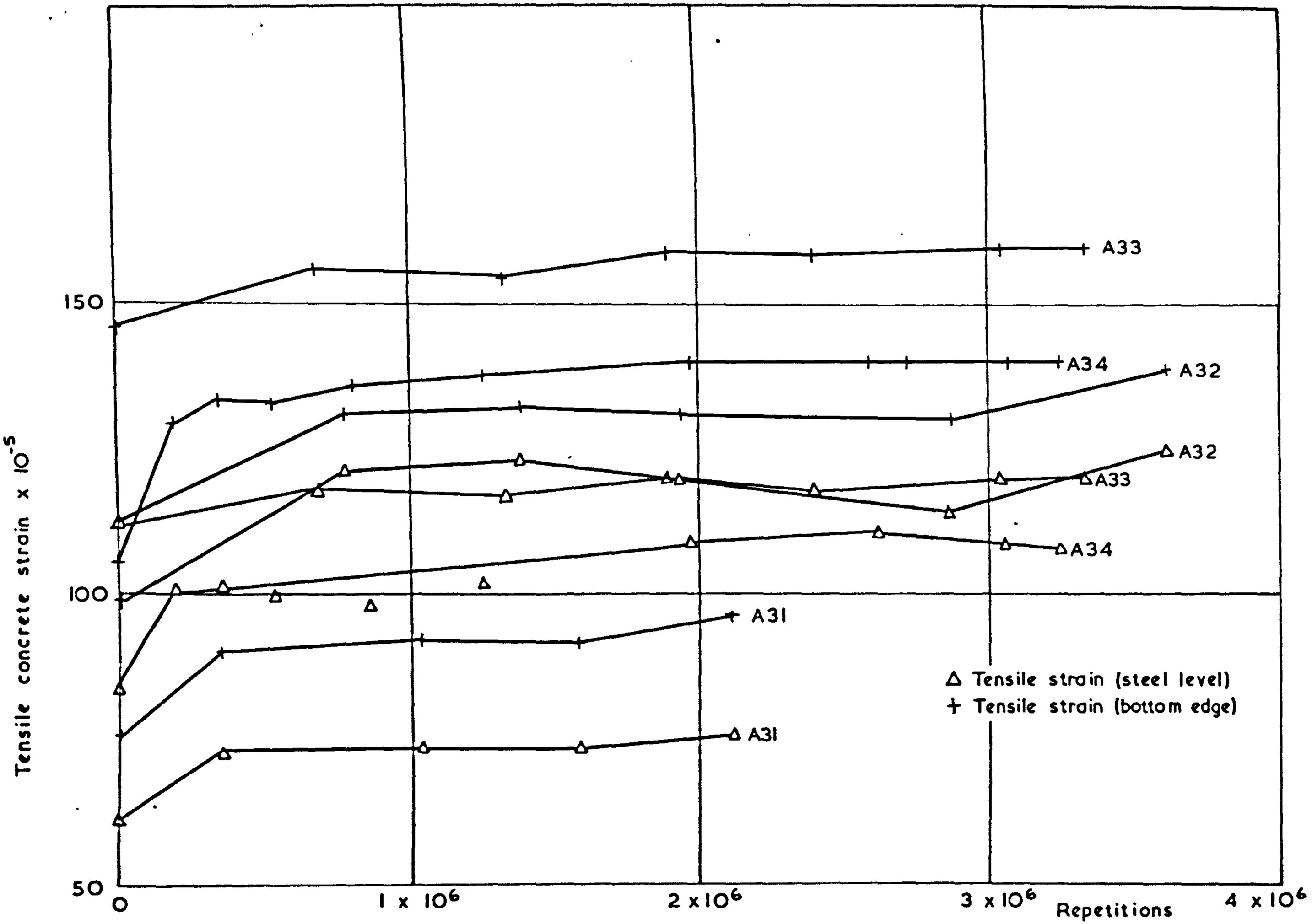

FIG.(106) VARIATION OF CONCRETE STRAIN WITH REPETITIONS

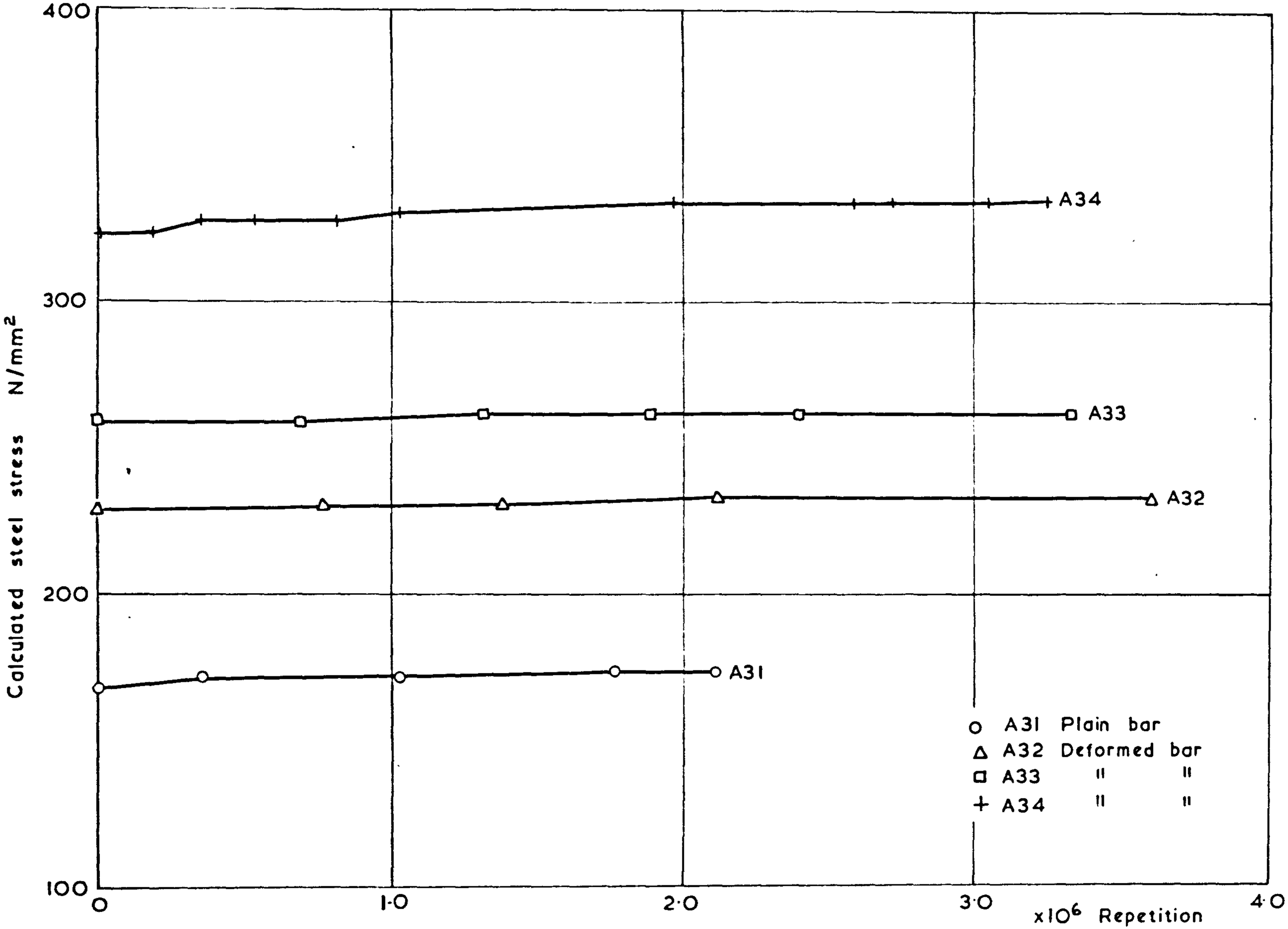

FIG.(107) VARIATION OF STEEL STRESS WITH REPETITIONS

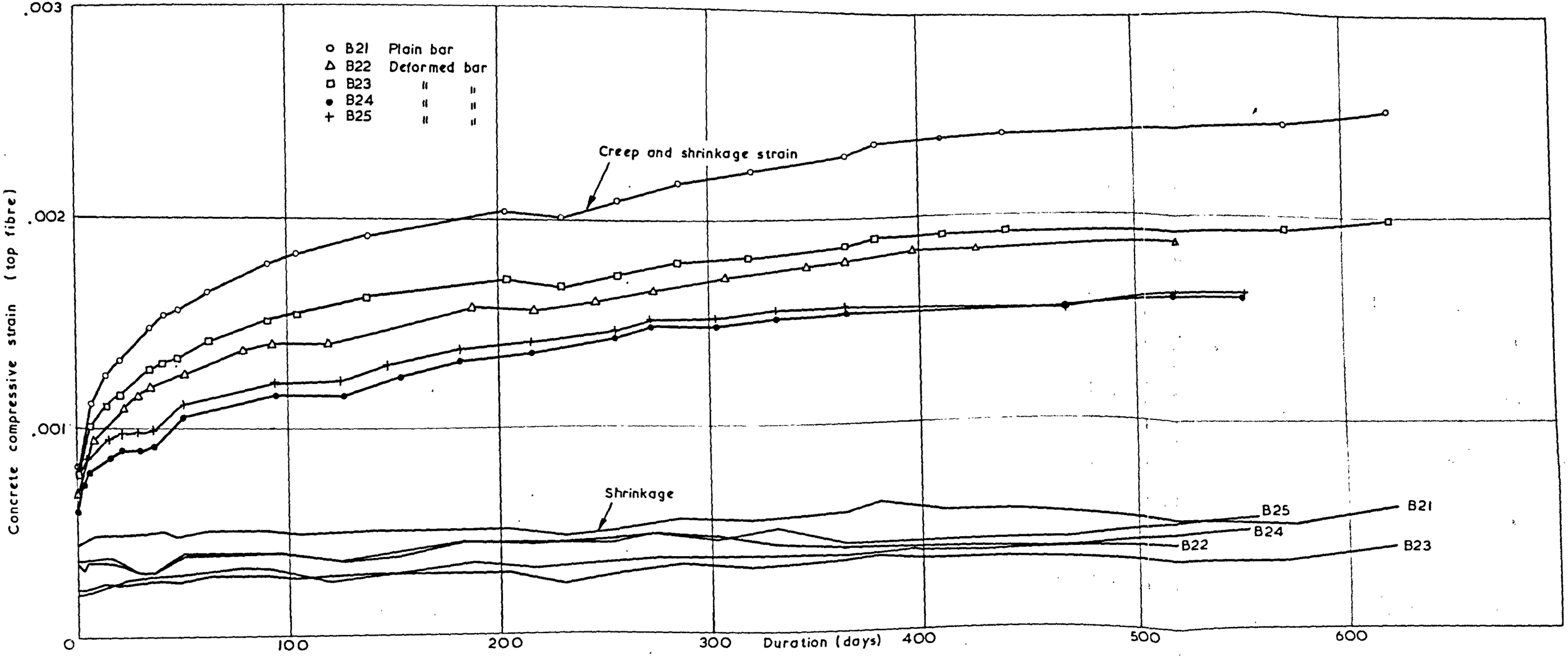

FIG.(108) VARIATION OF CONCRETE STRAIN WITH TIME (SUSTAINED LOAD)

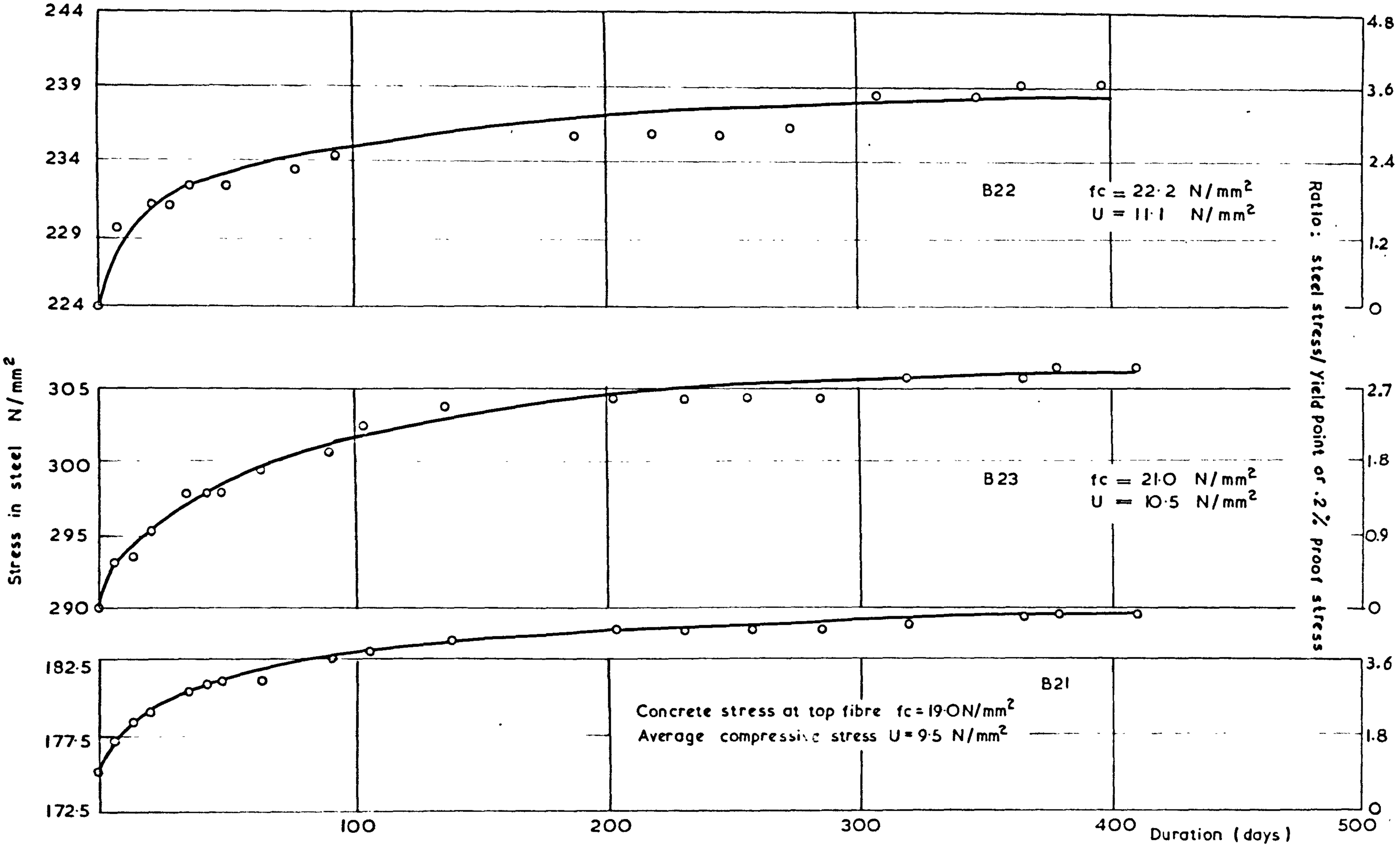

FIG. (109) VARIATION OF STEEL STRESS WITH TIME (SUSTAINED LOAD)

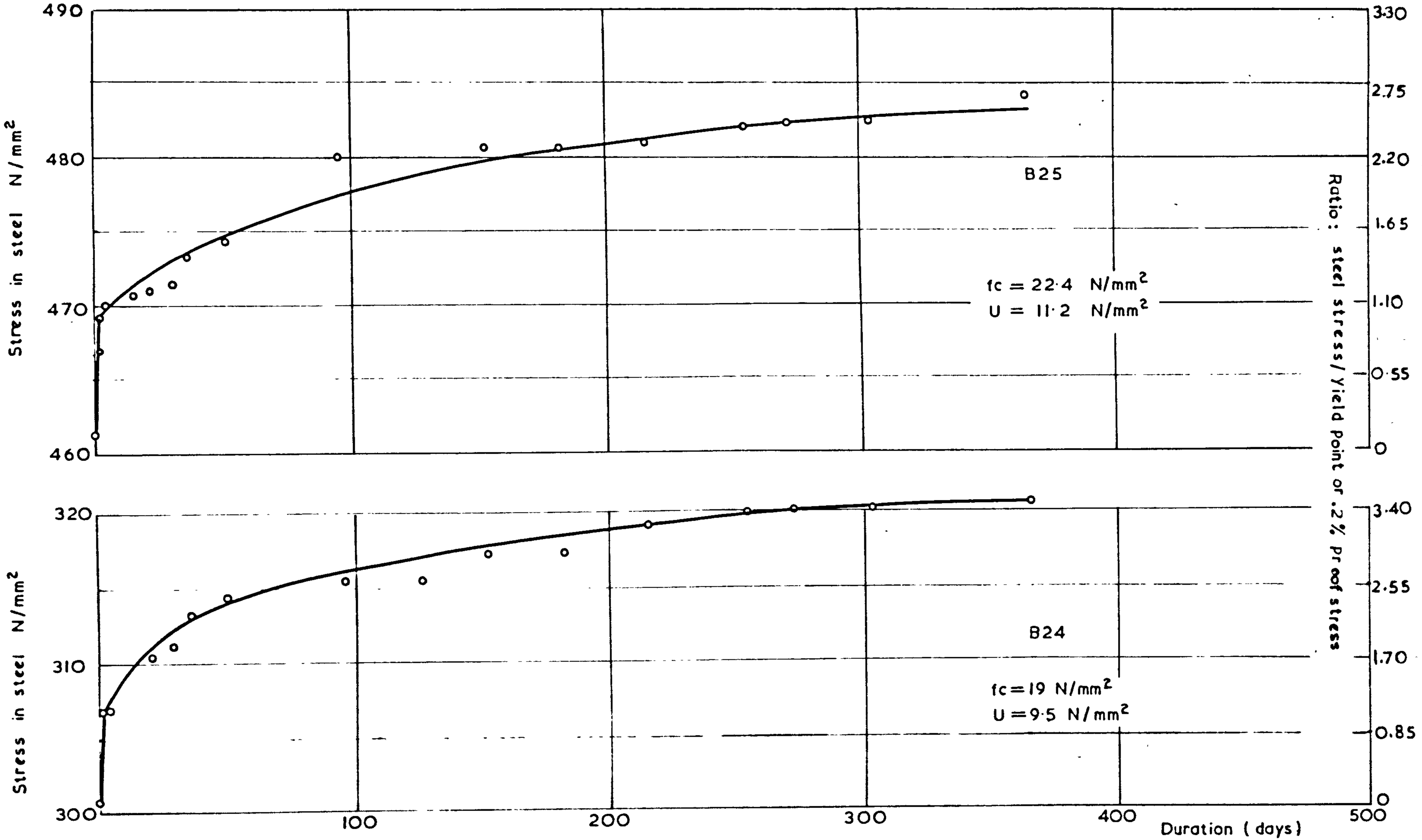

FIG. (110) VARIATION OF STEEL STRESS WITH TIME (SUSTAINED LOAD)

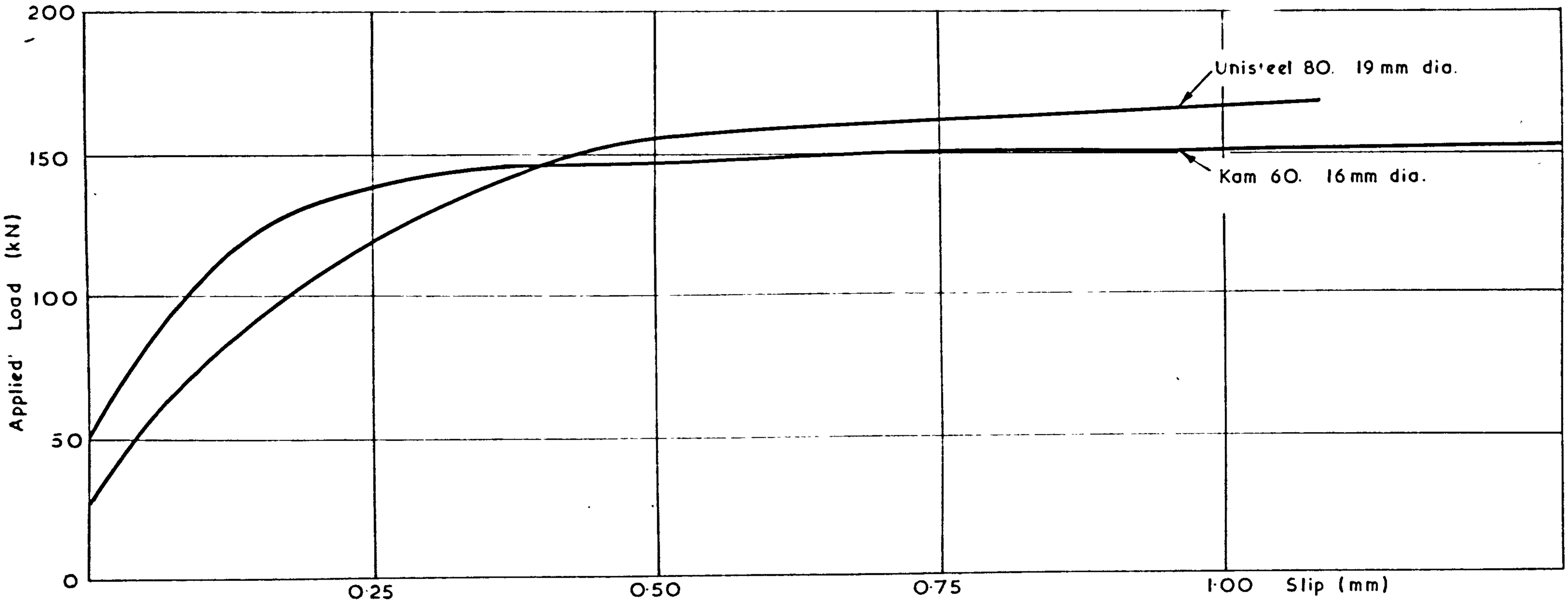

FIG. (III) LOAD – SLIP CURVES FOR UNISTEEL 80 AND KAM 60.

APPENDIX A

Ultimate Strength Design Using High Tensile Reinforcing Bars in Reinforced Concrete Beams

It has been pointed out that the ultimate strength design concept when coupled with the use of high tensile reinforcement, permits the design of more economical structures than can be obtained by working stress methods using mild steel reinforcement. However, more restrictive requirements must be added. Concrete strength requirements are more restrictive, deflections and cracking are limited. To illustrate the effects of the limited deflection and crack width on the choice of using high tensile steel, a detailed design of a typical beam is presented in the following:

Design of Rectangular Beam

Span: 4570 mm Third point loading system

Cube Strength: 41.4 N/mm^2

Load:	Live:		41.75 KN
	Dead: Beam 0.11 KN/m	3.77 KN	
	Weights (spreader)	1.08	
	Total dead load =		4.85KN
	Working load		46.6 KN

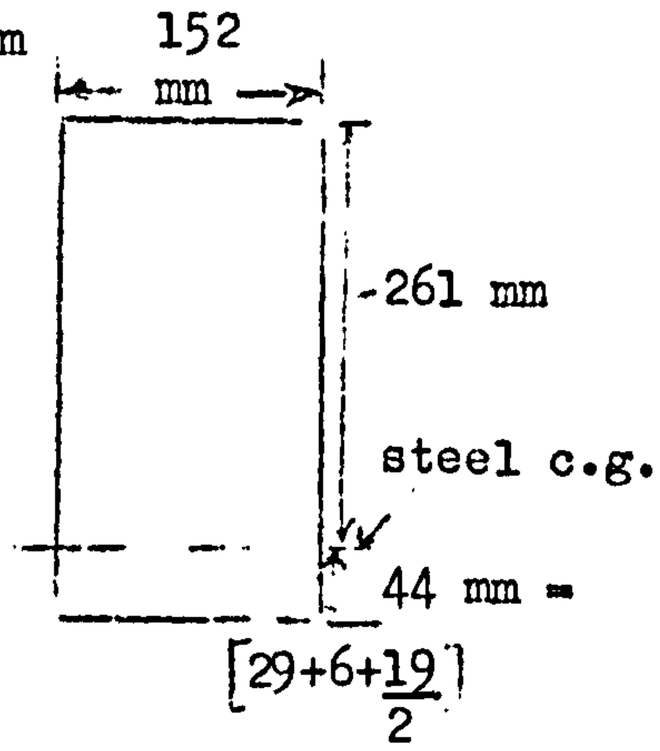

Design Loads:

W = 1.4 D.L. + 1.6 L.L. (For load factors reference should be made to the Draft Code[23])

$W = 1.4\,(4.85) + 1.6\,(41.75) = 73.6$ KN

$M = \frac{WL}{6} = \frac{(73.6)\,(4570)}{6} = 56600$ KN - mm

Steel required:

$$M_r = 0.87\,qU_w bd_1^2\,(1 - 1.1q)$$

$$56600 = 0.87\,(41.4)(152)(261)^2\,q(1 - 1.1q)$$

$$q = 0.195 = \frac{A_s}{bd_1}\,\frac{f_y}{U_w}$$

$$A_s = (0.195)\,\left(\frac{41.4}{550}\right)(152)\,(261) = 583\ mm^2$$

$$p = \frac{583}{261 \times 152} \times 100 = 1.47\%$$

Use 2 - 19 mm deformed Unisteel 80 bars

$\therefore A_s = 570\ N/mm^2$ and $p = 1.44\%$

Deflections

γ_f = 1.0 for Dead and Live Load (see Draft Code)

γ_m = 1.0 for steel and concrete

$E_c = 4\sqrt{U_w} = 4\sqrt{41.4} = 25.7\ KN/mm^2$ ..... § 9.3.2.

$f_t = 0.458\sqrt{U_w} = 0.458\sqrt{41.4} = 2.95\ N/mm^2$ ..... § 9.3.2.

$M_c = \frac{f_t I_o}{d - d_n} = \frac{2.95 \times 406 \times 10^6}{305 - 162} = 8700\ KN - mm$

On the first cycle of loading:

$$\Delta_1 = \beta \left[\frac{M_c}{E_c I_o} + \frac{M - M_c}{0.9\ E_c I_c} \right] L^2 \quad \text{..... § 9.3.2.}$$

$$= \frac{23}{216} \left[\frac{8700}{25.7 \times 406 \times 10^6} + \frac{35500 - 8700}{0.9 \times 25.7 \times 168 \times 10^6} \right] 4570^2$$

$$= 17.3\ mm$$

The stress in the steel, at which this deflection occurred can be calculated as follows:

$\frac{M}{M_u} = \frac{35500}{65000} \times 100 = 54.5\% > 30\%$ ..... § 8.2

use a fully cracked section based on a modular ratio of

$\frac{200}{25.7} \simeq 8$

$dn_{cr} = d_1 \sqrt{m^2p^2 + 2mp} - mpd_1$ ..... § 8.2

$dn_{cr} = 261\sqrt{8^2 \times .0144^2 + 2 \times 8 \times .0144} - 8 \times .0144 \times 261 = 98\ mm$

$e_o = \sqrt{\frac{U_w}{5000}} = \sqrt{\frac{41.4}{5000}} = 129 \times 10^{-5}$

assume $\alpha = 0.33$ $f_s = \frac{35500}{570(261 - 0.33 \times 98)} = 272\ N/mm^2$

$f_s A_s = \frac{f_c}{2} A_c$

$f_c = 2 \times \frac{272 \times 570}{98 \times 152} = 20.8\ N/mm^2 < 0.8 \times 41.4 = 33.1\ N/mm^2$

$\therefore e < e_o$ use triangular stress distribution with $\alpha = 0.33$ (see Fig. 12)

$f_s = 272\ N/mm^2$

When the whole of the live load is sustained for a period of 1000 days:

$\Delta_T = F_d \Delta_1 = 1.85 \times 17.3 = 32\ mm \gg L/360 = 12.7\ mm$

Where (F_d) is obtained from Fig. (101) for a steel stress of 272 N/mm^2 and adding a Unity.

When the structural member is cracked before the application of the load, the deflection at design load can be obtained from:

$$\Delta_2 = \beta \left(\frac{M}{1.3E_cI_c}\right) L^2 + \tfrac{1}{4}\Delta_1 \qquad \ldots\ldots \S\ 9.3.2.$$

$$= \frac{23}{216}\left(\frac{35500}{1.3 \times 25.7 \times 168 \times 10^6}\right) \times 21 \times 10^6 + \tfrac{1}{4} \times 17.3$$

$$= 14.18 + 4.30 = 18.48 \text{ mm}$$

When the whole live load is sustained for a period of 1000 days:

$$\Delta_T = F_d\Delta_2 = 1.85 \times 18.48 = 34.2 \text{ mm} \gg 12.7 \text{ mm}$$

Therefore under such a high steel stress of 272 N/mm^2 the section depth and the beam span must be altered. The use of camber is recommended.

Cracking:

γ_f = 1.0 for dead and live load (see Draft Code)
γ_m = 1.0 for steel and concrete
f_s = 272 N/mm^2

On the first application of the load, the maximum crack width can be calculated as follows:

$$W_{(max)_1} = RC\left(f_s - \frac{K_s}{p}\right) \times 10^{-6} \qquad \ldots\ldots \S\ 9.2.2.$$

Where R = 16.0 for deformed bar
K_s = 69.5 N/mm^2

$$W_{(max)_1} = 16 \times 35\left(f_s - \frac{69.5}{1.44}\right) \times 10^{-6}$$

$$= 560\left(272 - \frac{69.5}{1.44}\right) \times 10^{-6}$$

= 0.125 mm at the level of reinforcement

When the live load is sustained for 1000 days:

$$W_{(max)_T} = F_c W_{(max)_1} = 1.41 \times 0.125 = 0.176 \text{ mm}$$

Where F_c is obtained from Fig. (75)

Allowable maximum crack width (under normal conditions of exposure)

= 0.2 mm > 0.176 mm

When the structural member is cracked before the application of loading, the crack width at design load can be obtained from:

$$W_{(max)_2} = C\left[f_s\,(R + k_1) - k_1k_2\right] \times 10^{-6} \qquad \ldots\ldots \S\ 9.2.2.$$

$$= 35\left[272\,(12.9 + 5.28) - 5.28 \times 138\right] \times 10^{-6} = 0.148 \text{ mm at the level of reinforcement}$$

When the whole live load is sustained for 1000 days:

$$W_{(max)_T} = F_c W_{(max)_2} = 1.41 \times 0.148 = 0.209 \text{ mm} \simeq 0.200 \text{ mm}$$

Comparison between Measured and Calculated Behaviour of Beams:

Beam Behaviour	Neutral Axis (mm)	Steel Stress N/mm²	Short-Term				Long-Term After 1000 days	
			Deflection (mm)		Crack Width (mm)		Deflection (mm)	Crack Width (mm)
			1st cycle	2nd cycle	1st cycle	2nd cycle		
Calculated § 11.2	98	272	17.30	18.48	0.125	0.148	32.00	0.176
Measured	95	272	16.12	17.00	0.100	0.130	30.90	0.160

Economic Consideration

When mild steel bars are replaced by Unisteel 80 bars the saving in steel area and steel cost is calculated as follows:

Assumptions: The section size is kept constant: b = 152 mm, d = 305
The strength of concrete is kept constant: $U_w = 41.4 \text{ N/mm}^2$
The ultimate strength of beams is kept constant: W = 73.6 KN

$$M_r = 0.87 \; qU_w \; bd_1^2 \; (1 - 1.1q)$$

For mild steel bars ($f_y = 276 \text{ N/mm}^2$)

$$56600 = 0.87 \; (41.4) \; (152) \; (256)^2 q(1 - 1.1q)$$

$$56600 = 35.8 \times 10^7 \; q \; (1 - 1.1 \; q)$$

$$q(1 - 1.1q) = \frac{56600}{35.8 \times 10^7} = 0.158$$

$$q = 0.20$$

$$A_s = (0.20) \left(\frac{41.4}{276}\right) (152)(256) = 1160 \text{ mm}^2$$

As has been shown earlier in this Appendix for Unisteel 80 bars ($f_y = 550 \text{ N/mm}^2$) $A_s = 570 \text{ mm}^2$

Saving in steel area $= \frac{1160 - 570}{1160} \times 100 = 51\%$

Unisteel 80 bars cost 12% more than mild steel bars

Increase in steel area due to increase in cost $= 0.12 \times 570 = 68.5 \text{ mm}^2$

Reduction in saving $= \frac{68.5}{1160} \times 100 = 5.9\%$

Net saving $= 45.1\%$

Shear

$$Q = \frac{73600}{2} = 36800$$

$$q = \frac{Q}{bd_1} = \frac{36800}{152 \times 261} = 0.94\ N/mm^2 > q_c = 0.916\ N/mm^2$$

Stirrups must be supplied.

$$0.4\ N/mm^2 \leq (0.87\ fyq)\ \frac{Asq}{bs} \geq q - 0.8q_c \qquad \text{(see Draft Code)}$$

$$0.4 = \frac{(0.87)\ (276)\ (56.6)}{152\ S}$$

$$S = \frac{13580}{152 \times 0.4} = 224\ mm > 196\ mm = 0.75d_1 \qquad \text{(see Draft Code)}$$

use 6 mm vertical stirrups at 196 mm spacing

In the present investigation 24 - 6 mm diameter vertical stirrups spaced at 152 mm were used. (In the shear spans only)

Bond

$$U_f \text{ (flexural)} = \frac{Q}{\sum_o l_a} = \frac{36800}{119.4 \times 206} = 1.49\ N/mm^2 < 5.07\ N/mm^2$$

(see Draft Code)

$$U_a \text{ (anchorage)} = \frac{f_s A_s}{\sum_o l}$$

$$= \frac{550 \times 570}{119.4 \times 1523} = 2.38\ N/mm^2 < 3.26\ N/mm^2$$

(See Draft Code)

Derivation of Equations

The derivation of equations (21) and (22) is based on the elastic theory:

The neutral axis depth for the uncracked section (Eqn. 21)

$$bd\ (d/2) + (m - 1)\ A_s\ (d - d_1) = [bd + (m-1)\ A_s]\ \bar{y}$$

$$\bar{y} = \frac{\frac{bd^2}{2} + (m - 1)\ A_s\ (d-d_1)}{bd + (m - 1)\ A_s}$$

$$\bar{y} = \frac{d/2 + (m - 1)\ \frac{As}{bd}\ (d - d_1)}{1 + (m - 1)\ \frac{As}{bd}}$$

$$= \frac{d/2 + (m - 1)\ g\ (d - d_1)}{1 + (m - 1)\ g} \quad ; \qquad g \simeq p$$

$$\bar{y} = \frac{d/2 + (m - 1)\ p\ (d - d_1)}{1 + (m - 1)\ p}$$

$$dn_{ucr} = d - \bar{y} = d - \frac{d/2 + (m - 1)p\ (d - d_1)}{1 + (m-1)\ p}$$

<u>The neutral axis depth for the cracked section (Eqn. 22)</u>

$$bdn_{cr}\left(\frac{dn_{cr}}{2}\right) = mA_s\ (d_1 - dn_{cr})$$

$$dn_{cr}^2 + \frac{2mA_s\ dn_{cr}}{b} - \frac{2m}{b} A_s\ d_1 = 0$$

$$p = \frac{A_s}{bd_1}$$

$$dn_{cr}^2 + 2mpdn_{cr}d_1 - 2md_1^2p = 0$$

$$dn_{cr}^2 + 2mpdn_{cr}d_1 + m^2p^2d_1^2 - m^2p^2d_1^2 - 2md_1^2p = 0$$

$$(dn_{cr} + mpd_1)^2 = m^2p^2d_1^2 + 2md_1^2p$$

$$dn_{cr} = d_1\sqrt{m^2p^2 + 2mp} - mpd_1$$

APPENDIX B

Bond Tests

In the present investigation it was observed that beams reinforced with Kam steel bars showed better crack control than beams with Unisteel bars. Kam 60 steel and Unisteel 80 had similar yield strengths, but different surface deformation characteristics, as can be seen in Plate (1). They were both provided with lateral ribs on their surfaces, which were of different shapes, face angles and inclinations to the bar axis. So it was decided to carry out pull-out tests, for the purpose of comparison only, between the two types of reinforcement from the standpoint of bond characteristics and slip resistance.

As stated in §§ 7.4.4.3., six pull-out specimens were made; three for each type of steel. Fig. (5) and Table (7) show the details of the specimen which was made with the same type of concrete used in the main beams. Fig. (111) shows the load-slip curves for both types of steel. The average of 3 is reported. The average was taken because there was a large variation in the results of the specimens of the same type. The differences can be explained by the presence of a great many variables affecting the behaviour of the pull-out specimen viz. the random nature of concrete, compaction, the degree of chemical adhesion between the steel and concrete etc.

Bond can be defined as the shearing stress or force between the bar and the surrounding concrete, and it can be assumed to be made up of (a) chemical adhesion, (b) friction and (c) mechanical interlocking between the steel and concrete. Deformed bars depend primarily upon the mechanical interlocking for their bond properties, which are superior to those of plain bars; the chemical adhesion and friction can be considered as secondary components. The slip in the case of deformed bars may occur either by the rib pushing the concrete away from the bar (wedging action) or the rib crushing the concrete in front of it, depending on the face angle of the rib. Detailed investigation of the mechanics of bond and slip of deformed bars has been reported by Lutz.[194]

Initially, chemical adhesion combined with mechanical interlocking prevents slip. After the adhesion is broken and slip occurs the rib of a bar restrains this movement by bearing against the concrete between the ribs (concrete key). Hence the rib face angle and the rib orientation

relative to the bar axis are the determining factors in the bond characteristics and bond failure of deformed bars.[194]

In the present investigation, if the load does not exceed 27 KN the bond characteristics of both types of steel shows no marked difference. With a load of 27 KN (2.38 N/mm^2 average bond stress) the first relative movement of Unisteel bar occurred while the adhesion of the Kam steel was unaffected, in spite of the fact that the latter had a smaller bar diameter. With a load of 52 KN (5.44 N/mm^2 average bond stress) the adhesion-bond strength of the Kam steel came into play, while the Unisteel showed a slip of .045 mm. After this the high shear bond and the interlocking characteristics of both types of steel prevented excessive slip. However, the rate of slip with Unisteel 80 was higher than that with Kam 60. In the latter the increase in slip was very rapid after a load of about 120 KN until failure, while in the former the slip continued to increase gradually with increasing load until a load of about 155 KN, after which slipping occurred with no change of load until failure.

Therefore, it can be observed from Fig. (111) that Kam 60 had higher slip resistance and higher average bond stresses than Unisteel 80, but the average bond strength at pull-out was slightly higher in the latter. This can be explained by the fact that Unisteel 80 bar had a bigger diameter than the Kam 60 bar. Similar behaviour has been reported by Lutz.[194] In both cases slip occurred almost entirely by crushing of the concrete in front of the rib, as can be observed in the compacted powder lodged in front of the rib when the bar was pulled out. However, the difference in the face angles and the orientation of the ribs relative to the bar axis resulted in different wedge action, and different resistance to slip. Table (7) shows that the average bond stresses at 0.025 mm and 0.25 mm slips are greater for Kam 60 than for Unisteel 80. Similar observations have been reported by Lutz.[194,195]

All the specimens failed in bond. Bond failure is defined as a failure accompanied by excessive slip at the free end of the bar. Excessive slip is associated with a rapid increase in the movement of the free end of the bar with only a slight increase in the applied load. The mode of failure is shown in Plate (4B).

In all cases the bar was stressed to its yield strength at the

maximum load, but the failure was classified as bond failure because of large slip at the free end of the bar.

Due to the circumferential stresses in the concrete, fine longitudinal splitting cracks appeared on the surface of the specimens. These cracks did not progress any further, but they remained constant. The progress of these cracks was inhibited by the presence of adequate confinement provided by the transverse reinforcement, permitting the increased bond strength. Similar observations have been reported by Lutz.[194,195]

By way of conclusion, Kam steel had higher bond stress and slip resistance than Unisteel at the same load level. The reason for the difference is due to the difference in the resistance to slip brought about by the difference in the rib orientation and wedge action. Kam steel, which had ribs perpendicular to the bar axis, offered more resistance to slip than Unisteel, which had ribs orientated at an angle to the bar axis.

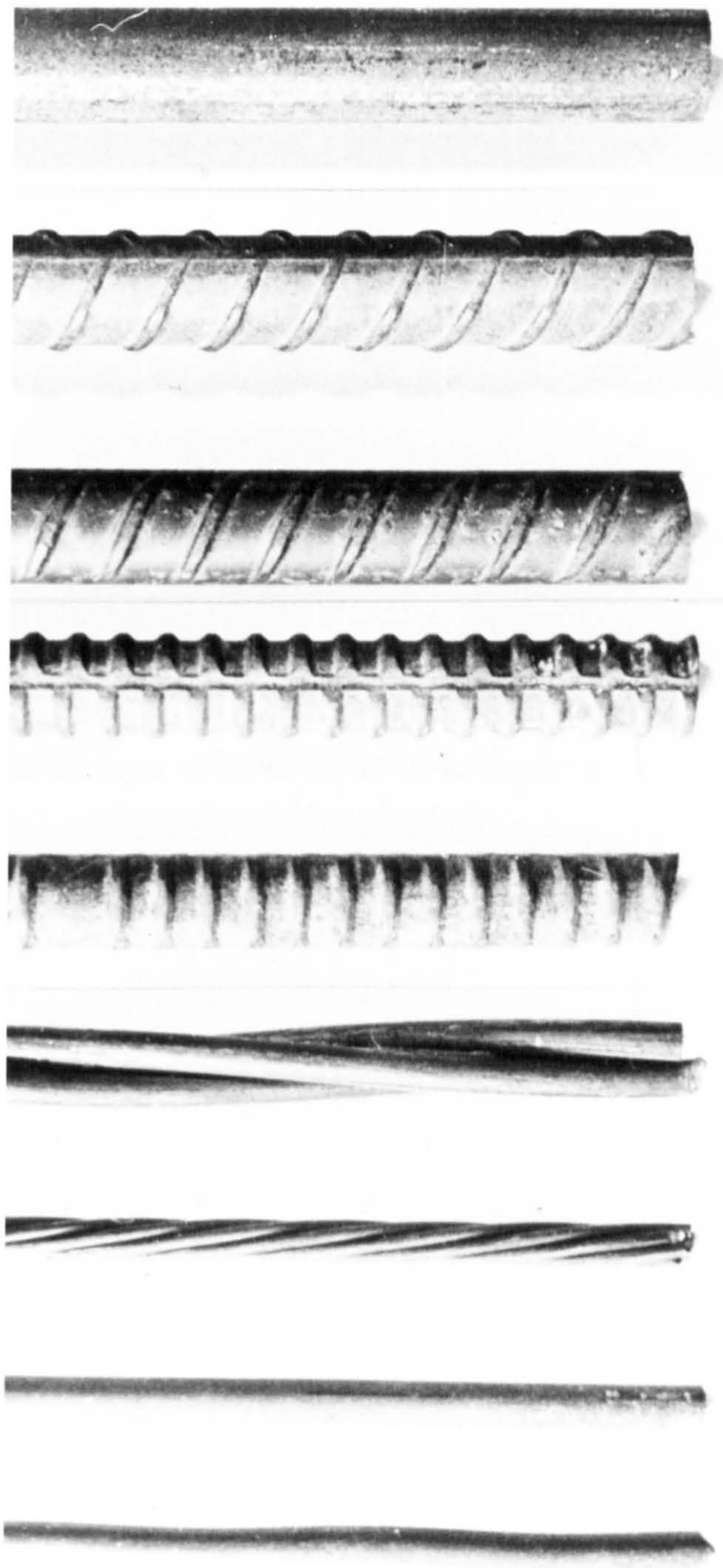

A. Mild Steel

B. Unisteel 60 & 80

C. Kam Steel 60 & 90

D. Bristrand 100

E. Prestressing Strand

F. Plain
Prestressing Wire

G. Crimped
Prestressing Wire

PLATE (1) TYPES OF REINFORCEMENT

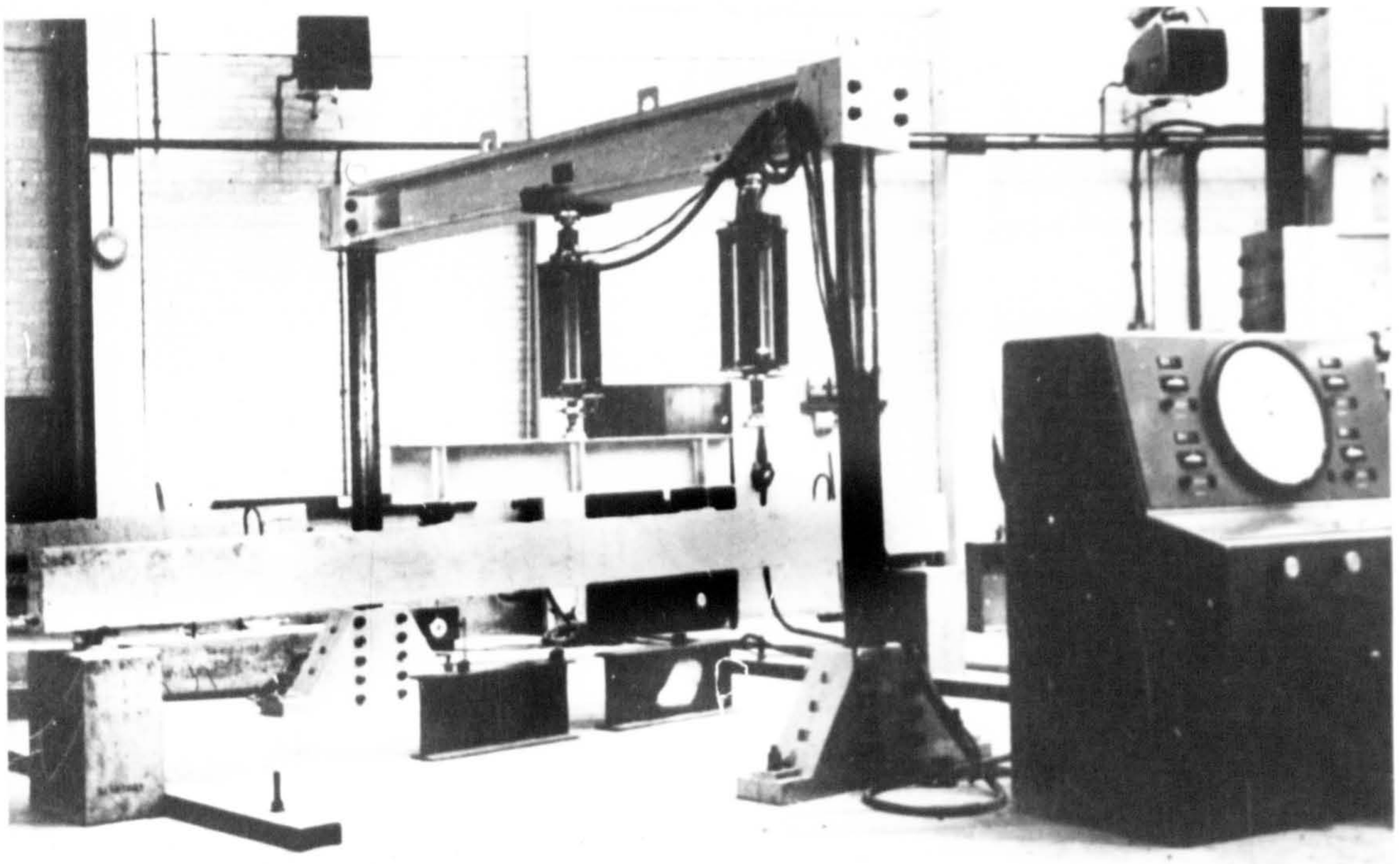

A. Static and Fatigue Tests (Simple Frame)

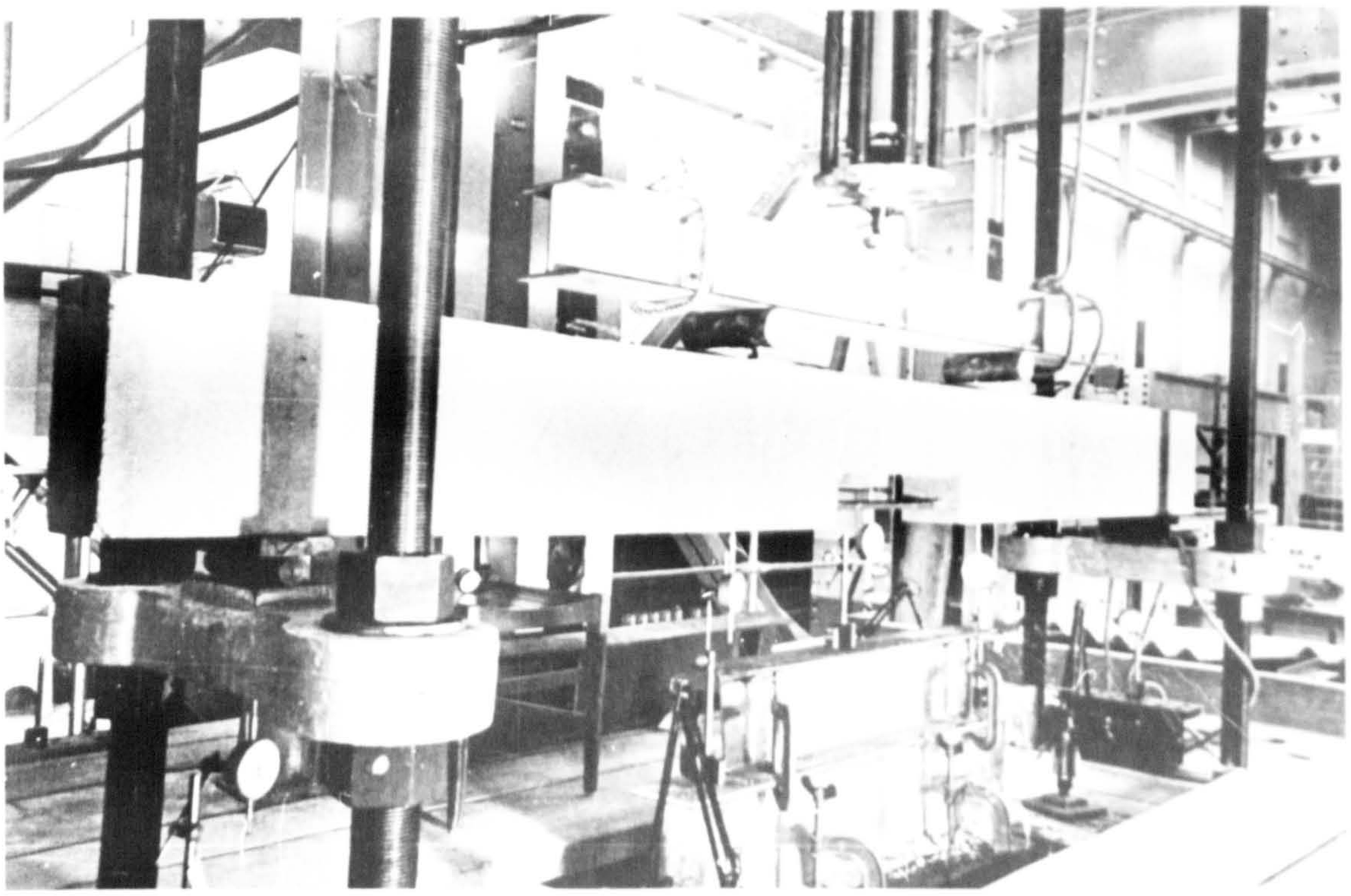

B. Static Tests (Self-Straining Frame)

PLATE (2) STATIC AND FATIGUE TEST ARRANGEMENT

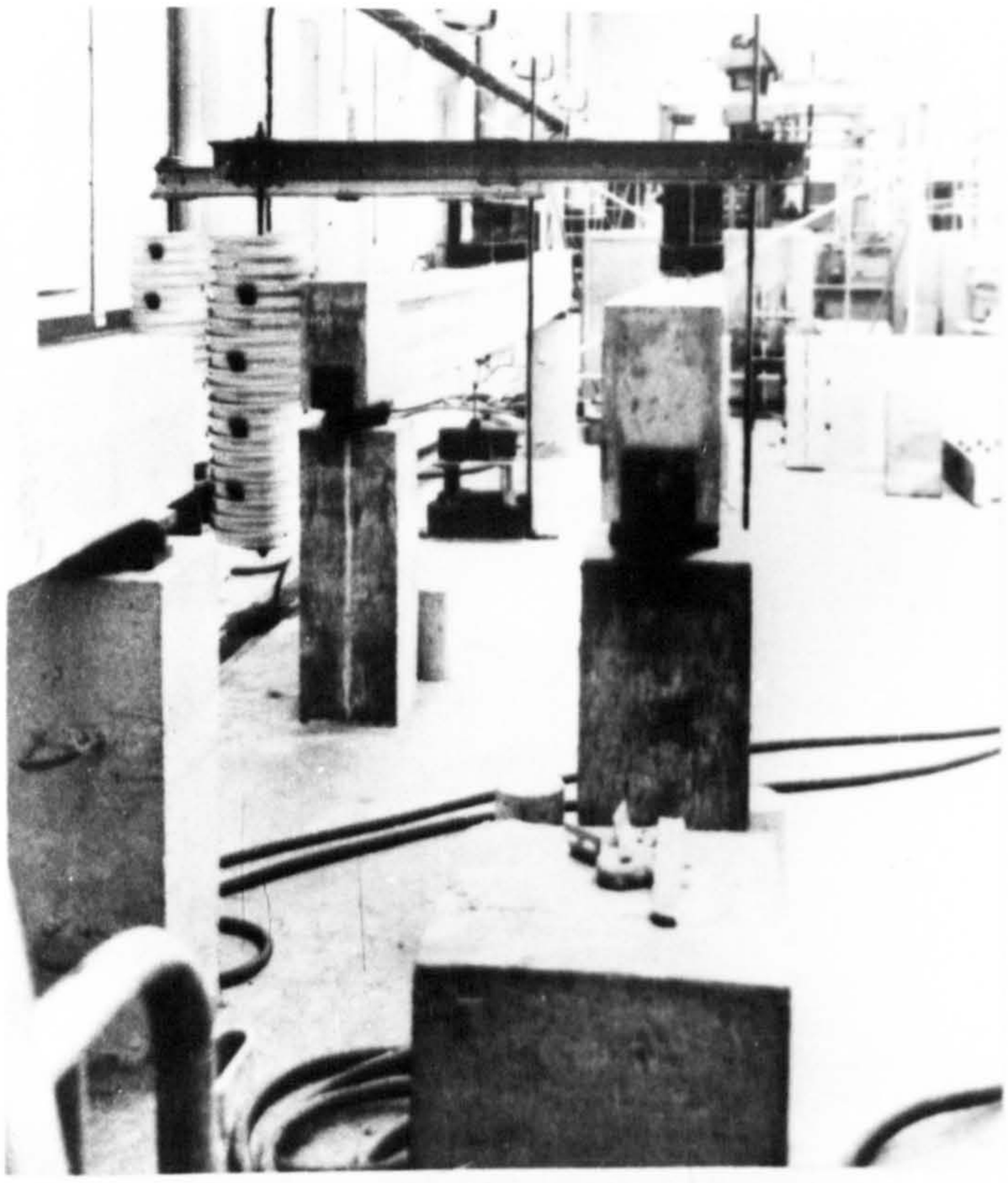

A. Simple Arrangement

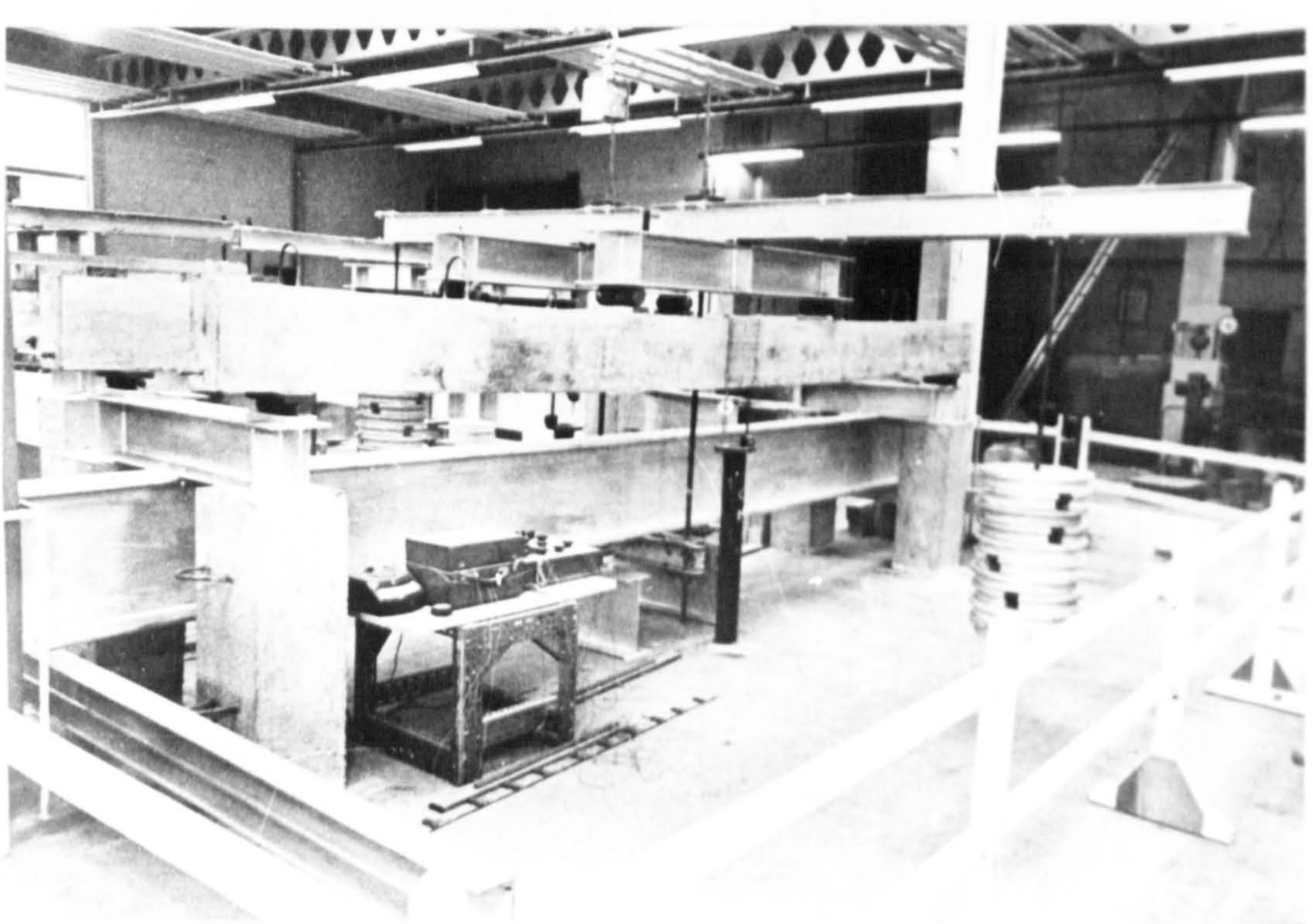

B. Self-Straining Arrangement

PLATE (3) LEVER ARRANGEMENT FOR SUSTAINED LOADING

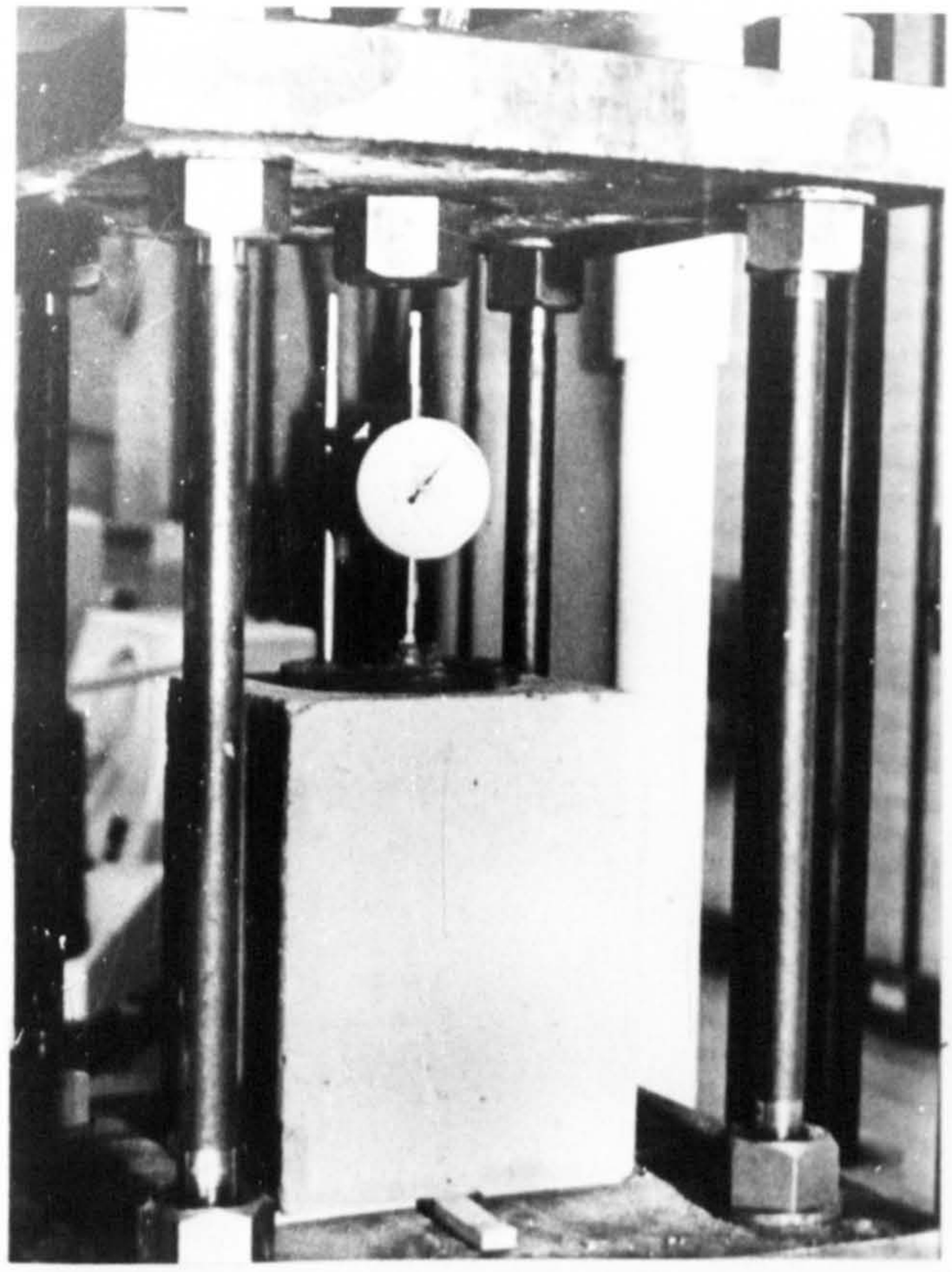

A. Test Arrangement

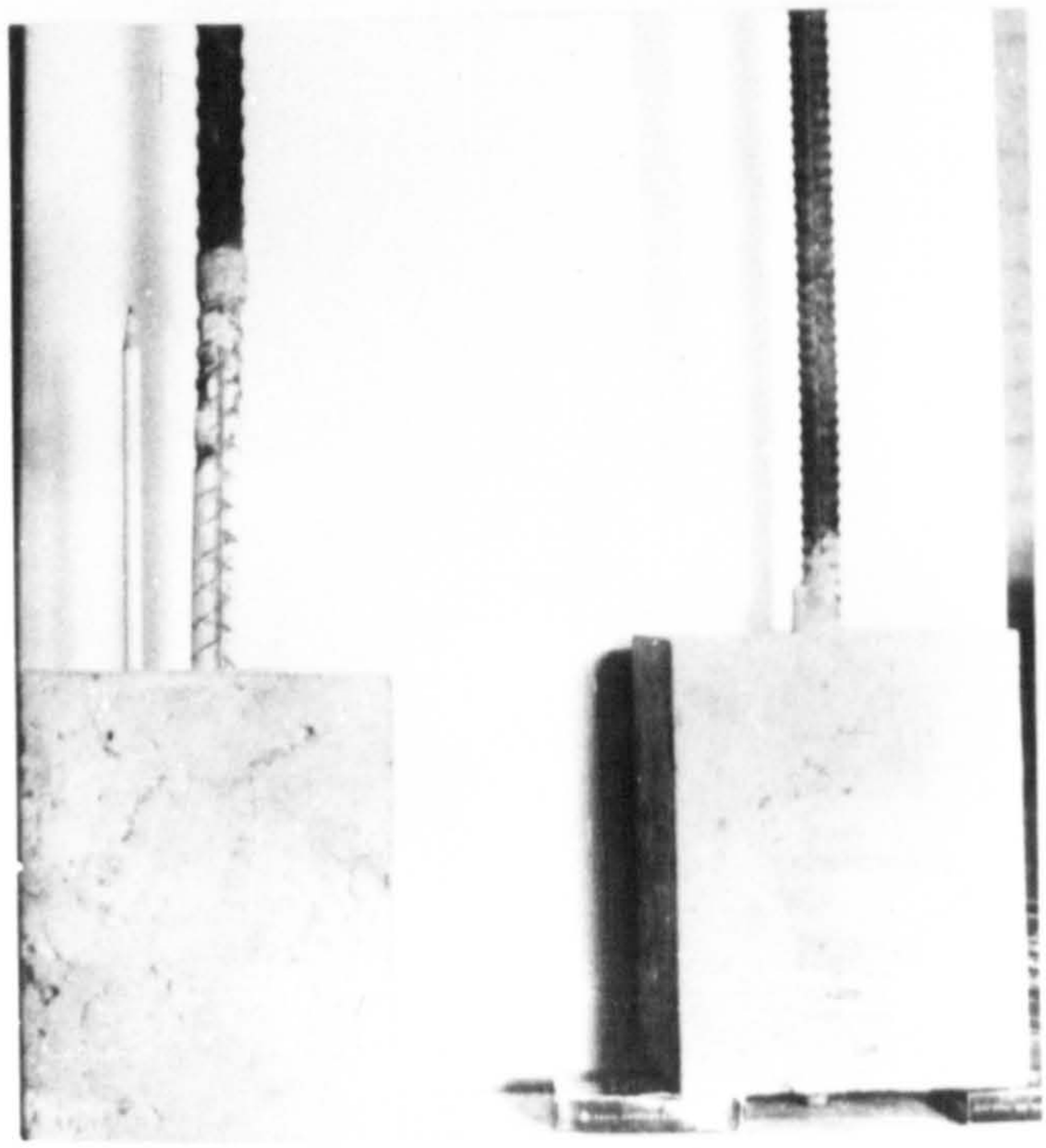

B. Failed Specimen

PLATE (4) PULL-OUT TEST ARRANGEMENT

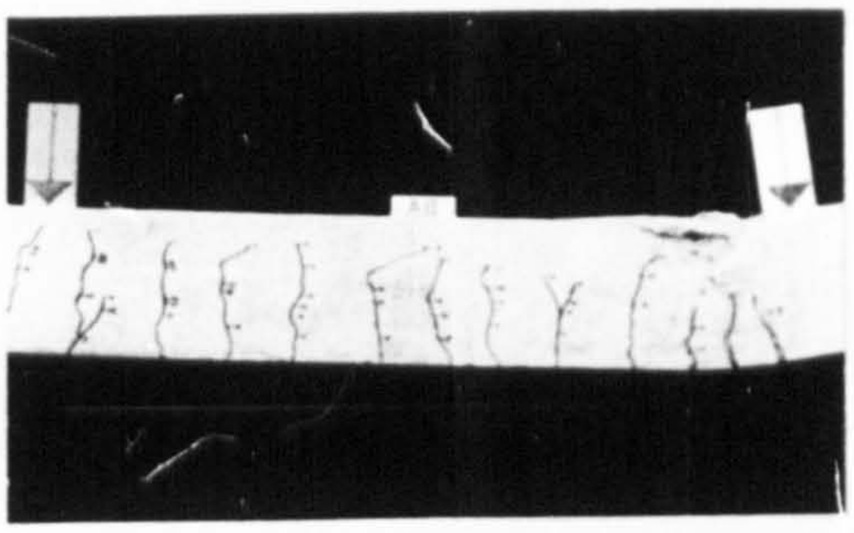

a) Plain mild steel (All)

b) Deformed Kam 60 (A34)

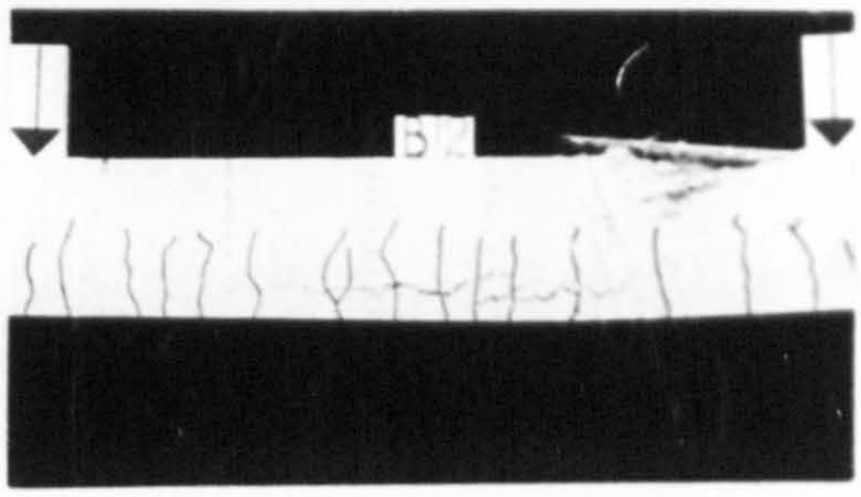

c) Deformed Unisteel (B12)

A. Beams with steel having definite yield point

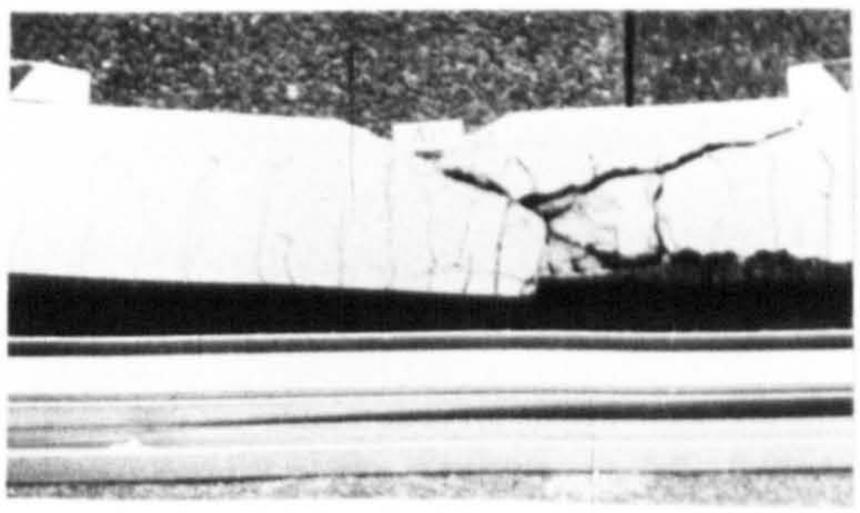

a) Deformed Kam 90 (A15)

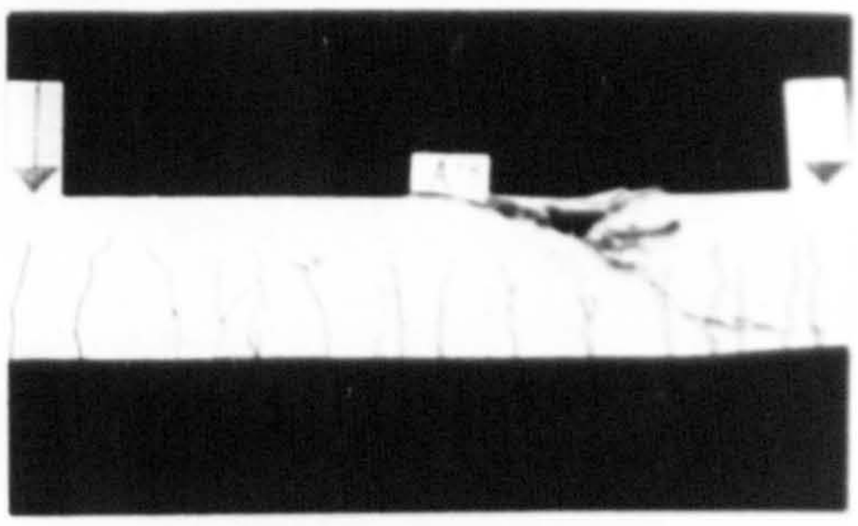

b) Deformed Unisteel 80 (A13)

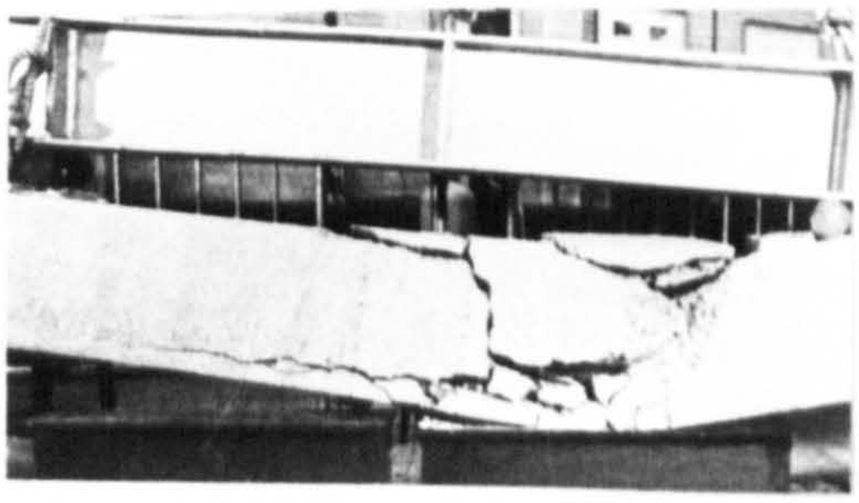

c) Bristrand 100 (B19)

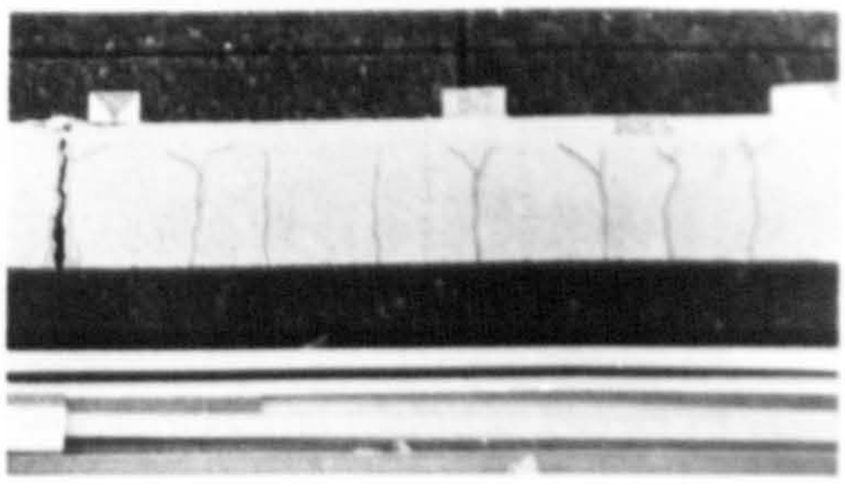

d) Plain Prestressing Wire (B17)

B. Beams with steel having indefinite yield point

PLATE (5) TYPICAL FAILURE MODES

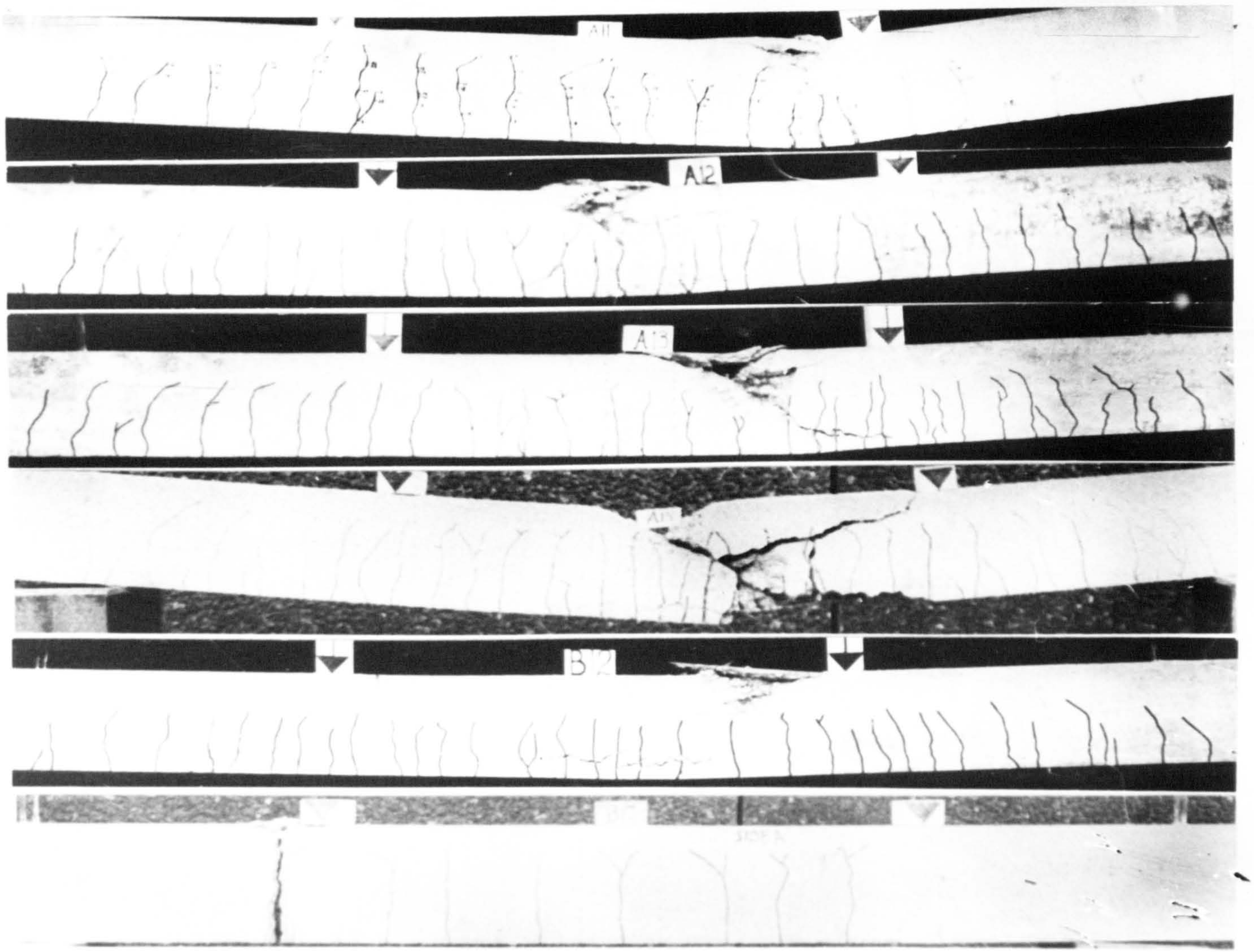

PLATE (6) FINAL CONDITION OF BEAMS